

# Catalysts for the production of sustainable biopolymers

Whitelaw, Emma

*Award date:*
2011

*Awarding institution:*
University of Bath

# Catalysts for the Production of Sustainable Biopolymers

Emma L. Whitelaw

A thesis submitted for the degree of Doctor of Philosophy

Department of Chemistry

University of Bath

September 2011

# Contents

# Acknowledgements

Firstly I would like to thank Dr Matthew Jones for the opportunity to carry out my PhD within his research group. His support and guidance throughout the three years is very much appreciated.

The University of Bath and Johnson Matthey are gratefully acknowledged for their financial support.

Drs Mary Mahon, Gabriele Kociok-Köhn are thanked for their help with the X-ray crystal structure determination and Dr John Lowe is very gratefully thanked for all his help with NMR problems. He is also thanked for his kindness in permitting me so much time on the NMR spectrometers for kinetic experiments.

Thanks go to all the Jones and Davidson group with special mention to Dr Cathy Frankis and Dr Daniel Garcia for helping me with everything, you were both missed incredibly. To all the lab and office buddies, as well as adopted ones (Chris Hawkins), my PhD time wouldn't have been the same without you all – good luck to you all! Special mentions include Chrissie Cooper for your lab tunes, Ben Jeffery for your enormous fountain of knowledge and malt loaf. Tom Forder for helping me train for my first half marathon, Kirsty Barber for always being there when I need a drink and just someone to talk to, Chris Ready for eating my soup when no one else will, Dr Justin O'Byrne the Irishman who corrected my English, Lois Manton for her endless amounts of tea and cereal and biscuits and Kinder Surprise, and Carlo Di Iulio who without his presence Anaheim, Disney and Hollywood wouldn't have been the same. Thanks also go to Casey Case for always making me smile. I hope to get a fruit party bag soon!

Finally, enormous thanks go to Dr Gareth Lamb: without you it wouldn't have been possible. I look forward to being Mrs Lamb.

# Abstract

The development of biodegradable plastics from sustainable sources is at the forefront of chemical research. One such example is the production of polylactide (PLA) *via* the ring-opening polymerisation (ROP) of the cyclic ester lactide (LA). Current industrial metal initiators utilised for the ROP of LA do not allow control over the stereochemistry of the resulting product. This thesis will investigate various initiators containing a variety of ligand sets for the ROP of *rac*-LA.

Chapter 1 introduces the ROP of *rac*-LA, the mechanisms utilised and the methods employed for characterisation of PLA. A review of the current literature of recent developments in the production of PLA *via* various metal initiators is also included.

Chapter 2 reports the development of a series of group (IV) complexes containing various amine *tris*(phenolate) ligands, where the sterics and electronics have been varied. Such complexes were trialled for the ROP of *rac*-LA as well as the ROP of trimethylene carbonate (TMC). The ability of such initiators to produce copolymers of *rac*-LA/TMC and *rac*-LA/isosorbide was also investigated and discussed.

Chapter 3 describes the synthesis of a range of group (IV) complexes containing Salalen ligands. The sterics of the ligands have been varied and the ability of the initiators to initiate the ROP of *rac*-LA in a stereocontrolled fashion has been investigated. Furthermore, the complexes have been trialled for the degradation of PLA into methyl lactate, an important starting material in the production of LA.

Chapter 4 investigates the development of Al(III) Salalen complexes for the ROP of *rac*-LA, where the sterics and electronics of the ligand have been varied. Kinetic investigations have been carried out to aid the understanding of the polymerisation process.

Chapter 5 provides details of the reaction procedures for the synthesis of ligands, complexes and polymers. Kinetic procedures are also reported together with details of the analytical techniques employed.

# Publications

- E. L. Whitelaw, M. D. Jones, M. F. Mahon and G. Kociok-Köhn, *Dalton Trans.*, **2009**, 9020-9025
- E. L. Whitelaw, M. D. Jones, M. F. Mahon, *Inorg. Chem.*, **2010**, 49, 7176-7181
- E. L. Whitelaw, M. G. Davidson and M. D. Jones, *Chem. Comm.*, **2011**, 47(36), 10004-10006
- E. L. Whitelaw, G. Loraine, M. F. Mahon and M. D. Jones, *Dalton Trans.*, **2011**, DOI: 10.1039/c1dt11438g
- B. J. Jeffery, E. L. Whitelaw, D. Garcia-Vivo, J. A. Stewart, M. F. Mahon, M. G. Davidson and M. D. Jones, *Chem. Comm.*, Submitted manuscript.

# Glossary of Abbreviations

| | |
|---|---|
| LA | lactic acid or lactide |
| GA | glycolic acid or glycolide |
| PLA | polylactic acid or polylactide |
| PGA | polyglycolic acid or polyglycolide |
| ROP | ring-opening polymerisation |
| $k_p$ | polymerisation rate constants |
| $k_{int}$ | rate of initiation |
| $k_{prop}$ | rate of propagation |
| $k_{app}$ | apparent rate of propagation |
| GPC | gel permeation chromatography |
| PDI | polydispersity index |
| $M_w$ | weight average molecular weight |
| $M_n$ | number average molecular weight |
| $M_n$ (theo.) | theoretical number average molecular weight |
| $P_r$ | probability of *racemic* enrichment |
| $P_m$ | probability of *meso* enrichment |
| *rac*-LA | racemic-lactide |
| *"i"* | isotactic |
| *"s"* | syndiotactic |
| $[LA]_o$ | initial concentration of lactide |
| $[LA]_t$ | concentration of lactide at a specific time, t |
| | |
| FDA | Food and Drug Administration |
| DIPP | 2,6-di-isopropylphenyl |
| Pipp | *p*-isopropylphenyl |
| *fac* | facial |
| *mer* | meridional |
| TMC | trimethylene carbonate or 1,3-dioxan-2-one |
| ε-CL | ε-caprolactone |
| CPIS | cyclic poly(isosorbide suberate) |
| DSDOP | 2,2-dimethyl-2-stanna-1,3-dioxepane |
| acac | acetylacetonate |

| | |
|---|---|
| DMAP | 4-dimethylaminopyridine |
| | |
| MALDI-ToF | matrix-assisted laser desorption/ionization – time-of-flight |
| MS | mass spectrometry |
| ESI-ToF | electro-spray-ionisation - time-of-flight |
| NMR | nuclear magnetic resonance |
| s | singlet |
| d | doublet |
| dd | doublet of doublets |
| t | triplet |
| td | triplet of doublets |
| q | quartet |
| sept | septet |
| m | multiplet |
| δ | chemical shift |
| ppm | parts per million |
| J | coupling constant |
| DSC | differential scanning calorimetry |
| $T_g$ | glass transition temperature |
| $T_m$ | polymer melting temperature |
| $T_c$ | polymer crystallisation temperature |
| | |
| SPS | solvent purification system |
| UV | ultra-violet |
| DRI | differential refractometer |
| IR | infrared |
| LALLS | low angle light scattering |
| MALLS | multi angle light scattering |

# Chapter 1

# Introduction

# 1. Introduction

## 1.1 Biopolymers

Due to diminishing stocks of petrochemical resources, and the overall price of oil ever increasing, the demand for a replacement of petroleum-based plastics has been at the forefront of research over the last few decades.[1] In succession with this, the recent concerns over the environmental impact of such products has led to research being focussed on the production of biodegradable and sustainable substitutes for petroleum-based plastics. One such example is the development of photodegradable plastics, which require continual exposure to sunlight for complete degradation, which at present, are not suitable for landfill disposal.[2, 3] A more desirable goal is the production of biodegradable plastics from plants, more specifically, from starch or cellulose. An example of such is the production of Coca-Cola PlantBottles® in 2009 which was the first PET bottle with up to 30 % plant-based content that was shown to reduce the carbon impact by up to 12 %.[4]

Biodegradable plastics can be split into two sub definitions:

- Biodegradable plastics which degrade from the action of naturally occurring micro-organisms such as bacteria, fungi and algae, over a period of no longer than six months.
- Compostable plastics which undergo degradation by a biological process which yield $CO_2$, water, inorganic compounds and biomass leaving no visually distinguishable or toxic residues.

One area of extensive research in the development of biodegradable plastics is in the production of linear aliphatic polyesters, particularly those derived from lactic acid (LA) and glycolic acid (GA). Such polyesters are used in a broad range of commodity applications such as food packaging to more intricate biomedical devices.[1] The production of PLA and PGA by polycondensation reactions occurs *via* an equilibrium which limits the molecular weight of the resulting polymer. Hence a preferred method of producing such polymers is to dehydrate the monomers to their corresponding cyclic esters which can further be ring-opened in the presence of an initiator to produce linear aliphatic polyesters in a more controlled fashion, as shown in Figure 1.01.[5]

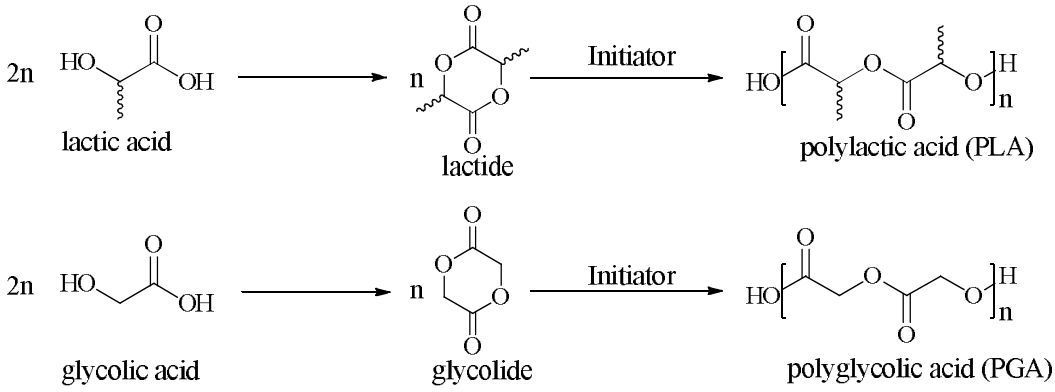


**Figure 1.01**: Production of PLA and PGA *via* their corresponding cyclic monomers

Both PLA and PGA are not only biodegradable but are biocompatible, since the hydrolysis of their products in physiological media gives lactic and glycolic acids. Such products are non-toxic and can be eliminated *via* the Krebs cycle as water and carbon dioxide.[1] Another advantage of PLA is that it can be derived from a sustainable source: from the fermentation of corn and sugar beets.[1] PLA is a polymer of lactic acid (2-hydroxypropionic acid) and was first developed by Dow Chemicals in the 1950s. Due to the high cost of production, its main use was limited to specialised medical devices.[2] However, in recent years there has been a major cost reduction in the production of PLA allowing commodity applications to be explored. NatureWorks® part of Dow-Cargill, produce over 140,000 tonnes of PLA per year in their plant in the United States.[6]

One of the major obstacles in the wider implementation of PLA as a commercial plastic is the cost of the platform chemical lactic acid, which can be produced from batch fermentation of aqueous glucose under anaerobic conditions.[7] However this process generates a large amount of salt waste, as approximately one tonne of gypsum ($CaSO_4$) is produced per tonne of lactic acid.[8] Often the esterification of lactic acid to methyl lactate is necessary to facilitate the purification.[9] Recent developments have been concerned with the production of methyl lactate directly from sugars, which would eliminate the need for esterification and generate LA from methyl lactate without the large amount of waste.[9]

## 1.2 Ring-Opening Polymerisation of Lactide

### 1.2.1 Mechanistic Studies

As mentioned in Section 1.1, the ring-opening polymerisation (ROP) of LA is the preferred method of producing PLA due to the ability to achieve higher control over the polymer produced. Various mechanistic approaches are reported for the ROP of LA, for example the reaction to taking place *via* an anionic or cationic mechanism (Figures 1.02 and 1.03 respectively).[1]

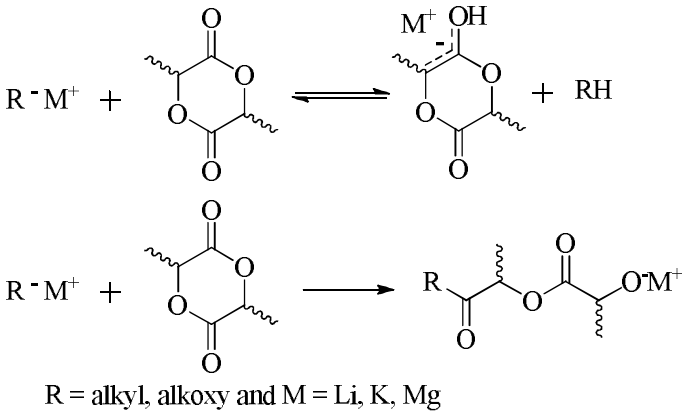


**Figure 1.02**: Anionic Mechanism for the production of PLA[1]

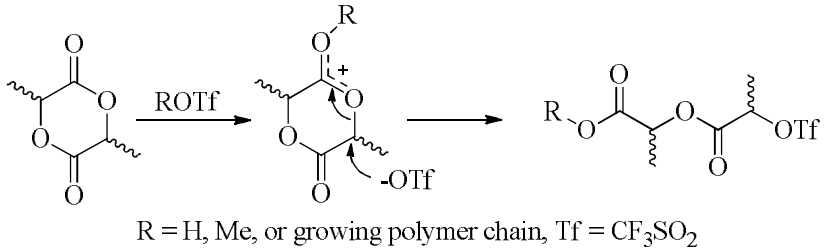


**Figure 1.03**: Cationic Mechanism for the production of PLA[1]

Despite the ability to obtain PLA *via* an anionic or cationic mechanism, the approach that is more widely reported is a coordination and insertion mechanism (Figure 1.04). This typically requires a metal initiator and is seen to occur in three steps first formulated in 1971 by Dittrich and Schulz.[1, 10]

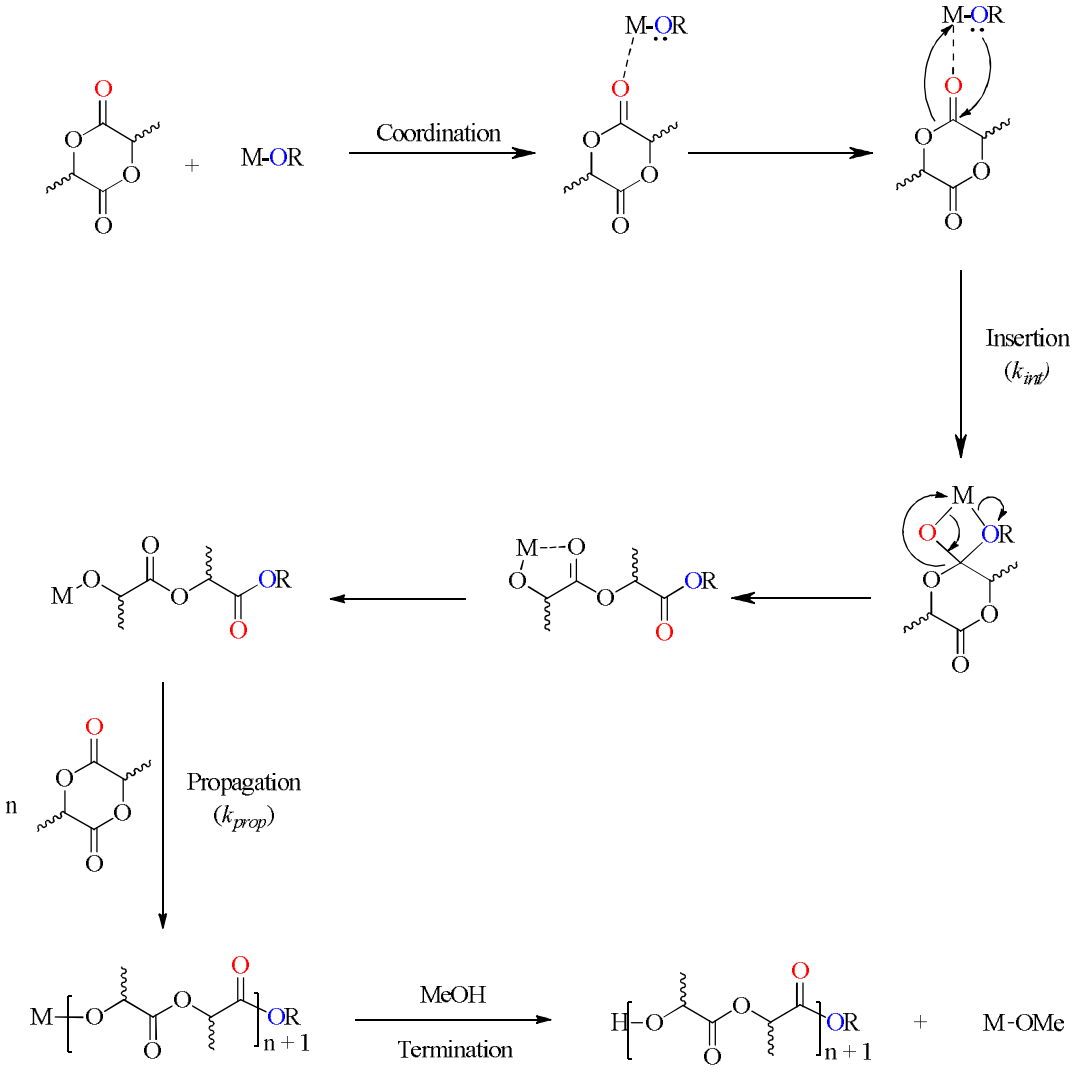


**Figure 1.04**: Coordination-insertion mechanism for the ROP of LA

The first step is the coordination of the monomer to the Lewis-acidic metal centre after which the monomer inserts into one of the metal-alkoxide bonds *via* nucleophillic addition of the alkoxy group on the carbonyl carbon. The ring is then opened *via* acyl-oxygen cleavage, followed by propagation of the polymer chain by addition of LA monomer units. Finally the metal-alkoxide bond is hydrolysed to form a hydroxyl end group, typically by addition of methanol. Study of end-group analysis can also be utilised to support the mechanism of the reaction. The mechanism of LA ROP has been studied by Gibson *et al.* using DFT analysis for the consecutive ring-opening of two LA molecules.[11] It was observed through such analysis that the polymerisation proceeds *via* two major

transition states, which is also observed with other coordinative initiator systems.[11]

For polymerisation reactions proceeding *via* a coordination-insertion mechanism, one of the controlling factors of molecular weight is the ratio of $k_{propagation}/k_{initiation}$. For example if $k_{propagation} << k_{initiation}$ then the polymer chain growth is well controlled resulting in a narrow molecular weight distribution due to the growth of the polymer from each initiator occurring simultaneously. This will also result in good theoretical molecular weight (Equation 1.01) correspondence with the experimental data obtained from GPC (gel permeation chromatography) analysis.

$$M_n\,(calculated) = \left(\left(\frac{conversion}{100}\right) \times 144\right) \times 100 + (\,end\ groups)$$

**Equation 1.01**: Equation to calculate theoretical molecular weight with a 100:1 monomer to initiator ratio; in most cases the end group are H and O$^{i}$Pr groups

However, if $k_{propagation} >> k_{initiation}$ then the polymer chains will grow at various rates resulting in a broad molecular weight distribution.

A further contribution to molecular weight control is the extent of side-reactions that are also occurring. For example transesterification which can proceed in two ways: *via* an intramolecular reaction (Figure 1.05) which results in backbiting producing a macrocyclic structure and shorter chains, or *via* an intermolecular reaction which gives chain redistribution (Figure 1.06).

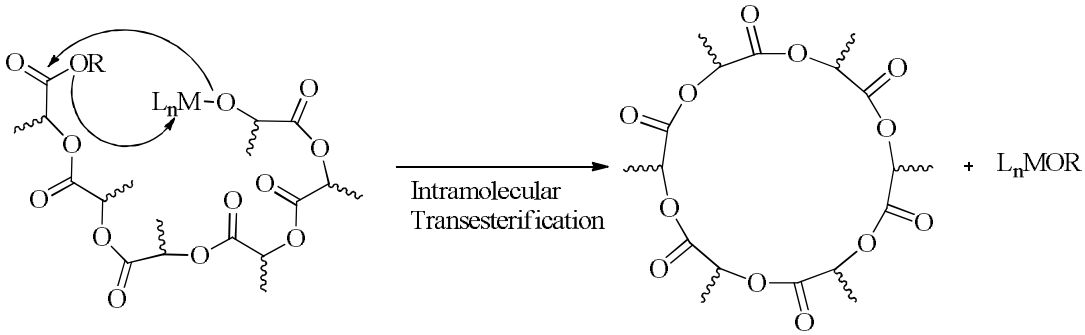


**Figure 1.05**: Transesterification *via* intramolecular reactions

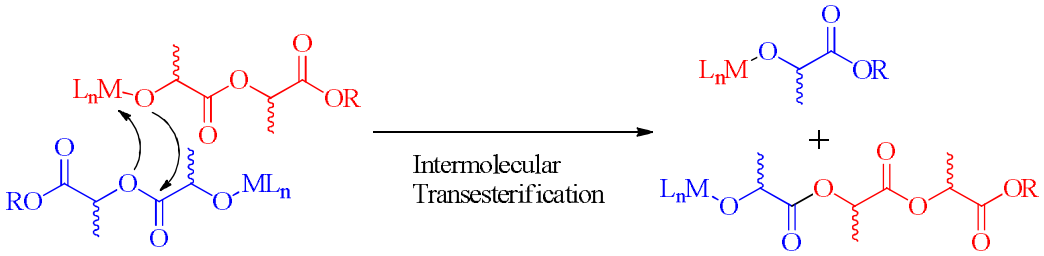


**Figure 1.06**: Transesterification *via* intermolecular reactions

The extent to which transesterification is occurring can be monitored by analysis of MALDI-ToF mass spectrometry which measures the distribution of molecular weight within the polymeric product. The presence of cyclic polymers can also be detected by MALDI-ToF mass spectrometry.

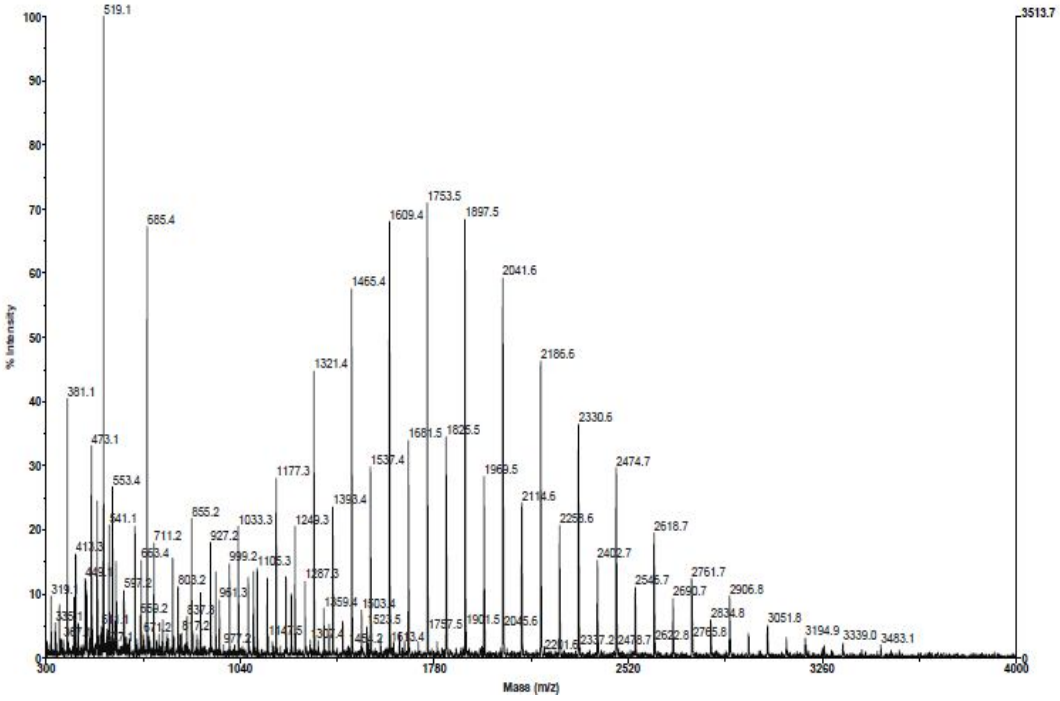


**Figure 1.07**: MALDI-ToF mass spectrum of PLA

Figure 1.07 shows a PLA product with a degree of transesterification occurring. This is visible by analysing the mass difference between peaks within the distribution such that if no transesterification was occurring then the distribution would show one series of peaks with a repeat unit of 144 $gmol^{-1}$ (for a LA monomer) between the peaks. However, , if transesterification is occurring there would be the presence of multiple extra series of curves in one spectrum and the difference between the peaks would no longer be 144 $gmol^{-1}$, but 72 $gmol^{-1}$.

The activity for the polymerisation reaction is normally assessed by analysis of the polymerisation rate constants ($k_p$) which given that most LA polymerisation reactions obey a second order rate law, can be deduced from:

$$\frac{-d[LA]}{dt} = k_p[LA]_0[I]_0^n$$

**Equation 1.02**: Second order rate equation of LA where $[I]_0$ is the initial concentration of initiator

Typically, n is equal to 1, but this can vary if there is aggregation of the catalyst. However, in practice to calculate $k_p$, it is necessary to carry out pseudo first order rate experiments to determine $k_{app}$ (apparent rate of propagation) which is given as:

$$\frac{-d[LA]}{dt} = k_{app}[LA]_0 \text{ where } k_{app} = k_p[I]_0^n$$

**Equation 1.03**: Pseudo first rate order equation for determination of $k_{app}$

Therefore a plot of $k_{app}$ against [initiator] can be used to determine $k_p$ from elucidation of the gradient of the plot if n = 1. However, if n ≠ 1 a ln–ln graph is necessary. Use of only $k_{app}$ values can provide distorted values for the initiator in question's activity and mechanism and it is of higher importance to calculate $k_p$ if possible.[12] However, $k_{app}$ values are very useful for comparing rates of polymerisations at a constant initiator concentration.

The ROP of LA can be carried out under either solution conditions or under industrially preferred solvent-free or melt conditions. If the polymerisation is carried out in solution, the desired solvent (usually $CH_2Cl_2$ or toluene) is added to the LA and initiator and the reaction heated to the desired temperature to ensure all LA becomes soluble in the solvent. Under solvent-free conditions, the polymerisation is carried out in the absence of solvent, mixing the LA and initiator together at an elevated temperature, usually >130 °C to ensure good mass transfer of monomer and initiator.

### 1.2.2 Gel-Permeation Chromatography (GPC)

GPC can be used to characterise polymeric material *via* the principle of size exclusion chromatography. A GPC instrument contains a column that is packed with crosslinked polystyrene beads containing pores of various sizes. The

polymer sample to be analysed is dissolved in a solvent, usually THF and injected down the column. Different polymer molecules take varying lengths of time to pass through the column, for example larger polymer molecules cannot fit into the pores of all the polystyrene beads and therefore will take less time to travel down the column, whereas smaller polymer molecules can fit into the majority of the beads and will have an increased elution time (Figure 1.08).

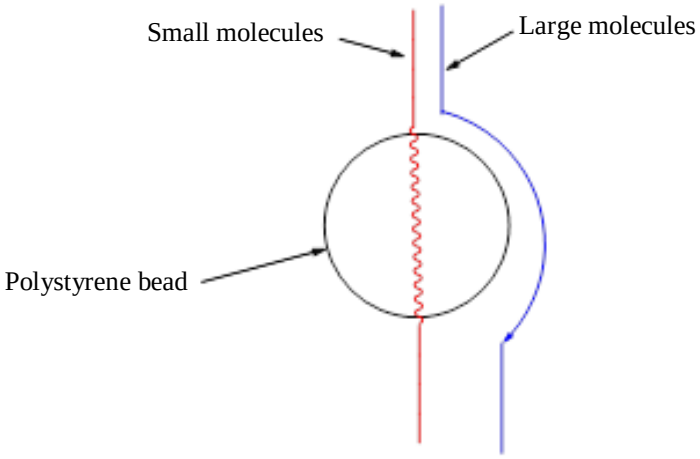


**Figure 1.08**: Schematic diagram of a GPC column and size exclusion principle

The time the polymer takes to travel down the column can be used to calculate the molecular weight of the sample, based on how the instrument is calibrated. Calibration is usually carried out using samples of polystyrene of known molecular weights and recording the elution time of the samples. A calibration graph of elution time *vs* molecular weight is determined, from which all unknown samples are compared against. The value of the molecular weights obtained from GPC analysis can vary from that expected due to the hydrodynamic volume difference between PLA and the polystyrene standards. A correction of multiplying the $M_n$ (observed) by 0.58 can be applied to account for such differences in THF.[13]

GPC samples are usually dissolved in an appropriate solvent (most frequently THF), filtered and injected into the column. The separation occurs on the column and the concentration by weight of the polymer in the solvent is monitored by the detector (Figure 1.09).

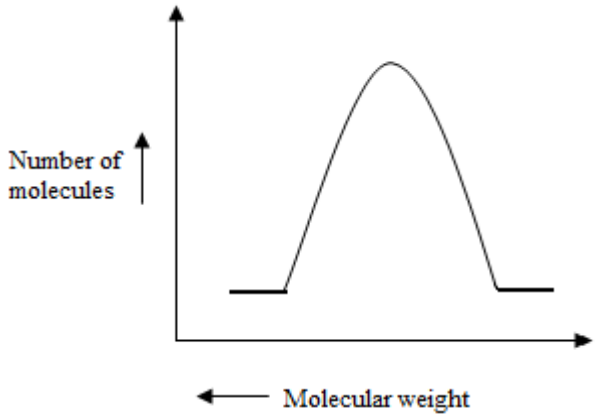


**Figure 1.09**: Distribution curve obtained for polymeric products

The weight average molecular weight ($M_w$) and the number average molecular weight ($M_n$) of the unknown sample can then be obtained from Equation 1.04 and 1.05. The polydispersity index (PDI) can be calculated from the ratio of $M_w$ to $M_n$.

$$M_w = \sum W_i M_i \text{ where } W_i = \frac{N_i M_i}{\sum N_i M_i}$$

**Equation 1.04**: Determination of $M_w$ where $N_i$ is the number of molecules of mass $M_i$

$$M_n = \frac{\sum N_i M_i}{\sum N_i}$$

**Equation 1.05**: Determination of $M_n$ where $N_i$ is the number of molecules of mass $M_i$

The types of detectors available include concentration sensitive detectors such as ultra-violet (UV) absorption, differential refractometer (DRI) and infrared (IR) absorption. Other types of detectors available are molecular weight sensitive detectors such as low angle light scattering (LALLS) and multi angle light scattering (MALLS) which gives a weight distribution of the polymer as a function of the retention volume.[14] The advantage of light scattering detectors is that they are quantitative. The technique measures the light scattered due to optical density inhomogeneities from the polymer solutions, and requires a precise measure of the difference in refractive index between the solution and solvent.[15]

### 1.2.3 Differential Scanning Calorimetry

Differential scanning calorimetry or DSC is used to study the thermal transitions of a polymer, *i.e* changes that occur when the polymer is heated or cooled. DSC measures the difference in heat input when two pans are heated at the same rate, one containing the polymeric material, and the other empty (reference pan). The pan containing the polymer will require more heat to maintain it at the same temperature as the reference pan in an endothermic transition (melting) or less heat in an exothermic transition (crystallisation). A measure of this extra heat needed is recorded and a plot of the temperature *vs*. difference in heat output is measured.

DSC can be used to measure the glass transition temperature ($T_g$), the polymer crystallisation temperature ($T_c$) and the polymer melting temperature ($T_m$). $T_g$ is the temperature in which there is a point of inflection in the DSC plot corresponding to an increase in the heat capacity of the polymer. The $T_g$ is used to measure the temperature at which a polymeric material will be in its glassy state – below the $T_g$ the polymeric material will be brittle, but above the $T_g$, the polymer will be softer and seen to be more rubber like. $T_c$ is the polymer crystallisation temperature, and is achieved when the polymers become crystalline, which in return gives out heat. This is then observed as a dip in the graph produced from the DSC. $T_c$ is an exothermic transition. $T_m$ is the polymer melting temperature and is achieved when the polymeric material is heated even further than the $T_c$. Enough energy is therefore supplied to break the interchain interactions present, resulting in a peak in the DSC plot. The $T_m$ is measured from the top of the curve and is an endothermic transition.

DSC can be used to analyse the physical properties of PLA and differences in the PLA microstructure can be observed from changes to the $T_m$ and $T_g$. Enantiopure PLLA has been reported to give a $T_g$ of around 50 °C and a $T_m$ of 180 °C. A 50: 50 mix of PLLA and PDLA also displays a $T_g$ of approximately 50 °C, but has a significantly larger $T_m$ of around 230 °C.[16]

### 1.2.4 Stereochemistry of PLA

LA can exist in three forms: *L*-lactide, *D*-lactide and meso-lactide, with the former being the naturally occurring enantiomer, and *rac*-lactide (*rac*-LA) consisting of a 50: 50 mix of the *L* and *D* enantiomer.

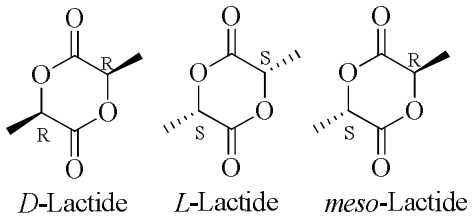


**Figure 1.10**: Possible enantiomeric forms of lactide

The monomeric units shown in Figure 1.10 can be used to synthesise PLA containing different stereochemistry, which are shown in Figure 1.11.

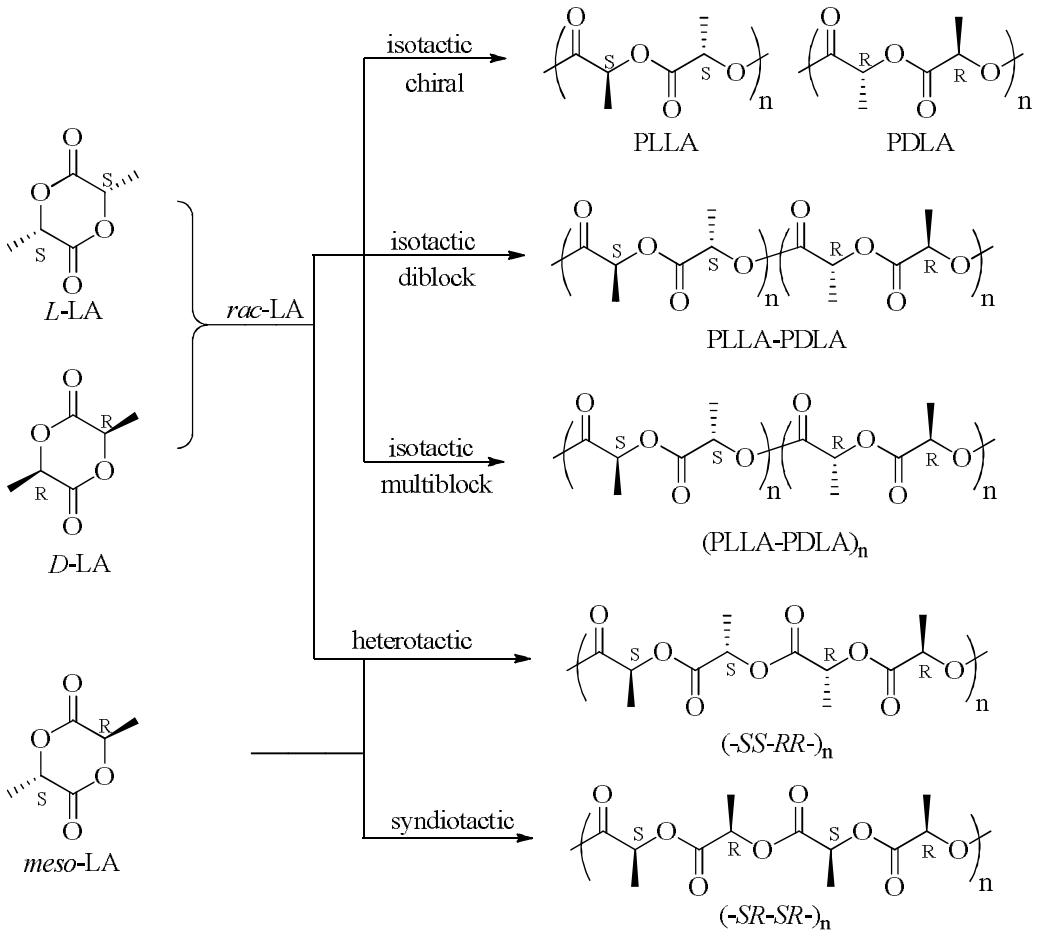


**Figure 1.11**: Lactide stereochemistry and PLA microstructures[17]

As reported in Section 1.2.3, the physical properties of the resulting polymer can be affected by the degree of stereoregularity in the polymer backbone. This can be

summarised in that atactic PLA is amorphous, heterotactic PLA displays some degree of crystallinity having a $T_m$ of 130 °C but is generally considered amorphous. Interestingly isotatic PLA has a $T_g$ of around 50 °C and a $T_m$ of 180 °C, but stereoblock isotactic PLA displays a significantly higher $T_m$ of around 230 °C.

The crystallisation is dependent on the order of stereocentres in the polymer. If consecutive stereogenic centres are equivalent, (*R* followed by *R* or *S* followed by *S*), then this is given the symbol '*i*' (isotactic). Consequently if the stereogenic centres are inequivalent (*R* followed by *S* or *S* followed by *R*), then this is given the symbol '*s*' (syndiotactic). The importance of the neighbouring stereocentres gives an indication of the overall crystallinity of the PLA product and hence the degree of stereocontrol achieved during the polymerisation. For example if the polymerisation of *L*-LA is carried out then the polymer backbone will contain all equivalent stereocentres and the only possibility will be '*i*' indicative of isotactic PLA. An example is shown in Figure 1.12.

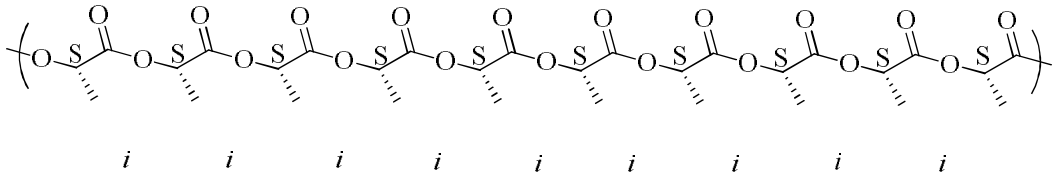


**Figure 1.12**: Assignment of neighbouring stereogenic centres in isotactic PLA

For analysis of polymeric products, the overall stereochemistry of the backbone can be determined from analysis of the $^1$H homonuclear decoupled NMR spectrum which analyses the methine *tetrads* i.e. 4 neighbouring methine stereocentres. This is such that for isotactic PLA the only possible combination of *tetrads* is *iii*.

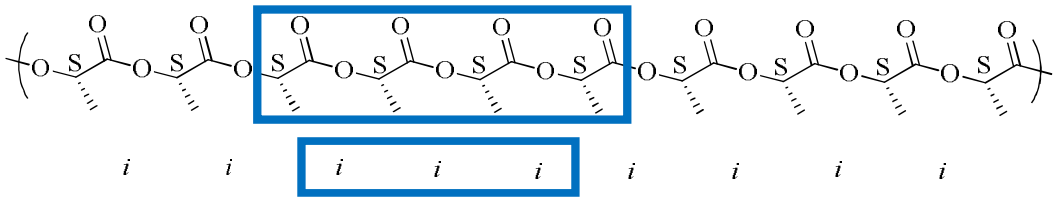


**Figure 1.13**: PLA backbone highlighting *tetrad* and therefore assignment of the neighbouring stereocentres

This would be indicated by the presence of only one resonance for the methine protons in the $^{1}$H homonuclear decoupled NMR spectrum corresponding to *iii* (Figure 1.14).

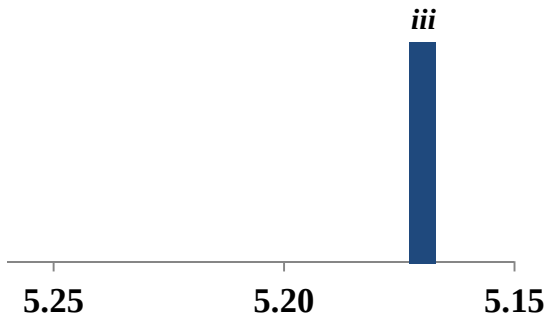


**Figure 1.14**: Schematic diagram of $^{1}$H homonuclear decoupling NMR spectrum of isotactic PLA

However, if heterotactic PLA is produced, then there is an alternation of the stereocentres (*R/R* followed by *S/S*), which results in two possibilities of *tetrad* assignment from the $^{1}$H homonuclear decoupled NMR spectroscopy: *sis* and *isi*.

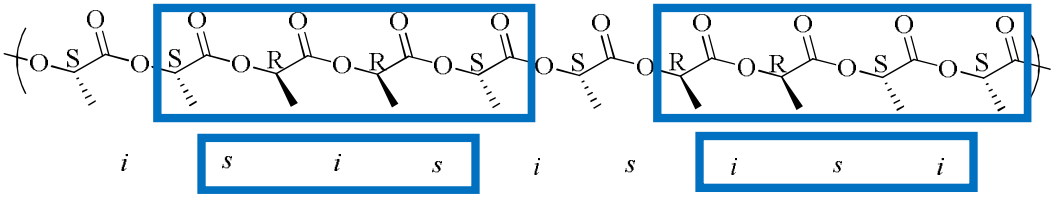


**Figure 1.15**: Assignment of neighbouring sterocentres for heterotactic PLA highlighting the two *tetrad* possibilities.

Therefore in the $^{1}$H homonuclear decoupled NMR spectrum, there would only be two resonances present for the two possible *tetrads*: *sis* and *isi* (Figure 1.16).

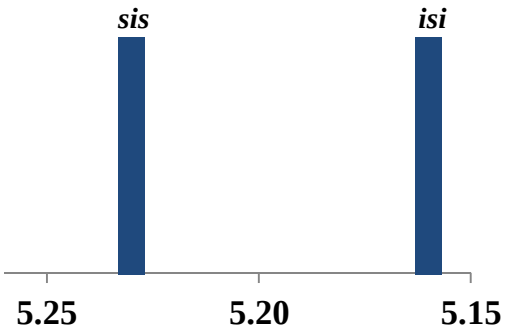


**Figure 1.16**: Schematic diagram of $^{1}$H NMR homonuclear decoupled NMR spectrum of heterotactic PLA

For atatic PLA, there is a random orientation of the methyl groups resulting in no control of neighbouring stereocentres. The assignment of *tetrads* results in the possibility of five combinations that are possible.

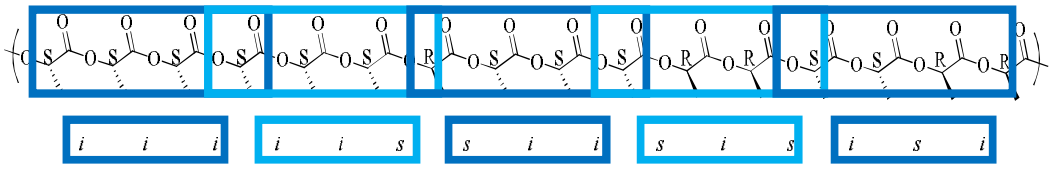


**Figure 1.17**: Assignment of neighbouring stereogenic centres in atactic PLA

These five combinations of *tetrads* result in the presence of five methine peaks in the $^{1}$H homonuclear decoupled NMR spectrum in a ratio of 1:1:1:3:2 (Figure 1.18).

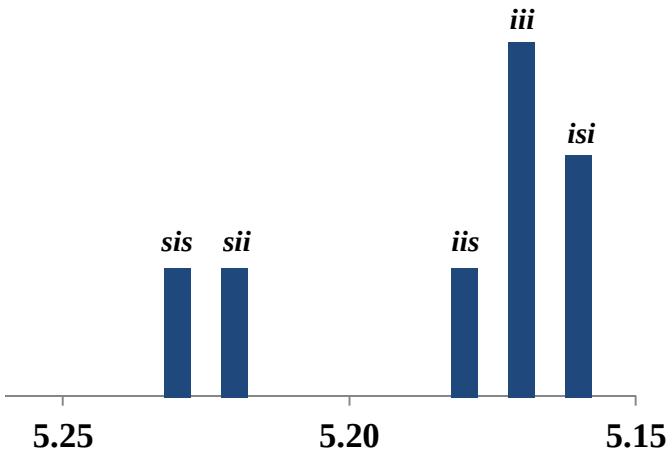


**Figure 1.18**: Schematic diagram of the $^{1}$H homonuclear decoupled NMR spectrum of atactic PLA

The presence of the five possible *tetrads* in PLA derived from *rac*-LA and *meso*-LA can be determined from Bernoullian statistics, and the probability of the *tetrad* appearing in the $^{1}$H homonuclear decoupling NMR spectrum of the methine region can be calculated using the equations in Table 1.01.[17]

| tetrad | Probability | |
|---|---|---|
| | *rac*-LA | *meso*-LA |
| [*iii*] | $P_m^2 + P_rP_m/2$ | 0 |
| [*iis*] | $P_rP_m/2$ | 0 |
| [*sii*] | $P_rP_m/2$ | 0 |
| [*sis*] | $P_r^2/2$ | $(P_m^2 + P_rP_m)/2$ |
| [*sss*] | 0 | $P_r^2 + P_rP_m/2$ |
| [*ssi*] | 0 | $P_rP_m/2$ |
| [*iss*] | 0 | $P_rP_m/2$ |
| [*isi*] | $(P_r^2 + P_rP_m)/2$ | $P_m^2/2$ |

**Table 1.01**: Tetrad probabilities based on Bernoullian statistics[17]

For ease of calculation, and omitting the need for simultaneous equations, [*sis*] is normally calculated for *rac*-LA and used to determine the $P_r$ value and hence the tacticity or stereoregularity of the polymeric product. $P_m$ is the probability of *meso* enrichment and $P_r$ is the probability of racemic enchainment. If $P_r = 1$ then there is 100 % chance that the next stereocentre in the polymer chain will be racemic and therefore heterotactic PLA is produced. If $P_r = 0$ then there is no chance of the neighbouring stereocentre being different, or racemic, which is indicative of either isotactic PLA from *L*-LA or *D*-LA or stereoblock isotactic PLA from *rac*-LA. When $P_r = 0.5$ there is a 50 % chance of the neighbouring site being racemic and hence atactic PLA is present.

## 1.3 Metal Initiators

As mentioned in Sections 1.1 and 1.2, the ROP of *rac*-LA requires an initiator to produce PLA, and the choice of initiator used can alter the stereochemistry of the polymer produced. In general terms, it is believed that multidentate ligands that contain heteroatoms encapsulate metal ions to form single-site complexes of the formula $L_mMR$ where $L_m$ is the ligand and R the initiation group. It has been reported that the choice of ligand can control the steric and electronic properties of the metal, and the initiation group can affect the activity of the overall complex.[18] The need for an initiation group can be further emphasised when looking at the mechanism of the reaction (Figure 1.04, Section 1.21). Although

this thesis deals with the utilisation of metal initiators, it should be noted that there are also metal free initiators reported for the polymerisation.[19-21]

### 1.3.1 Tin Initiators

At present, the industrial processes manufacturing PLA, uses tin(II)bis(2-ethylhexanoate) (Figure 1.19) as the initiator under solvent-free conditions (discussed in Section 1.2.1) due to its commercial availability, ease of handling and solubility in most common organic solvents.

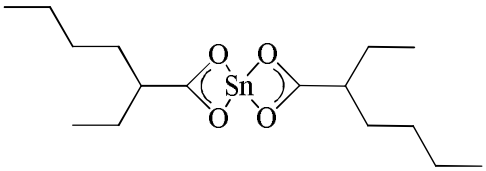

**Figure 1.19**: Structure of Sn(II)(octanoate): $Sn(Oct)_2$

The further advantages of using $Sn(Oct)_2$ as an initiator in the ROP of *rac*-LA is that it is highly active, producing high molecular weight polymers within a few hours at temperatures ranging from 140 – 180 °C.[1, 22] It has been shown however that better control of the molecular weight can be achieved when $Sn(Oct)_2$ is combined with a protic reagent such as an alcohol indicating a coordination and insertion mechanism is taking place – Figure 1.20.[23]

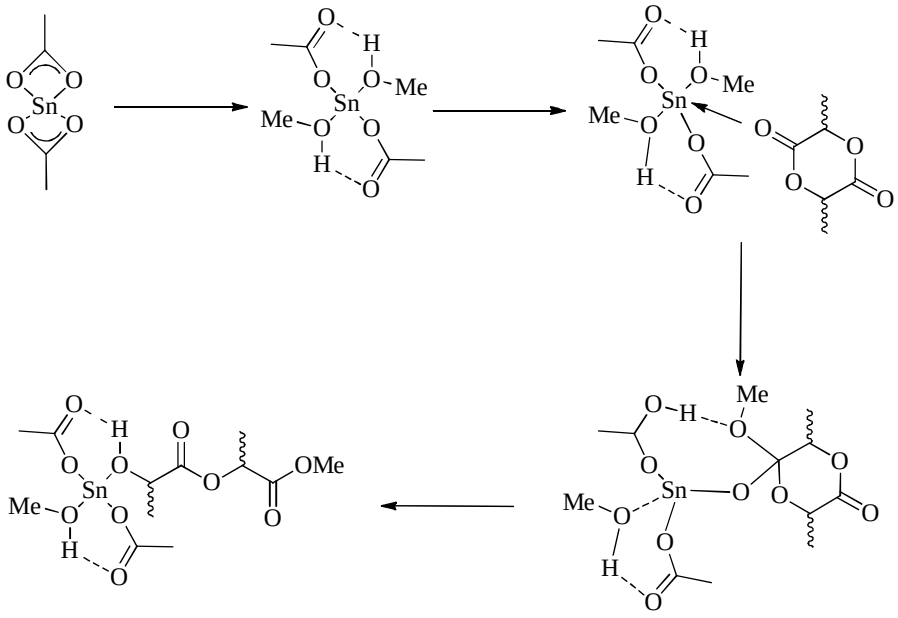

**Figure 1.20**: Predicted mechanism for the $Sn(Oct)_2$ catalysed ROP of *rac*-LA in the presence of methanol[23]

It has been reported that $Sn(Oct)_2$ itself does not initiate the reaction. It is widely assumed that a Sn-OR is formed *in situ* during the reaction of $Sn(Oct)_2$ and a corresponding alcohol.[22] Although $Sn(Oct)_2$ has been approved by the Food and Drug Administration (FDA), for packing materials, its toxicity issues still remain a concern especially for the use of PLA in more niche applications such a surgical stents and sutures.

Gibson *et al.*. synthesised a range of Sn(II) complexes containing *β*-diketiminate ligands, shown in Figure 1.21.[24, 25]

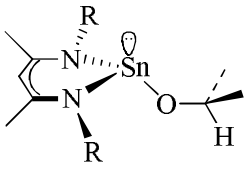


**Figure 1.21**: Sn(II) complex isolated by Gibson *et al.*[24, 25]

Results indicated that when R = Ar in the complex shown in Figure 1.21, the ROP of 100 equivalents of *rac*-LA in $CH_2Cl_2$, carried out at ambient temperature gives high conversion to PLA after 96 hours. When the reaction was repeated in toluene at 60 °C, 85 % conversion to PLA was observed after 4 hours, producing a heterotactically enriched product.[24] When R = DIPP (2,6-di-isopropylphenyl), the ROP of *rac*-LA at room temperature requires a reaction time of 50 hours to attain > 95 % conversion.[25] The polymerisation is well controlled, with good correlation between theoretical and measured molecular weights, producing heterotactic PLA. When R = DIPP, the polymerisation is seen to show higher activity than when R = Ar, achieving > 90 % to PLA after 4 hours in toluene at 60 °C, again showing a linear correlation between monomer conversion and monomer-to-initiator stoichiometry.[25]

More recent work by Gibson *et al.* reports the use of *tert*-butylamidinate tin(II) complexes for the ROP of *rac*-LA (Figure 1.22).[26]

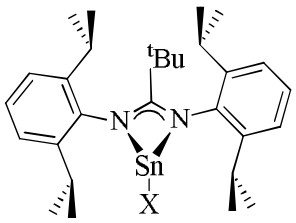


X = O$^i$Pr (**1**)
X = $NMe_2$ (**2**)
X = $N(SiMe_3)_2$ (**3**)

**Figure 1.22**: *tert*-bulylamidinate tin(II) complexes reported by Gibson *et al.* for the ROP of *rac*-LA[26]

The complexes shown in Figure 1.22 were trialled for the ROP of *rac*-LA in toluene at 60 °C using 100 equivalents of LA. A plot of $M_n$ *vs* monomer conversion is linear when the reactions are carried out using complex **1** in Figure 1.22, indicating that the polymerisation is well-controlled. Kinetic investigations using **1** as the initiator over a range of initiator concentrations revealed a non-first-order dependence of 0.21 on **1** presumably due to aggregation of the initiator in solution. This is in contrast to that observed for the complexes shown in Figure 1.21.[26] Complex **1** however is reported to have a higher activity than the $\beta$-diketiminate initiators shown in Figure 1.21, achieving the same levels of conversion after 90 minutes, compared to 4 hours for $\beta$-diketiminate initiators. When complexes **2** and **3** were trialled for the ROP of *rac*-LA, it was seen that **2** gave comparable molecular weights to **1**, however, **3** produced PLA with much higher molecular weights and broader molecular weight distributions.[26] The reaction rates observed with **2** and **3** are slower than that for **1** requiring a reaction time of 180 minutes and 240 minutes respectively to achieve similar conversions.[26] All complexes isolated in Figure 1.22 produced PLA with a heterotactic bias.

Alkoxides of other metals containing free p, d or f orbitals of the appropriate energy and a bound initiation group were therefore considered as alternatives to $Sn(Oct)_2$. Such metal alkoxides may be capable of initiating the reaction and allowing the ROP of *rac*-LA to occur *via* the coordination and insertion mechanism in Figure 1.04.

### 1.3.2 Aluminium Initiators

The use of aluminium alkoxides, even as simple as $Al(O^iPr)_3$ are examples of alternatives to $Sn(Oct)_2$ for the ROP of *rac*-LA. However, $Al(O^iPr)_3$ has been reported to be significantly less active than $Sn(Oct)_2$ in bulk and generates PLA with lower molecular weight, as well as having an induction period of a few minutes for the polymerisation reaction.[1] $Al(O^iPr)_3$ is known to exist in two different forms: the trimer and the tetramer with evidence suggesting that the trimer is more reactive than the tetramer at catalysing the ROP of *L*-LA.[27]

One of the earliest examples of LA polymerisation *via* metal initiators utilised tetraphenylporphyrin aluminium alkoxides for the ROP of *D*-LA to achieve control of the molecular weight and molecular weight distribution.[28]

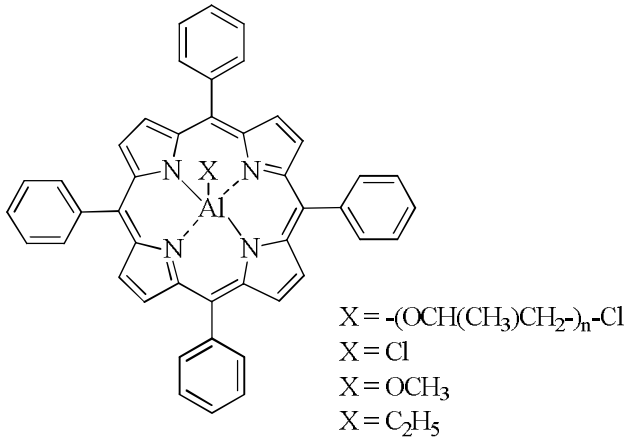


**Figure 1.23**: Tetraphenylporphyrin aluminium alkoxides used in the ROP of *D*-LA[28]

The polymerisation reaction using the complexes shown in Figure 1.23, when X = $(OCH(CH_3)CH_2)_nCl$ where n = 20 and when X = $OCH_3$ were reported to proceed in a very similar manner. It was reported that the ROP of *D*-LA at 100 °C achieved 94 % conversion after 96 hours yielding PLA with a $M_n$ of 16,400 $gmol^{-1}$.[28] When the temperature was lowered to room temperature, the rate of polymerisation decreased resulting in no substantial polymeric product.[28] When the complex in Figure 1.23 where X = Cl was trialled for the ROP of *D*-LA, no conversion to polymeric product was observed.[28]

Development from this early work led to the polymerisation of LA being carried out using aluminium alkoxide Schiff base complexes.[29, 30] An example of which is from Spassky *et al.* who utilised an aluminium complex of a chiral binaphthyl

Schiff base to produce stereoblock isotactic PLA from *rac*-LA in solution at 70 °C (Figure 1.24).[30]

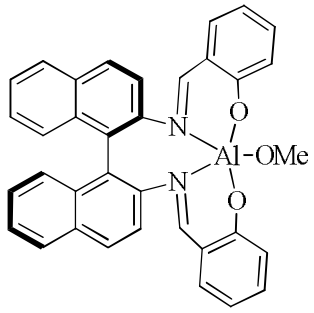


**Figure 1.24**: (*R)*-Binaphthyl Schiff base aluminium complex developed by Spassky *et al.*[30]

It was reported that at 70 °C a 20:1 preference for the polymerisation of (*R,R*)-lactide over (*S,S*)-lactide was occurring meaning that at conversions less than 50 % the polymer microstructure was predominantly isotactic as all the (*R,R*)-lactide is used up. Above 50 % conversion, only (*S,S*)-lactide remains and the end result is the formation of stereoblock PLA with a high melting temperature of 187 °C.[31] A modified racemic version of the complex shown in Figure 1.24 where the OMe group is replaced by an O$^{i}$Pr group was developed by Baker and Smith.[32] They reported a living polymerisation of *rac*-LA to yield a mixture of PLLA and PDLA *via* a site control mechanism, where the key step is governed by the chiral binaphthyl ligand.[32] Coates *et al* re-evaluated the results reported by Baker and Smith, and concluded that their modified version of the initiator shown in Figure 1.24 did not produce a mixture of PLLA and PDLA, but an isotactic stereoblack PLA.[31]

Feijen *et al.* advanced this work by ustilising a Salen aluminium alkoxide complex which employs Jacobsen ligand (Figure 1.25).[29]

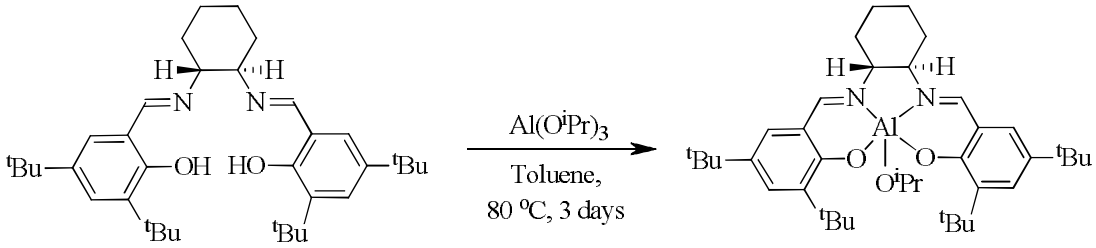


**Figure 1.25**: Preparation of (*R,R*)-Salen aluminium alkoxide complex from Jacobsen ligand[29]

Jacobsen ligand itself is an inexpensive commercial starting material and can be used to provide high isospecificity and control the polymerisation of LA at higher temperatures both in solution and under melt conditions.[33] The complex shown in Figure 1.25 polymerises *L*-LA significantly faster than *D*-LA with a $k_I/k_D$ of around 14. Furthermore, the ROP of *rac*-LA *via* the (*R,R*) Salen aluminium alkoxide complex produces isotactic stereoblock PLA *via* an enantiomorphic site control mechanism.[29]

A further example of aluminium Salen complexes producing stereoblock-isotactic PLA from *rac*-LA is given by Nomura shown in Figure 1.26. It was reported that such catalysts exploit a chain-end control mechanism in the polymerisation where the pre-catalyst does not contain any chirality but the stereochemistry is determined by the last inserted monomer in the polymeric chain.[32]

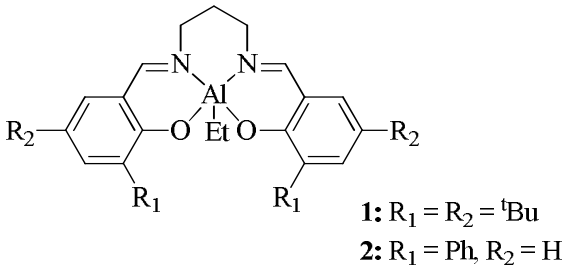


**Figure 1.26**: Aluminium complexes reported by Nomura to achieve isotactic PLA[32]

Polymerisations carried out using complex **1** in Figure 1.26 in toluene at 70 °C using a 100: 1: 1 ratio of [LA]:[initiator]:[benzyl alcohol], achieved 95 % conversion to PLA after 14 hours producing a polymeric product with a $M_n$ of 22,000 $gmol^{-1}$. Incorporation of Ph-substituents into the aromatic rings accelerated the polymerisation rate with complex **2** achieving 94 % conversion to PLA with a $M_n$ of 20,000 $gmol^{-1}$ after just 1.3 hours.[32] In both cases, narrow polydispersity values were achieved suggesting that the polymerisations are carried out with a degree of control.[32]

The addition of benzyl alcohol is not required when alkoxide groups are present on the aluminium centre. An example of such is reported by Fulton *et al.* who also reported no activity for the ROP of *rac*-LA when alkoxy aluminium complexes containing a chelating ligand with a piperazine ring present are used as initiators (Figure 1.27). The complex shown in Figure 1.27 does, however, show activity for the ROP of $\varepsilon$-caprolactone.[34]

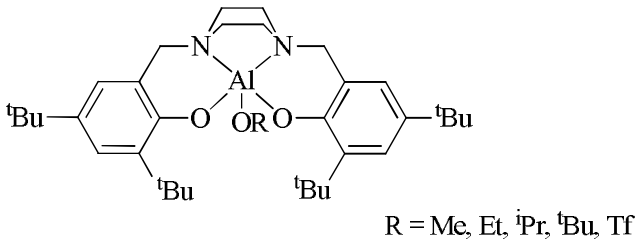


**Figure 1.27**: Aluminium alkoxy complexes containing a piperazine chelating ligand showing no activity for the ROP of *rac*-LA[34]

Gibson *et al.* have synthesised a range of aluminium complexes containing Salan type ligands (tetradentate phenoxyamines) which showed high stereocontrol in the ROP of *rac*-LA with the benefit of the complexes being colourless unlike the Salen counterparts. This is particularly important for the commercial aspect of such complexes since decolourisation steps on an industrial scale can be avoided.[35]

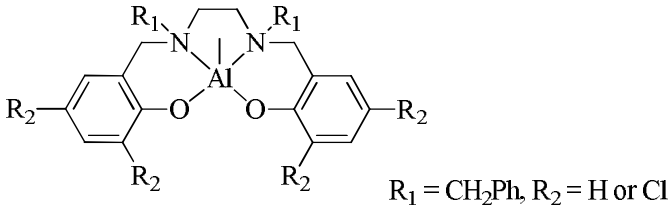


**Figure 1.28**: Salan aluminium complexes developed by Gibson *et al.*[35]

It was reported that kinetically the 3,5-dichlorophenoxide equivalent was slower than the unsubstituted equivalent with a $k_{app}$ of 37.8 × $10^{-6}$ $s^{-1}$ compared to a $k_{app}$ of 79.8 × $10^{-6}$ $s^{-1}$ for the un-substituted aluminium complex.[35] When the ROP of *rac*-LA was performed in toluene at 80 °C, using a 100: 1 ratio of [LA]: [Al], the chloro substituted complex in Figure 1.28 gave 94 % conversion to PLA after 21 hours ($M_n$ = 17,770 $gmol^{-1}$, PDI = 1.06). The unsubstituted initiator however showed higher activity giving 98 % conversion to PLA after the same length of time producing a product with $M_n$ = 21,180 $gmol^{-1}$ and PDI = 1.08. Furthermore when the phenoxide groups are unsubstituted ($R_2$ = H), high levels of isoselectivity is observed (spectra **a** in Figure 1.29) in the $^1H$ homonuclear decoupled NMR spectrum with a $P_r$ = 0.21, however when $R_2$ = Cl, heterotactic PLA is produced with a $P_r$ = 0.96 (spectra **b** in Figure 1.29).[35]

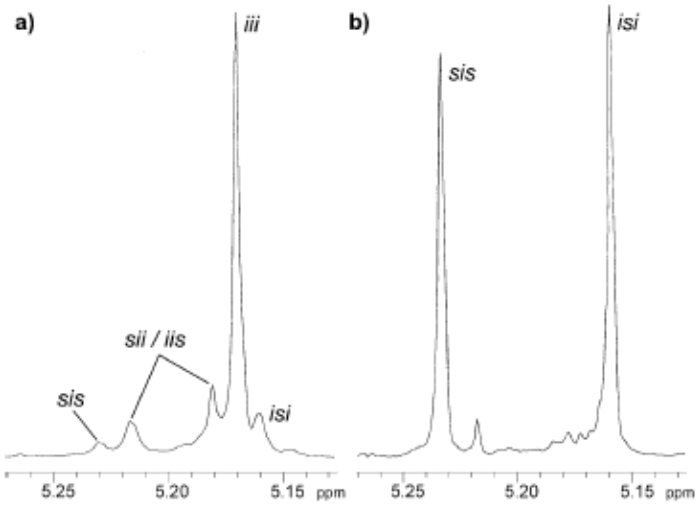


**Figure 1.29**: $^{1}$H homonuclear decoupled NMR spectra of the methine region of PLA. a) $R_2$ = H, b) $R_2$ = Cl[35]

A further example in the use of tetradentate phenoxyamine (Salan-type) ligands has been reported by Feijen, which were reported to be active for the ROP of *rac*-LA with various degrees of stereocontrol producing both isotactic and heterotactic PLA.[36]

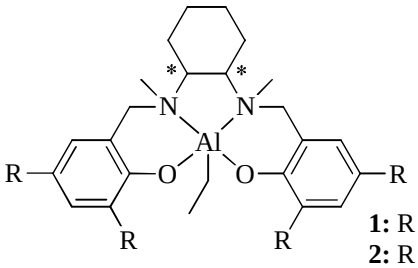


**1:** R = H, *(*R*,*R*)
**2:** R = Cl, *(*R*,*R*)
**3:** R = Me, *(*R*,*R*)
**4:** R = H, *(*rac*)
**5:** R = Cl, *(*rac*)
**6:** R = Me, *(*rac*)

**Figure 1.30**: Aluminium complexes of tetradentate phenoxyamine ligands with either (*R,R)* or *rac* stereochemistry at the chiral centres[36]

The active initiators were generated *in situ* by addition of propan-2-ol and were all seen to be active in producing PLA in a well-controlled manner with molecular weights from 4.38 – 8.00 × $10^3$ gmol$^{-1}$ being in good correlation with the theoretical $M_n$ values.[36] Both the optically pure and the *racemic* version of the complexes were synthesised, but very little distinction in the stereochemistry of the PLA produced or the activity was observed with either version of the complexes.[36] When R = H, 70 % conversion to isotactically enriched PLA was produced after 10 hours with the optically pure (*R,R*)-tetradentate phenoxyamine

aluminium complex, compared with 89 % conversion after the same period of time using the *racemic* initiator. However, when the R groups on the phenoxide rings were methyl groups, no stereocontol was observed in the polymerisation resulting in atactic PLA being produced. To achieve high conversions when R = Me, longer reaction times of 69 hours for the optically pure initiator and 53 hours for the *racemic* complex were required.[36] Heterotactic PLA could be produced when R = Cl achieving greater than 80 % conversion after 57 hours for the optically pure initiator and 34 hours when the *racemic* complex was utilised.[36] Since heterotactic PLA cannot be obtained from *rac*-LA *via* an enantiomeric site control mechanism with the use of an enantiomeric pure complex, it was indicative that a propagating chain-end control mechanism was occurring.

Kinetic studies were used to further understand the mechanism of polymerisation, using the enantiomeric pure complex **1** in Figure 1.30, with the addition of propan-2-ol to generate the active initiator *in situ*. The kinetic data was recorded at 70 °C in toluene at initial *rac*-LA concentrations of 0.534 M and 0.267 M with varying concentrations of initiator. In each case, a deviation from a first-order plot for $\ln[LA]_0/[LA]_t$ *vs* time was observed at high conversions, suggesting that there is a preference for one LA enantiomer over the other, i.e. preference for (*S*,*S*)-LA or (*R*,*R*)-LA.[36] When the same initiator was used to polymerise (*S*,*S*)-LA then (*R*,*R*)-LA there was a clear difference in rates showing a preference for (*S*,*S*)-LA ($k_{app}$ = 517 × $10^{-3}$ $h^{-1}$) over (*R*,*R*)-LA ($k_{app}$ = 51.0 × $10^{-3}$ $h^{-1}$) which is indicative of a site control mechanism. However, when the polymerisation was repeated where the R groups on the phenoxide rings were either Me or Cl, the reaction shows a preference towards (*R*,*R*)-LA with $k_{SS}/k_{RR}$ = 0.62 (for R = Cl) and 0.82 (for R = Me). A graph of conversion *vs* time was collected for the polymerisations in toluene at 70 °C using both the enantiomerically pure and *racemic* version of the initiators where R = Me or Cl. Results indicated 1$^{st}$ order kinetics in the monomer suggesting a positive cooperation effect between a chain-end control mechanism and site control mechanism. This results from the occurrence of polymer exchange, i.e. there is coexistence of both mechanisms in LA polymerisation using such initiators.[36]

Unlike the complexes shown in Figures 1.24 – 1.28 and Figure 1.30, which contain an (ONNO)-type ligand, it has been reported that (OSSO)-type are also

active for the ROP of *rac*-LA. Examples of such are (OSSO)-type *bis*(phenolate) ligands complexed to $AlMe_3$ to produce both monomeric (complexes containing ligands **1**-**4**, Figure 1.31) and dimeric complexes (complexes containing ligand **4**, Figure 1.31).[37]

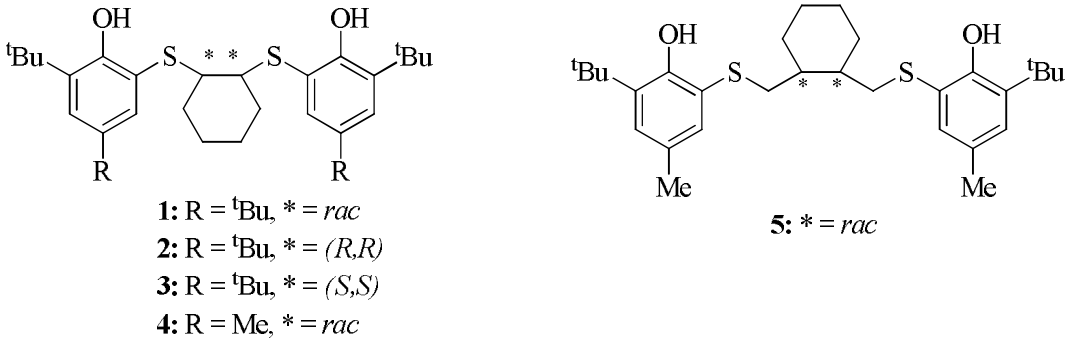


**Figure 1.31**: (OSSO)-type bis(phenolate) ligands which were complexed to $AlMe_3$[37]

Results indicate that the polymerisation *via* aluminium complexes containing the ligands in Figure 1.31 occurs in a controlled manner with $M_n$ increasing linearly with conversion to produce atactic PLA. Higher activity was observed with the monomeric complexes containing ligands **1-4**, with 90 % conversion to PLA achieved after 6 hours compared with a reaction time of 49 hours to achieve the same conversion when the initiator contains ligand **5**.[37] The polymerisations also showed no solvent dependence and no stereoselectivity was observed when the reactions were carried out in either toluene or THF.[37]

Amidinate aluminium complexes have been considered as potential initiators for the ROP of *rac*-LA due to the high Lewis acidity of the metal centre which could help facilitate the coordination step in the polymerisation mechanism. An example of such is a range of unsymmetric *N*-substituted amidinate ligands which were synthesised in the hope that the non-symmetrical ligands might induce a degree of enantiomorphic site control over the LA coordination/insertion during the ROP.[38]

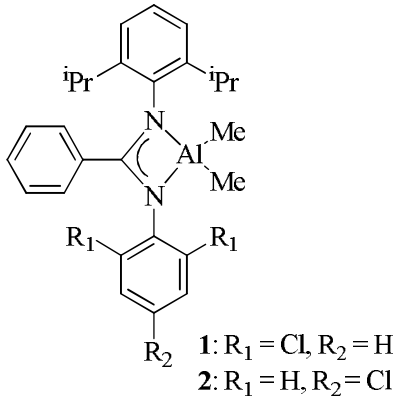


**Figure 1.32**: Amidinate aluminium complexes with a non-symmetrical ligand[38]

Changes to the substituents on one of the *N*-phenyl rings, has an effect on the activity of the polymerisation. For example, complex **1** shown in Figure 1.32, where chloro groups are present at both *ortho* positions, gives high activity with 94 % conversion to PLA achieved after 12 hours. However, if electron withdrawing groups are present at the *para* position on the *N*-phenyl ring (**2** in Figure 1.32), a decrease in activity is observed with a 75 % conversion to PLA after 72 hours.[38]

Investigations into the mechanism of the complexes in Figure 1.32 for the ROP of *rac*-LA showed that when the polymerisations were carried out using isopropanol or benzyl alcohol, the active initiator was generated *in situ*. On close inspection, it was observed that the initiation was occurring *via* the alkyl elimination of $Me_2Al(O^iPr)$ or $MeAl(O^iPr)_2$ or $Al(O^iPr)_3$ highlighting the instability of the metal complexes.[38] The polymerisations were therefore carried out without the addition of an alcohol, *i.e*. using the complexes as single component initiators. Studies into the mechanism of these polymerisations ruled out the generation of free radicals, but reported that the reactions were occurring by either monomer insertion into a Al-N or Al-Me bond.[38]

Unlike those complexes in Figure 1.32, Gibson *et al.* have reported that for *bis*(phenoxy)-amine aluminium complexes in the presence of electron withdrawing chloro groups, did not significantly affect the rate of LA polymerisation. However, Gibson and Phomphrai have reported that there is a dramatic change in rate observed for such compounds when the steric bulk around the metal is altered.[39, 40]

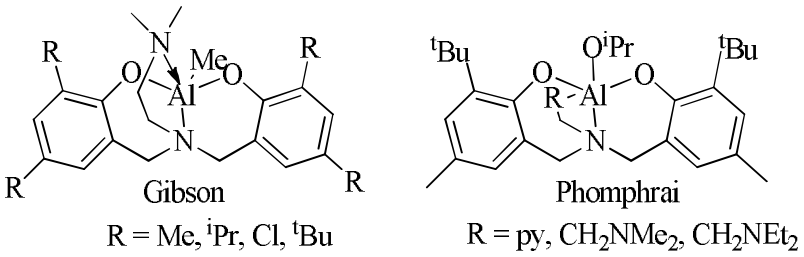


**Figure 1.33**: *Bis*(phenoxy)amine aluminium complexes isolated by Gibson and Phomphrai[39, 40]

Gibson observed that when the R groups on the phenoxy ring are changed from $^{i}$Pr to $^{t}$Bu, there is a dramatic decrease in rate indicative that an increase in size of the R group causes an almost prohibitive barrier to monomer binding and/or ring opening. When R = Me and there is less steric bulk on the ligand, high stereoselectivity is observed with isotactically enriched PLA produced.[39] Unlike Gibson, who observed changes in rate with changes to the phenoxy ring, Phomphrai reported changes in activity when the R group on the nitrogen centre is altered. After 16 hours, no product was observed in the polymerisation of *rac*-LA when the bulkier groups are attached (R = $CH_2NMe_2$ or $CH_2NEt_2$). However, when R = pyridine, the polymerisation with 50:1 of [LA]:[Al] achieved a 92 % conversion after 16 hours to yield PLA with enhanced isotactic bias and a $M_n$ = 6,900 gmol$^{-1}$.[40]

### 1.3.3 Group (IV) initiators

Although heteroleptic group (IV) initiators are more common, a few examples of homoleptic group (IV) initiators have been reported, for example the use of Ti($O^{i}Pr$)$_4$ and Zr($O^{i}Pr$)$_4$ for the ROP of *L*-LA.[41, 42]

Heteroleptic group (IV) complexes containing different ancillary ligands have been reported to produce well-defined alkoxide complexes depending on the steric bulk of such ligands. The rate of polymerisation can be controlled by the type of ancillary ligand, with the general order being: diamine *bis*(phenolates) > bulky alcohol/phenol clusters > Salens > titanatranes > tellurium *bis*(phenolates) > amine *bis*(phenolates) > amine *tris*(phenolates).[12] Pertinent to this study is the use of Salens, amine *bis*(phenolates) and *tris*(phenolates), however this chapter will report work of initiators containing various ancillary ligands. In general the titanium complexes are the most investigated, however zirconium and hafnium analogues can display greater activity and sterocontrol with the same ligands.[12]

Nakamura, Harada and co-workers have reported the preparation of tellurium *bis*(phenolates), as well as other chalcogen-bridged *bis*(phenolates) for the preparation of monomeric and dimeric titanium complexes (Figure 1.34).[43-45]

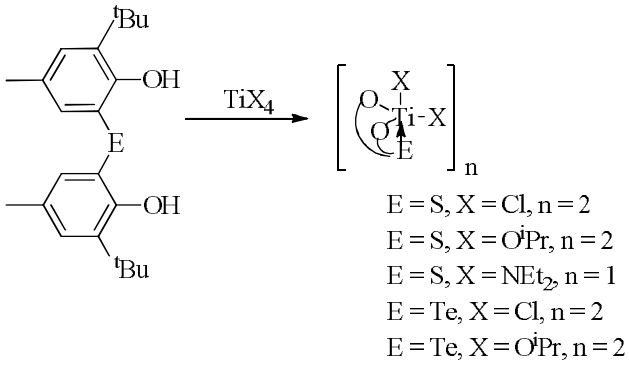


**Figure 1.34**: Monomeric and dimeric titanium complexes[43-45]

The compounds in Figure 1.34 were prepared to investigate the effect of monomeric and dimeric titanium complexes in the ROP of *rac*-LA.[43-45] The complexes isolated contain either sulphur or tellurium chalcogen-bridged biphenolate ligands. Results indicated that the dimeric tellurium complex where X = Cl gave the best results when carried out in anisole or dioxane at 100 °C with a [LA]:[Ti] ratio of 200: 1. For example, when the ROP of *L*-LA was carried out in anisole, 84 % yield was achieved after 32 hours, producing PLA with a $M_n$ of 24,200 $gmol^{-1}$ and a PDI of 1.08.[45] Narrow molecular weight distributions reported for the ROP of *L*-LA in anisole indicates that no backbiting is occurring, with the $M_n$ value increasing proportionally with the monomer conversion.[45]

Similar five-coordinate titanium complexes containing atrane-type ligands were trialled for the ROP of *rac*-LA, and were shown to be active both in solution and under more industrially preferred melt conditions.[46]

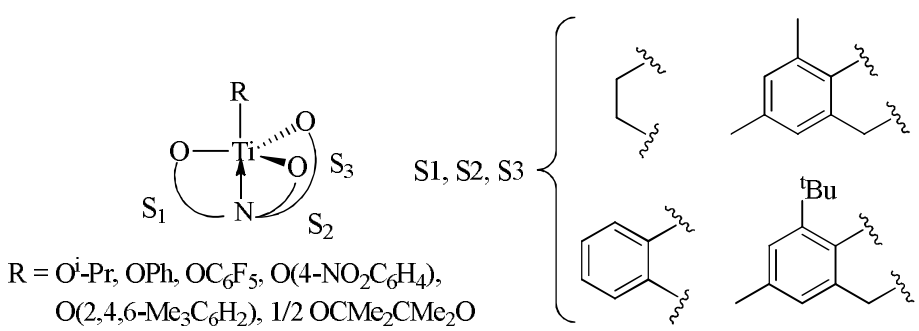


**Figure 1.35**: Five-coordinate titanium complexes containing atrane-type ligands[46]

As the number of five-membered rings in the tetradentate ligand increases, the bulk polymerisation activity and PDI also increase (1.42 – 1.97).[46] This was seen to be attributed to transesterification during propagation which led to bimodal type molecular weight distributions.[46] Developed from this work the same group utilised the compounds in Figure 1.35, and also reported the use of $TiCl_x(O^iPr)_{4-x}$ type initiators for the ROP of *rac*-LA.[47] It was thought that utilising alkoxy titanatranes would be effective for the ROP of *rac*-LA due to their possession of a transannular Ti-N bond that could potentially labilize the *trans* axial OR group. This in turn facilitates dissociation of the initiating alkoxide group allowing it to function as an end group, and therefore control the molecular weight.[47] It was shown that under solvent free conditions, as x increases in $TiCl_x(O^iPr)_{4-x}$ there was a general increase in molecular weight of the polymeric material and a decrease in the polydispersity.[47] This decrease in polydispersity indices as the number of chlorine atoms increases was also observed in solution, suggesting that a greater degree of control during the polymerisation is achieved.[48] This greater control could be attributed to the chlorotitanium alkoxides permitting only one $O^iPr$ group to dissociate. In this case PLA with a heterotactic bias was observed.[47, 48]

Further research in this area investigated the dependence of a controlled polymerisation reaction on the number of titanium metal centres in the initiator. They screened tetranuclear, trinuclear and dinuclear titanium alkoxide complexes in the ROP of LA and comparing results to those from $TiCl_x(O^iPr)_{4-x}$.[48]

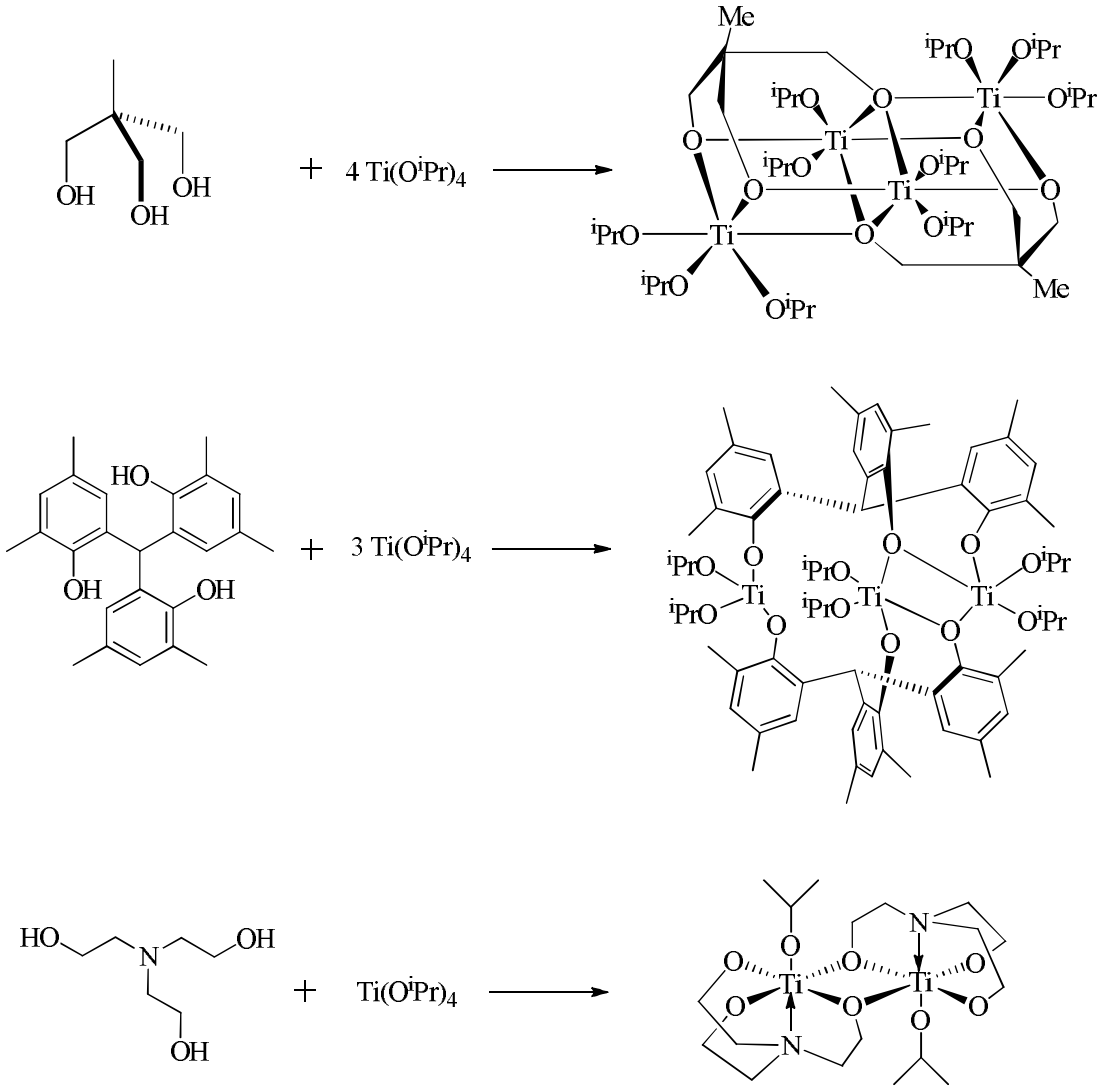


**Figure 1.36**: Synthesis of tetranuclear, trinuclear and dinuclear titanium alkoxide complexes[48]

Although all of the complexes were mainly tested for the ROP of *L*-LA, the tetranuclear and trinuclear compounds (Figure 1.36), were tested in the ROP of *rac*-LA in toluene at 70 °C. The tetranuclear compound produced 75 % yield of PLA in 24 hours, and it was shown that the polymerisation occurs in a well-controlled manner. It was also suggested that for the tetranuclear compound produced, all isopropoxide groups could be active in the initiation step. This is evident from a linear correlation of $M_w$ and PDI against [LA]/[Ti], which shows a high y intercept related to a slow initiation step during the polymerisation.[48] The tetranuclear titanium alkoxide complex: $(MeC(CH_2\text{-}\mu_3\text{-}O)(CH_2\text{-}\mu\text{-}O)_2)_2Ti_4(O^iPr)_{10}$ is another example of an initiator containing more than one metal centre, and has been investigated for the ROP of *rac*-LA under both solution and solvent-free conditions.[49] It was thought that the tetranuclear titanium compound would be

highly active for the polymerisation due to the presence of ten isopropoxide groups, one or more of which could act as an initiator for the production of *iso*-propoxy-terminated PLA.[49] A further reason for such a complex to be successful in the ROP of *rac*-LA is due to it being readily soluble in toluene and exhibiting stability both in the solid state and in toluene at ambient temperatures over an extended period of time.

Under industrially preferred melt conditions, the tetranuclear titanium alkoxide complex achieves 100 % conversion to PLA after 30 minutes, although with a certain degree of transesterification due to high polydispersity values recorded (up to 2.33 for *L*-LA). This was indicative of decomposition of the initiator.[49] In an attempt to prevent decomposition, the polymerisation was repeated in solution at room temperature resulting in a more controlled reaction but at the expense of high yield and molecular weight due to solubility of the monomer and polymer at lower temperatures. A plot of $M_n$ and PDI as a function of [LA]/[Ti] in solution at 70 °C again indicated that all isopropoxide groups could be active in the initiation step due to the linearity of the slope. Furthermore, the high *y* intercept observed for both graphs can be attributed to intramolecular transesterification reactions taking place.[49]

Neutral titanium (IV) dialkoxide complexes and zirconium (IV) dichloride complexes have been synthesised and tested in the ROP of *rac*-LA(Figure 1.37).[50]

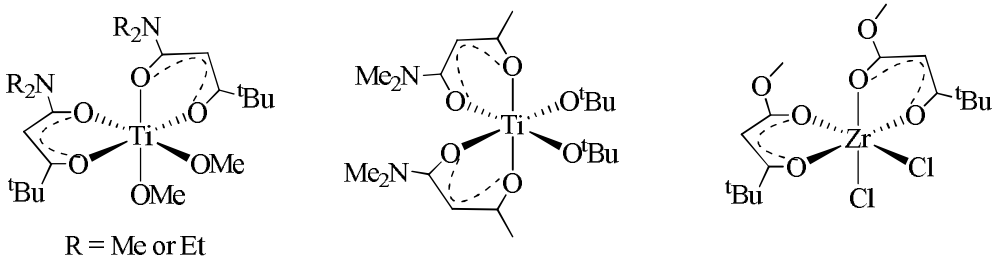


**Figure 1.37**: Titanium (IV) dialkoxide complexes and zirconium (IV) dichloride complexes[50]

The zirconium dichloride complex shown in Figure 1.37, displays higher activity than the titanium (IV) dialkoxide complexes, achieving 72 % conversion to PLA after 12 hours under solvent-free conditions compared with 13 – 64 % for the titanium (IV) dialkoxides.[50] This highlights the need for more research into zirconium and hafnium complexes for the ROP of *rac*-LA. Investigation into the polymerisation revealed that there is not a linear correlation between $M_w$ and PDI

*vs* time, indicating that the polymerisation does not proceed in a living manner, but is entropically driven as the polymer chain breaks down during the polymerisation and does not grow further.[50]

Titanium Salen initiators have been synthesised (Figure 1.38) and trialled for the ROP of *rac*-LA, and compared to analogous aluminium complexes containing tetradentate Salen ligands, which have shown to facilitate the ROP of LA at elevated temperatures.[51] It was reported that the polymerisation rate, tacticity and molecular weight control was dependant on the diimine backbone.[51]

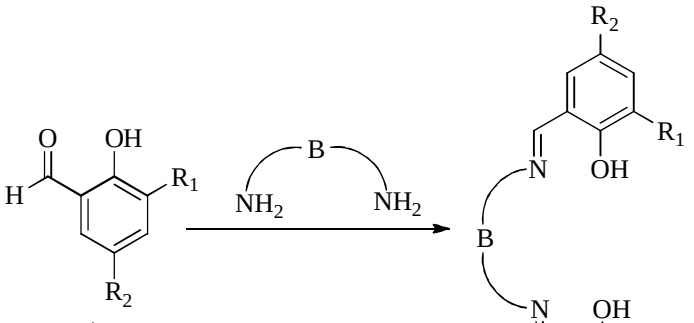


**1:** $R_1 = {}^tBu$, $R_2$ = OMe, B=$CH_2CH_2$
**2:** $R_1 = {}^tBu$, $R_2$ = H, B=$CH_2CH_2$
**3:** $R_1 = {}^tBu$, $R_2 = {}^tBu$, B=$CH_2CH_2$
**4:** $R_1 = {}^tBu$, $R_2$ = I, B=$CH_2CH_2$
**5:** $R_1 = {}^tBu$, $R_2$ = Cl, B=$CH_2CH_2$
**6:** $R_1 = {}^tBu$, $R_2 = {}^tBu$, B=(*R*,*R*)-cyclohexyl

**Figure 1.38**: Ligands used to prepare titanium Salen complexes for the ROP of *rac*-LA[51]

Symmetric tetradentate ligands such as those shown in Figure 1.38, can wrap around octahedral metal centres in three geometries designated as *mer-mer* (*trans*), *fac-fac* (*α-cis*) or *fac-mer* (*β-cis*) as shown in Figure 1.39, where X is a labile group.[52, 53] For the complexes prepared using the ligands in Figure 1.38, X is an isopropoxide group.[51]

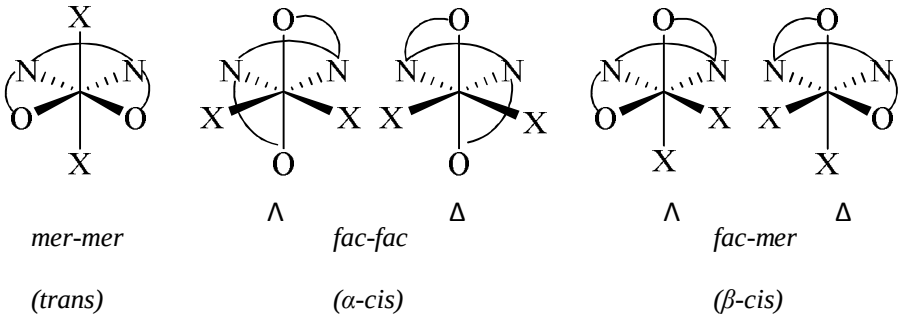


**Figure 1.39**: Possible geometries for tetradentate ligands around octahedral metal centres[53]

From analysis of the titanium structures containing the ligands in Figure 1.38, it was reported that when B = $CH_2CH_2$, the complexes adopt a *trans*-planar geometry which is in contrast to when B = (*R*,*R*)-cyclohexyl which instead adopts a *β-cis* geometry in solution.[51] This geometry is significant for the ROP of *rac*-LA as the initiator containing the (*R*,*R*)-cyclohexyl ring was shown to be the least active presumably due to the configuration of the complex. The polymerisation of *rac*-LA in solution proceeded in a well-controlled manner with GPC analysis of the $M_n$ indicating that for all initiators only one PLA chain propagates from each titanium centre. This is presumably due to the steric control around the metal centre by the presence of bulky *ortho* tert-butyl groups on the Salen phenoxy units.[51] Kinetic studies indicated that increased rates of propagation for the initiators in Figure 1.38 are observed in comparison to Al(Salen) systems.[51] For example, initiator **3** in Figure 1.38 is reported to give a $k_{app}$ = 2.59 × $10^{-5}$ $s^{-1}$ which is an order of magnitude faster than the corresponding aluminium Salen complex ($k_{app}$ = 0.13 × $10^{-5}$ $s^{-1}$).[51] Variation in the substituents on the phenoxy rings has been shown to have an effect on the polymerisation such that when $R_1$ and $R_2$ are electron donating OMe groups the initiator shows the most activity. However, when $R_2$ is electron withdrawing *i.e.* I or Cl, there is a reduction in the rate of polymerisation. This is in stark contrast to the results reported for Al(Salen) complexes which showed enhanced activities when halides were present at the *para* position of the phenoxy ring.[51]

Chiral Schiff base ligands (Figure 1.40) complexed to group (IV) alkoxides could be utilised for the ROP of *rac*-LA.[54]

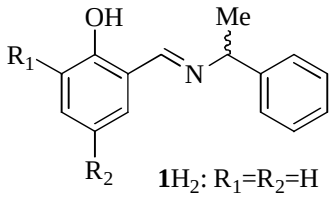


**1**$H_2$: $R_1$=$R_2$=H
**2**$H_2$: $R_1$=H, $R_2$=OMe
**3**$H_2$: $R_1$=H, $R_2$=Me
**4**$H_2$: $R_1$=$R_2$=Cl

**Figure 1.40**: Schiff base ligands complexed to Ti(IV) and Zr(IV) alkoxides reported by Davidson *et al.*.[54]

The solid-state structure of ligand **4**$H_2$ in Figure 1.40 with *R* configuration is determined by an intramolecular OH•••••N hydrogen bond shown in Figure 1.41.[54]

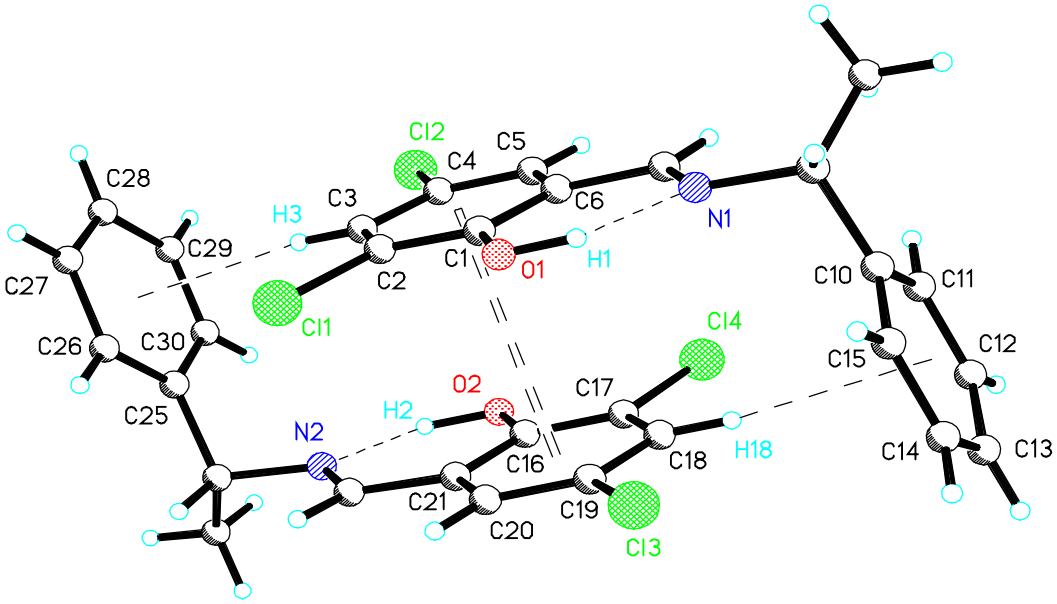


**Figure 1.41**: X-ray crystal structure of Schiff base ligand used by Davidson *et al.* with Ti(IV) and Zr(IV).[54]

The metal complexes are all six-coordinate pseudo octahedral, and the polymerisation in solution indicated that the titanium complexes were all inactive. Good activity was observed for the zirconium complexes in toluene at both 20 °C and 80 °C to produce PLA with a heterotactic bias.[54] Analysis of the polymeric material by MALDI-ToF mass spectrometry revealed that intermolecular transesterification was occurring. When the polymerisation was repeated under solvent-free conditions both the titanium and zirconium initiators were active showing good polymerisation control but again no selectivity for titanium. In comparison to the polymeric material produced in solution, the zirconium initiators offered less control under melt conditions.[54]

*Bis*(aniline-phenolate) group (IV) complexes reported by Kol *et al.* have been shown to be highly active for the ROP of *rac*-LA – Figure 1.42. The complexes all adopt similar geometies to that see in Salan type complexes with *cis*-N/*trans*-O binding of the ligand.[55]

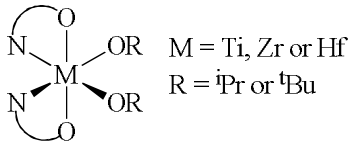


**Figure 1.42**: *Bis*(aniline-phenolate) group (IV) complexes showing *trans*-O and *cis*-N[55]

The complexes shown in Figure 1.42 were used for the polymerisation of *rac*-LA at 130 °C under solvent-free conditions, resulting in PLA with molecular weights half that of expected suggesting two growing polymer chains on each metal centre. From analysis of the $^{1}$H homonuclear decoupled NMR spectrum all catalysts showed stereoselectivity towards heterotactic PLA, with higher heteroselectivity observed with zirconium and hafnium than titanium. Further enhancement of stereoselectivity was observed when the temperature was lowered from 130 °C to 75 °C.[55] A further example of tetradentate *bis*(phenolate) ligands complexed to a group (IV) metal was reported by Okuda, who synthesised a titanium complex containing analogous ligands to that complexed to aluminium in Figure 1.31.[56] The titanium complex was shown to achieve 96 % conversion to produce PLA with a $M_n$ = 14,000 gmol$^{-1}$ after 72 hours in a controlled manner (PDI = 1.16), resulting in a polymer with $P_r$ = 0.4.[56]

Another set of tetradentate *bis*(phenolate) ligands complexed to not only Ti(IV), but also zirconium and hafnium for the ROP of *rac*-LA, is tetradentate amine *bis*(phenolates) exhibiting ONNO coordination – Figure 1.43. These ligands fall into two categories with their complexes either displaying $C_2$ or $C_s$ symmetry.[57]

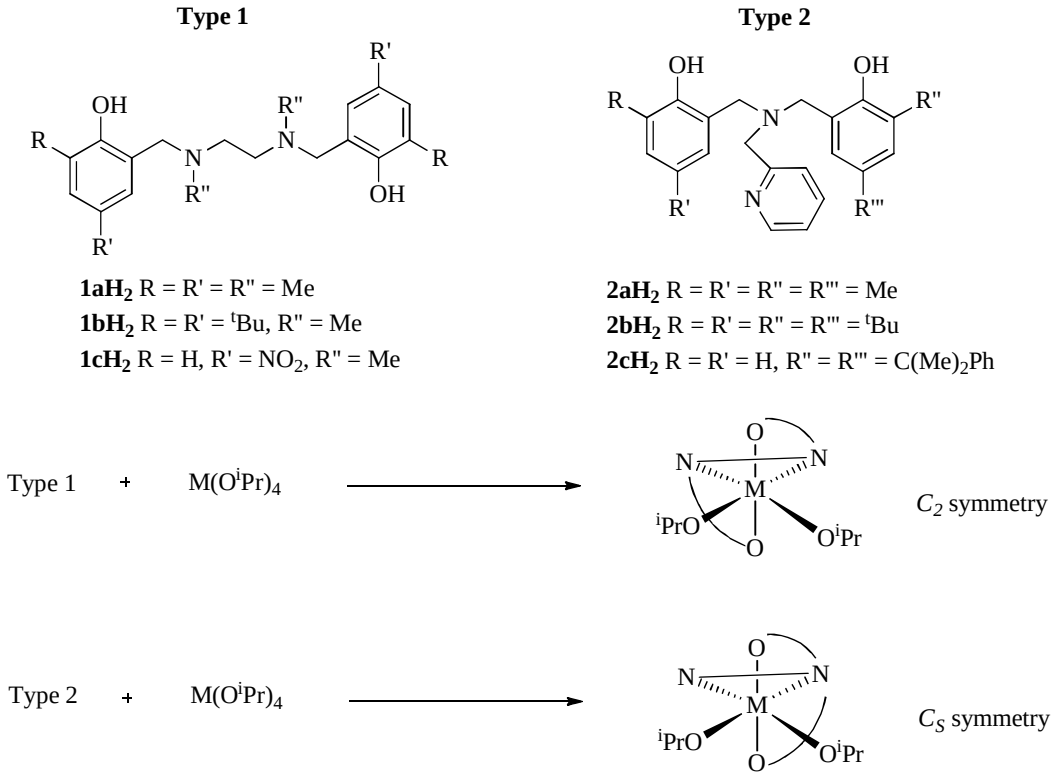


**Figure 1.43**: Tetradentate amine *bis*(phenolate) ligands and their structural motifs[57]

It was shown that although the Ti(IV) complexes were inactive in solution, they exhibited activity under solvent-free conditions producing atactic PLA in moderate yield after two hours. In contrast, it was seen that the Zr(IV) and Hf(IV) complexes led to the production of isotactically enriched PLA under both solvent-free and solution conditions, when less bulky ligands were complexed. It was reported that the ligands of Type 1 form pseudo $C_2$-symmetric chiral complexes ($\Delta$ or $\Lambda$) with octahedral Zr(IV) centres, whereas Type 2 ligands form nonchiral complexes with $C_s$ symmetry. It was hypothesised that this could explain why complexes exhibiting Type 1 ligands show greater stereocontrol than those containing Type 2 ligands. The difference in the group (IV) metals giving different stereoselectivity was reported to be caused by the ability of zirconium and hafnium to achieve greater chelation of the growing polymer than titanium complexes, favouring approach of (*R*,*R*)-LA or (*S*,*S*)-LA.[57]

An analogous symmetric amine-pyridine-*bis*(phenolate) ligand to Type 2 in Figure 1.43 was recently reported for the preparation of a homoleptic zirconium complex.[58] This group also reported the use of the same ligand (Figure 1.44) for

the preparation of enantiomeric dinuclear zirconium and hafnium complexes containing two homochiral nitrogen atoms.[58]

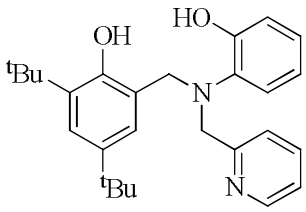


**Figure 1.44**: Amine-pyridine *bis*(phenolate) ligand that can be complexed to zirconium and hafnium[58]

When the ligand in Figure 1.44 is complexed to zirconium and hafnium, to produce dinuclear complexes, the N atom of the tertiary amine in the ligand becomes a chiral centre.[58] This is due to the restriction on the conformation of inversion of the unsymmetric tertiary amine when it is complexed to the metal centre, resulting in the dinuclear complexes possessing two chiral N atoms. It was possible to characterise all four possible enantiomers {Zr/Hf N(*R*),N(*R*) and Zr/Hf N(*S*),N(*S*)} by single crystal X-ray analysis, all of which were tested for the ROP of *rac*-LA.[58] Interestingly, when the racemic dinuclear complexes of zirconium and hafnium were utilised for the ROP of *rac*-LA in toluene at 130 °C isotactically enriched PLA was produced which was gave $P_r$ values in the range of 0.35 – 0.28 which are higher than those reported by Davidson *et al.* for the mononuclear zirconium and hafnium complexes containing the analogous Type 2 ligand in Figure 1.42 ($P_r$ = 0.5 – 0.4).[57, 58]

Ligands with $C_2$ symmetry, displaying {OSSO} coordination were reported by Kol *et al.* – Figure 1.45.[52]

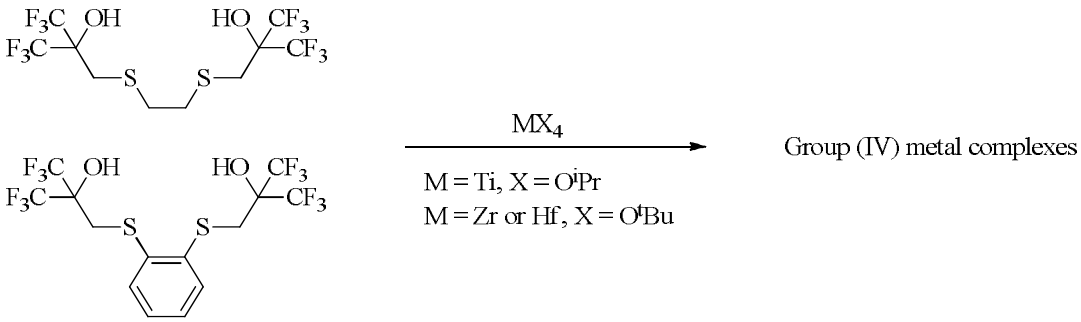


**Figure 1.45**: Preparation of group (IV) {OSSO}-type dithiodidate complexes[52]

Single crystal X-ray analysis of one of the titanium complexes prepared shows the complexes are mononuclear with octahedral geometry around the metal centre with the ligand binding in a *fac-fac* mode (*α-cis*). This is in contrast to the complexes containing the ligands shown in Figure 1.38 which demonstrated both *mer-mer* (trans) and *fac-mer* (*β-cis*) geometry.[52]

The initiators were tested for the ROP of *rac*-LA under both solvent-free conditions and in toluene at 75 °C. The stereoselectivity and activity did not alter greatly when the nature of the bridge between the two sulphur atoms changes, whereas stereoselectivity and activity were dependant on the choice of metal centre.[52] Results indicated that Ti(IV) gave the lowest activities and produced atactic PLA. However when the metal was zirconium or hafnium, higher activities were seen as well as a tendency towards PLA with a heterotactic bias ($P_r$ = 0.7). This heterotacticity could be further increased ($P_r$ = 0.89) by lowering the temperature of the polymerisation in toluene.[52]

Davidson *et al.* further developed the use of Group (IV) metals for the ROP of *rac*-LA reporting the production of heterotactic PLA under solvent-free conditions using a zirconium or hafnium complex containing an amine *tris*(phenolate) ligand (Figure 1.46).[59]

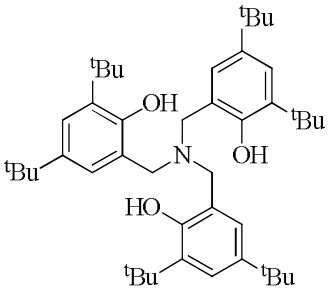


**Figure 1.46**: Bulky amine *tris*(phenolate) ligand developed by Davidson *et al.*[59]

The initiators were originally developed by Kol *et al.* who reported the use of such compounds for the ROP of *L*-LA.[60] Results indicated that the zirconium analogues demonstrated a 10 fold higher activity than the corresponding titanium complexes.[60] Such compounds contain a bulky amine *tris*(phenolate) ligand (Figure 1.46) which were isolated as five-coordinate monomeric species with a $C_3$-symmetric propeller-like arrangement of the ligand around the metal.[59, 60] The titanium analogue of the complex gave atactic PLA under solvent-free conditions

using a [LA]:[initiator] ratio of 300: 1 to yield PLA with a $M_n$ = 37,100 gmol$^{-1}$ in a 50 % yield after 30 minutes. Under the same conditions, the hafnium initiator produced PLA in a 95 % yield after 30 minutes yielding a polymeric product with a $M_n$ = 71,150 gmol$^{-1}$. The zirconium initiator however, showed higher activity producing 78 % yield of PLA after 6 minutes with a $M_n$ = 32,300 gmol$^{-1}$ and a PDI = 1.22. Under solvent free conditions both the zirconium and hafnium initiators carried out the ROP of *rac*-LA with a high level of stereocontrol yielding heterotactic PLA with $P_r$ values of 0.96 for Zr and 0.88 for Hf.[59] The mechanism accounting for the heteroselectivity when the metal is zirconium or hafnium is thought to be from either inversion of axial chirality during chain propagation which leads to the stereochemistry at the metal centre alternating or a chain-end control mechanism based on the steric bulk of the ligand.[59]

Pseudo $C_3$-symmetric *tris*(sulphonamide) amide ligands analogous to $C_3$-symmetric amine (*tris*)phenolate ligands, have been synthesised by Mountford *et al.* bearing $NSO_2Me$ donors which are sterically less encumbering to help improve the activity.[61]

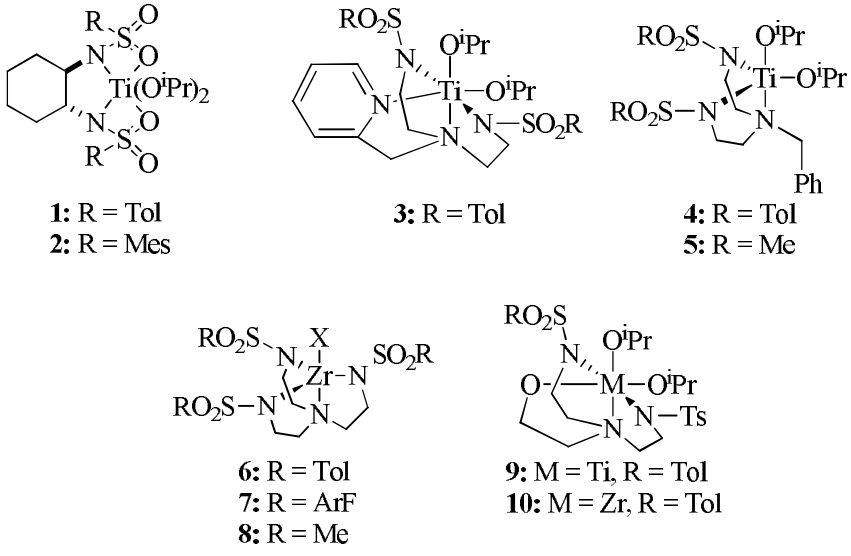


**Figure 1.47**: *Tris*(sulphonamide) amide ligands complexed to group (IV) metals[61]

Figure 1.47 shows a series of four, five and six coordinate initiators all of which were used for the ROP of *rac*-LA. The titanium *bis*(isopropoxide) complexes all produced atactic PLA. Furthermore, analysis of all polymers by MALDI-ToF mass spectrometry showed the presence of isopropoxide chain ends but with peak

envelopes separated by m/z values of 72 $gmol^{-1}$ which corresponds to half of a LA unit indicative of extensive transesterification.[61] The zirconium initiators shown in Figure 1.47 carried out the ROP of *rac*-LA in toluene at 70 °C using a 100: 1 ratio of [LA]: [initiator]. The polymerisations proceeded very slowly achieving 66 - 84 % conversion after 61 – 66 hours,[61] which is in contrast to that reported by Davidson *et al.* who showed higher activity for zirconium initiators than titanium equivalents using $C_3$-symmetric amine *tris*(phenolate) ligands for the ROP of *rac*-LA.[59, 60] Analogous to titanium, all zirconium complexes containing the ligands in Figure 1.45 produced atactic PLA and analysis of the MALDI-ToF spectra showed extensive transesterification was occurring.[61] The polymerisations with zirconium initiators gave PLA with extremely narrow polydispersities and good agreement between experimental and predicted molecular weights. A plot of $M_n$ *vs* percentage conversion gave gradients in the range of 144(2) – 159(4) $gmol^{-1}$ (% conversion)$^{-1}$ which is in agreement with that expected {144.1 $gmol^{-1}$ (% conversion)$^{-1}$} for one poly(*rac*-LA) chain growing per metal centre.[61]

Mountford *et al.* utilised a similar zirconium initiator to that of structures **9** and **10** in Figure 1.47 to polymerise *rac*-LA. It was reported that the zirconium complex produced atactic PLA in toluene at 100 °C, and under solvent-free conditions at 130 °C.[62] When the polymerisation is carried out in solution, a plot of $M_n$ *vs* conversion indicates that two *rac*-LA chains are growing per metal centre, however, when the reaction is carried out under solvent-free conditions, the gradient of the plot is indicative of only one polymer chain growing per metal centre.[62]

Another example of using group (IV) trisphenolate ligands for the ROP of *rac*-LA utilises dimeric titanium (IV) alkoxide complexes of trisphenols – Figure 1.48.[63]

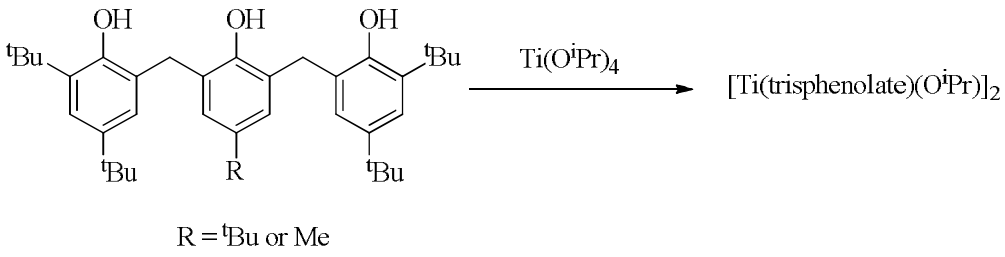


**Figure 1.48**: Dimeric titanium(IV) alkoxide complexes of trisphenols[63]

The ligands shown in Figure 1.48 adopt a chiral conformation when complexed to titanium and therefore could potentially produce isotactic stereoselectivity *via* enantiomorphic site control, if the chirality at the metal centre was preserved in the ROP of *rac*-LA. For both isolated initiators, the polymerisation reaction proceeds in a well-controlled manner in $CH_2Cl_2$ at 80 °C using a 100:1 ratio of [LA]: [initiator], to achieve > 90 % conversion after 12 hours when R = $^t$Bu, and 89 % conversion after 6 hours when R = Me.[63] Analysis of the PLA product showed heterotactic enrichment and although changes in temperature and choice of solvent had an effect on the reaction rate, very little effect was seen in the stereoregularity of the product. This bias towards heterotactic addition and not isotactic enrichment as previously predicted suggests that if the chirality at the titanium centre is retained during the reaction, it does not provide sufficient enantiomorphic site control.[63] When the reaction time is increased to 72 hours for the polymerisation reaction with R = $^t$Bu, analysis of the product *via* GPC shows the presence of a bimodal molecular weight distribution and an increase in the polydispersity indicating the presence of intermolecular chain transfer, which was not evident during the early stages of the ROP. The difference observed between the two initiators isolated is that when R = $^t$Bu the polymerisation requires a slight induction period which is not necessary when R = Me. It was reported that such a difference could be due to the steric size of the *para* substituent on the central ring, and that any isomerisation or reorganisation before initiation of the ROP must be more facile for the smaller *para*-methyl derivative than the *para-tert*-butyl derivative.[63]

The preparation of group (IV) benzofuranoxides has recently been reported for the ROP of *rac*-LA, in particular titanium complexes - Figure 1.49.[64]

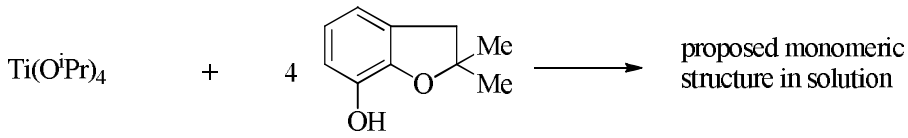


**Figure 1.49**: Synthesis of titanium 7-benzofuranoxide for the ROP of *rac*-LA[64]

The titanium monomeric initiator has been shown to produce PLA with a preference for heterotactic addition.[64] The advantage of such an initiator is that it is relatively stable in air, as no change was observed in the $^{1}$H NMR spectrum after four weeks of exposure of the complex to the atmosphere.[64]

Although many group (IV) initiators have been reported to be successful for the ROP of *rac*-LA, with some examples exhibiting isotactic stereocontrol (Okuda *et al.*)[56] or high activity (Davidson *et al.*)[59], there is still scope to develop an initiator that demonstrates both high activity and high isotactic stereocontrol. Development by Davidson *et al.* showed high activity for amine *tris*(phenolate) complexes (Figure 1.46)[59] but obtained heterotactic PLA, and therefore it is of interest to develop such a ligand system that will maintain the high activity but achieve isotactic PLA. Another set of ligands of interest are the Type 1 ligands shown in Figure 1.43 which showed isotactic enrichment in the production of PLA. Further work to develop such group (IV) complexes to achieve higher isotacticity and high activity will be reported.

### 1.3.4 Recent Developments in group (III) and Lanthanide Complexes

It has been reported that some ligand sets can be used in the complexation to both group (III) metals and lanthanides to produce complexes for the ROP of *rac*-LA. An example of such is the chiral biaryl-based NNO-donor ligands, Figure 1.50.[65]

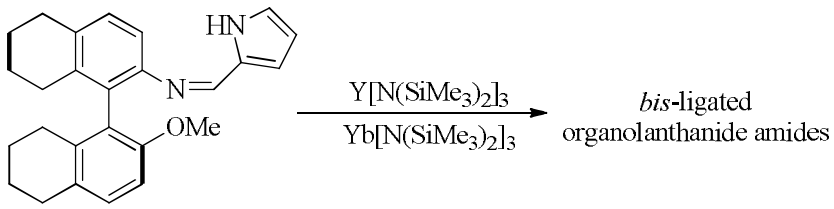


**Figure 1.50**: Preparation of *bis*-ligated organolanthanide amides[65]

Such lanthanide complexes were reported to be active for the polymerisation of *rac*-LA in solution at room temperature affording high conversion to PLA after just one hour.[65] Higher conversion of the LA was observed when THF was used

as the solvent (100 %), compared with toluene (67 %) when the same catalyst was used. Narrow polydispersities were observed (1.23 – 1.29) and PLA with a slight isotactic bias was produced.[65]

Further use of lanthanides as metal initiators for the ROP of *rac*-LA was investigated using a series of *bis*(thiophosphinic amido) yttrium complexes (Figure 1.51), which exhibit high rates and enhanced stereocontrol in the reaction.[66]

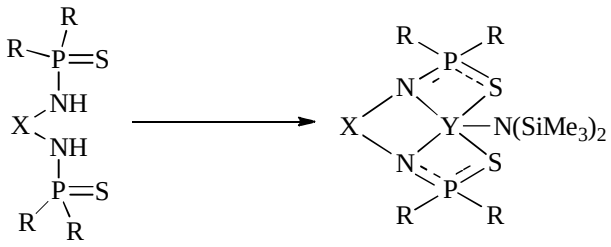


X = 2,2-dimethylpropylene, ethylene or *trans*-1.2-cyclohexylene
R = iso-propyl, phenyl or ethoxy

**Figure 1.51**: *bis*(thiophosphinic amindo) yttrium complexes isolated for the ROP of *rac*-LA[66]

Due to the difficult handling of yttrium initiators, the polymerisation of *rac*-LA using the complexes isolated in Figure 1.51 were performed *in situ*. All initiators were active for the ROP of *rac*-LA in $CH_2Cl_2$ at 298 K, with the rate affected by the R group, such that *iso*-propyl ($k_{app}$ = 7.82 – 10.70 × $10^{-3}$ $s^{-1}$) > phenyl ($k_{app}$ = 0.83 – 1.95 × $10^{-3}$ $s^{-1}$) > ethoxy ($k_{app}$ = 0.078 – 0.36 × $10^{-3}$ $s^{-1}$).[66] This was reported to be due to differences in electronics given that the difference in steric hindrance between a phenyl and *iso*-propyl group would not account for such differences observed in the rates.[66] Good polymerisation control was observed with all initiators from a linear fit of $M_n$ *vs* percentage conversion and good correlation between the degree of polymerisation observed and that predicted. Transesterification was evident from high polydispersity indices and a repeat unit of 72 $gmol^{-1}$ seen in the MALDI-ToF spectra corresponding to half a lactide molecule.[66] When R = iso-propyl or phenyl atactic PLA was produced, however when R = ethoxy, PLA with a heterotactic bias ($P_r$ = 0.68 and 0.79) was produced. The stereocontrol was seen to decrease when the reaction was carried out in THF compared to dichloromethane.[66]

The same group also reported the synthesis of yttrium *bis*(phosphinic) diamido complexes for the ROP of *rac*-LA.[67] Such complexes displayed a similar structure to those shown in Figure 1.51, where the labile group was not limited to $N(SiMe_2H)_2$, but alkoxide and aryloxide complexes were also reported.[67] The alkoxide complexes were all reported to be dimeric in both the solution and solid-state. The amide complexes however were shown to be dimeric in solution and in the solid-state when the phosphorus substituents were iso-propyl. However, upon increasing the steric hindrance of the phosphorus substituents to a $^{t}$Bu group, a monomeric yttrium complex is observed.[67] Although all yttrium *bis*(phosphinic) diamido complexes were active for the ROP of *rac*-LA, the mononuclear complex displayed the most stereocontrol producing PLA with a heterotactic bias ($P_r$ = 0.85) in THF at room temperature with a monomer to initiator ratio of 200: 1. However, all other complexes showed little stereocontrol producing PLA with $P_r$ = ~0.6 in THF at room temperature with a monomer to initiator ratio of either 200: 1 or 400:1.[67] The heteroselectivity observed in the mononuclear complex was reported to be due to a chain end control mechanism enhanced by solvent coordination at the active site.[67]

High activity and good polymerisation control demonstrated by the use of yttrium initiators was also reported using tridentate phosphide-diphosphine ligands, Figure 1.52.[68]

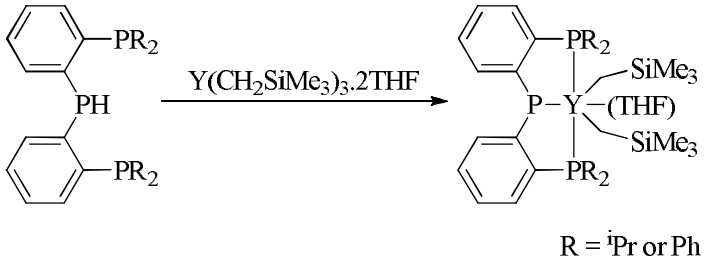


**Figure 1.52**: Phosphido-diphosphine pincer yttrium complexes[68]

It was reported that the yttrium complexes in Figure 1.52 produced PLA at room temperature in THF with a slightly heterotactic bias, $P_r$ = 0.64. Analogous complexes using scandium were synthesised, which showed lower activity and control than the yttrium equivalents for the ROP of LA. This is thought to be due to the bulky pincer ligand coordinating to a small metal centre hindering coordination and/or nucleophilic attack of the monomer.[68] The scandium

complexes also produced PLA with a slight heterotactic bias, albeit with slightly less stereocontrol ($P_r$ = 0.62). Higher polymerisation activities are observed when the reaction is carried out in toluene compared with THF, due to THF being a strongly coordinating solvent with a high affinity for the oxophilic catalytic centre seen with such group (III) metals. THF is therefore competing with the monomer in the coordination step during the polymerisation, reducing the polymerisation activity.[68] More recent developments by the same group have reported the use of the complexes in Figure 1.52 for the ROP of other cyclic esters for example $\varepsilon$-caprolactone, $\delta$-valerolactone and $\beta$-butyrolactone.[69]

A naphthoxy based ligand platform is thought to be an apt choice for the ROP of cyclic esters. This is due to the ability of such chelating ligands to accommodate metal centres with different ionic radii allowing a comparison of various metals centres to be carried out. Furthermore, the influence that hard *vs* soft donating heteroatoms and *ortho*-silyl groups have on the polymerisation can be studied. Examples of complexes containing naphthoxy based ligands was reported by Carpentier *et al.* who explored group (III) complexes supported by tridentate bis(*ortho*-silyl-substituted naphtholate)- donor ligands, Figure 1.53.[70]

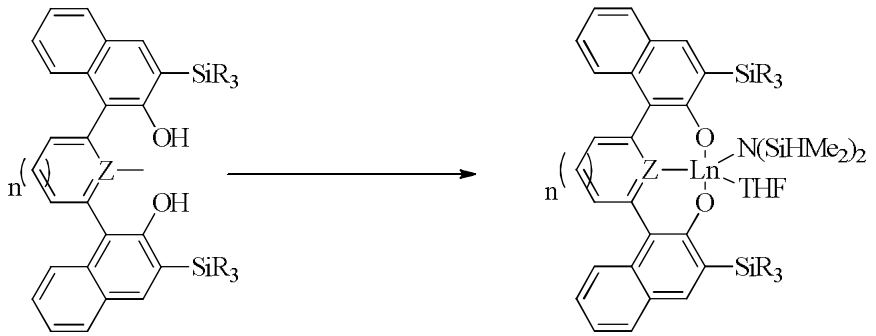


**{OZO$^R$}H$_2$**
Z = N, n = 1, $SiR_3$ = $SiPh_3$, $Si^tBuMe_2$
Z = S, n = 0, $SiR_3$ = $SiPh_3$

{ONO$SiPh_3$}Ln[$N(SiHMe_2)_2$](THF) Ln = Sc, Y, La
{ONO$Si^tBuMe_2$}Ln[$N(SiHMe_2)_2$](THF) Ln = Sc, Y, La
{OSO$SiPh_3$}Ln[$N(SiHMe_2)_2$](THF) Ln = Sc, Y, La

**Figure 1.53**: Tridentate bis(*ortho*-silyl-substituted naptholate)-donor ligands complexed to group (III) metals[70]

All complexes were active for the ROP of *rac*-LA at room temperature in toluene and THF with faster rates observed in toluene. This difference in rate is analogous to that observed for the initiators in Figure 1.52. For example when

{ONO$^{SiPh_3}$}Y[N(SiHMe$_2$)$_2$(THF) is used as the initiator, 100 % conversion to PLA was achieved after three minutes in toluene compared to only 71 % conversion to PLA after sixty minutes in THF.[70] Molecular weights for the polymers obtained were closely related to those calculated confirming the presence of one polymer chain per metal centre and overall the polymerisation was seen to exhibit a good degree of control with polydispersity values all under 2.[70]

Such initiators showed a varying degree of stereocontrol with the probability of racemic linkages ($P_r$) ranging from 0.5 to 0.93 demonstrating that atactic and heterotactic PLA could be produced.[70] The degree of stereocontrol can be influenced by many factors. For example, when the polymerisation is carried out in toluene atactic PLA is produced, however when the reaction is repeated in THF, heterotactic PLA is produced with a $P_r$ value of 0.93.[70] This indicates that the initiators shown in Figure 1.53 clearly exhibit a greater degree of stereocontrol than other tridentate group (III) initiators such as those in Figure 1.52. Other factors affecting the degree of tacticity are the choice of metal, the central linker in the framework and the *ortho*-silyl substituent, for example when the *ortho*-silyl substituent is $^t$Bu, the degree of stereocontol is altered such that the tacticity decreases with increasing ionic radius, i.e. $P_r$: Sc, 0.93; Y, 0.84; La, 0.50.[70] Interestingly when an O-SiPh$_3$ substituent is present on the naphtholate ring the initiators are also active for the ROP of *rac*-*β*-butyrolactone. The results indicating that, in contrast to the ROP of *rac*-LA, higher stereocontrol is achieved when the polymerisation is performed in toluene, compared to THF where $P_r$ = 0.5.[70]

A series of achiral lanthanide alkyl complexes bearing N,O multidentate ligands have been investigated as initiators for the ROP of *rac*-LA, more specifically mono(alkyl), bis(alkyl) and Salan complexes, Figure 1.54.[18]

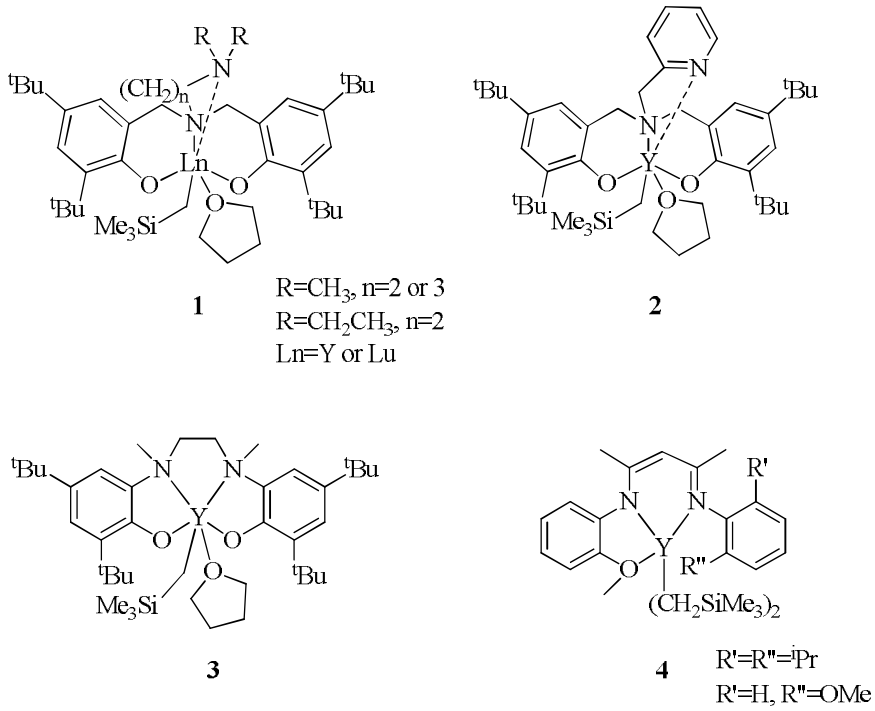


**Figure 1.54**: Series of achiral lanthanide alkyl complexes bearing N,O multidentate ligands[18]

For the mono(alkyl) complexes (**1** and **2** in Figure 1.54), almost complete conversion to PLA was achieved within one hour at room temperature with the exception of complex **1** where R = $CH_3$ and n = 3, which showed only trace conversion after six hours at room temperature, but a 70 % conversion was achieved after one hour at 70 °C.[18] The molecular weights of the PLA produced from such complexes correlated well with theoretical values and narrow PDI values were seen. With the noted exception, all complexes of **1** in Figure 1.54 produced PLA with modest activity but were highly selective producing heterotactic PLA with $P_r$ values over 0.94.[18]

The lanthanide Salan complex (**3** in Figure 1.54) unfortunately showed little selectivity in the production of PLA ($P_r$ = 0.65) which is in stark contrast to its aluminium counterpart which was reported to produce highly heterotactic PLA with a $P_r$ value of 0.96 (Figure 1.28).[18, 35] Investigation into the $\beta$-diiminate-ligated lanthanide *bis*(alkyl) complexes (**4** in Figure 1.54) for the ROP of *rac*-LA in THF at 20 °C, reported complete conversion to PLA after 30 minutes with molecular weights close to the theoretical values based on both metal alkyl species being active.[18] The *bis*(alkyl) complexes produced atactic PLA with a broad molecular weight distribution. It was also observed that for complexes

shown in Figure 1.54, there was a dependence on the solvent used in the polymerisation such that when the reactions were carried out in dichloromethane instead of THF, the conversion and stereoselectivity both reduced. When the reactions were attempted in toluene at room temperature, no conversion to PLA was observed, however at 70 °C in toluene the reaction was seen to be rapid, producing low molecular weight PLA with broad molecular weight distribution.[18]

Similar alkyl lanthanide complexes to those in Figure 1.54 were synthesised containing a piperazidine-bridged *bis*(phenolate) ligand (Figure 1.55) and trialled for the ROP of *rac*-LA.[71]

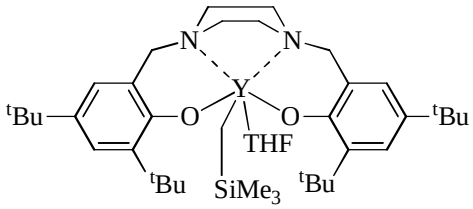


**Figure 1.55**: Yttrium alkyl complex supported by a piperazidine-bridged *bis*(phenolate) ligand[71]

In general for such complexes, it was reported that when the piperazidine ring adopts a chair conformation a bimetallic piperazidine-bridged *bis*(phenolate) lanthanide complex is isolated. However, when the piperazidine bridge adopts a boat conformation a mononuclear piperazidine-bridged *bis*(phenolate) lanthanide complex is observed.[71] In this case when a piperazidine bridged bis(phenol) was used to prepare a series of lanthanide alkyl complexes, only the mononuclear *bis*(phenolate) lanthanide mono(alkyl) complexes were isolated, Figure 1.55.[71] The yttrium complex shown in Figure 1.55 was trialled for the ROP of *rac*-LA and was reported to exhibit higher activity than that of the *N,N'* bridged *bis*(phenolate) yttrium alkyl complexes in Figure 1.54, polymerising 700 equivalents of *rac*-LA in two hours at 20 °C in THF achieving 100 % conversion to PLA with a $M_n$ = 63,000 gmol$^{-1}$ and a PDI = 1.61.[71] Unlike the mono(alkyl) yttrium complexes in Figure 1.54, the piperazidine yttrium complex showed no stereoselectivity producing atactic PLA.[18, 71]

A more recent example shown to have comparable stereocontrol and activity in the ROP of *rac*-LA as the yttrium alkyl complexes shown in Figure 1.54, was

reported using an amine bridged *bis*(phenolate) lanthanide aryloxide (Figure 1.56).[72]

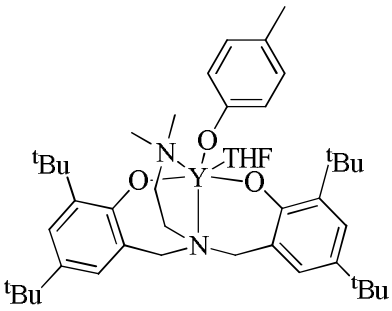


**Figure 1.56**: Amine bridged *bis*(phenolate) lanthanide aryloxide using for the ROP of *rac*-LA[72]

The complex shown in Figure 1.56 produced PLA in THF at room temperature, at various monomer to initiator ratios. Both the amine bridged *bis*(phenolate) yttrium aryloxide (Figure 1.56) and the amine bridged *bis*(phenolate) yttrium alkyl complex shown in Figure 1.54 (complex **1**), are able to polymerise 500 equivalents of *rac*-LA in one hour to produce heterotactic PLA: $P_r$ = 0.95 for aryloxide complex and $P_r$ = 0.94 for alkyl complex.[72] An improvement in activity from both the aryloxide and alkyl yttrium complexes is reported for methoxy-amino bridged *bis*(phenolate) yttrium alkoxides which can polymerise 1000 equivalents of *rac*-LA in 40 minutes under the same conditions. However with less stereocontrol, producing PLA with $P_r$ = 0.80.[72] This indicates that the initiating group does not have as crucial an effect on the stereocontrol as the ancillary ligand.

It was recently reported that dicationic and zwitterionic yttrium complexes (Figure 1.57) can be synthesised and used for the production of PLA *via* the ROP of *rac*-LA.[73]

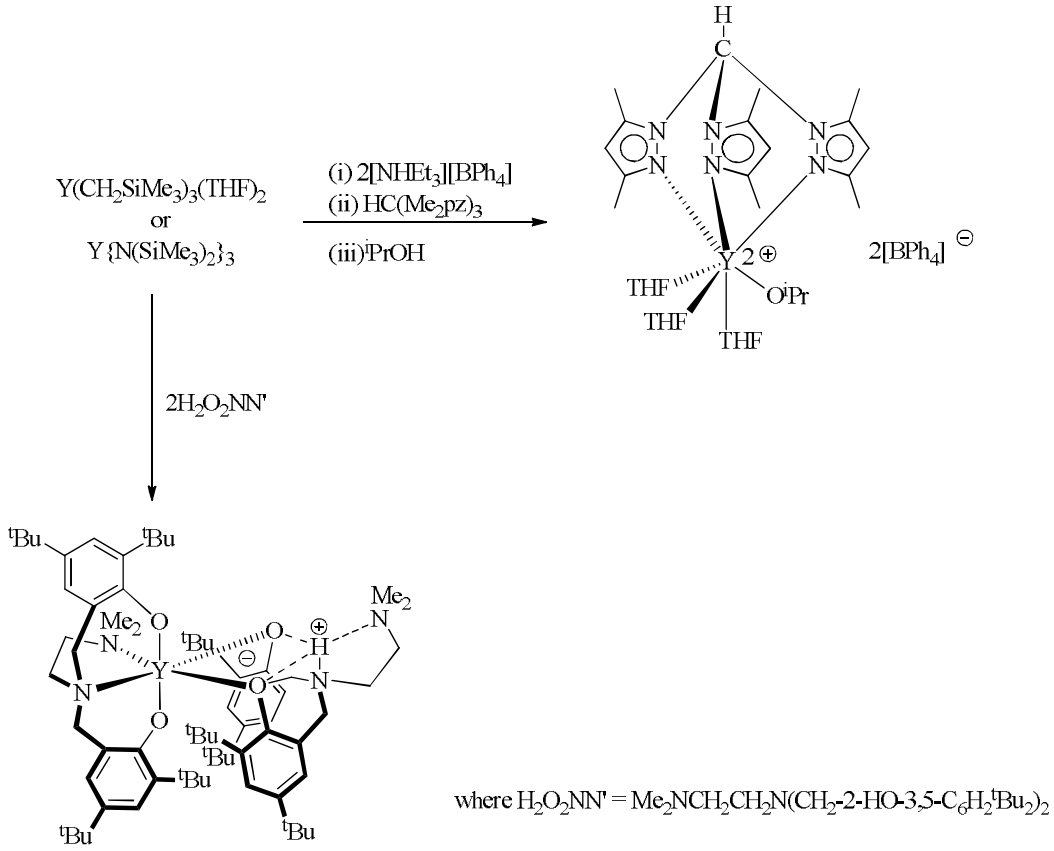


**Figure 1.57**: Preparation of dicationic and zwitterionic yttrium complexes[73]

The dicationic yttrium complexes have been reported to be effective for both the living and immortal polymerisation of *rac*-LA in THF at 70 °C in the presence of five equivalents of isopropanol.[73] High conversions to PLA were also achieved when the reaction was repeated with five equivalents of $BnNH_2$ instead of $^{i}$PrOH. In both cases, the molecular weights were consistent with six polymer chains growing simultaneously per Y centre, yielding atactic PLA.[73] An improvement from the dicationic complex was the preparation of a zwitterionic complex as shown in Figure 1.57. Although charge-neutral overall, the complex contains both a Lewis acidic yttrium centre and a Brønsted acidic proton in close proximity creating a potential "doubly-activating" site for initiation with $BnNH_2$. The zwitterionic complex achieved high conversions after 20 minutes which is greatly improved compared with the dicationic species which took 12 hours to achieve high conversions under the same conditions.[73] More significantly the zwitterionic species produced highly heterotactic PLA ($P_r$ = 0.96) with little transesterification observed.[73]

Following on from this work, low coordinate rare-earth metals have also been reported to be active for the ROP of *rac*-LA. An example is the mononuclear complexes: $[Nd(dbp)_3(thf)_3]$ and $[Gd(dbp)_3(thf)_3]$ where dbp = 2,4-di-*tert*-butylphenol.[74] Both complexes were shown to give > 90 % conversion to PLA within one hour with observed molecular weights higher than expected if one polymer chain was growing per Ln-dbp bond, suggesting that $k_{prop} \gg k_{int}$.[74] The polymerisations are not well-controlled with high polydispersity indices observed (> 2.2), however when the polymerisations were repeated with the addition of benzyl alcohol the PDI values reduced (< 1.6) suggesting a more controlled system. For the polymerisations carried out in the presence of benzyl alcohol lower molecular weight products are obtained, which are close to those expected for one polymer chain per equivalent of benzyl alcohol indicative of an immortal polymerisation occurring.[74] Further analysis of the polymer indicated extensive transesterification was occurring and no control of the stereochemistry was observed.

The polymerisations using $[Nd(dbp)_3(thf)_3]$ and $[Gd(dbp)_3(thf)_3]$ were repeated but with the addition of $BnNH_2$ as the co-initiator. Results indicated that 100 equivalents of *rac*-LA in the presence of five equivalents of $BnNH_2$ in THF at room temperature, gave 94 % conversion in 10 minutes to a benzyl amine-terminated PLA.[74] Although a decrease in the PDI values had already been seen with the addition of benzyl alcohol, the values were seen to further decrease to 1.3 when $BnNH_2$ was used as the initiator. The molecular weights were close to those expected for five polymeric chains forming per metal centre, however unlike the zwitterionic complexes of yttrium, no stereocontrol was observed with atactic PLA produced.[74]

*Bis*(phenolate) amine-supported samarium borohydride complexes have been synthesised and reported to be active for the ROP of *rac*-LA.[75]

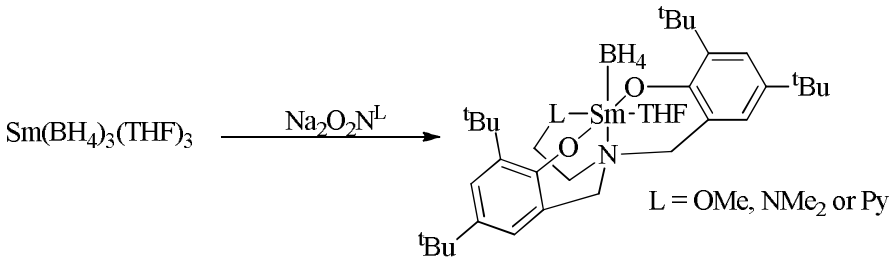


**Figure 1.58**: Preparation of *bis*(phenolate) amine-supported samarium borohydride complexes[75]

The polymerisation of *rac*-LA using the complexes shown in Figure 1.58, was carried out in THF at room temperature using a ratio of 200: 1 of [LA]: [Sm]. All three complexes showed 80 – 90 % conversion of *rac*-LA after 30 minutes to yield heterotactic PLA, with 80 % conversion achieved after 5 minutes when L = $NMe_2$.[75] The complex containing L = $NMe_2$ showed greater correlation between measured and theoretical molecular weights and a narrower PDI value compared to L = OMe and L = Py, suggesting transesterification is occurring to a lower degree.[75] In terms of correlation between measured and theoretical $M_n$ and PDI values, the order of ROP control is L = $NMe_2$ > Py > OMe.[75]

A further set of samarium complexes based on those in Figure 1.58, have also been prepared using a amide group instead of a borohydride group on the metal centre, (Figure 1.59), and tested for the ROP of *rac*-LA.[75]

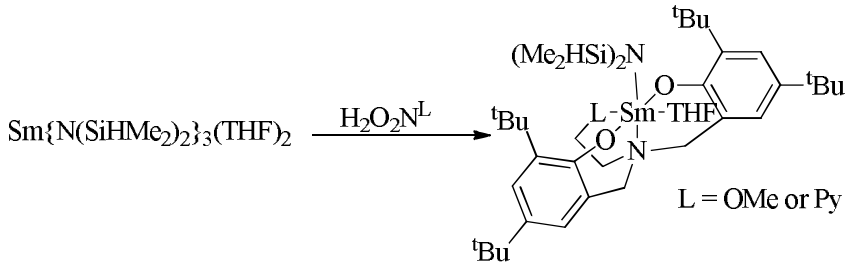


**Figure 1.59**: Preparation of *bis*(phenolate) amine-supported samarium amide complexes[75]

Polymerisation results indicated that the amide is more active than the borohydride equivalent under the same conditions (THF, room temperature, 200:1 ratio of [LA]: [Sm]), achieving > 89 % conversion to PLA after just five minutes. When L = OMe, a PLA product with a $M_n$ = 58,200 $gmol^{-1}$ and a PDI value of 1.43 is produced, compared with a $M_n$ = 48,200 $gmol^{-1}$ and a PDI value of 1.39 when L = Py.[75] However, it was observed that the $M_n$ values were considerably higher than the predicted molecular weights for one polymer chain per metal

centre, which could be due to poor rate of initiation over propagation or side reactions of the initiators.[75] If the reactions are left for a longer period of time (30 minutes), an increase in the polydispersity indices are observed (1.43 to 1.94 for L = OMe and 1.39 to 2.05 for L = Py) again indicating post-enchainment transesterification. Analogous to the borohydride complexes, the amide samarium complexes shown in Figure 1.59 produce heterotactically enriched PLA with little effect on the stereocontrol observed when the L group is altered. For example when L = OMe a $P_r$ value of 0.81 is achieved after 5 minutes in THF at room temperature, compared with a $P_r$ value of 0.78 when L = Py.[75]

Recent research has reported the preparation of heteroscorpionate neodymium amides for the ROP of *rac*-LA.[76]

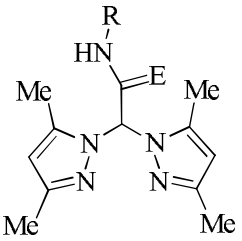


**1**: R = (*S*)-PhMeCH, E = O
**2**: R = sBu, E = O
**3**: R = Ph, E = S
**4**: R = $^{t}$Bu, E = S

**Figure 1.60**: Ligand complexed to $[Nd\{N(SiHMe_2)_2\}_3(thf)_2]$ to synthesise initiators for the ROP of *rac*-LA[76]

Two equivalents of the heteroscorpionate ligand shown in Figure 1.60 are reacted with two equivalents of $[Nd\{N(SiHMe_2)_2\}_3(thf)_2]$ to produce a dimeric neodymium species that has shown to be active for the production of PLA in toluene at 50 °C.[76] Results indicate varying degrees of activity dependant on the ancillary ligand such that the enantiopure complex of **1** achieves 71 % conversion to PLA after 25 hours, yet complex **3** achieves 69 % conversion after only 7 hours.[76] Higher activity is observed with complexes of **2** and **4** achieving 45 % conversion after 0.45 hours and 4.5 hours respectively. The high level of control in the polymerisations using all initiators can be seen with low PDI values (< 1.20) and a linear correlation between conversion and $M_n$, suggestive of well-controlled propagation steps and a single type of reaction site.[76]

The racemic complex containing **2** and the achiral complexes containing **3** and **4** in Figure 1.59 showed no stereoselectivity in the ROP of *rac*-LA. However, analysis of the microstructure of the polymeric material produced *via* the

enantiopure heteroscorpionate complex containing ligand **1** from Figure 1.58 gave PLA with an isotactic bias ($P_m$ = 0.61) at low conversions of around 10 %.[76] The optical activities of the polymer products at 10 % showed a preference for polymerisation of *L*-LA indicating an enantiomorphic site-control mechanism is occurring. However, at a slightly higher conversion of 52 %, a random incorporation of *L*-LA and *D*-LA is seen and hence the PLA produced at higher conversions is atactic.[76]

Arnold *et al.* reported the use of bifunctional yttrium *N*-heterocyclic carbene (NHC) catalysts for the ROP of *rac*-LA.[77]

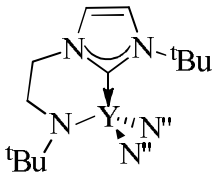


**Figure 1.61**: Bifunctional yttrium *N*-heterocyclic carbine catalysts[77]

The bifunctional nature of the complex shown in Figure 1.61 was reported to be from the LA binding to the Lewis acidic yttrium centre, which consequently allows the labilized NHC to function as a Lewis base and ring-open the LA monomer.[77] The complex was reported to be extremely active for the polymerisation of *rac*-LA even at very low concentrations (0.01 %). For example, a 85 % yield of PLA was achieved after 15 minutes in toluene using a monomer to initiator ratio of 10,000: 1.[77] The ROP of *rac*-LA utilising the complex in Figure 1.61 produced highly heterotactic PLA at 20 °C in toluene, in a controlled manner (PDI < 1.47).[77]

### 1.3.5 Other Initiators: Zinc and Magnesium

The biocompatible nature of zinc makes it an attractive initiator for the further development of environmentally friendly products for biomedical and pharmaceutical applications. One of the first examples using a zinc complex as a single-site catalyst for the ROP of *rac*-LA was reported by Coates *et al.*, who utilised $\beta$-diiminate (BDI) zinc complexes to produce PLA at room temperature – Figure 1.62.[78]

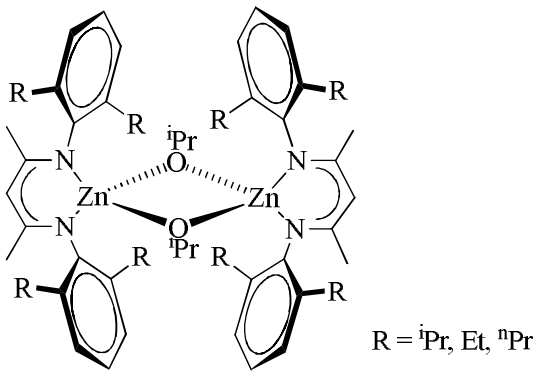


**Figure 1.62**: Single-site $\beta$-diiminate zinc complex [(BDI)ZnO$^{i}$Pr] reported by Coates et al.[17, 78]

It was reported that when R = $^{i}$Pr (Figure 1.62), the ROP of *rac*-LA occurs in a well-controlled living manner at 20 °C in $CH_2Cl_2$. The polymerisation using a 200: 1 ratio of [LA]: [initiator], produced PLA after 20 minutes with a narrow polydispersity value of 1.10 and a $M_n$ = 37,900 gmol$^{-1}$.[78] Furthermore, analysis of the microstructure of the polymeric material showed highly heterotactic PLA ($P_r$ = 0.90) was produced, and an increase in this stereoregularity was observed when the polymerisation was repeated at lower temperature of 0 °C ($P_r$ = 0.94). The polymers produced at both 20 °C and 0 °C are amorphous with a $T_g$ of 49 °C.[78] When the substituents of the $\beta$-diiminate ligand (R in Figure 1.62) are altered, there is a significant effect in the stereochemistry of the resulting polymer, such that when R is changed from isopropyl to ethyl, there is a decrease in the heterotacticity ($P_r$ = 0.79). A further decrease is observed when R = *n*-propyl ($P_r$ = 0.76).[17] The rate of polymerisation also increases in the order of $^{i}$Pr > Et > $^{n}$Pr with 97 % conversion to PLA achieved after 0.33 hours when R = $^{i}$Pr compared to 97 % PLA produced after 19 hours when R = $^{n}$Pr.[17] Consequently, $k_{app}$ is also effected by altering the substituent on the $\beta$-diiminate ligand, such that when R = $^{i}$Pr a $k_{app}$ of 0.22 min$^{-1}$ is reported, but when R = Et or $^{n}$Pr the rate is decreased ($k_{app}$ = 0.017 min$^{-1}$ and 0.0066 min$^{-1}$).[17]

The effect of the initiating group on the polymerisation of *rac*-LA was investigated using: -N(SiMe$_3$)$_2$, -Et, -OAc, -O$^{i}$Pr (Figure 1.62) and –OCH(Me)CO$_2$Me. It was reported that the latter two initiating groups were superior showing predictable molecular weights and narrow molecular weight distribution. This is presumably due to the initiating groups closely mimicking the propagation species. In the case of –N(SiMe$_3$)$_2$, -Et and –OAc, the initiation does

not occur *via* insertion into the acyl-oxygen bond but is thought to react with impurities in the monomer, to synthesise a new initiating group, resulting in a slower rate of initiation ($k_{int}$) than propagation ($k_{prop}$).[17]

Analogous to the zinc *β*-diiminate complexes shown in Figure 1.62, a series of magnesium *β*-diiminate complexes were also synthesised and reported by Coates *et al.*.[17] When R = $^{t}$Bu, the polymerisation of *rac*-LA occurs extremely fast achieving complete conversion to PLA after 2 minutes at 20 °C with a [LA]/[Mg] ratio of 200: 1. The magnesium complex however is less stereoselective than the zinc analogue, producing atactic PLA, with a broad molecular weight distribution (PDI = 1.59). Narrow molecular weight distributions could be achieved with the same initiator by repeating the reaction in the presence of one equivalent of 2-propanol, albeit still without good chain-end control.[17]

Chisholm *et al.* further developed this work by increasing the steric bulk around the metal centre, for zinc and magnesium, by developing similar structures to those in Figure 1.62, but where the methyl groups in the ligand backbone have been replaced by *tert*-butyl groups.[79] It was thought that by increasing the steric pressure around the metal it would enhance the influence of end-group in the polymerisation control and hence increase the selectivity in the production of PLA. However, it was reported, that such complexes showed a decrease in stereoselectivity and instead produced atactic PLA on both occasions.[79]

Just like the *β*-diiminate ligand complexes of zinc and magnesium, it was thought that other ligand systems that were complexed to magnesium which were successful for the ROP of cyclic esters could be transferred to zinc. An example of such is the preparation of amidinate-based heteroscorpionate alkyl zinc complexes.[80] Similar amidine-heteroscorpionate ligands have been used to synthesise lanthanide complexes that too have been reported to be active for the production of PLA (See Section 1.3.4, Figure 1.60).[76]

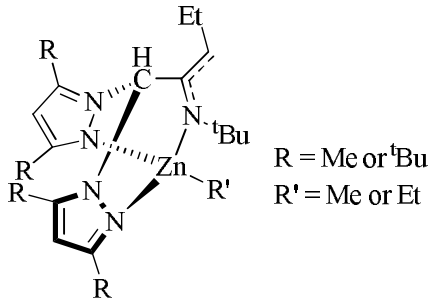


**Figure 1.63**: Heteroscorpionate alkyl zinc complexes prepared for the ROP of *rac*-LA[80]

The complexes in Figure 1.63 can be prepared from the reaction of $ZnMe_2$ or $ZnEt_2$ with the corresponding ligand, which are hydrolysis products of heteroscorpionate lithium acetamidinates.[80] All complexes in Figure 1.63 were trialled for the ROP of *rac*-LA in toluene at 110 °C, with a [LA]: [initiator] ratio of 100: 1. It was reported that the initiators showed 70 % conversion to PLA after 48 hours in solution with narrow polydispersity values (1.08 – 1.23). However, under solvent-free conditions, when R = $^t$Bu and R' = Me, 61 % conversion is achieved after 45 minutes although with a loss of control with a higher PDI value of 1.43. All products showed slight stereoselectivity towards heterotactic PLA when R = $^t$Bu, however atactic PLA was produced when R = Me, probably due to methyl substituents contributing less steric demand in the pyrozolic rings leading to a less congested, more flexible and less selective initiator to the incoming LA monomer.[80]

It has been reported that heteroscorpionate alkyl magnesium complexes are highly effective single-component living initiators for the ROP of *rac*-LA.[81] Based on this, and that the more sterically hindered alkyl zinc complexes in Figure 1.63, led to the production of heterotactic PLA, it was assumed that an alternative magnesium initiator containing scorpionate/cyclopentadienyl hybrid ligand would show high activity and stereocontrol in the ROP of *rac*-LA.[81]

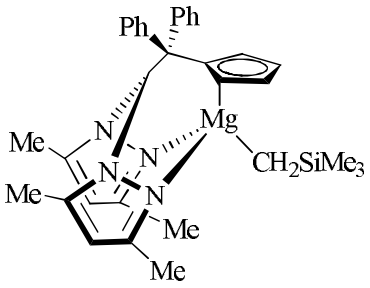


**Figure 1.64**: Hybrid scorpionate/cyclopentadienyl magnesium complex used for the ROP of *rac*-LA[81]

The magnesium complex shown above in Figure 1.64 was active in the ROP of *rac*-LA in toluene at 90 °C giving 59 % conversion to PLA after eight hours at a ratio of 200: 1 of [LA]: [initiator].[81] Under solvent-free conditions, 41 % of *rac*-LA had been converted after two hours, however with a broader molecular weight distribution (PDI = 1.41) than under solution conditions (PDI = 1.12), presumably attributed to gradual catalyst decomposition at a higher temperature as well as some transesterification. Unlike the zinc complex in Figure 1.64, no stereoselectivity was observed with this magnesium analogue, producing atactic PLA under both solvent and solvent-free conditions.[81]

As already shown for the *β*-diiminate complexes, changes to the ligand backbone or the metal centre can alter the activity and stereoselectivity in the ROP of *rac*-LA. It has been reported that a series of NNO-tridentate ketiminate ligands (Figure 1.65) complexed to magnesium and zinc are active for the production of PLA at low temperature.[82]

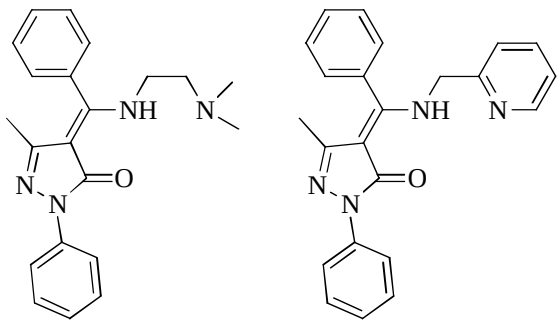


**L[1]H** **L[2]H**

**Figure 1.65**: NNO-tridentate ketiminate ligands used to synthesise magnesium and zinc benzylalkoxy complexes[82]

Results indicated that out of all four complexes (magnesium and zinc complexes of both ligands shown in Figure 1.65), $[(\mathbf{L^1})_2Mg_2(\mu\text{-}OBn)_2]$ exhibits the highest stereocontrol with a $P_r$ value of 0.85 when the polymerisation is carried out at 30 °C in THF.[82] A slight loss of heterotacticity is observed when the temperature of the reaction is increased to 50 °C, and a slight increase to $P_r = 0.87$ is reported when the temperature is reduced to 0 °C.[82] The degree of stereoselectivity is also altered with the choice of solvent, for example with the initiator $[(\mathbf{L^1})_2Mg_2(\mu\text{-}OBn)_2]$, when the solvent is changed from THF to $CH_2Cl_2$ at 30 °C, a dramatic change in the $P_r$ value is seen, decreasing from 0.85 in THF to 0.36 in $CH_2Cl_2$.[82] Changes to the terminal group in the magnesium complexes *i.e.* a ligand change from $\mathbf{L^1H}$ to $\mathbf{L^2H}$, significantly decreases the stereocontrol of the reaction, no longer producing heterotactic PLA, but an atactic product with $P_r = 0.54$ with initiator $[(\mathbf{L^2})_2Mg_2(\mu\text{-}OBn)_2]$.[82]

Analogous to the magnesium complexes, $[(\mathbf{L^1})_2Zn_2(\mu\text{-}OBn)_2]$ shows higher activity than $[(\mathbf{L^2})_2Zn_2(\mu\text{-}OBn)_2]$ achieving 95 % conversion to PLA within 90 minutes at 0 °C compared to 93 % conversion to PLA in 4 hours for $[(\mathbf{L^2})_2Zn_2(\mu\text{-}OBn)_2]$ when the polymerisation is carried out in THF with a [LA]: [M] ratio of 200: 1.[82] Although an increase in the activity is observed for the zinc complexes upon changing the terminal group from 2-(*N*,*N*'-dimethylamino)ethyl to 2-pyridinyl-methyl *i.e.* $\mathbf{L^1H}$ to $\mathbf{L^2H}$, no improvement is seen in the stereoselectivity producing PLA with a slight heterotactic bias on both occasions: $P_r = 0.61$ for $\mathbf{L^1H}$ and $P_r = 0.60$ for $\mathbf{L^2H}$.[82]

The preparation of zinc (II) alkoxide complexes supported by a mononucleating ligand has been reported by Hillmyer and Tolman *et al.* for the ROP of *rac*-LA.[83]

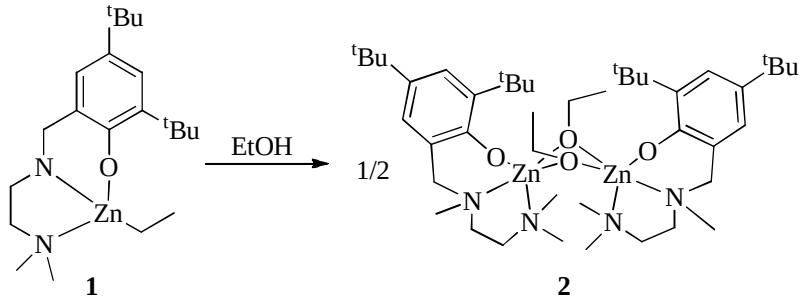


**1** **2**

**Figure 1.66**: Preparation of zinc(II) alkoxide complexes for the ROP of *rac*-LA[83]

Although complex **1** in Figure 1.66 was reported to show no activity in the ROP of *rac*-LA *via* a coordination and insertion mechanism, complex **2** in Figure 1.66 was highly active in $CH_2Cl_2$ at 25 °C achieving > 90 % conversion to PLA in under 20 minutes even at high [LA]: [initiator] ratio of 1500: 1.[83] Figure 1.66 shows complex **2** as a dimeric species, as reported to be in the solid state.[83] However, further analysis confirmed that in solution complex **2** actually exists in a monomeric form, and it is thought to be the monomeric structure that is present during the polymerisation reactions.[83] Although good molecular weight control was demonstrated, the overall molecular weights are lower than expected, particularly at high concentrations, for example at 98.5 % conversion for $[LA]_o/[\mathbf{2}]_o = 1500$, the expected molecular weight should be 214 $kgmol^{-1}$, yet the experimental value is 130 $kgmol^{-1}$. This was reported to be due to rapid chain exchange which could arise from impurities that are present in the reaction.[83]

It has been reported that unlike phenoxides, alkoxides do not lead to mononuclear, discrete complexes, but rather are noted to produce highly aggregated polynuclear species. This is reported to be attributed to the more basic alkoxide having a high tendency to cause bridging. One reported approach to reduce this bridging and generate a less basic alkoxide O-atom is to incorporate $CF_3$ groups $\alpha$ to the alkoxide, which are electron-withdrawing and generate intra and inter molecular repulsions.[84] Examples of such complexes (Figure 1.67), have been prepared and explored for their reactivity in the ROP of *rac*-LA.[84]

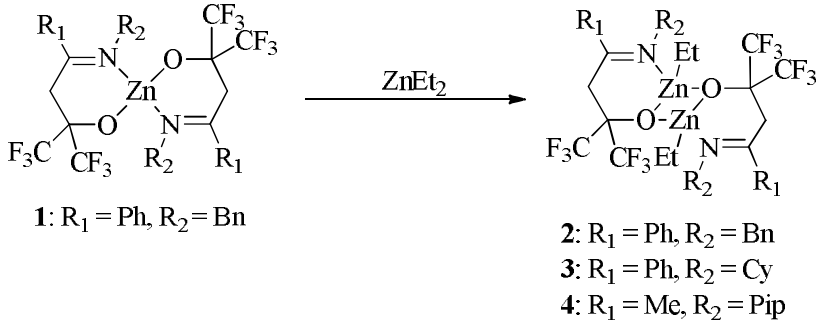


**Figure 1.67**: Preparation of zinc complexes of fluorous alkoxide-imino ligands of the type{$ON^{R1R2}$}$ZnEt$[84]

The heteroleptic zinc complexes shown in Figure 1.67 were trialled for the ROP of *rac*-LA with initial results showing low conversions at 20 °C in THF using a 100: 1 ratio of [LA]: [initiator]. However, upon addition of one equivalent of

benzyl alcohol to the polymerisation reaction, a more efficient initiating species was produced. High conversions were achieved, for example complex **2** gave 92 % conversion to PLA after 23 hours generating a product with $M_n$ = 10,700 gmol$^{-1}$.[84] The activity of the polymerisation could be significantly improved using initiators **2-4** with the addition of benzyl alcohol, by increasing the temperature to 50 °C, achieving > 94 % conversion after 1.5 hours.[84] The polymeric products produced at this higher temperature in THF showed relatively narrow molecular weight distributions (PDI = 1.25 – 1.33) and a close correlation between experimental and theoretical molecular weights based on one polymer chain growing per metal centre.[84] An increase in the amount of benzyl alcohol added to the polymerisation resulted in an "immortal" polymerisation taking place enabling the growth of more than one polymer chain per metal centre, and allowing the benzyl alcohol to act as a chain transfer agent.[84] Using complex **1** as an initiator for the production of PLA led to poor conversion of *rac*-LA. However, upon addition of one-equivalent of benzyl alcohol, 92 % conversion to PLA could be achieved at 50 °C in toluene. The activity of complex **1** in Figure 1.67 is slower than the ethyl(alkoxide) zinc initiators **2-4**, with 92 % conversion achieved after 36 hours in toluene compared to 15 hours for complex **2** in toluene under the same conditions: 50 °C, 100: 1: 1 of [LA]: [Zn]: [BnOH].[84] For all systems shown in Figure 1.67, containing the fluorous alkoxide-imine ligands, no degree of stereocontrol was observed.[84]

The synthesis of dinuclear zinc alkoxide complexes of the type [$LZn_2(\mu$-$OEt)X_2$] where X is a halide and L is a pentadentate phenolate ligand, have been synthesised and trialled for the ROP of *rac*-LA.[85, 86]

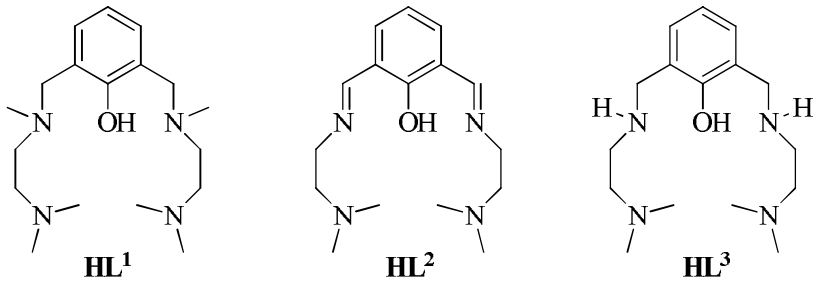


**Figure 1.68**: Pentadentate phenolate ligands used in the preparation of dinuclear zinc complexes of the type [$LZn_2(\mu$-$OEt)X_2$] where X is a halide [85, 86]

The preparation of the dinuclear zinc complexes containing the three ligands in Figure 1.68 have been optimised and the complexes are reported to be active for the ROP of *rac*-LA with varying degrees of activity, in all cases generating the initiator *in situ*.[86] The polymerisation using **HL$^1$** where X = Cl, Br and I, have shown > 90 % conversion to PLA in $CH_2Cl_2$ at 25 °C, with an overall order of reactivity being: [$L^1Zn_2(\mu\text{-OEt})Br_2$] > [$L^1Zn_2(\mu\text{-OEt})Cl_2$] > [$L^1Zn_2(\mu\text{-OEt})I_2$].[86] This highlights that the order of polymerisation activity is not reflective of the electronegativity of the halide present.[86] With X = Br showing the best activity achieving 91 % conversion after 22 minutes, the resulting ligands (**HL$^2$** and **HL$^3$**) were also used to prepare analogous compounds: [$L^2Zn_2(\mu\text{-OEt})Br_2$] and [$L^3Zn_2(\mu\text{-OEt})Br_2$] and trialled for the ROP of *rac*-LA under the same conditions. Results indicate that for the complex containing **HL$^2$**, the reaction rate is extremely slow, however when ligand **HL$^3$** is employed, 92 % conversion to PLA can be achieved after just one minute.[86] Good correlation between experimental molecular weights and the theoretical value ($M_n$ = 26,000 gmol$^{-1}$) was observed, with the best fit seen for the highly active species and significantly lower molecular weights obtained for the slower [$L^2Zn_2(\mu\text{-OEt})Br_2$] complex with a $M_n$ = 14,200 gmol$^{-1}$.[86] It was reported that the higher reactivity seen with [$L^1Zn_2(\mu\text{-OEt})Br_2$] and [$L^3Zn_2(\mu\text{-OEt})Br_2$] over [$L^2Zn_2(\mu\text{-OEt})Br_2$] was due to the increased flexibility of the amine ligand in the complexes over the imine ligand **HL$^2$**.[86]

The effect of the metal centre on the rate of polymerisation has also been investigated using **HL$^1$** shown in Figure 1.68, complexed to zinc, magnesium and cobalt.[87] The reactions were carried out under similar conditions to that of the zinc complexes discussed above (25 °C, $CH_2Cl_2$) and the results indicated that only the dinuclear zinc complex was able to produce PLA with a high molecular weight, with the magnesium and cobalt complexes showing poor kinetic activity and only producing low molecular weight oligomers.[87] Under the industrially preferred melt conditions, the same reactivity was observed. The magnesium and cobalt complexes have inferior activity converting only 18 % of *rac*-LA after 16 hours for magnesium and 40 % for cobalt under the same conditions with a [LA]: [initiator] ratio of 300: 1. The dinuclear zinc complex however was able to achieve 81 % conversion after five minutes under melt conditions with a

[LA]: [initiator] ratio of 5000: 1, albeit with lower than expected molecular weights. From studies of reaction rates, it was reported that the magnesium and cobalt complexes show similar initial rates for the polymerisation of *rac*-LA, with the zinc complex being around ninety times faster.[87]

*Bis*(phosphinimine) ligands have been reported to be ideal frameworks for the preparation of complexes for the ROP of *rac*-LA due to the rigidity of the ligands as well as the modular nature of the phosphinimine functionality. Hayes *et al.* have synthesised a range of cationic organozinc complexes containing such *bis*(phosphinimine) pincer ligands with methyl-(*S*)-lactate as an initiating group (Figure 1.69).[88, 89]

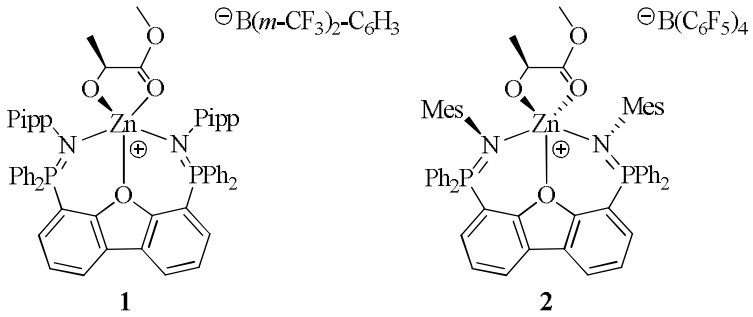


**Figure 1.69**: Cationic organozinc complexes containing *bis*(phosphinimine) ligands[88, 89]

When a Mes (2,4,6-trimethylphenyl) group was present (**2**), atactic PLA was produced after 3.5 hours at 60 °C in $C_6D_5Br$ with 50 equivalents of LA.[88] However, when the steric demand at the phosphinimine N-aryl site is reduced, to a Pipp (*p*-isopropylphenyl) group (**1**), the polymerisation can be carried out at room temperature in a highly active manner achieving 90 % conversion of 200 equivalents of *rac*-LA in 50 minutes.[89] Unlike compound **2**, the complexes containing Pipp groups produced PLA with heterotactic enrichment ($P_r$ = 0.63).[89]

## 1.4 Other monomers for co-polymerisation with *rac*-LA

Although production of PLA on its own is of commercial value, its combination with other viable monomers for the production of copolymers has received increased interest due to the ability to tune the physical properties depending on the ratio of each monomer in the copolymerisation reaction. An example of such is the material Vicryl™ used in bioassimilable sutures which contains 8 % lactic

acid and 92 % glycolic acid.[1] Although a vast amount of research has been carried out on a variety of different monomers for the copolymerisation with LA (for example, $\delta$-valerolactone, $\varepsilon$-caprolactone and $\beta$-butyrolactone), this report will focus on the development of copolymers of LA and isosorbide as well as LA and trimethylene carbonate (TMC).

Different types of copolymers can be produced depending on the initiator and synthetic method employed, with block, random or alternating copolymers possible. Block copolymers are polymers consisting of multiple sequences of the same monomer alternating with a sequence of a different monomer.[90] A random copolymer is a polymer that is made up of more than one monomeric unit, in which the probability of the next polymer site is independent of the previous unit.[91] An alternating copolymer consists of more than one monomer which alternate along the polymeric chain.

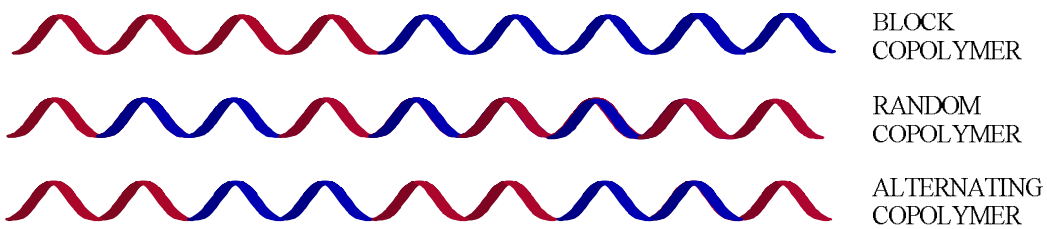


**Figure 1.70**: Schematic representation of the types of copolymers possible

### 1.4.1 Copolymerisation of *rac*-LA and isosorbide

Isosorbide (Figure 1.71) is a relatively inexpensive diol that can be produced from renewable resources such as glucose in large quantities.

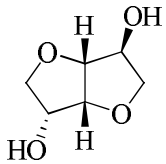


**Figure 1.71**: Structure of Isosorbide

When isosorbide is incorporated into polymers containing alkane or aliphatic ether building blocks, it increases the glass transition temperature ($T_g$).[92] It is a chiral thermostable monomer which allows its polymers to be heated for a short time at 300 °C without decomposition or significant racemisation.[92] Taking the

above into account and also the fact that it does not show sensitivity to racemisation under acidic or basic condition, isosorbide is seen to be a good candidate for incorporation into copolymers.

Research carried out by Kricheldorf *et al.* utilised $SnOct_2$ as an initiator for the copolymerisation of $\varepsilon$-caprolactone ($\varepsilon$-CL) and a cyclic polyester consisting of isosorbide and suberic acid {CPIS: cyclic poly(isosorbide suberate), Figure 1.72}, to produce a biodegradable polyester.[92]

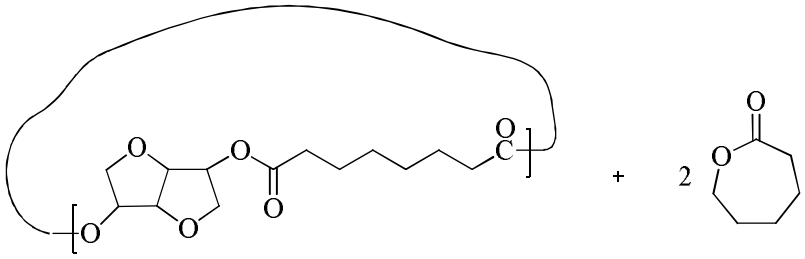


CPIS $\varepsilon$-CL

**Figure 1.72**: CPIS and $\varepsilon$-CL used for the production of a biodegradable polyester[92]

$SnOct_2$ has already been discussed in Section 1.3.1 for the homopolymerisation of *rac*-LA, which at present is the initiator used for the production of PLA within the polymer industry. It was reported to be successful for the copolymerisation of ε-CL and CPIS, when the reaction was carried out under solvent-free conditions with a 1: 2 ratio of CPIS: ε-CL. However a high temperature of 200 °C was required to achieve the copolymerisation in the presence of a co-initiator of benzyl alcohol.[92]

$Sn(Oct)_2$ was reported to be used in the synthesis of various copolymers composed of *L*-LA and isosorbide succinate moieties.[93] The isosorbide succinate moieties have been incorporated into poly(*L*-LA), PLLA, backbone to produce four different copolymeric products with low average molecular weights:

**I**: monomer mixtures of *L*-LA , isosorbide and succinic anhydride

**II**: PLLA, isosorbide and succinic anhydride

**III**: oligo(isosorbide succinate) (PIS) and *L*-LA

**IV**: transesterification between PLLA and PIS

The products of **II-IV** were all reported to produce block copolymers, with the product of **I** giving a random copolymer. In the reaction of **II** and **III**, block copolymers of shorter sizes are formed due to transesterification occurring. Polymers of **I** are completely amporphous yet **II-IV** are crystalline with **II** and **III** less so due to transesterification.[93] Further studies of the polymer produced form **III** revealed that the block copolymer (Figure 1.73) produced a better scaffold than PLLA for fibroblast cell adhesion and proliferation.[94]

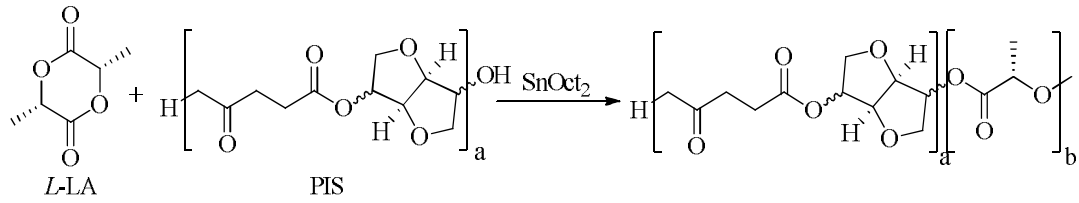


**Figure 1.73**: Proposed structure of poly(isosorbide succinate – *b* – *L*-LA)[94]

A further tin catalyst studied for the production of a copolymer of ε-CL and CPIS is 2,2-dimethyl-2-stanna-1,3-dioxepane (DSDOP) which is a cyclic tin alkoxide, Figure 1.74.

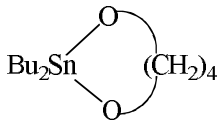


**Figure 1.74**: Structural representation of DSDOP (2,2-dimethyl-2-stanna-1,3-dioxepane)[92]

Initial results indicated that the catalyst shown in Figure 1.74 was an effective initiator for the polymerisation of ε-CL, but was shown to give partial degradation of CPIS. Evidence was also present to indicate intensive transesterification was occurring in the reaction, with a tendency for the formation of random sequences.[92] The use of La($O^iPr$)$_3$ and Y($O^iPr$)$_3$ were also investigated as potential initiators for the copolymerisation of *rac*-LA and isosorbide. Results indicated that Y($O^iPr$)$_3$ had a preference for the polymerisation of CPIS, and La($O^iPr$)$_3$ had a preference for the polymerisation of ε-CL, over the production of a copolymer.[92]

Just as shown for LA, there is a need to develop initiators that are more sustainable and less toxic for the development of new copolymers. This report will investigate the ability of group (IV) amine *tris*(phenolates) for the

copolymerisation of *rac*-LA with isosorbide, and compare the products with the homopolymers of LA.

### 1.4.2 Copolymerisation of *rac*-LA and TMC

The development of polycarbonates has received a lot of recent interest within academic research,[95] with one example being the ROP of TMC (trimethylene carbonate or 1,3-dioxan-2-one), to produce a polycarbonate.

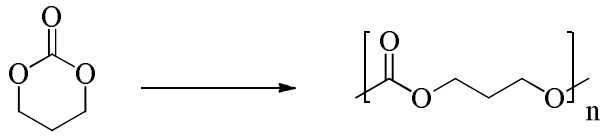

**Figure 1.75**: Production of a polycarbonate from TMC

TMC has the same advantage as PLA in that its products are biodegradable and suitable for use in many medical applications. However, aliphatic carbonates have a lower electrophilicity of the CO group than aliphatic polyesters meaning that they are less sensitive to hydrolytic degradation. This is advantageous for pharmaceutical applications when a slow resorption in the human body is desired.[96] TMC has been used as a co-monomer on many occasions because it lowers the $T_g$ which improves the flexibility of the product and reduces the rate of hydrolytic degradation making it suitable for soft tissue engineering applications.[97, 98]

Like PLA, many different metals have been researched to carry out the polymerisation of TMC.[99] Kricheldorf *et al.* used various butyl tin trichloride compounds for the ROP of TMC to achieve the desired polymeric product in high yields.[100] It was reported that the reactivity decreases from $BuSnCl_3$ to $Bu_2SnCl_2$ to $Bu_3SnCl$, with the molecular weights of the product showing the same trend.[100] Studies using $SnOct_2$ as an initiator for the ROP of TMC showed no conversion after 24 hours at temperatures less than 60 °C, with slight conversion at 80 °C albeit with a slow reaction rate, and higher rates of polymerisation at 100 °C.[97] It was reported that the polymerisation using $SnOct_2$ in the presence of benzyl alcohol as a co-initiator was carried out *via* a coordination-insertion mechanism with tin benzyloxide groups initiating the polymerisation.[97] The use of a co-initiator is required for such reactions at temperatures less than 120 °C, but

above this temperature, for example 160 °C, the TMC can undergo insertion into the Sn-Oct bond giving a high weight polymer over a shorter period of time.[97]

Kricheldorf *et al.* also utilised $TiCl_4$ and $SbCl_5$ for the same reaction which again produced the product in high yield (> 90 %), and in both cases formed a complex with the monomer *via* the carbonyl group.[101] It was reported that $SbCl_5$ was more reactive than $TiCl_4$ and was able to carry out the polymerisation at 25 °C in $CHCl_3$.[101] More recent work by the same group highlighted the use of $Ph_2BiOEt$ and $Ph_2BiBr$ as active initiators for the ROP of TMC achieving conversions ≥ 98 %.[96] $SnCl_4$, $SnBr_4$ and $SnI_4$ have also been investigated for the polymerisation of TMC with results indicating that a high molecular weight polymer can be obtained for all three, with $SnI_4$ giving the highest. The reaction was reported to proceed *via* a cationic polymerisation mechanism which results however in side reactions occurring yielding $CH_2$-X compounds.[102]

Darensbourg *et al.* investigated the use of Al(III) and Sn(IV) Salen chloride compounds (Figure 1.76) as initiators for the ROP of TMC due to their Lewis acidic nature.[103]

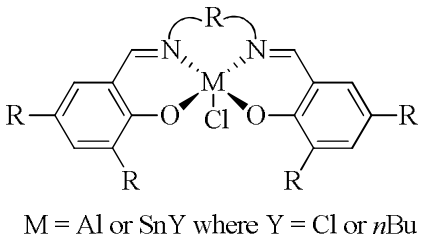

M = Al or SnY where Y = Cl or *n*Bu

**Figure 1.76**: General structure of Salen chloride compounds for the ROP of TMC[103]

Both the aluminium and tin complexes were effective catalysts and produced polycarbonates that contained no ether linkages, with aluminium showing preference over the tin complex due to the reduction in Lewis acidity at the Sn(IV) metal centre.[103]

Like PLA, although the homopolymerisation of TMC is of industrial importance, the copolymerisation of it with other viable monomers is also of interest. One such example is the copolymerisation of *rac*-LA and TMC. By incorporation of TMC into PLA products, the brittle nature of PLA alone can be reduced making it important for biomedical materials such as thermoplastic elastomers.[104] Since

$Sn(Oct)_2$ is a successful initiator for the homopolymerisation of TMC and LA, examples of its use and other tin complexes for the production of copolymers of both monomers also exist.[105-107] However, it was reported by Darensbourg that it is of value to carry out the copolymerisation of TMC with PLA using complexes derived from biocompatible metals, for example calcium complexes with tridentate Schiff base ligands (Figure 1.77).[104]

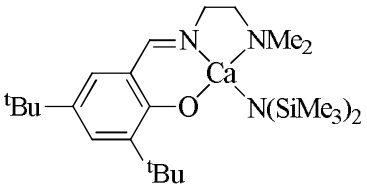


**Figure 1.77**: Tridentate Schiff base biocompatible calcium complex used for the copolymerisation of *rac*-LA and TMC[104]

Complexes of the type shown above in Figure 1.77 were effective for the homopolymerisation of TMC and LA independently to produce high molecular weight polymers with narrow polydispersities, as well as being successful at the copolymerisation of the two monomers.[104]

Random copolymerisation of TMC and *rac*-LA has been investigated using zinc lactate $Zn(Lac)_2$ as an initiator producing high molecular weight polymeric material with polydispersity indices in the range of 1.7 – 2.0 at 140 °C for 72 hours.[108, 109] The degradation of such amorphous copolymers was reported to be faster than the homopolymer of TMC with faster rates observed for polymeric products with higher LA content.[109]

Another example using a less toxic metal initiator for copolymerisation reactions is the use of zirconium (IV) acetylacetonate $Zr(acac)_4$, which has shown to be successful for the synthesis of bioresorbable aliphatic copolyesters and copolymers of glycolide and TMC.[110] It was reported that $Zr(acac)_4$ was a successful initiator for the copolymerisation of *L*-LA and TMC, but owing to the large difference between the reactivity ratios of *L*-LA and TMC, only copolymers with high amounts of LA units could be achieved.[110] The copolymerisation was conducted under solvent-free conditions at a range of temperatures. Results indicated that when the reaction is carried out at high temperatures of 180 °C, amorphous materials with identical compositions but highly randomised chain

structures were produced. This could be attributed to intensive intermolecular transesterification taking place at the same time as copolymer chain growth. When the copolymerisation is repeated at a lower temperature of 110 °C, the degree of transesterification is reduced resulting in a semicrystalline material with multi-block structures.[110]

Very few examples exist in the literature for the copolymerisation of *rac*-LA and TMC using group (IV) initiators, and therefore this report, will investigate the ability of group (IV) amine *tris*(phenolates) for the homopolymerisation of TMC as well as its copolymerisation with *rac*-LA.

1. O. Dechy-Cabaret, B. Martin-Vaca and D. Bourissou, *Chem. Rev.*, 2004, **104**, 6147-6176.
2. B. P. Mooney, *Biochem. J.*, 2009, **418**, 219-232.
3. L. Zan, W. J. Fa and S. L. Wang, *Environmental Science & Technology*, 2006, **40**, 1681-1685.
4. Chemistry and Industry, Issue 10, 2011
5. C. J. Frankis, PhD Thesis, 2010
6. http://www.natureworksllc.com
7. R. M. West, M. S. Holm, S. Saravanamurugan, J. M. Xiong, Z. Beversdorf, E. Taarning and C. H. Christensen, *J. Catal.*, 2010, **269**, 122-130.
8. R. Datta and M. Henry, *J. Chem. Technol. Biotechnol.*, 2006, **81**, 1119-1129.
9. M. S. Holm, S. Saravanamurugan and E. Taarning, *Science*, 2010, **328**, 602-605.
10. W. Dittrich and R. C. Schulz, *Angew. Makromol. Chem.*, 1971, **15**, 109-&.
11. E. L. Marshall, V. C. Gibson and H. S. Rzepa, *J. Am. Chem. Soc.*, 2005, **127**, 6048-6051.
12. R. H. Platel, L. M. Hodgson and C. K. Williams, *Polym. Rev.*, 2008, **48**, 11-63.
13. T. Biela, A. Duda and S. Penczek, *Macromol. Symp.*, 2002, **183**, 1-10.
14. B. Trathnigg, *Prog. Polym. Sci.*, 1995, **20**, 615-650.
15. http://www.pharmacopeia.cn - 20th November 2011
16. M. J. Stanford and A. P. Dove, *Chem. Soc. Rev.*, 2010, **39**, 486-494.
17. B. M. Chamberlain, M. Cheng, D. R. Moore, T. M. Ovitt, E. B. Lobkovsky and G. W. Coates, *J. Am. Chem. Soc.*, 2001, **123**, 3229-3238.
18. X. L. Liu, X. M. Shang, T. Tang, N. H. Hu, F. K. Pei, D. M. Cui, X. S. Chen and X. B. Jing, *Organometallics*, 2007, **26**, 2747-2757.
19. L. Zhang, F. Nederberg, J. M. Messman, R. C. Pratt, J. L. Hedrick and C. G. Wade, *J. Am. Chem. Soc.*, 2007, **129**, 12610-12611.
20. A. P. Dove, H. Li, R. C. Pratt, B. G. G. Lohmeijer, D. A. Culkin, R. M. Waymouth and J. L. Hedrick, *Chem. Commun.*, 2006, 2881-2883.
21. T. R. Jensen, L. E. Breyfogle, M. A. Hillmyer and W. B. Tolman, *Chem. Commun.*, 2004, 2504-2505.
22. P. Degee, P. Dubois, R. Jerome, S. Jacobsen and H. G. Fritz, *Macromol. Symp.*, 1999, **144**, 289-302.
23. M. Ryner, K. Stridsberg, A. C. Albertsson, H. von Schenck and M. Svensson, *Macromolecules*, 2001, **34**, 3877-3881.
24. A. P. Dove, V. C. Gibson, E. L. Marshall, A. J. P. White and D. J. Williams, *Chem. Commun.*, 2001, 283-284.
25. A. P. Dove, V. C. Gibson, E. L. Marshall, H. S. Rzepa, A. J. P. White and D. J. Williams, *J. Am. Chem. Soc.*, 2006, **128**, 9834-9843.
26. N. Nimitsiriwat, V. C. Gibson, E. L. Marshall, A. J. P. White, S. H. Dale and M. R. J. Elsegood, *Dalton Trans.*, 2007, 4464-4471.
27. A. Kowalski, A. Duda and S. Penczek, *Macromolecules*, 1998, **31**, 2114-2122.
28. L. Trofimoff, T. Aida and S. Inoue, *Chem. Lett.*, 1987, 991-994.
29. Z. Y. Zhong, P. J. Dijkstra and J. Feijen, *J. Am. Chem. Soc.*, 2003, **125**, 11291-11298.
30. N. Spassky, M. Wisniewski, C. Pluta and A. LeBorgne, *Macromol. Chem. Phys.*, 1996, **197**, 2627-2637.
31. T. M. Ovitt and G. W. Coates, *J. Am. Chem. Soc.*, 2002, **124**, 1316-1326.
32. N. Nomura, R. Ishii, M. Akakura and K. Aoi, *J. Am. Chem. Soc.*, 2002, **124**, 5938-5939.
33. Z. Y. Zhong, P. J. Dijkstra and J. Feijen, *Angew. Chem., Int. Ed. Engl.*, 2002, **41**, 4510-4513.

34. N. C. Johnstone, E. S. Aazam, P. B. Hitchcock and J. R. Fulton, *J. Organomet. Chem.*, 2010, **695**, 170-176.
35. P. Hormnirun, E. L. Marshall, V. C. Gibson, A. J. P. White and D. J. Williams, *J. Am. Chem. Soc.*, 2004, **126**, 2688-2689.
36. H. Z. Du, A. H. Velders, P. J. Dijkstra, J. R. Sun, Z. Y. Zhong, X. S. Chen and J. Feijen, *Chem. Eur. J.*, 2009, **15**, 9836-9845.
37. B. Lian, H. Y. Ma, T. P. Spaniol and J. Okuda, *Dalton Trans.*, 2009, 9033-9042.
38. F. Qian, K. Y. Liu and H. Y. Ma, *Dalton Trans.*, 2010, **39**, 8071-8083.
39. Z. H. Tang and V. C. Gibson, *Eur. Polym. J.*, 2007, **43**, 150-155.
40. K. Phomphrai, P. Chumsaeng, P. Sangtrirutnugul, P. Kongsaeree and M. Pohmakotr, *Dalton Trans.*, 2010, **39**, 1865-1871.
41. H. R. Kricheldorf, M. Berl and N. Scharnagl, *Macromolecules*, 1988, **21**, 286-293.
42. J. Baran, A. Duda, A. Kowalski, R. Szymanski and S. Penczek, *Macromol. Symp.*, 1997, **123**, 93-101.
43. Y. Nakayama, K. Watanabe, N. Ueyama, A. Nakamura, A. Harada and J. Okuda, *Organometallics*, 2000, **19**, 2498-2503.
44. Y. Takashima, Y. Nakayama, T. Hirao, H. Yasuda and A. Harada, *J. Organomet. Chem.*, 2004, **689**, 612-619.
45. Y. Takashima, Y. Nakayama, K. Watanabe, T. Itono, N. Ueyama, A. Nakamura, H. Yasuda, A. Harada and J. Okuda, *Macromolecules*, 2002, **35**, 7538-7544.
46. Y. Kim and J. G. Verkade, *Organometallics*, 2002, **21**, 2395-2399.
47. Y. Kim, G. K. Jnaneshwara and J. G. Verkade, *Inorg. Chem.*, 2003, **42**, 1437-1447.
48. Y. Kim and J. G. Verkade, *Macromol. Symp.*, 2005, **224**, 105-117.
49. Y. J. Kim and J. G. Verkade, *Macromol. Rapid Commun.*, 2002, **23**, 917-921.
50. F. Gornshtein, M. Kapon, M. Botoshansky and M. S. Eisen, *Organometallics*, 2007, **26**, 497-507.
51. C. K. A. Gregson, I. J. Blackmore, V. C. Gibson, N. J. Long, E. L. Marshall and A. J. P. White, *Dalton Trans.*, 2006, 3134-3140.
52. E. Sergeeva, J. Kopilov, I. Goldberg and M. Kol, *Inorg. Chem.*, 2010, **49**, 3977-3979.
53. E. Sergeeva, J. Kopilov, I. Goldberg and M. Kol, *Inorg. Chem.*, 2009, **48**, 8075-8077.
54. A. J. Chmura, D. M. Cousins, M. G. Davidson, M. D. Jones, M. D. Lunn and M. F. Mahon, *Dalton Trans.*, 2008, 1437-1443.
55. A. Stopper, I. Goldberg and M. Kol, *Inorg. Chem. Commun.*, 2011, **14**, 715-718.
56. J. C. Buffet and J. Okuda, *Chem. Commun.*, 2011, **47**, 4796-4798.
57. A. J. Chmura, M. G. Davidson, M. D. Jones, M. D. Lunn, M. F. Mahon, A. F. Johnson, P. Khunkamchoo, S. L. Roberts and S. S. F. Wong, *Macromolecules*, 2006, **39**, 7250-7257.
58. M. G. Hu, M. Wang, H. J. Zhu, L. Zhang, H. Zhang and L. C. Sun, *Dalton Trans.*, 2010, **39**, 4440-4446.
59. A. J. Chmura, M. G. Davidson, C. J. Frankis, M. D. Jones and M. D. Lunn, *Chem. Commun.*, 2008, 1293-1295.
60. M. Kol, M. Shamis, I. Goldberg, Z. Goldschmidt, S. Alfi and E. Hayut-Salant, *Inorg. Chem. Commun.*, 2001, **4**, 177-179.
61. A. D. Schwarz, K. R. Herbert, C. Paniagua and P. Mountford, *Organometallics*, 2010, **29**, 4171-4188.
62. A. D. Schwarz, A. L. Thompson and P. Mountford, *Inorg. Chem.*, 2009, **48**, 10442-10454.
63. S. K. Russell, C. L. Gamble, K. J. Gibbins, K. C. S. Juhl, W. S. Mitchell, A. J. Tumas and G. E. Hofmeister, *Macromolecules*, 2005, **38**, 10336-10340.

64. K. Krauzy-Dziedzic, J. Ejfler, S. Szafert and P. Sobota, *Dalton Trans.*, 2008, 2620-2626.
65. G. F. Zi, Q. W. Wang, L. Xiang and H. B. Song, *Dalton Trans.*, 2008, 5930-5944.
66. L. M. Hodgson, R. H. Platel, A. J. P. White and C. K. Williams, *Macromolecules*, 2008, **41**, 8603-8607.
67. R. H. Platel, A. J. P. White and C. K. Williams, *Inorg. Chem.*, 2011, **50**, 7718-7728.
68. M. Mazzeo, M. Lamberti, I. D'Auria, S. Milione, J. C. Peters and C. Pellecchia, *J. Polym. Sci., part A: Polym Chem.,* 2010, **48**, 1374-1382.
69. I. D'Auria, M. Mazzeo, D. Pappalardo, M. Lamberti and C. Pellecchia, *Journal of Polymer Science Part a-Polymer Chemistry*, 2011, **49**, 403-413.
70. E. Grunova, E. Kirillov, T. Roisnel and J. F. Carpentier, *Dalton Trans.*, 2010, **39**, 6739-6752.
71. Y. J. Luo, W. Y. Li, D. Lin, Y. M. Yao, Y. Zhang and Q. Shen, *Organometallics*, 2010, **29**, 3507-3514.
72. K. Nie, X. Y. Gu, Y. M. Yao, Y. Zhang and Q. Shen, *Dalton Trans.*, 2010, **39**, 6832-6840.
73. L. Clark, M. G. Cushion, H. E. Dyer, A. D. Schwarz, R. Duchateau and P. Mountford, *Chem. Commun.*, 2010, **46**, 273-275.
74. L. Clark, G. B. Deacon, C. M. Forsyth, P. C. Junk, P. Mountford and J. P. Townley, *Dalton Trans.*, 2010, **39**, 6693-6704.
75. H. E. Dyer, S. Huijser, N. Susperregui, F. Bonnet, A. D. Schwarz, R. Duchateau, L. Maron and P. Mountford, *Organometallics*, 2010, **29**, 3602-3621.
76. A. Otero, A. Lara-Sanchez, J. Fernandez-Baeza, C. Alonso-Moreno, I. Marquez-Segovia, L. F. Sanchez-Barba, J. A. Castro-Osma and A. M. Rodriguez, *Dalton Trans.*, 2011, **40**, 4687-4696.
77. D. Patel, S. T. Liddle, S. A. Mungur, M. Rodden, A. J. Blake and P. L. Arnold, *Chem. Commun.*, 2006, 1124-1126.
78. M. Cheng, A. B. Attygalle, E. B. Lobkovsky and G. W. Coates, *J. Am. Chem. Soc.*, 1999, **121**, 11583-11584.
79. C. N. Ayala, M. H. Chisholm, J. C. Gallucci and C. Krempner, *Dalton Trans.*, 2009, 9237-9245.
80. C. Alonso-Moreno, A. Garces, L. F. Sanchez-Barba, M. Fajardo, J. Fernandez-Baeza, A. Otero, A. Lara-Sanchez, A. Antinolo, L. Broomfield, M. I. Lopez-Solera and A. M. Rodriguez, *Organometallics*, 2008, **27**, 1310-1321.
81. A. Garces, L. F. Sanchez-Barba, C. Alonso-Moreno, M. Fajardo, J. Fernandez-Baeza, A. Otero, A. Lara-Sanchez, I. Lopez-Solera and A. M. Rodriguez, *Inorg. Chem.*, 2010, **49**, 2859-2871.
82. Y. Huang, W. C. Hung, M. Y. Liao, T. E. Tsai, Y. L. Peng and C. C. Lin, *J. Polym. Sci. Part A: Polym. Chem.* 2009, **47**, 2318-2329.
83. C. K. Williams, L. E. Breyfogle, S. K. Choi, W. Nam, V. G. Young, M. A. Hillmyer and W. B. Tolman, *J. Am. Chem. Soc.*, 2003, **125**, 11350-11359.
84. E. Grunova, T. Roisnel and J. F. Carpentier, *Dalton Trans.*, 2009, 9010-9019.
85. C. K. Williams, N. R. Brooks, M. A. Hillmyer and W. B. Tolman, *Chem. Commun.*, 2002, 2132-2133.
86. P. D. Knight, A. J. P. White and C. K. Williams, *Inorg. Chem.*, 2008, **47**, 11711-11719.
87. L. E. Breyfogle, C. K. Williams, V. G. Young, M. A. Hillmyer and W. B. Tolman, *Dalton Trans.*, 2006, 928-936.
88. C. A. Wheaton and P. G. Hayes, *Dalton Trans.*, 2010, **39**, 3861-3869.
89. C. A. Wheaton and P. G. Hayes, *Chem. Commun.*, 2010, **46**, 8404-8406.
90. www.blockcopolymers.com

91. http://goldbook.iupac.org
92. S. Chatti and H. R. Kricheldorf, *J. Macromol. Sci., Part A: Pure Appl. Chem.,* 2006, **43**, 967-975.
93. R. Casarano, D. F. S. Petri, M. Jaffe and L. H. Catalani, *J. Braz. Chem. Soc.*, 2009, **20**, 1414-1424.
94. R. Casarano, R. Bentini, V. B. Bueno, T. Iacovella, F. B. F. Monteiro, F. A. S. Iha, A. Campa, D. F. S. Petri, M. Jaffe and L. H. Catalani, *Polymer*, 2009, **50**, 6218-6227.
95. B. D. Ulery, L. S. Nair and C. T. Laurencin, *J. Polym. Sci., Part B: Polym. Phys.,* 2011, **49**, 832-864.
96. H. R. Kricheldorf, G. Behnken, G. Schwarz, P. Simon and M. Brinkmann, *J. Macromol. Sci., Part A: Pure Appl. Chem.,*2009, **46**, 353-359.
97. H. R. Kricheldorf and A. Stricker, *Macromol. Chem. Phys.*, 2000, **201**, 2557-2565.
98. Z. Zhang, R. Kuijer, S. K. Bulstra, D. W. Grijpma and J. Feijen, *Biomaterials*, 2006, **27**, 1741-1748.
99. J. Y. Liu, C. Zhang and L. J. Liu, *J. Appl. Polym. Sci.*, 2008, **107**, 3275-3279.
100. H. R. Kricheldorf and B. Weegenschulz, *J. Polym. Sci. Part A: Polym. Chem.,*1995, **33**, 2193-2201.
101. H. R. Kricheldorf and B. Weegenschulz, *J. Macromol. Sci., Part A: Pure Appl. Chem.,* 1995, **A32**, 1847-1862.
102. H. R. Kricheldorf and B. WeegenSchulz, *Polymer*, 1995, **36**, 4997-5003.
103. D. J. Darensbourg, P. Ganguly and D. Billodeaux, *Macromolecules*, 2005, **38**, 5406-5410.
104. D. J. Darensbourg, W. Choi, O. Karroonnirun and N. Bhuvanesh, *Macromolecules*, 2008, **41**, 3493-3502.
105. D. Pospiech, H. Komber, D. Jehnichen, L. Haussler, K. Eckstein, H. Scheibner, A. Janke, H. R. Kricheldorf and O. Petermann, *Biomacromolecules*, 2005, **6**, 439-446.
106. J. Cai, K. J. Zhu and S. L. Yang, *Polymer*, 1998, **39**, 4409-4415.
107. A. P. Pego, A. A. Poot, D. W. Grijpma and J. Feijen, *Macromol. Biosci.*, 2002, **2**, 411-419.
108. J. A. Yang, F. Liu, S. Tu, Y. W. Chen, X. L. Luo, Z. Q. Lu, J. Wei and S. M. Li, *J. Biomed. Mater. Res., Part A,*2010, **94A**, 396-407.
109. J. Yang, F. Liu, L. Yang and S. M. Li, *Eur. Polym. J.*, 2010, **46**, 783-791.
110. P. Dobrzynski and J. Kasperczyk, *J. Polym. Sci., Part A: Polym. Chem.,*2006, **44**, 3184-3201.

# Chapter 2

# Group (IV) amine *tris*(phenolate) complexes as initiators for the ROP of *rac*-LA

# 2. Group (IV) amine *tris*(phenolate) complexes as initiators for the ROP of *rac*-LA.

## 2.1 Preamble

As mentioned in Chapter 1, Section 1.3.3, Davidson *et al.* reported the use of group (IV) $C_3$-symmetric amine *tris*(phenolate) complexes for the ROP of *rac*-LA. Results indicated that highly heterotactic PLA could be produced under solvent-free conditions after just 6 minutes.[1] It was also shown that when tetradentate amine *bis*(phenolate) ligands were complexed to zirconium and hafnium, the resulting pseudo $C_2$-symmetric initiators showed stereoselectivity in the ROP of *rac*-LA. Isotactically enriched PLA was produced under both solution and solvent-free conditions, however a longer reaction time was necessary to achieve high yields, than the $C_3$-symmetric amine *tris*(phenolate) complexes.[2]

This chapter therefore describes the preparation and complexation of a range of pseudo $C_2$-symmetric amine *tris*(phenolate)s to group (IV) metals. It is the intention that by utilising *tris*(phenolate) ligands, high activity and control will be observed, and the polymerisation will occur with stereocontrol from the complexes exhibiting pseudo $C_2$-symmetry. The ligands described herein are modified versions of the $C_3$-symmetric amine (*tris*)phenolate ligands reported by Davidson *et al.* where a methylene bridge has been removed. Such ligands have previously been complexed to Fe(III) for the epoxidation of styrene.[3] The sterics and electronics of the substituents on one of the phenoxide moieties have been varied and their effect on the ROP of *rac*-LA also compared.

Investigation into the use of such initiators for the production of copolymers has also been carried out. It is the goal that by synthesising copolymers of *rac*-LA and either 1,3-dioxan-2-one (TMC) or isosorbide, the resulting properties of the polymer can be tuned to be more applicable to the end use. For example the water solubility of the resulting polymer could be increased

by incorporating isosorbide into the PLA chain. The homopolymerisation of TMC is also discussed using the group (IV) complexes reported here in.

## 2.2 Preparation of amine *tris*(phenolate) ligands

The ligands used were all prepared according to literature procedures,[3, 4] (Figure 2.01) and were achieved in yields > 55 % after purification.

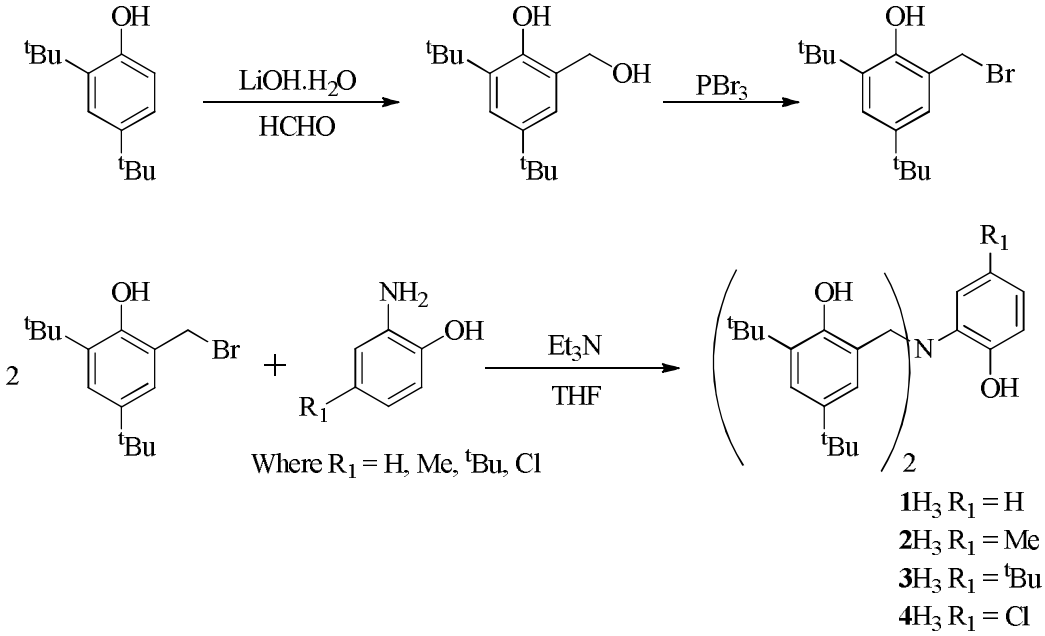


**Figure 2.01**: Preparation of amine (*tris*)phenolate ligands[3, 4]

The ligands shown in Figure 2.01, not only allow a comparison in the effect of varying the sterics on the ROP of *rac*-LA (ligands **1**$H_3$ to **3**$H_3$) but also the effect of varying the electronic nature of the ligand (**4**$H_3$). Unfortunately, it was not possible to obtain single crystal X-ray diffraction structures for any of the ligands shown in Figure 2.01. However, all ligands were characterised by $^{1}H$ and $^{13}C\{^{1}H\}$ NMR spectroscopy together with high resolution mass spectrometry. After initial analysis of the crude ligand, it was observed from $^{1}H$ NMR spectroscopy that in some instances resonances corresponding to $Et_3N^+Br^-$ were present. It was therefore necessary to carry out flash chromatography to isolate pure material using $CHCl_3$ as the solvent, Figure 2.02.

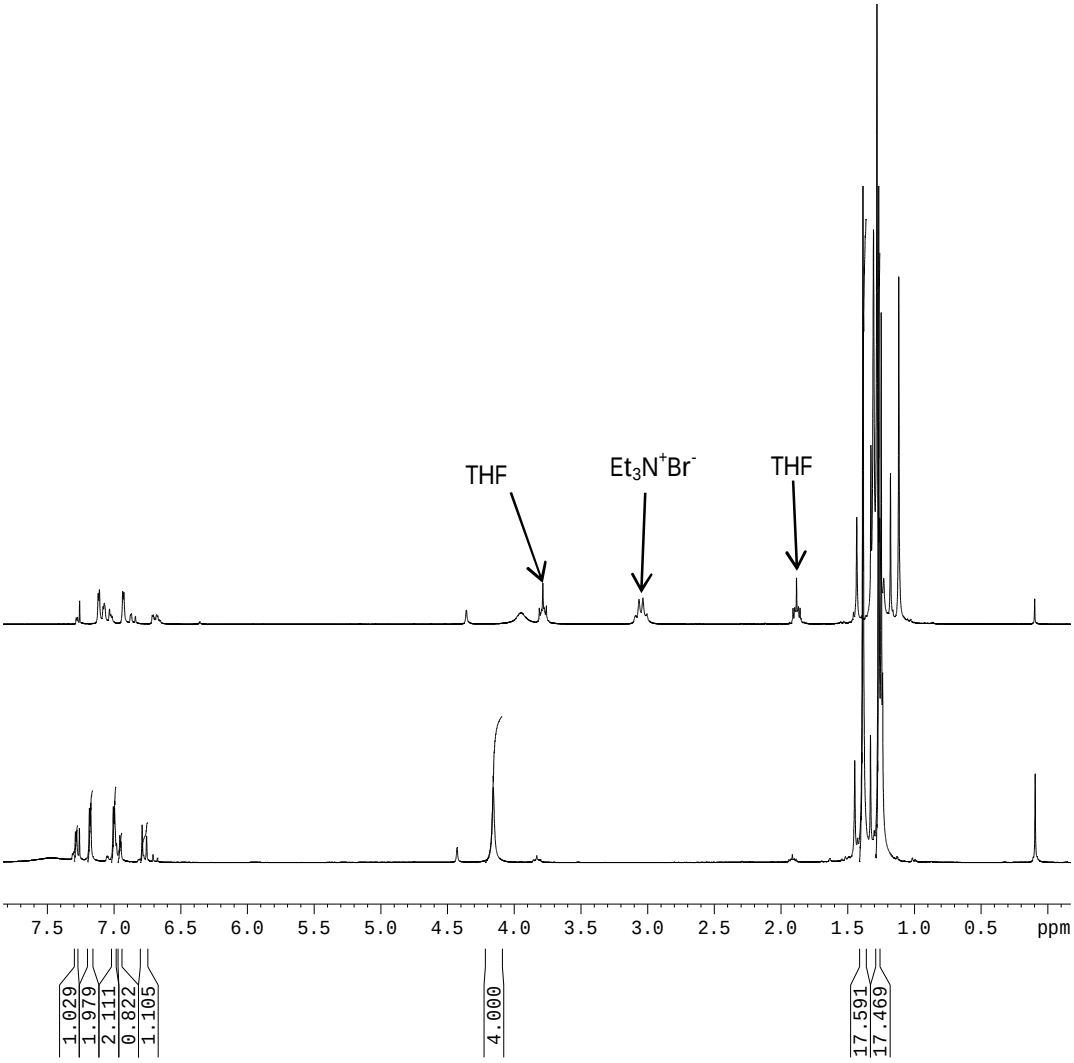


**Figure 2.02**: $^{1}$H NMR spectra - top: **3**$H_3$ before purification *via* flash chromatography, lower: **3**$H_3$ after purification *via* flash chromatography.

It can be seen from Figure 2.02 that the top spectrum clearly indicates the presence of not only a triethylamine hydrobromide salt produced in the second stage of ligand preparation, but also the presence of additional $CH_3$ resonances between 1.0 – 1.5 ppm. These additional $CH_3$ resonances are due to the presence of remaining starting material, which can be removed upon purification – lower spectrum Figure 2.02.

## 2.3 Complexing amine *tris*(phenolate) ligands to group (IV) metals

The ligands shown in Figure 2.01 were complexed to group (IV) metals using a 1:1 stoichiomery of the appropriate ligand and metal alkoxide in toluene, as shown in Figure 2.03.[5]

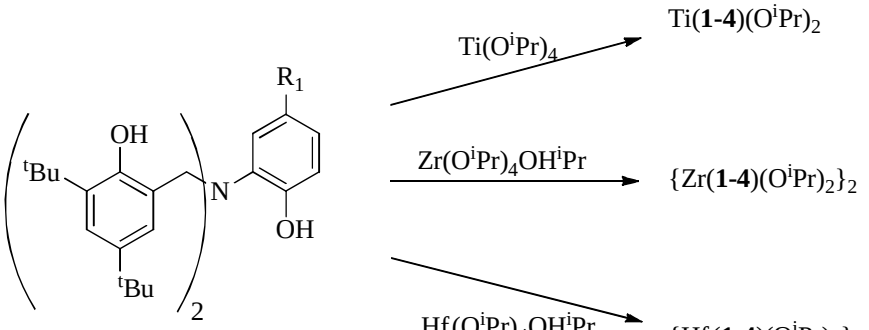


**1**H$_3$ R$_1$ = H
**2**H$_3$ R$_1$ = Me
**3**H$_3$ R$_1$ = $^t$Bu
**4**H$_3$ R$_1$ = Cl

**Figure 2.03**: Complexes prepared using amine *tris*(phenolate) ligands

### 2.3.1 Titanium amine *tris*(phenolate) complexes

The titanium complexes were characterised by $^1$H NMR, $^{13}$C{$^1$H} NMR spectroscopy, elemental analysis and single crystal X-ray diffraction. All of the complexes were shown to be monometallic even when the steric bulk of the ligand was increased to incorporate a $^t$Bu group Ti(**3**)O$^i$Pr (Figure 2.04), or the electronics were altered – Ti(**4**)O$^i$Pr (Figure 2.05).

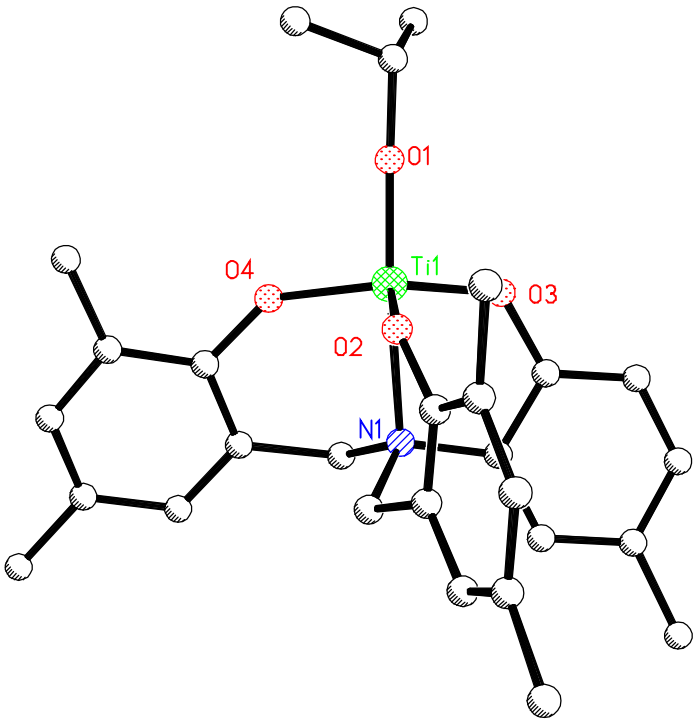


**Figure 2.04**: Solid-state structure of Ti(**3**)O$^{i}$Pr where the methyl groups of all the $^{t}$Bu's have been removed for clarity as have the H atoms.

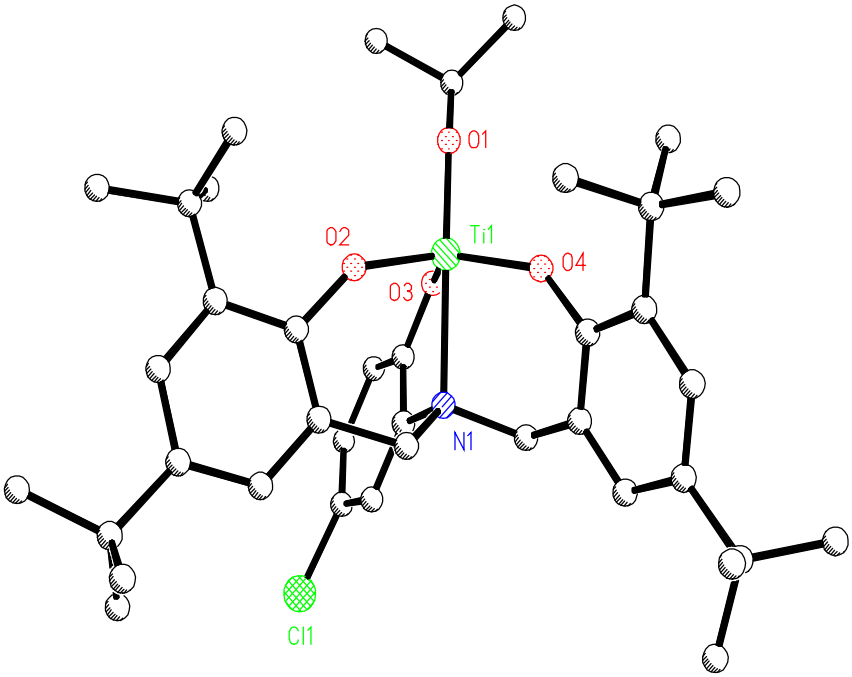


**Figure 2.05**: Solid-state structure of Ti(**4**)O$^{i}$Pr where the H atoms have been removed for clarity.

The complexes are pseudo trigonal bipyramidal, with a typical {O(4)-Ti(1)-O(2)} angle of around 120 $^{o}$.

| | Ti(**1**)O$^{i}$Pr | Ti(**2**)O$^{i}$Pr | Ti(**3**)O$^{i}$Pr | Ti(**4**)O$^{i}$Pr | [$O_3$N]Ti(O$^{i}$Pr)$^{6}$ |
|---|---|---|---|---|---|
| Ti(1)-O(1) | 1.769(16) | 1.767(2) | 1.767(19) | 1.785(2) | 1.778(4) |
| Ti(1)-O(2) | 1.8524(16) | 1.8570(19) | 1.8168(19) | 1.818(2) | 1.833(6) |
| Ti(1)-O(3) | 1.8729(17) | 1.8680(2) | 1.8841(19) | 1.886(2) | 1.866(6) |
| Ti(1)-O(4) | 1.8237(16) | 1.8200(19) | 1.8430(19) | 1.835(2) | 1.825(6) |
| Ti(1)-N(1) | 2.332(2) | 2.328(2) | 2.347(2) | 2.313(3) | 2.334(5) |
| O(1)-Ti(1)-O(3) | 99.44(8) | 102.59(10) | 97.74(9) | 94.06(11) | - |
| N(1)-Ti(1)-O(1) | 176.74(8) | 172.39(10) | 173.45(9) | 170.85(11) | - |
| Ti(1)-O(1)-C$^{i}$Pr | 162.80(16) | 164.0(3) | 177.9(2) | 143.5(2) | 164.4(6) |

**Table 2.01**: Selected bond lengths (Å) and bond angles (°) for Ti(**1-4**)O$^{i}$Pr and [$O_3$N]Ti(O$^{i}$Pr)$^{6}$

It can be seen from Table 2.01 that the {Ti(1)-O(1)-C$^{i}$P$_r$} bond angle increases as the steric bulk is increased but drastically decreases for Ti(**4**)O$^{i}$Pr, which contains a chloro substituent. By incorporation of a chloro group into the ligand, the length of the {Ti(1)-O(1)} bond is statistically longer than those observed for other ligands. However, the {Ti(1)-N(1)} bond is decreased in length. The metric data shown in Table 2.01 for the titanium complexes are consistent with previously characterised titanium complexes, such as the *C*$_3$-symmetric complexes reported by Kol *et al.* which contain $^{t}$Bu substituents at the *ortho* and *para* positions on the phenolate rings.[6] The data for such compounds are also shown in Table 2.01.[6] Titanium complexes containing *C*$_3$-symmetric amine *tris*(phenolate) ligands similar to that reported by Kol *et al.*[6] where the labile isopropoxide group has been replaced with, for example, a chloro group have also been reported in the literature.[7] Substitution of the isopropoxide group with a poorer π donor results in a longer Ti-Cl bond of 2.3074(7) Å compared with Ti-O(1) values shown in Table 2.01.[7] Consequently, the Ti-N bond length for such a compound is statistically shorter {2.216(2) Å}.[7] The data

shown in Table 2.01 is also consistent with another titanium complex containing an achiral *tris*(phenol) ligand, with a Ti-O-C$^{i}$Pr angle of 154.5(2) °.[8] Such complexes however have been reported to exist in a dimeric form with O-Ti-O angles ranging from 107 – 112 °.[8] Kol *et al.* have isolated monomeric titanium *bis*(phenolate) complexes which show larger O-Ti-O angles of around 160 ° but analogous Ti-N bond lengths of around 2.3 Å.[9]

Both the $^{1}$H and $^{13}$C{$^{1}$H} NMR spectra were recorded in $CDCl_3$ at room temperature, and in a typical $^{1}$H NMR spectrum an AX spin system (J = 13.5 Hz) is observed. The methylene protons appear as discrete diastereotopic doublets indicating that the solid-state structure is maintained in solution (Figure 2.06, top spectrum).

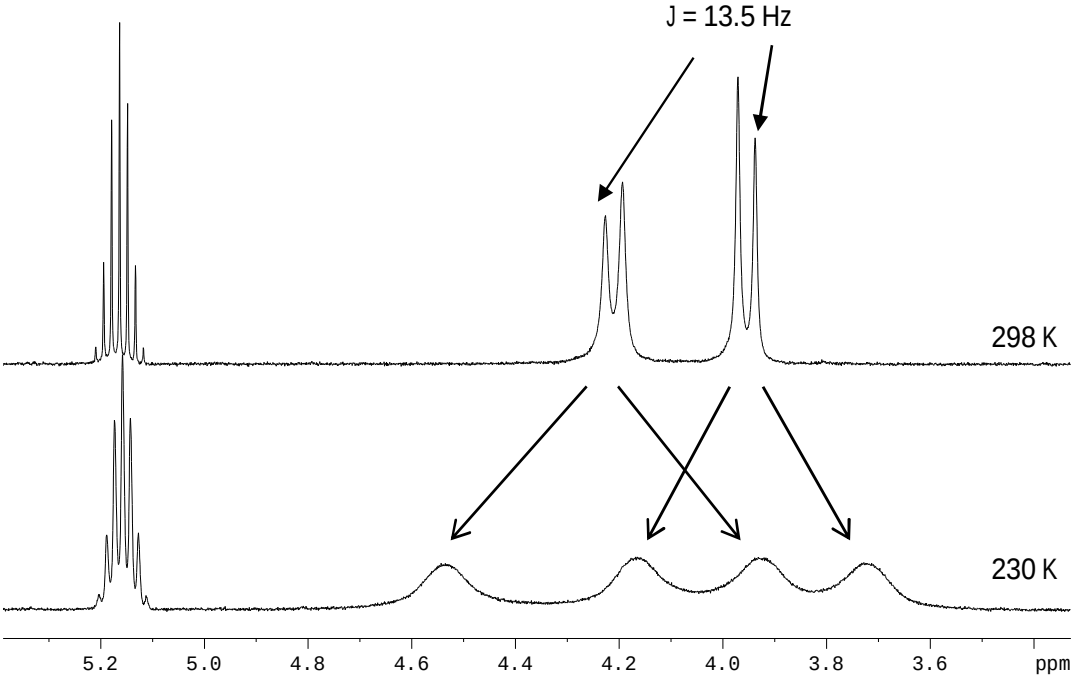


**Figure 2.06**: $^{1}$H NMR spectrum of Ti(**3**)O$^{i}$Pr at 298 K and 230 K in $CDCl_3$

However, when the solution was cooled to 230 K four broad methylene proton resonances of equal intensity were observed in the $^{1}$H NMR spectrum indicating that all the methylene protons have become inequivalent at 230 K - Figure 2.06, lower spectrum. It is hypothesised that at room temperature there is a distinction between the axial and equatorial protons in the methylene groups, but the $CH_2$ groups are equivalent. The J values reported here are in agreement with other AX spin systems reported in literature, such as titanium amine phenolate

complexes reported by Kol *et al.* with J values between 13.4 – 13.9 Hz for the equivalent methylene protons.[5] At lower temperature, the equivalence is lost and therefore, there is now a distinction not only between the axial and equatorial protons but also between the two methylene groups. This is turn results in all four methylene protons becoming inequivalent and hence four resonances are observed in the $^{1}$H NMR spectrum – Figure 2.06, lower spectrum. This is schematically shown in Figure 2.07.

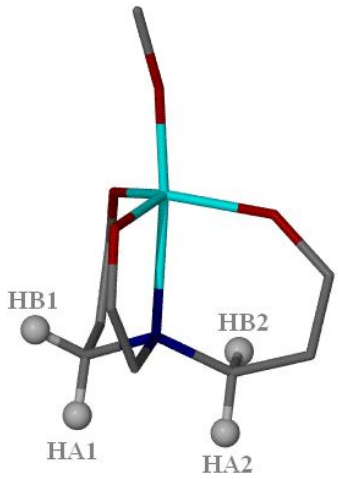


**Figure 2.07**: Schematic representation of Ti complexes labelling methylene protons

Figure 2.07 schematically indicates that at 298 K analysis of the $^{1}$H spectra can be interpreted that $HA_1$ and $HA_2$ are equivalent as are $HB_1$ and $HB_2$. Whereas at 230 K, $HA_1$ and $HA_2$ are inequivalent, as are $HB_1$ and $HB_2$.

### 2.3.2 Zirconium amine *tris*(phenolate) complexes

In contrast to the titanium initiators in Section 2.3.1, the zirconium complexes were isolated as dimers in the solid-state regardless of the steric bulk around the metal (Figures 2.08 and 2.09). In all cases the phenoxide moiety containing the $R_1$ group (Figure 2.01) bridges the two metal centres.

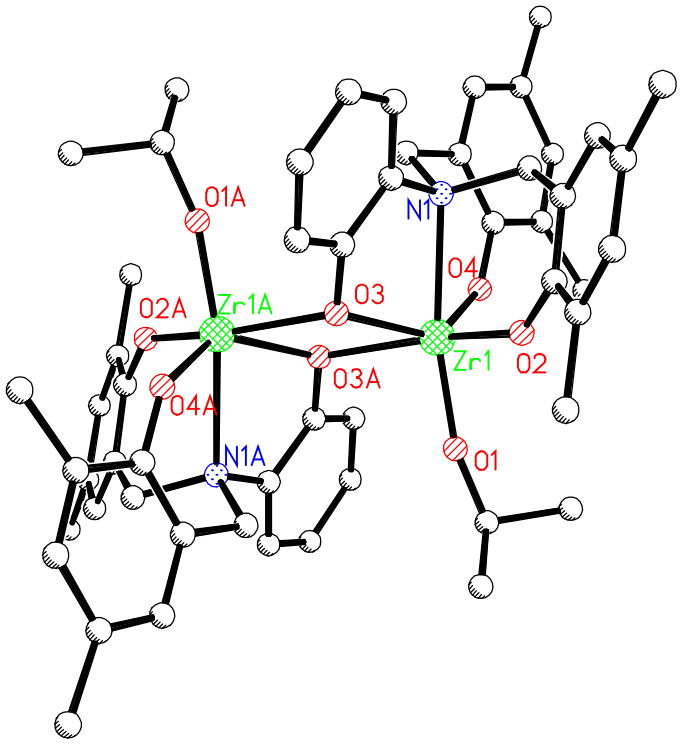


**Figure 2.08**: Solid-state structure of {Zr(**1**)O$^{i}$Pr}$_2$ where the methyl groups of the $^{t}$Bu moieties have been removed for clarity as have the hydrogen atoms. The atoms labelled with an 'A' can be generated by the following symmetry operation: $x + 1, -y + 1, -z$.

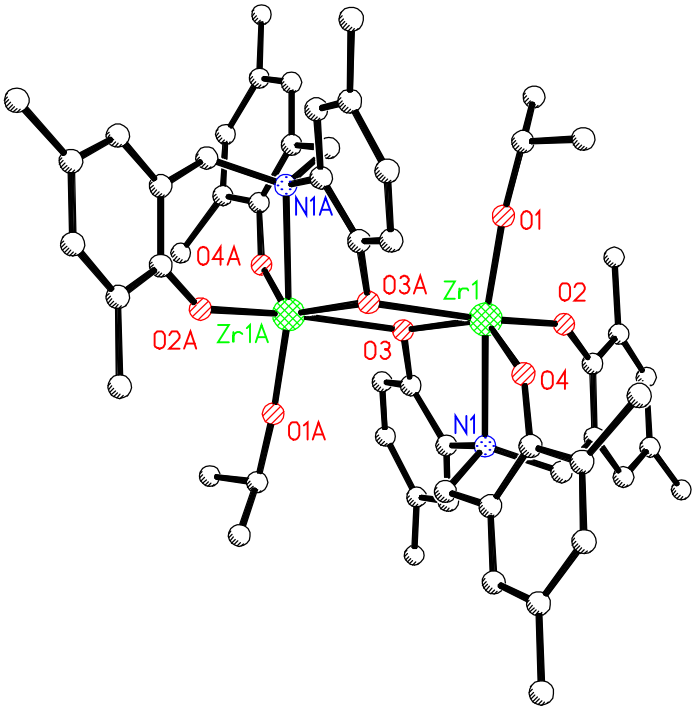


**Figure 2.09**: Solid-state structure of {Zr(**3**)O$^{i}$Pr}$_2$ where the methyl groups of the $^{t}$Bu moieties have been removed for clarity as have the hydrogen atoms. The atoms labelled with an 'A' can be generated by the following symmetry operation: $-x, -y + 1, -z + 1$.

The structures isolated are in contrast to that observed for the more common $C_3$ symmetric zirconium amine *tris(*phenolate) ligand complexes, where monometallic complexes are typically isolated or zwitterionic complexes depending on the steric bulk of the ligand.[5, 10, 11] Unlike the titanium complexes which were pseudo trigonal bipyramidal, the zirconium metal centres are pseudo octahedral with a typical {N(1)-Zr(1)-O(1)} angle of around 170 °. The metric data for the Zr(IV) complexes isolated are given in Table 2.02.

| | {Zr(**1**)O$^i$Pr}$_2$ | {Zr(**2**)O$^i$Pr}$_2$ | {Zr(**3**)O$^i$Pr}$_2$ | (ONO)Zr(O$^i$Pr)$_2$[5] |
|---|---|---|---|---|
| Zr(1)-O(1) | 1.9178(19) | 1.913(2) | 1.916(3) | 1.955(4) & 1.925(4) |
| Zr(1)-O(2) | 1.9950(19) | 1.981(2) | 1.996(3) | 2.038(4) |
| Zr(1)-O(3) | 2.1568(18) | 2.148(2) | 2.151(3) | 2.044(4) |
| Zr(1)-O(3A) | 2.2686(18) | 2.303(2) | 2.288(3) | - |
| Zr(1)-O(4) | 1.9878(19) | 1.991(2) | 1.988(3) | - |
| Zr(1)-N(1) | 2.438(2) | 2.447(3) | 2.443(3) | 2.447(5) |
| O(2)-Zr(1)-O(4) | 109.61(8) | 107.93(9) | 106.55(11) | - |
| N(1)-Zr(1)-O(1) | 168.18(8) | 168.87(9) | 169.01(11) | - |
| Zr(1)-O(1)-C$^i$Pr | 164.8(2) | 173.7(2) | 172.4(3) | 151.3(3) & 167.8(3) |

**Table 2.02**: Selected bond lengths (Å) and bond angles (°) for {Zr(**1-3**)O$^i$Pr}$_2$ and (ONO)Zr(O$^i$Pr)$_2$ for comparison[5]

Due to O(3) bridging the two Zr(IV) centres, the {Zr(1)-O(3)} bond length is longer than {Zr(1)-O(1)} and {Zr(1)-O(2)}. As the steric bulk of the ligand increases, the angle {O(2)-Zr(1)-O(4)} is reduced and upon addition of a substituent on the bridging phenoxide ring, the angle {Zr(1)-O(1)-C$^i$Pr} increases. The data shown in Table 2.02 is consistent with previously reported monomeric zirconium $C_3$ amine *tris*(phenolate) complexes, for example Kol *et al.* reported a

Zr-O$^{i}$Pr bond length of 1.921(5) Å and a Zr-N bond length of 2.439(7) Å.[5] The complexes reported here show comparable bond lengths and angles to analogous zirconium *bis*(phenolate) complexes prepared by Kol *et al.*.[5] An example of such is reported in Table 2.02 {(ONO)Zr(O$^{i}$Pr)$_2$} and contains the ligand shown in Figure 2.10.

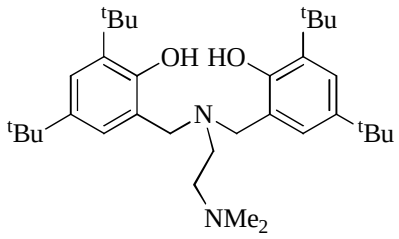


**Figure 2.10**: Amine *bis*(phenolate) ligand used in the preparation of (ONO)Zr(O$^{i}$Pr)$_2$[5]

Two values for {Zr(1)-O(1)} and {Zr(1)-O(1)-C$^{i}$P$_r$} are reported in Table 2.02 for the *bis*(phenolate) complex due to the presence of an additional isopropoxide group which is not observed in the *tris*(phenolate) complexes.

For comparison with the isolated titanium complexes shown in Section 2.3.1, the $^{1}$H NMR spectra of the zirconium complexes were also recorded in $CDCl_3$ at room temperature and at 230 K. In both cases, the spectra were inconclusive and failed to yield any meaningful NMR data (Figure 2.11).

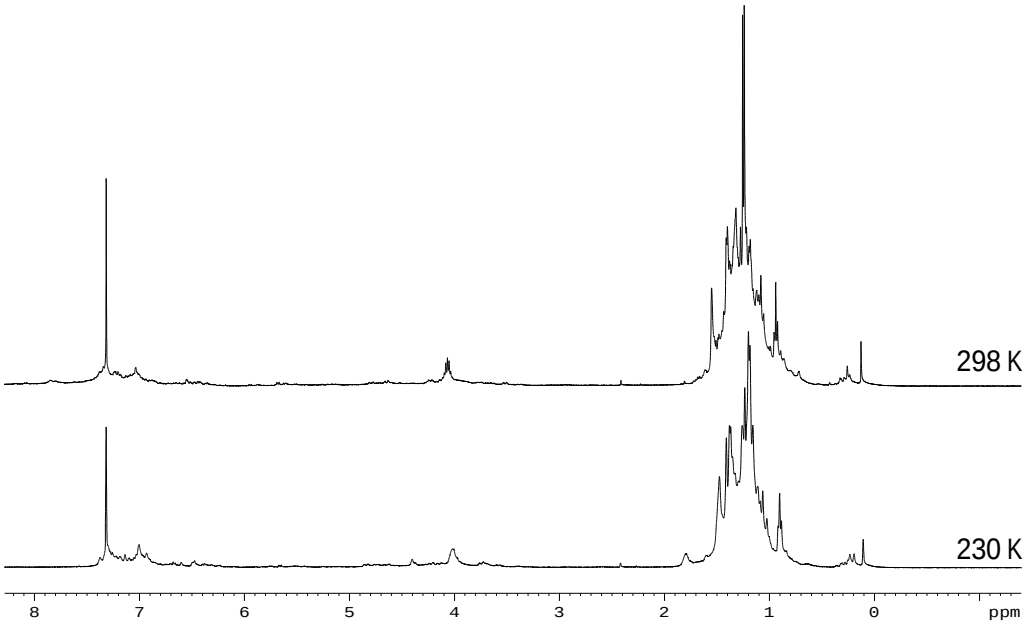


**Figure 2.11**: $^{1}$H NMR spectra of {Zr(**3**)O$^{i}$Pr}$_2$ at 230 K and 298 K in $CDCl_3$

The $^{1}$H NMR spectrum was also recorded in $d_8$-toluene at room temperature (Figure 2.12), but again no meaningful information was garnered.

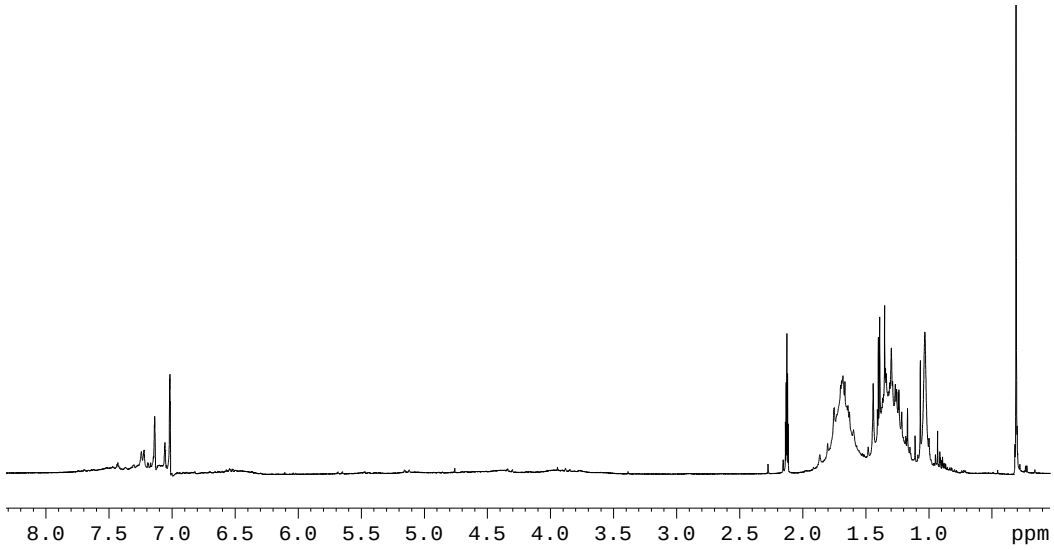


**Figure 2.12**: $^{1}$H NMR spectrum of {Zr(**3**)O$^{i}$Pr}$_2$ in $d_8$-toluene at 298 K

The spectra recorded in both $CDCl_3$ and $d_8$-toluene suggests that there is a considerable degree of fluxionality occurring, presumably due to monomer – oligomer exchange processes occurring on the NMR timescale. A coordinating solvent – $d_8$-THF – was therefore chosen as the preferred solvent to record the NMR spectra of the zirconium complexes, in an attempt to hinder any exchange processes.

At room temperature, the spectrum recorded in $d_8$-THF shows two discrete resonances for the methylene bridges, (Figure 2.13): a broad singlet and a doublet in a 1: 1 ratio.

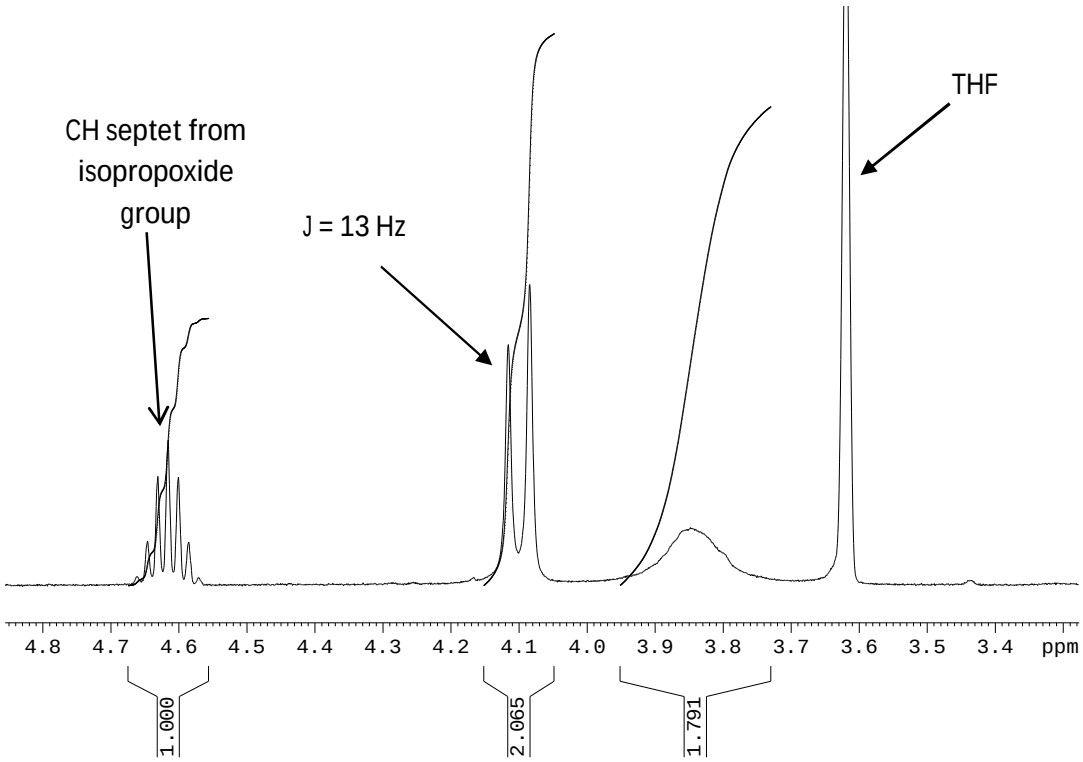


**Figure 2.13**: $^{1}$H NMR spectrum of {Zr(**1**)O$^{i}$Pr}$_2$ in $d_8$-THF at 298 K

It can be seen from Figure 2.13 that the broad singlet corresponding to a methylene $CH_2$ is not clearly defined. This suggests that there is still some degree of fluxionality occurring at room temperature, whether it is between the monomer and oligomer or between THF coordinating and dissociating from the metal centre. To understand more about the structure in solution, the sample in $d_8$-THF was cooled to 230 K (Figure 2.14).

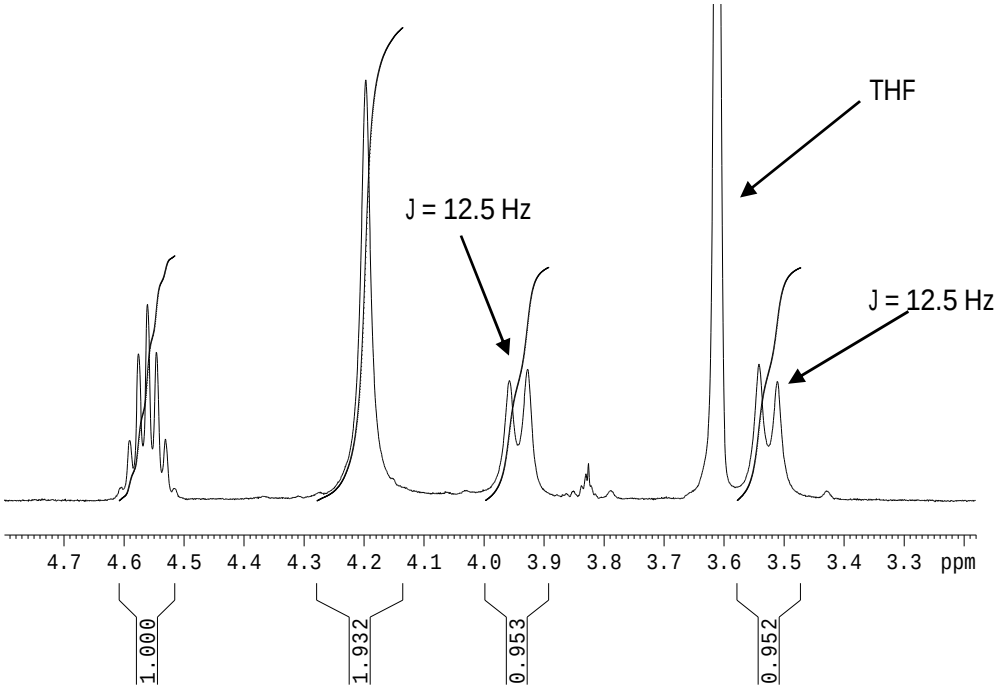


**Figure 2.14**: $^{1}$H NMR spectrum of (Zr(**1**)O$^{i}$Pr)$_2$ in $d_8$-THF at 230 K

As seen from Figure 2.14 the broad singlet has now become two discrete doublets of equal intensity and the distinguished doublet has become a singlet. This must mean that two protons are equivalent and the other two protons of the methylene $CH_2$'s are inequivalent. It is hypothesised that this is consistant with monomeric pseudo octahedral symmetrical complexes with a THF molecule coordinated to the metal centre. For example a similar $^{1}$H NMR spectrum was observed by Brown *et al.* for Ti(IV) amine *tris*(phenolate) systems with acac type ancillary ligands.[12]

The difference in the environment of the diastereotopic methylene protons can be further observed by analysis of the $^{1}$H NMR spectrum of {Zr(**3**)O$^{i}$Pr}$_2$ which contains a more bulky substituted ligand – Figure 2.15.

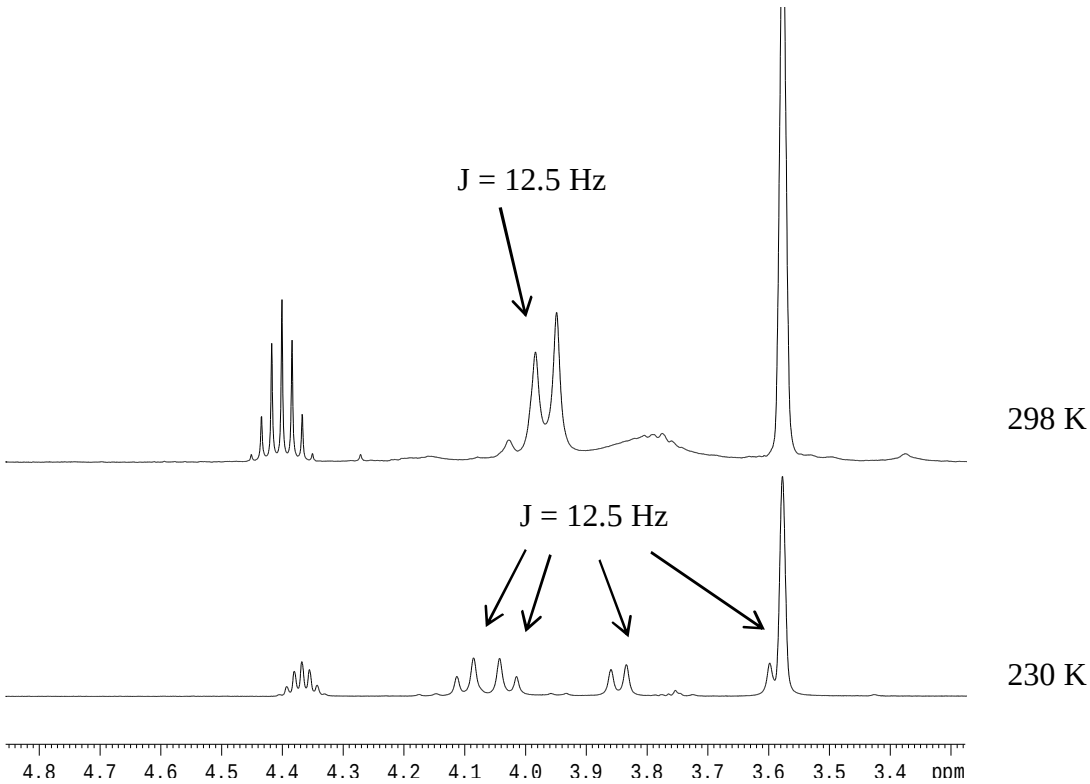


**Figure 2.15**: $^{1}$H NMR spectra of {Zr(**3**)O$^{i}$Pr}$_2$. Top spectrum at 298 K, lower spectrum at 230K

The top spectrum of Figure 2.15 shows the $^{1}$H NMR spectrum of {Zr(**3**)O$^{i}$Pr}$_2$ at room temperature which is analogous to that observed for {Zr(**1**)O$^{i}$Pr}$_2$. The $^{1}$H NMR at 298 K shows a discrete doublet and a broad resonance for the methylene protons. However, when {Zr(**3**)O$^{i}$Pr}$_2$ in $d_8$-THF is cooled to 230 K (lower spectrum), the resonances corresponding to the methylene protons are now distinguished into four separate doublets indicating that all protons are no longer equivalent. One doublet is present under the THF resonance however, from COSY analysis the resonance at 1.85 ppm in the bottom spectrum of Figure 2.15, can be determined as a doublet. Group (IV) monomeric pseudo octahedral complexes at low temperature, were reported to show six discrete resonances for the diastereotopic methylene protons. This is consistent with the doublets observed in Figure 2.14.[12] Upon increasing the temperature it was observed that the resonances broaden and coalesce which is consistent with the data observed in the top spectrum in Figure 2.15.[12]

The difference observed in the $^{1}$H NMR spectra at low temperature for {Zr(**1**)O$^{i}$Pr}$_2$ and {Zr(**3**)O$^{i}$Pr}$_2$ must be attributed to a steric effect from the R group changing from an H to a $^{t}$Bu substituent. The presence of this bulky group

in {Zr(**3**)O$^{i}$Pr}$_2$ dictates that all four methylene protons are no longer equivalent and hence there is the presence of four doublets in the $^1$H NMR spectrum. However, in the absence of a bulky substituent ({Zr(**1**)O$^{i}$Pr}$_2$), not all methylene protons can be distinguished and hence two are observed as a singlet at low temperature in the $^1$H NMR spectrum.

### 2.3.3 Hafnium amine *tris*(phenolate) complexes

The hafnium initiators were prepared in the exact same manner to the titanium initiators in Section 2.3.1 and the zirconium counterparts in Section 2.3.2. Unsurprisingly, ligands **1**H$_2$ – **4**H$_2$ afforded dimeric structures when complexed to hafnium, analogous to the zirconium initiators.

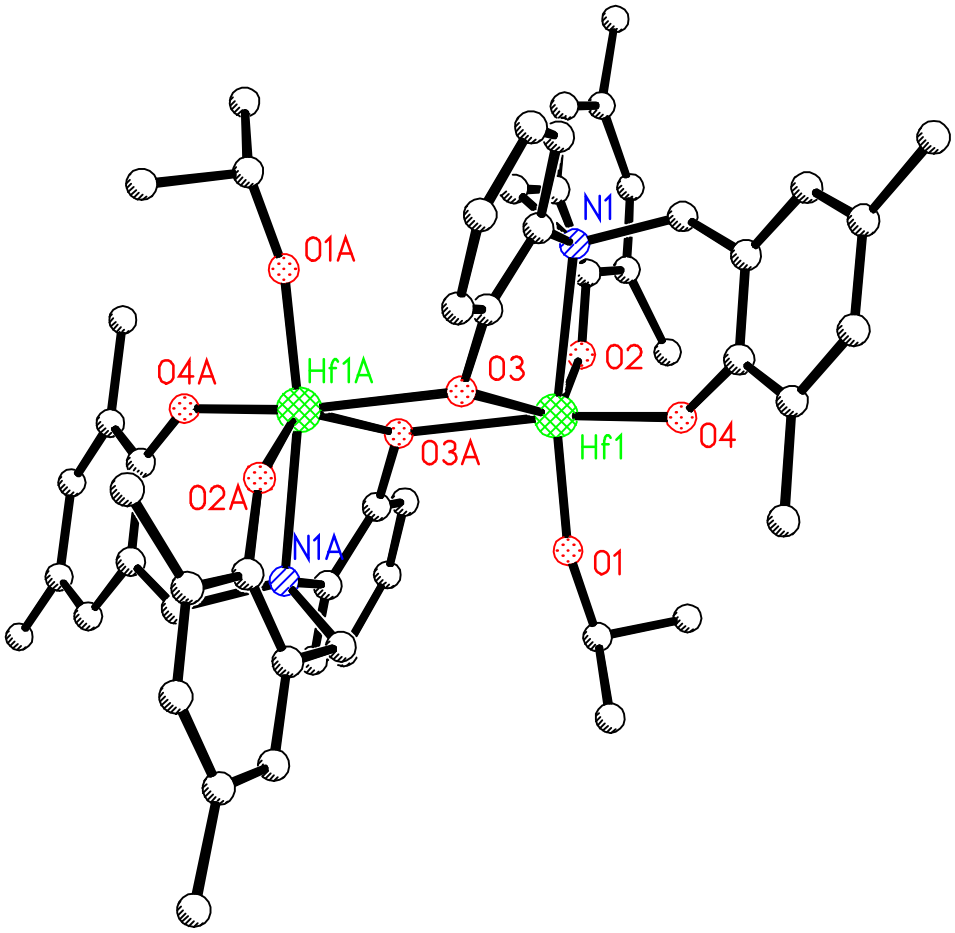


**Figure 2.16**: Solid-state structure of {Hf(**1**)O$^{i}$Pr}$_2$ where the methyl groups of the $^{t}$Bu moieties have been removed for clarity as have the hydrogen atoms. The atoms labelled with an 'A' can be generated by the following symmetry operation: $-x+1, -y, -z$.

Unfortunately, after several attempts it was not possible to achieve X-ray diffraction structures for any other hafnium complexes than {Hf(**1**)O$^i$Pr}$_2$ shown in Figure 2.16.

| | {Hf(**1**)O$^i$Pr}$_2$ | (O$_3$N)Hf(O$^i$Pr)$_2$[1] | {Zr(**1**)O$^i$Pr}$_2$ | Ti(**1**)O$^i$Pr |
|---|---|---|---|---|
| Hf(1)-O(1) | 1.913(3) | 1.920(2) | 1.9178(19) | 1.769(16) |
| Hf(1)-O(2) | 1.972(3) | 1.949(3) | 1.9950(19) | 1.8524(16) |
| Hf(1)-O(3) | 2.142(3) | 1.944(3) | 2.1568(18) | 1.8729(17) |
| Hf(1)-O(3A) | 2.252(3) | - | 2.2686(18) | - |
| Hf(1)-O(4) | 1.987(3) | 1.999(3) | 1.9878(19) | 1.8237(16) |
| Hf(1)-N(1) | 2.417(4) | 2.406(2) | 2.438(2) | 2.332(2) |
| O(2)-Hf(1)-O(4) | 109.09(13) | 116.31(13) | 109.61(8) | 99.44(8) |
| N(1)-Hf(1)-O(1) | 168.61(13) | 179.33(9) | 168.18(8) | 176.74(8) |
| Hf(1)-O(1)-C$^i$Pr | 163.4(4) | 177.6(8) | 164.8(2) | 162.80(16) |

**Table 2.03**: Selected bond lengths (Å) and bond angles (°) for {Hf(**1**)O$^i$Pr}$_2$, (O$_3$N)Hf(O$^i$Pr)$_2$[1], {Zr(**1**)O$^i$Pr}$_2$ and Ti(**1**)O$^i$Pr

As previously reported in Section 2.3.2 for the zirconium initiators, the hafnium complexes isolated also contain pseudo octahedral metal centres with a {N(1)-Hf(1)-O(1)} angle of 168.61(13) °. The bond lengths and angles for {Hf(**1**)O$^i$Pr}$_2$ are comparable with *C*$_3$-symmetric amine *tris*(phenolate) hafnium complexes (see Figure 1.46, Chapter 1) reported by Davidson *et al.* as indicated in Table 2.03 for (O$_3$N)Hf(O$^i$Pr)$_2$.[1] (O$_3$N)Hf(O$^i$Pr)$_2$ has a larger {O(2)-Hf(1)-O(4)} angle than {Hf(**1**)O$^i$Pr)}$_2$ presumably due to the *C*$_3$-symmetric amine *tris*(phenolate) hafnium complex existing in a monomeric form, unlike the dimeric structure shown in Figure 2.16 for {Hf(**1**)O$^i$Pr}$_2$.[1]

The data reported in Table 2.03 is consistent with that for {Zr(**1**)O$^i$Pr}$_2$ and hence for further analysis, the $^1$H and $^{13}$C{$^1$H} NMR spectrum were not

investigated in $CDCl_3$ or $d_8$-toluene. Due to the distinction seen between the resonances in the $^1H$ NMR spectrum when $d_8$-THF is used as the solvent, characterisation of hafnium initiators containing ligands **1**$H_2$ – **4**$H_2$ were analysed in this manner.

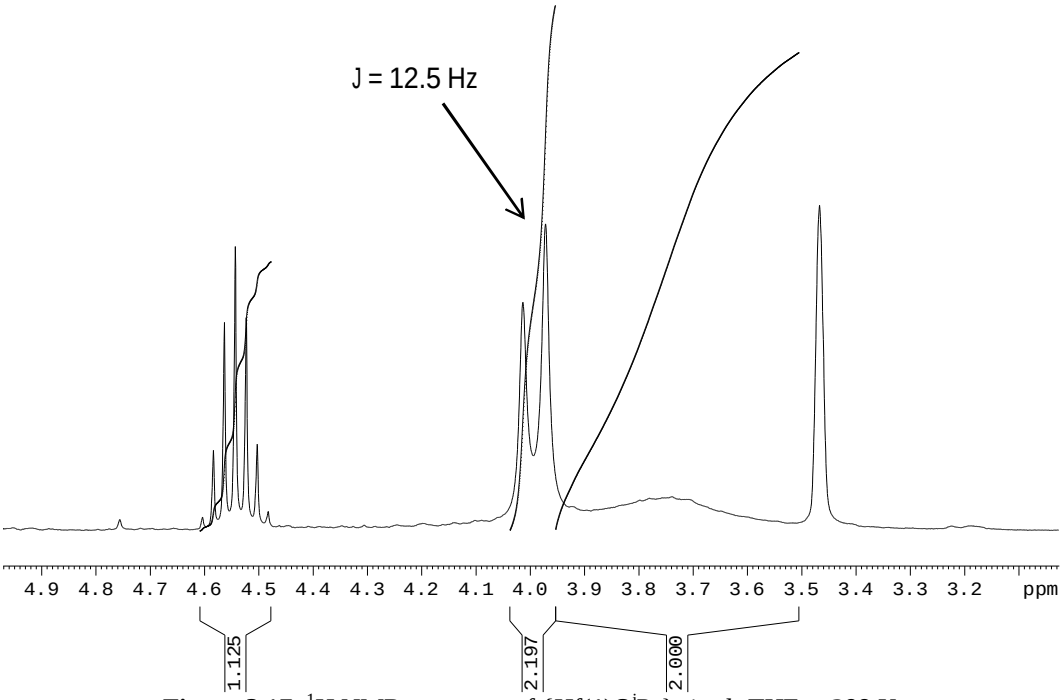


**Figure 2.17**: $^1H$ NMR spectrum of {Hf(**1**)O$^i$Pr}$_2$ in $d_8$-THF at 298 K

Figure 2.17 shows that when the $^1H$ NMR of {Hf(**1**)O$^i$Pr}$_2$ is recorded in $d_8$-THF at 298 K, the methylene protons are observed as a discrete doublet at 4.0 ppm and a broad singlet at 3.7 ppm in a 1:1 ratio. This is in agreement with that observed for {Zr(**1**)O$^i$Pr}$_2$ in Figure 2.13. The presence of the broad singlet is indicative of fluctional processes occurring on the NMR timescale and hence the $^1H$ NMR spectrum was recorded at 230 K to try and resolve any exchange processes.

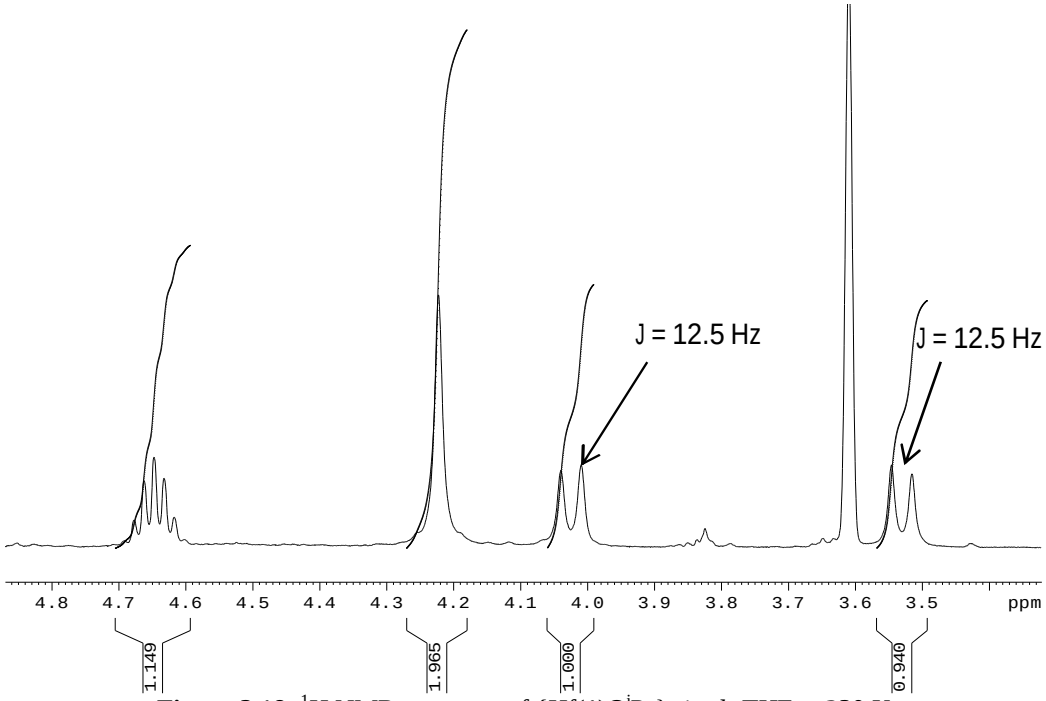


**Figure 2.18**: $^{1}$H NMR spectrum of {Hf(**1**)O$^{i}$Pr}$_2$ in $d_8$-THF at 230 K

When {Hf(**1**)O$^{i}$Pr}$_2$ in $d_8$-THF was cooled to 230 K and the $^{1}$H NMR recorded, the same separation of resonances observed for {Zr(**1**)O$^{i}$Pr}$_2$ was seen such that the broad singlet was split into two discrete doublets of equal intensity and the doublet a singlet. For completeness, the $^{1}$H NMR spectra at 298 K and 230 K were recorded in $d_8$-THF for {Hf(**3**)O$^{i}$Pr}$_2$ which contains the more bulky ligand where R = $^{t}$Bu. Analogous to the zirconium counterpart (Figure 2.13), and {Hf(**1**)O$^{i}$Pr}$_2$ the $^{1}$H NMR spectra of {Hf(**3**)O$^{i}$Pr}$_2$ at 298 K shows a discrete doublet and a broad singlet. However, upon cooling to 230 K, the $^{1}$H NMR spectrum now shows four doublets in a ratio of 1:1:1:1 indicating that all methylene protons are inequivalent. This is presumably due to the effect of the bulky substituent on the bridging phenoxy ring as discussed previously.

## 2.4 Polymerisation of *rac*-LA

The Ti(IV), Zr(IV) and Hf(IV) initiators were trialled for the ROP of *rac*-LA both under solution and melt conditions. For the solution polymerisations the reactions were carried out in ~5 ml of toluene at a temperature of 80 °C using [LA]/[initiator] of 100. The polymerisations were performed for a reaction time of either 2 hours or 24 hours and 0.7 g of *rac*-LA was utilised. In comparison the

solvent-free or melt polymerisations were carried out in the absence of solvent at a temperature of 130 °C. The [LA]:[initiator] ratio employed in such polymerisations was 300: 1 using 2 g of *rac*-LA in each case.

### 2.4.1 Titanium Initiators

The titanium initiators: Ti(**1-4**)O$^{i}$Pr were trialled for the ROP of *rac*-LA in toluene at 80 °C for 2 hours and 24 hours. Unfortunately, the polymerisations after a reaction time of 2 hours failed to produce any polymeric material and hence only the data obtained from the reaction after 24 hours are reported in Table 2.04 below.

| Entry | Initiator | Conversion[a] (%) | $M_n$[b] | $M_w$[b] | $M_n$ (theo.) | PDI[b] | $P_r$[c] |
|---|---|---|---|---|---|---|---|
| **1** | Ti(**1**)O$^{i}$Pr | 85 | 12100 | 13800 | 12300 | 1.14 | 0.5 |
| **2** | Ti(**2**)O$^{i}$Pr | 96 | 11350 | 23450 | 13900 | 2.07 | 0.5 |
| **3** | Ti(**3**)O$^{i}$Pr | - | - | - | - | - | - |
| **4** | Ti(**4**)O$^{i}$Pr | 96 | 23100 | 47600 | 13900 | 2.06 | 0.5 |

**Table 2.04**: ROP results for Ti(**1-4**)O$^{i}$Pr in toluene at 80 °C for 24 hours. 0.7 g of *rac*-LA, [LA]/[initiator] = 100. [a] conversion as determined *via* $^{1}$H NMR, [b] determined from GPC (in THF) referenced to polystyrene, [c] calculated from the $^{1}$H homonuclear decoupled NMR ($CDCl_3$) analysis.

It can be seen in Table 2.04, with the exception of Ti(**3**)O$^{i}$Pr, all initiators gave > 85 % conversion after 24 hours. The conversion to polymeric material can be calculated *via* $^{1}$H NMR spectroscopy, by analysis of the crude product before any remaining monomer is removed by washing with copious amounts of methanol.

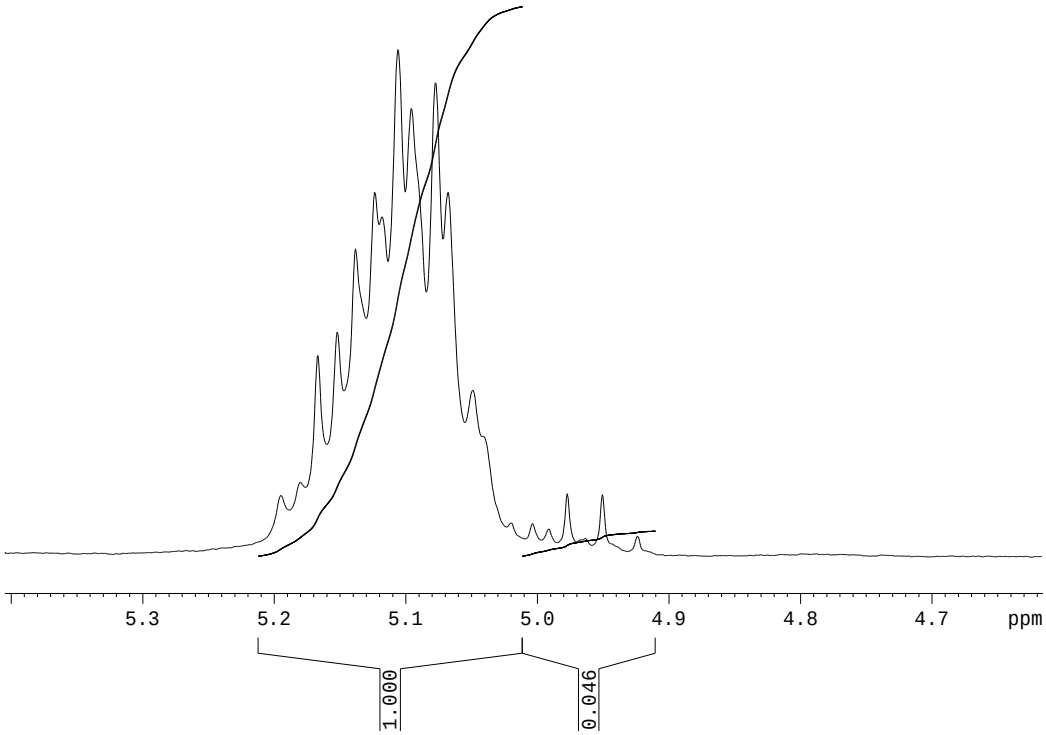


**Figure 2.19**: $^{1}$H NMR spectrum of polymer produced *via* Ti(**2**)O$^{i}$Pr – entry 2 Table 2.04

From Figure 2.19, the conversion can be calculated as the percentage of polymeric material present using the following equation:

$$\left(\frac{1}{1 + 0.046}\right) \times 100 = 96\ \%$$

**Equation 2.01**: Calculation for conversion to polymer

The titanium initiators in toluene at 80 °C all yield atactic PLA, as seen by $P_r$ values of 0.5, determined from the $^{1}$H homonuclear decoupled NMR spectrum – Figure 2.20. This is analogous to previous studies where Ti(IV) species on the whole afford atactic PLA.[1, 2]

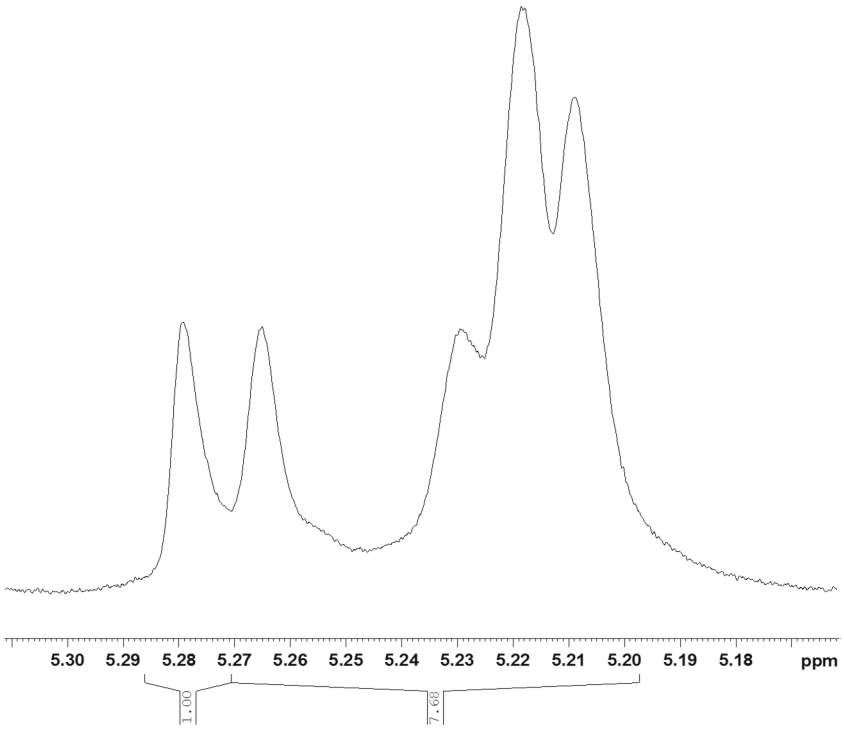


**Figure 2.20**: $^{1}$H homonuclear decoupled NMR of Ti(**2**)O$^{i}$Pr with a $P_r$ value of 0.5 – entry 2, Table 2.04

Using the equations reported by Coates *et al.* shown in Table 1.01 of Section 1.2.4 of Chapter 1, the degree of stereocontrol and hence the overall $P_r$ (probability of racemic enchainment) value can be calculated from the [*sis*] peak.[13] For example for the $^{1}$H homonuclear decoupled spectrum in Figure 2.20, the $P_r$ value can be calculated as:

$$\frac{P_r^2}{2} = [sis] \Rightarrow P_r^2 = 0.23 \Rightarrow P_r = \sqrt{0.23} = 0.48$$

**Equation 2.02**: Calculation of $P_r$ value for the polymer shown in Figure 2.20

The polymerisations carried out by the titanium initiators do not proceed with a great degree of control as exemplified by the high PDI values in Table 2.04, particularly for Ti(**2**)O$^{i}$Pr and Ti(**4**)O$^{i}$Pr. This is further emphasised by analysis of the MALDI-ToF mass spectrum which indicates that some degree of transesterification is occurring from the presence of more than one molecular weight distribution shown in Figure 2.21 with a repeat unit of 72 gmol$^{-1}$.

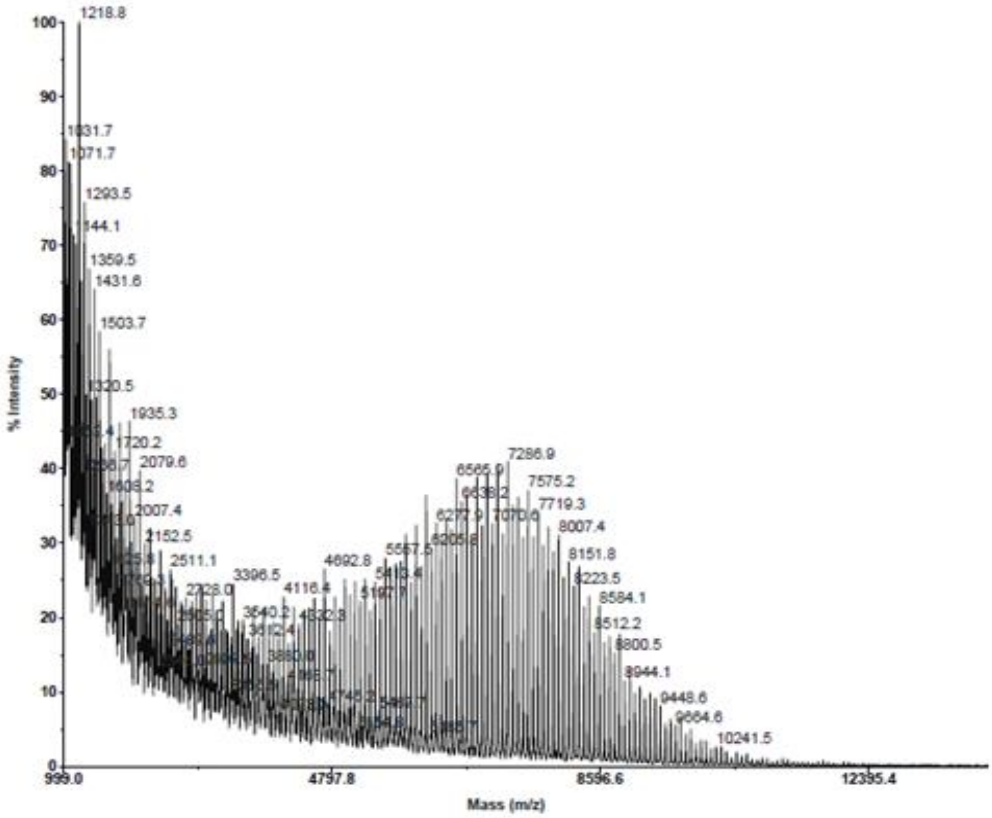


**Figure 2.21**: MALDI-ToF mass spectrum of Ti(**1**)O$^{i}$Pr in toluene at 80 °C for 24 hours – entry 1, Table 2.04

Analysis of the MALDI-ToF mass spectrum of a polymer sample produced by Ti(**1**)O$^{i}$Pr in solution at 80 °C shows good correlation between the theoretical and observed data for a polymer chain with an isopropoxide end group. This therefore confirms that the polymerisation is occurring *via* a coordination and insertion mechanism.

Under the more industrially preferred melt conditions, the titanium initiators were trialled at 130 °C in the absence of solvent with a [LA]/[initiator] of 300. To achieve a high level of polymeric material, the reactions were carried out for 2 hours. The results are shown in Table 2.05.

| Entry | Initiator | Conversion[a] (%) | $M_n$[b] | $M_w$[b] | $M_n$ (theo.) | PDI[b] | $P_r$[c] |
|---|---|---|---|---|---|---|---|
| **1** | Ti(**1**)O$^i$Pr | 74 | 39450 | 43050 | 32050 | 1.09 | 0.5 |
| **2** | Ti(**2**)O$^i$Pr | 95 | 124150 | 183350 | 41150 | 1.48 | 0.5 |
| **3** | Ti(**3**)O$^i$Pr | 51 | 18650 | 19800 | 22100 | 1.06 | 0.5 |
| **4** | Ti(**4**)O$^i$Pr | 95 | 117600 | 203450 | 41150 | 1.73 | 0.5 |

**Table 2.05:** ROP results for Ti(**1-4**)O$^i$Pr in the absence of solvent at 130 °C for 2 hours. 2.0 g of *rac*-LA, [LA]/[initiator] = 300. [a] conversion as determined *via* $^1$H NMR, [b] determined from GPC (in THF) referenced to polystyrene, [c] calculated from the $^1$H homonuclear decoupled NMR ($CDCl_3$) analysis.

Under melt conditions, it can be seen from Table 2.05 that all initiators are active for the ROP of *rac*-LA with Ti(**3**)O$^i$Pr being the least active, achieving only 51 % conversion to PLA after 24 hours. This is analogous to that shown in the solution studies – Table 2.04. The conversions reported in Table 2.05 are higher than those cited by Kol *et al.* who reported in one case a 43 % yield after 48 hours using a titanium amine t*ris*(phenolate) complex under solvent free conditions, albeit with *L*-LA.[5] The molecular weights obtained when Ti(**2**)O$^i$Pr and Ti(**4**)O$^i$Pr are the initiators, are higher than the theoretical values expected suggesting that the polymerisations are not well controlled. This is further emphasised by the high PDI values observed for these initiators. The theoretical molecular weights can be calculated based on the reaction conditions of 300: 1 of [monomer]: [initiator], such that the expected $M_n$ and $M_w$ for the reactions in Table 2.05 would be calculated as such:

$$300 \times 144\ (M_w\ of\ LA) \times \left(\frac{conversion}{100}\right) + end\ groups$$

**Equation 2.03**: Calculation of theoretical molecular weights

Further investigation into the polymerisation of *rac*-LA using Ti(**1**)O$^i$Pr as the initiator (which has the least discrepancy between calculated and theoretical $M_n$ values) was carried out using a monomer: initiator ratio of 50:1 and 600:1 in the absence of solvent and at 130 °C for 2 hours (Table 2.06).

| Entry | Initiator | Conversion[a] | [LA]:[initiator] | $M_n$[b] | $M_n$ (theo.) | PDI[b] |
|---|---|---|---|---|---|---|
| **1** | Ti(**1**)O$^i$Pr | 95 | 50:1 | 6600 | 6900 | 1.19 |
| **2** | Ti(**1**)O$^i$Pr | 74 | 300:1 | 39450 | 32050 | 1.09 |
| **3** | Ti(**1**)O$^i$Pr | 95 | 600:1 | 73400 | 82200 | 1.11 |

**Table 2.06**: ROP results for Ti(**1**)O$^i$Pr in the absence of solvent at 130 °C for 2 hours. 2.0 g of *rac*-LA, various [LA]/[initiator] ratios. [a] conversion as determined *via* $^1$H NMR, [b]determined from GPC (in THF) referenced to polystyrene

It can be seen from Table 2.06 that the $M_n$ obtained when the [LA]:[initiator] ratio is altered is consistent with the theoretical molecular weights calculated using Equation 2.03 for each of the different ratios. The values shown in Table 2.06 are relative to each other, for example, when the monomer: initiator ratio is doubled from 300:1 to 600:1, the $M_n$ observed is also effectively doubled from 39450 gmol$^{-1}$ to 73400 gmol$^{-1}$. This confirms that the polymerisation reaction in the absence of solvent using Ti(**1**)O$^i$Pr as the initiator is well controlled.

### 2.4.2 Zirconium Initiators

The zirconium initiators were also trialled for the ROP of *rac*-LA, with the assumption that the complex exists as a monomer in solution, and hence the mass of initiator utilised was calculated based on the molecular weight of the monomeric species. Unlike the titanium initiators, when the zirconium complexes were trialled for the ROP of *rac*-LA in toluene for 2 hours, they were seen to give enhanced activity producing PLA in near quantitative yields.

| Entry | Initiator | Conversion[a] (%) | $M_n$[b] | $M_w$[b] | $M_n$ (theo.) | PDI[b] | $P_r$[c] |
|---|---|---|---|---|---|---|---|
| **1** | {Zr(**1**)O$^i$Pr}$_2$ | 97 | 19200 | 20450 | 14050 | 1.07 | 0.50 |
| **2** | {Zr(**2**)O$^i$Pr}$_2$ | 84 | 20200 | 22050 | 12150 | 1.09 | 0.50 |
| **3** | {Zr(**3**)O$^i$Pr}$_2$ | 99 | 18650 | 20350 | 14350 | 1.09 | 0.60 |
| **4** | {Zr(**4**)O$^i$Pr}$_2$ | 99 | 13100 | 17350 | 14350 | 1.32 | 0.67 |

**Table 2.07**: ROP results for {Zr(**1-4**)O$^i$Pr}$_2$ in toluene at 80 °C for 2 hours. 0.7 g of *rac*-LA, [LA]/[initiator] = 100. [a] conversion as determined *via* $^1$H NMR, [b] determined from GPC (in THF) referenced to polystyrene, [c] calculated from the $^1$H homonuclear decoupled NMR ($CDCl_3$) analysis.

Table 2.07 shows the results from the ROP of *rac*-LA in toluene at 80 °C for 2 hours. Analysis of the $^{1}$H homonuclear decoupled NMR spectrum for initiators {Zr(**3**)O$^{i}$Pr)}$_2$ and {Zr(**4**)O$^{i}$Pr)}$_2$ indicates a slight degree of stereocontrol is occurring producing PLA with a heterotactic bias.

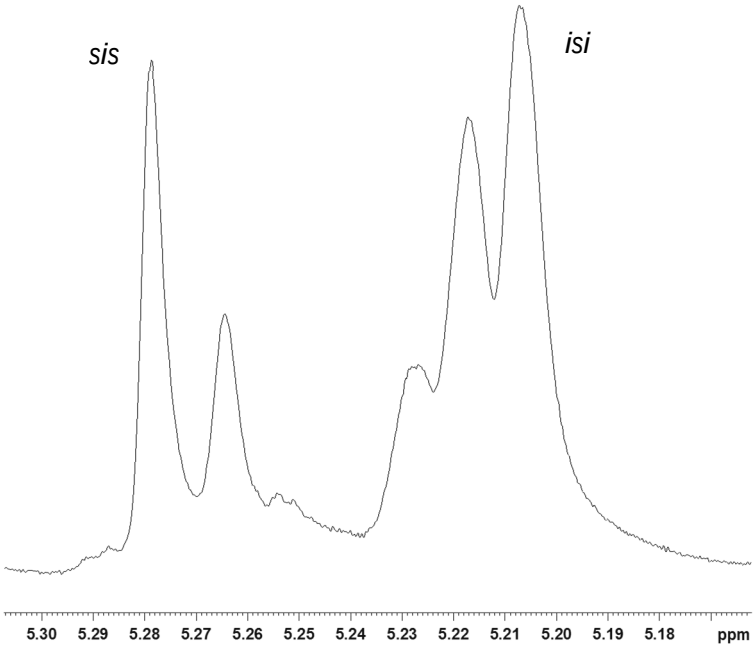


**Figure 2.22**: $^{1}$H homonuclear decoupled NMR spectrum of the polymer produced *via* {Zr(**3**)O$^{i}$Pr}$_2$ – entry 3 Table 2.07

The heterotacticity can be seen from an increase in the intensity of the *sis* and *isi* resonances in the $^{1}$H homonuclear decoupled NMR spectrum (Figure 2.22) and there is no longer an intensity ratio of 1:1:1:3:2 as observed for atactic PLA. The molecular weights reported in Table 2.07 are close to the theoretical molecular weight. This in conjunction with low PDI values which indicates that the polymerisations are occurring with some degree of control.

To allow comparison with the titanium initiators, the polymerisations *via* {Zr(**1-4**)O$^{i}$Pr)}$_2$ were repeated in toluene at 80 °C but for a longer reaction time of 24 hours.

| Entry | Initiator | Conversion[a] (%) | $M_n$[b] | $M_w$[b] | $M_n$ (theo.) | PDI[b] | $P_r$[c] |
|---|---|---|---|---|---|---|---|
| **1** | {Zr(**1**)O$^i$Pr}$_2$ | 98 | 26300 | 34100 | 14200 | 1.30 | 0.50 |
| **2** | {Zr(**2**)O$^i$Pr}$_2$ | 99 | 21300 | 28650 | 14350 | 1.34 | 0.59 |
| **3** | {Zr(**3**)O$^i$Pr}$_2$ | 99 | 28700 | 36200 | 14350 | 1.26 | 0.62 |
| **4** | {Zr(**4**)O$^i$Pr}$_2$ | 98 | 15200 | 22350 | 14200 | 1.47 | 0.60 |

**Table 2.08**: ROP results for {Zr(**1-4**)O$^i$Pr}$_2$ in toluene at 80 °C for 24 hours. 0.7 g of *rac*-LA, [LA]/[initiator] = 100. [a] conversion as determined *via* $^1$H NMR, [b] determined from GPC (in THF) referenced to polystyrene, [c] calculated from the $^1$H homonuclear decoupled NMR ($CDCl_3$) analysis.

After 24 hours at 80 °C in toluene all of the zirconium initiators give near quantitative conversion to PLA with a greater degree of control than the titanium equivalents with lower PDI values. Analogous to the polymerisations after 2 hours (Table 2.07) the zirconium initiators produce PLA with a slight degree of heterotacticity with $P_r$ values around 0.6. The polymerisation *via* {Zr(**3**)O$^i$Pr}$_2$ was also trialled at room temperature in dichloromethane but failed to produce any polymeric material.

The zirconium initiators were trialled for the ROP of *rac*-LA under the more industrially preferred conditions in the absence of solvent at 130 °C for 15 minutes.

| Entry | Initiator | Conversion[a] (%) | $M_n$[b] | $M_w$[b] | $M_n$ (theo.) | PDI[b] | $P_r$[c] |
|---|---|---|---|---|---|---|---|
| **1** | {Zr(**1**)O$^i$Pr}$_2$ | 99 | 23700 | 44400 | 42850 | 1.87 | 0.56 |
| **2** | {Zr(**2**)O$^i$Pr}$_2$ | 99 | 89250 | 114450 | 42850 | 1.28 | 0.50 |
| **3** | {Zr(**3**)O$^i$Pr}$_2$ | 99 | 41800 | 60900 | 42850 | 1.46 | 0.58 |
| **4** | {Zr(**4**)O$^i$Pr}$_2$ | 96 | 43900 | 64750 | 41550 | 1.47 | 0.62 |

**Table 2.09**: ROP results for {Zr(**1-4**)O$^i$Pr}$_2$ in the absence of solvent at 130 °C for 15 minutes. 2.0 g of *rac*-LA, [LA]/[initiator] = 300. [a] conversion as determined *via* $^1$H NMR, [b] determined from GPC (in THF) referenced to polystyrene, [c] calculated from the $^1$H homonuclear decoupled NMR ($CDCl_3$) analysis.

Again the zirconium initiators show high activity achieving near quantitative conversion to PLA after just 15 minutes. {Zr(**3**)O$^i$Pr}$_2$ and {Zr(**4**)O$^i$Pr}$_2$ show good correlation between the theoretical $M_n$ values and those

observed in Table 2.09 indicative of one polymer chain per metal centre. The stereocontrol observed still shows a tendency towards heterotactic PLA but to a lesser degree than that achieved in solution after 24 hours for the same initiators.

### 2.4.3 Hafnium Initiators

Analogous to the zirconium complexes, the hafnium initiators were trialled for the ROP of *rac*-LA in solution at 80 °C for 2 and 24 hours – Tables 2.10 and 2.11 respectively.

| Entry | Initiator | Conversion[a] (%) | $M_n$[b] | $M_w$[b] | $M_n$ (theo.) | PDI[b] | $P_r$[c] |
|---|---|---|---|---|---|---|---|
| **1** | {Hf(**1**)O$^i$Pr}$_2$ | 95 | 24250 | 27100 | 13750 | 1.12 | 0.6 |
| **2** | {Hf(**2**)O$^i$Pr}$_2$ | 25 | 550 | 550 | 3650 | 1.01 | - |
| **3** | {Hf(**3**)O$^i$Pr}$_2$ | 99 | 14900 | 16000 | 14350 | 1.07 | 0.6 |
| **4** | {Hf(**4**)O$^i$Pr}$_2$ | 25 | 450 | 450 | 3650 | 1.03 | - |

**Table 2.10**: ROP results for {Hf(**1-4**)O$^i$Pr}$_2$ in toluene at 80 °C for 2 hours. 0.7 g of *rac*-LA, [LA]/[initiator] = 100. [a] conversion as determined *via* $^1$H NMR, [b] determined from GPC (in THF) referenced to polystyrene, [c] calculated from the $^1$H homonuclear decoupled NMR ($CDCl_3$) analysis.

| Entry | Initiator | Conversion[a] (%) | $M_n$[b] | $M_w$[b] | $M_n$ (theo.) | PDI[b] | $P_r$[c] |
|---|---|---|---|---|---|---|---|
| **1** | {Hf(**1**)O$^i$Pr}$_2$ | 99 | 20000 | 24450 | 14350 | 1.22 | 0.6 |
| **2** | {Hf(**2**)O$^i$Pr}$_2$ | 26 | 2050 | 2200 | 3800 | 1.08 | - |
| **3** | {Hf(**3**)O$^i$Pr}$_2$ | 99 | 10000 | 15950 | 14350 | 1.60 | 0.6 |
| **4** | {Hf(**4**)O$^i$Pr}$_2$ | 38 | 550 | 550 | 5550 | 1.01 | - |

**Table 2.11**: ROP results for {Hf(**1-4**)O$^i$Pr}$_2$ in toluene at 80 °C for 24 hours. 0.7 g of *rac*-LA, [LA]/[initiator] = 100. [a] conversion as determined *via* $^1$H NMR, [b] determined from GPC (in THF) referenced to polystyrene, [c] calculated from the $^1$H homonuclear decoupled NMR ($CDCl_3$) analysis.

It can be seen from Tables 2.10 and 2.11 that initiators {Hf(**2**)O$^i$Pr}$_2$ and {Hf(**4**)O$^i$Pr}$_2$ are inefficient for the ROP of *rac*-LA and after several attempts at repeating the polymerisation reactions involving {Hf(**2**)O$^i$Pr}$_2$ and {Hf(**4**)O$^i$Pr}$_2$, there was no enhancement in the conversion or molecular weights. After both reaction times (2 hours and 24 hours) there is very little distinction between the

molecular weights and the stereoselectivity observed. For both the {Hf(**1**)O$^i$Pr}$_2$ and {Hf(**3**)O$^i$Pr}$_2$ initiators, PLA with a heterotactic bias is produced in solution at 80 °C for 2 hours and 24 hours. This can be observed from the $^1$H homonuclear decoupled NMR spectrum, which are similar to that observed for the zirconium initiators (for example {Zr(**3**)O$^i$Pr}$_2$ in Figure 2.22).

The hafnium initiators were also trialled for the ROP of *rac*-LA under solvent-free conditions to try and achieve conversion to PLA for all initiators.

| Entry | Initiator | Conversion[a] (%) | $M_n$[b] | $M_w$[b] | $M_n$ (theo.) | PDI[b] | $P_r$[c] |
|---|---|---|---|---|---|---|---|
| **1** | {Hf(**1**)O$^i$Pr}$_2$ | 97 | 24100 | 26200 | 42000 | 1.09 | 0.6 |
| **2** | {Hf(**2**)O$^i$Pr}$_2$ | 90 | 37750 | 43950 | 38950 | 1.16 | 0.55 |
| **3** | {Hf(**3**)O$^i$Pr}$_2$ | 98 | 63000 | 70550 | 42450 | 1.12 | 0.56 |
| **4** | {Hf(**4**)O$^i$Pr}$_2$ | 11 | 750 | 800 | 4800 | 1.01 | - [d] |

**Table 2.12**: ROP results for {Hf(**1-4**)O$^i$Pr}$_2$ in the absence of solvent at 130 °C for 15 minutes. 2.0 g of *rac*-LA, [LA]/[initiator] = 300. [a] conversion as determined *via* $^1$H NMR, [b] determined from GPC (in THF) referenced to polystyrene, [c] calculated from the $^1$H homonuclear decoupled NMR ($CDCl_3$) analysis, [d] $P_r$ value not obtained.

The data shown in Table 2.12 shows that under solvent-free conditions it is possible to obtain polymeric material when {Hf(**2**)O$^i$Pr}$_2$ is the initiator which is in contrast to that observed in toluene at 80 °C. Analogous to the polymeric material produced in toluene at 80 °C, under solvent free conditions the initiators were seen to produce PLA with a slight heterotactic bias. The molecular weight obtained when {Hf(**3**)O$^i$Pr}$_2$ is the initiator is slightly higher than that expected as observed in Table 2.12. When {Hf(**4**)O$^i$Pr}$_2$ was employed as the initiator, it failed to produce polymeric material after several attempts. The $P_r$ was therefore not recorded for {Hf(**4**)O$^i$Pr}$_2$.

The zirconium and hafnium initiators reported here, produce heterotactic PLA, with lower $P_r$ values than that observed for the $C_3$ amine *tris*(phenolate) group (IV) complexes isolated by Davidson *et al.* however, high activity is still observed.[1] This indicates the subtlety of the environment of the metal in the origin of stereocontrol in the ROP of *rac*-LA.

## 2.5 Kinetic Studies

Investigation into the reactivity rates of the amine *tris*(phenolate) complexes containing ligands **1**$H_3$ and **3**$H_3$ was carried out to obtain a $k_{app}$ for each initiator. Kinetic studies were carried out on a NMR scale ensuring that the initial concentration of LA ($[LA]_o$) was consistent for all initiators (0.578 mol $dm^{-3}$) and that all polymerisations were carried out in a similar manner on the same NMR spectrometer. $k_{app}$ was determined from analysis of a semilogarithmic plot of $\ln\{[LA]_o/[LA]_t\}$ *vs* time where $[LA]_o$ = 0.578 mol $dm^{-3}$ and $[LA]_t$ is the concentration of LA at a specific time. The polymerisations were carried out in $d_8$-toluene with a 100:1 ratio of [LA]:[initiator] over a period of 13 hours to mimic the solution polymerisations shown in Section 2.4.

### 2.5.1 Titanium Initiators

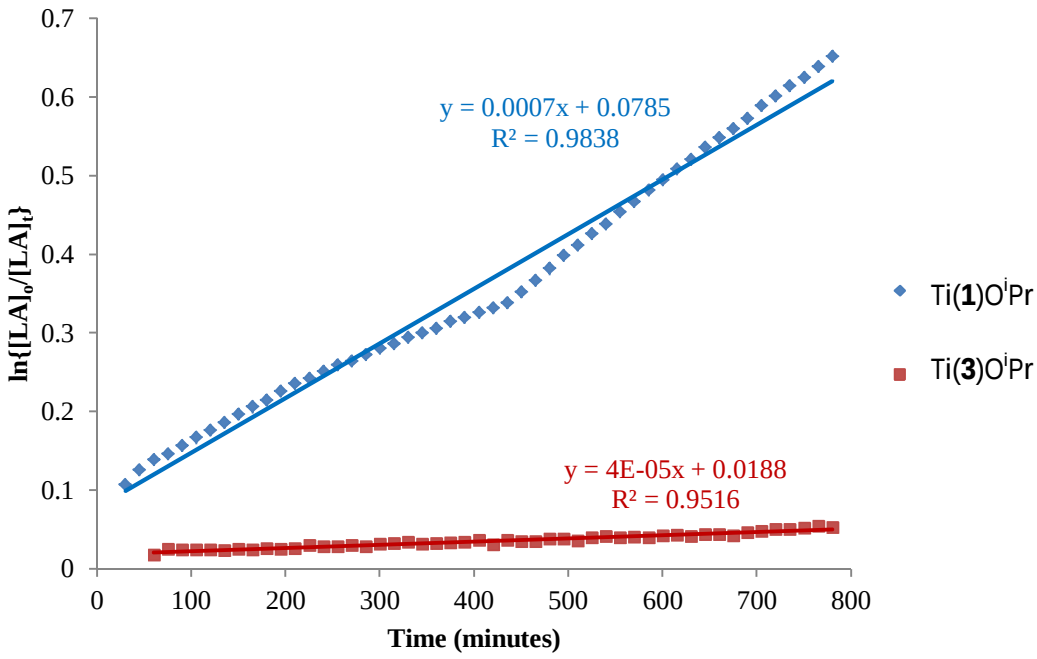


**Figure 2.23**: Semi-logarithmic plot of *rac*-LA using Ti(**1**)O$^i$Pr and Ti(**3**)O$^i$Pr at 80 °C in $d_8$-toluene

| Initiator | $k_{app}$ ($min^{-1}$) | $R^2$ |
|---|---|---|
| Ti(1)O$^i$Pr | 6.99 × $10^{-4}$ | 0.9838 |
| Ti(3)O$^i$Pr | 0.41 × $10^{-4}$ | 0.9516 |

**Table 2.13**: $k_{app}$ values for initiators Ti(**1**)O$^i$Pr and Ti(**3**)O$^i$Pr

Figure 2.23 and Table 2.13 show a difference in the rate of reactivity between the two initiators Ti(**1**)O$^{i}$Pr and Ti(**3**)O$^{i}$Pr, with the initiator where R is the more bulky $^{t}$Bu substituent showing the slower rate of polymerisation, as expected for the data presented in Table 2.04. The $k_{app}$ values obtained for Ti(**1**)O$^{i}$Pr and Ti(**3**)O$^{i}$Pr are lower than those reported for a [$^{t}$Bu-salen-$^{t}$Bu]Ti(O$^{i}$Pr)$_2$ complex isolated by Gibson *et al.*, who reported a $k_{app}$ of 1.55 × 10$^{-3}$ min$^{-1}$.[14] It should be noted however, that the plots shown in Figure 2.23 do not intercept at the origin and do not show absolute linearity suggesting that the polymerisation is more complex than first anticipated, and may not obey a definitive first order rate.

### 2.5.2 Zirconium Initiators

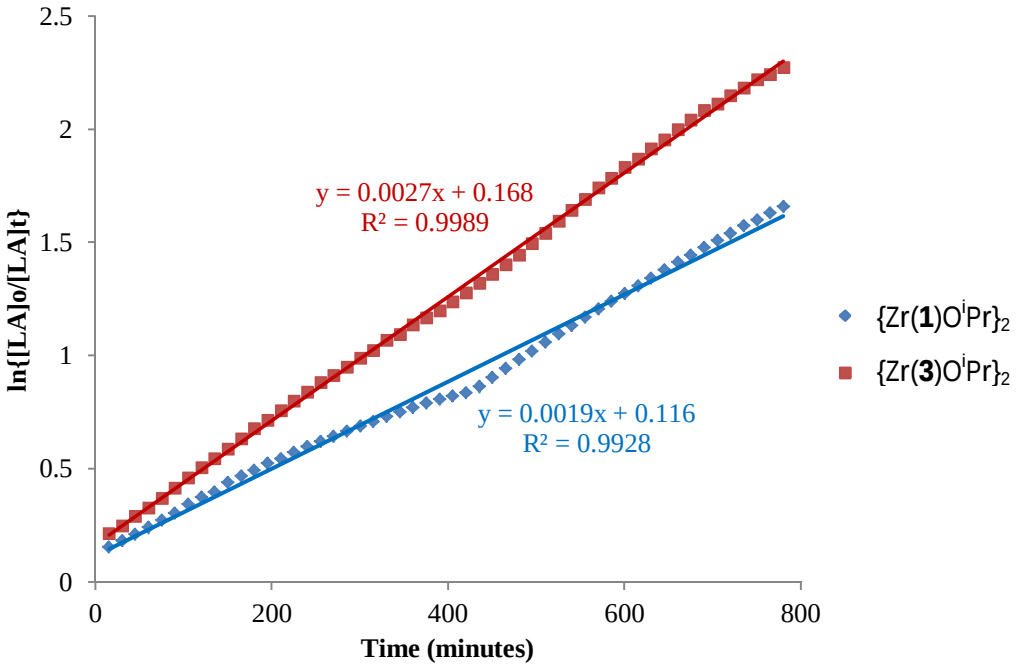


**Figure 2.24**: Semi-logarithmic plot of *rac*-LA using {Zr(**1**)O$^{i}$Pr}$_2$ and {Zr(**3**)O$^{i}$Pr}$_2$ at 80 °C in toluene

| Initiator | $k_{app}$ (min$^{-1}$) | $R^2$ |
|---|---|---|
| {Zr(1)O$^{i}$Pr}$_2$ | 1.93 × 10$^{-3}$ | 0.9928 |
| {Zr(3)O$^{i}$Pr}$_2$ | 2.74 × 10$^{-3}$ | 0.9989 |

**Table 2.14**: $k_{app}$ values for initiators {Zr(**1**)O$^{i}$Pr}$_2$ and {Zr(**3**)O$^{i}$Pr}$_2$

Figure 2.24 and Table 2.14 show that in contrast to the titanium amine *tris*(phenolate) complexes in Section 2.5.1, the initiator where R is the more bulky $^{t}$Bu substituent shows a slightly faster apparent rate of propagation than the unsubstituted counterpart. The $k_{app}$ values recorded for {Zr(**1**)O$^{i}$Pr}$_2$ and {Zr(**3**)O$^{i}$Pr}$_2$ are lower than that observed by Davidson *et al.* who reported a $k_{app}$ of 4.2 × $10^{-3}$ $min^{-1}$ for the zirconium $C_3$-amine *tris*(phenolate) complex.[1] In accordance with the data obtained in Table 2.06 and 2.07, the zirconium initiators show higher activity than the titanium equivalents with a faster rate of propagation in $d_8$-tolune at 80 °C. Analogous to that observed in Section 2.5.1, the kinetic plots obtained using the zirconium initiators do not intercept at the origin and do not show absolute linearity, suggesting that the polymerisation is more complex than first anticipated, and may not obey a definitive first order rate.

### 2.5.3 Hafnium Initiators

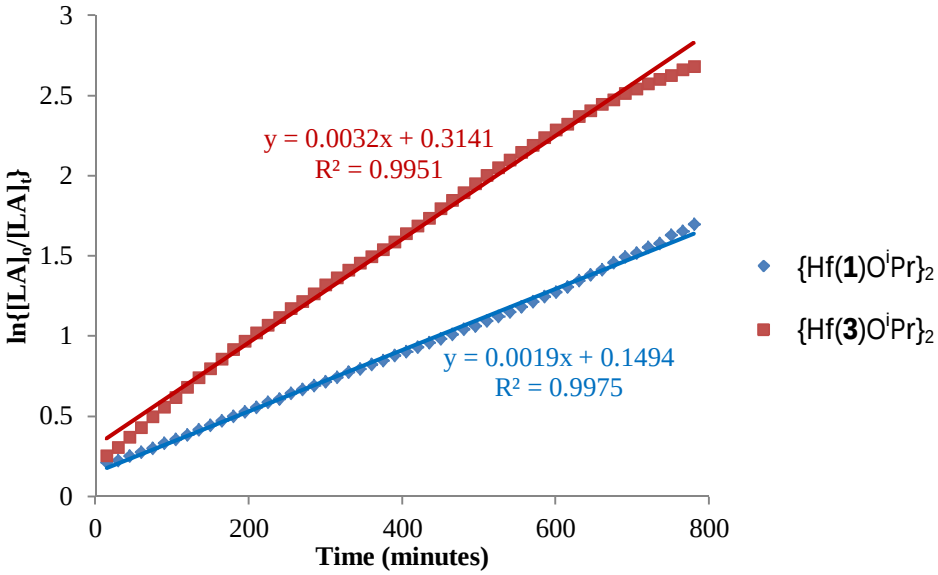


**Figure 2.25**: Semi-logarithmic plot of *rac*-LA using {H(**1**)O$^{i}$Pr}$_2$ and {Hf(**3**)O$^{i}$Pr}$_2$ at 80 °C in toluene

| Initiator | $k_{app}$ ($min^{-1}$) | $R^2$ |
|---|---|---|
| **{Hf(1)O$^{i}$Pr}$_2$** | 1.92 × $10^{-3}$ | 0.9975 |
| **{Hf(3)O$^{i}$Pr}$_2$** | 3.19 × $10^{-3}$ | 0.9951 |

**Table 2.15**: $k_{app}$ values for initiators {Hf(**1**)O$^{i}$Pr}$_2$ and {Hf(**3**)O$^{i}$Pr}$_2$

The $k_{app}$ values obtained for the hafnium initiators containing ligands **1**$H_3$ and **3**$H_3$ are comparable with those obtained for the analogous zirconium initiators, Figure 2.24. The value observed for {Hf(**3**)O$^i$Pr}$_2$ is comparable to that obtained for the zirconium $C_3$-symmetric amine *tris*(phenolate) complexes reported by Davidson *et al.* which gave a $k_{app}$ of 4.2 × $10^{-3}$ $min^{-1}$ for *rac*-LA.[1] Although the data obtained using {Hf(**1**)O$^i$Pr}$_2$ and {Hf(**3**)O$^i$Pr}$_2$ as initiators show an increase in linearity when compared to Figure 2.23 and Figure 2.24 for the other group (IV) initiators, there is still a deviation from the plots having a intercept at the origin. This suggests that the polymerisation is occurring in a more complex way that first anticipated for a first order reaction.

## 2.6 Polymerisation of TMC

The group (IV) complexes containing the amine *tris*(phenolate) ligands in Figure 2.01 were also trialled for the ROP of TMC (trimethylene carbonate or 1,3-dioxan-2-one) to produce polycarbonates – another biopolymer receiving a lot of interest in research recently.[15-18] As mentioned in Chapter 1, Section 1.4.2 polymers of TMC are biodegradable and developed for use in medical applications. Its application as a co-monomer to improve the flexibility of the resulting polymer has been of particular interest and therefore it would be of benefit to co-polymerise *rac*-LA and TMC, which is discussed here on in.

### 2.6.1 Homopolymerisation of TMC

TMC can be prepared in a one-step synthesis at room temperature according to literature procedures, as shown in Figure 2.26.[19]

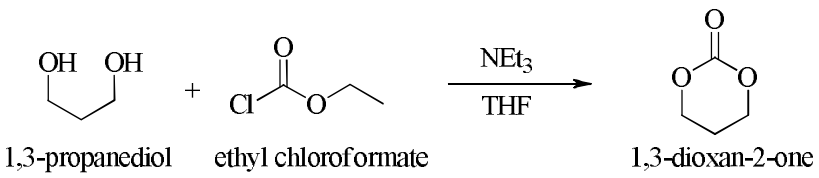


**Figure 2.26**: Preparation of TMC (1,3-dioxan-2-one)

It was not possible to prepare TMC in high yields only achieving ~36 % yield after recrystallisation. However, once synthesised it was then possible to carry out the ROP to produce a polycarbonate.

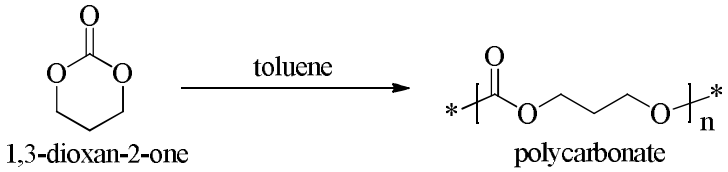


**Figure 2.27**: Polymerisation of TMC to produce polycarbonate

The ROP of TMC was carried out using the initiators produced in Figure 2.03 in toluene at 80 °C for 24 hours using a [TMC]:[initiator] ratio of 100: 1.

| Entry | Initiator | Conversion[a] (%) | $M_n$[b] | $M_w$[b] | $M_n$ (theo.) | PDI[b] |
|---|---|---|---|---|---|---|
| **1** | Ti(**1**)O$^i$Pr | 89 | 15450 | 42000 | 9150 | 2.72 |
| **2** | Ti(**2**)O$^i$Pr | 41 | 5800 | 9950 | 4250 | 1.71 |
| **3** | Ti(**3**)O$^i$Pr | 27 | 5950 | 9500 | 2800 | 1.60 |
| **4** | Ti(**4**)O$^i$Pr | 94 | 16900 | 32000 | 9650 | 1.90 |
| **5** | {Zr(**1**)O$^i$Pr}$_2$ | 99 | 40350 | 77300 | 10150 | 1.92 |
| **6** | {Zr(**2**)O$^i$Pr}$_2$ | 99 | 21250 | 48400 | 10150 | 2.28 |
| **7** | {Zr(**3**)O$^i$Pr}$_2$ | 99 | 47100 | 78500 | 10150 | 1.67 |
| **8** | {Zr(**4**)O$^i$Pr}$_2$ | 93 | 5550 | 11950 | 9550 | 2.14 |
| **9** | {Hf(**1**)O$^i$Pr}$_2$ | 97 | 12350 | 27250 | 9950 | 2.21 |
| **10** | {Hf(**2**)O$^i$Pr}$_2$ | 96 | 19950 | 35850 | 9850 | 1.80 |
| **11** | {Hf(**3**)O$^i$Pr}$_2$ | 98 | 9800 | 20000 | 10050 | 2.05 |
| **12** | {Hf(**4**)O$^i$Pr}$_2$ | 98 | 8800 | 18900 | 10050 | 2.15 |

**Table 2.16**: ROP results for Ti(**1-4**)O$^i$Pr and {Zr/Hf(**1-4**)O$^i$Pr}$_2$ in toluene at 80 °C for 24 hours. 0.493 g of TMC, [TMC]/[initiator] = 100. [a] conversion as determined *via* $^1$H NMR, based on the amount of recovered material, [b] determined from GPC (in THF) referenced to polystyrene

The initial concentration of TMC used in the polymerisations was calculated in accordance to the ROP of *rac*-LA, using the same molar equivalents in both cases. For determination of the conversion to polycarbonate, the integral of the polymer resonance (4.25 ppm) over the total integrals of the monomer and

polymer resonances was calculated from analysis of the $^{1}$H NMR spectrum as shown in Figure 2.28.

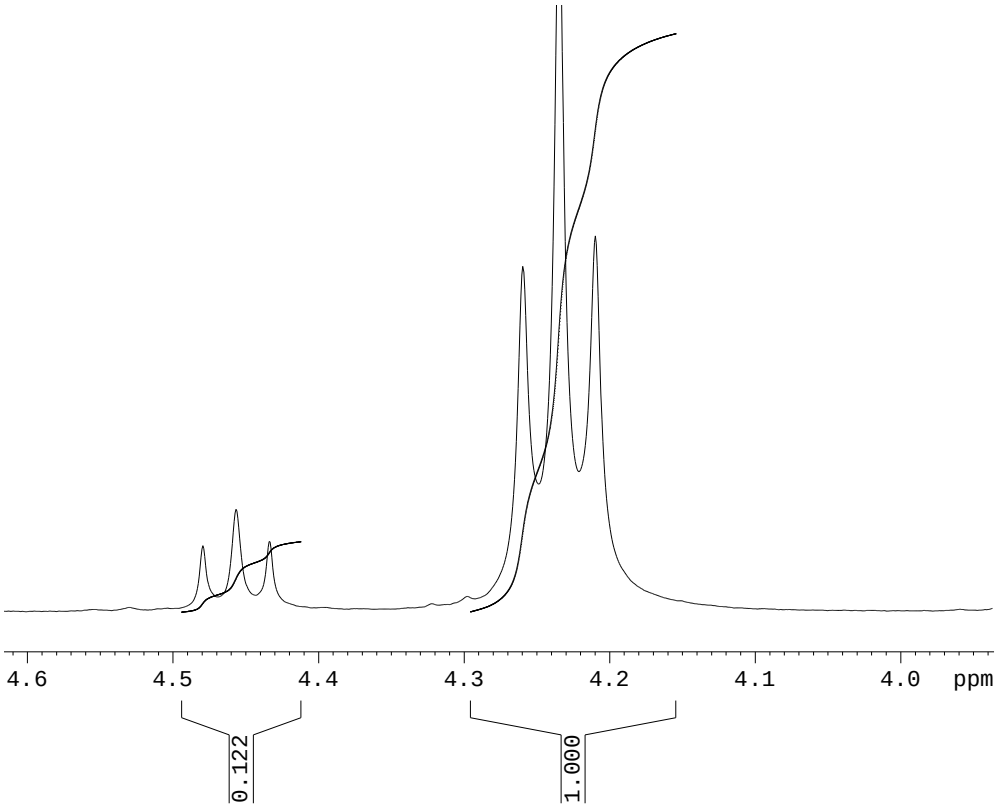


**Figure 2.28**: $^{1}$H NMR showing conversion to polycarbonate *via* Ti(**1**)O$^{i}$Pr at 80 °C in toluene – entry 1, Table 2.16

The theoretical molecular weight for conversion to polycarbonate in the ROP of *rac*-LA can be calculated using a modified version of that shown in Equation 2.03 where the molecular weight of TMC (102 gmol$^{-1}$) is substituted for 144 gmol$^{-1}$ (molecular weight of LA). For 100 % conversion to polycarbonate, the theoretical molecular weight should be:

$$100 \times 102 \times 1 + 60\left(O^{i}Pr + H\ end\ group\right) = 10300\ g\ mol^{-1}$$

The majority of the initiators for the ROP of TMC in Table 2.16 show good correlation of $M_n$ to the theoretical molecular weight, with the exception of {Zr(**1-3**)O$^{i}$Pr}$_2$. {Zr(**1-3**)O$^{i}$Pr}$_2$ shows higher than expected molecular weights suggesting that the rate of propagation is higher than the rate of initiation and could be indicative that some of the initiator is being destroyed during the polymerisation. This is further observed by the high polydispersity values for

such polymerisations indicating that the polymerisation is not well controlled for such initiators. The zirconium and hafnium initiators show higher activity than the titanium counterparts, with near quantitative conversion to polycarbonate after 24 hours, compared with only 27 % conversion when Ti(**3**)O$^{i}$Pr is the initiator.

The results indicated in Table 2.16 are superior to that reported by Kricheldorf *et al.* who reports only a slight conversion in the ROP of TMC at 80 °C using $SnOct_2$ as the initiator.[17] The use of amino acids for the ROP of TMC has been reported to give comparable conversions to that shown in Table 2.16, achieving > 90 % conversion after 24 hours at 80 °C however with slightly more control with PDI values under 1.70.[15]

### 2.6.2 Copolymerisation of *rac*-LA and TMC

Due to the initiators showing activity for the ROP of TMC, albeit with a low degree of control, it was therefore of interest to test the initiators for the production of a copolymer for enhanced flexibility of PLA with the incorporation of TMC. In this case only initiators containing ligands **1**$H_3$ and **3**$H_3$ were investigated at different monomer to initiator ratios under solvent-free conditions for a reaction time of 15 minutes.

| Entry | Initiator | [LA]:[TMC]:[initiator] | Yield[a] (%) | $M_n$[b] | $M_w$[b] | PDI[b] |
|---|---|---|---|---|---|---|
| **1** | Ti(**1**)O$^{i}$Pr | 300:10:1 | 90 | 47000 | 61400 | 1.31 |
| **2** | Ti(**1**)O$^{i}$Pr | 300:30:1 | 78 | 35800 | 44850 | 1.25 |
| **3** | Ti(**3**)O$^{i}$Pr | 300:10:1 | 24 | 9100 | 9700 | 1.06 |
| **4** | Ti(**3**)O$^{i}$Pr | 300:30:1 | 4 | - | - | - |
| **5** | {Zr(**1**)O$^{i}$Pr}$_2$ | 300:10:1 | 95 | 73950 | 106100 | 1.43 |
| **6** | {Zr(**1**)O$^{i}$Pr}$_2$ | 300:30:1 | 87 | 56350 | 85350 | 1.51 |
| **7** | {Zr(**3**)O$^{i}$Pr}$_2$ | 300:10:1 | 87 | 60400 | 81150 | 1.34 |
| **8** | {Zr(**3**)O$^{i}$Pr}$_2$ | 300:30:1 | 71 | 52550 | 75550 | 1.44 |
| **9** | {Hf(**1**)O$^{i}$Pr}$_2$ | 300:10:1 | 64 | 29900 | 50250 | 1.68 |
| **10** | {Hf(**1**)O$^{i}$Pr}$_2$ | 300:30:1 | 76 | 52750 | 66550 | 1.26 |
| **11** | {Hf(**3**)O$^{i}$Pr}$_2$ | 300:10:1 | 77 | 56400 | 65500 | 1.16 |
| **12** | {Hf(**3**)O$^{i}$Pr}$_2$ | 300:30:1 | 82 | 57700 | 66450 | 1.15 |

**Table 2.17**: ROP results for Ti(**1/3**)O$^{i}$Pr and {Zr/Hf(**1/3**)O$^{i}$Pr}$_2$ in the absence of solvent at 130 °C for 15 minutes. 2.0 g of *rac*-LA. [a] based on the amount of recovered material, [b] determined from GPC (in THF) referenced to polystyrene.

With the exception of Ti(**3**)O$^{i}$Pr all initiators show high activity after 15 minutes for the copolymerisation of *rac*-LA and TMC. The yields are based on the amount of recovered material and based on all monomer units. Analysis of the polymeric products produced in Table 2.17 by GPC, indicates that as the amount of TMC added to the copolymerisation reactions is increased, there is the appearance of a bimodal distribution suggesting that there are more than one type of polymer chain present in the sample. The polydispersity indices are in general seen to increase as the amount of TMC in the polymerisation reaction is increased, suggesting that the reactions are occurring with less control as the ratio is increased from [300:10:1] to [300:30:1] of [LA]:[TMC]:[initiator].

Analysis of $^{1}$H NMR spectrum of the copolymeric products from Table 2.17 (entries 5 and 6) with a comparison of a product containing no TMC (entry 1, Table 2.09) is shown in Figure 2.29.

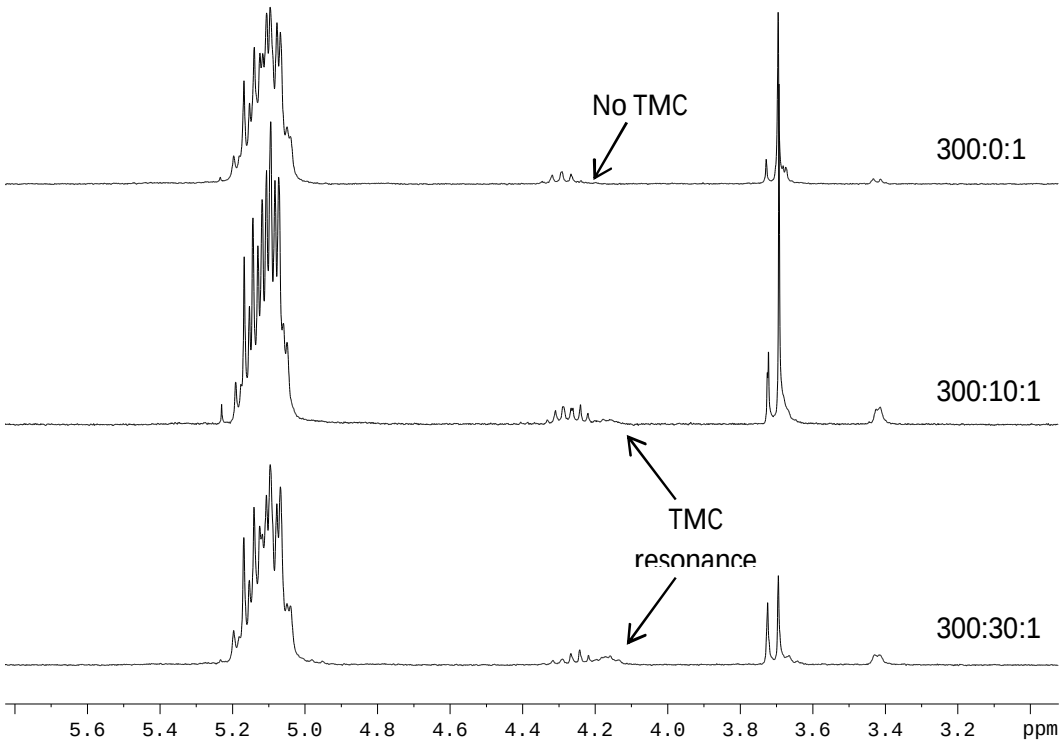


**Figure 2.29**: $^{1}$H NMR spectra of the co-polymeric products formed *via* {Zr(**1**)O$^{i}$Pr}$_2$ under solvent-free conditions at 130 °C at various [LA]:[TMC]:[initiator] ratios.

The spectra shown in Figure 2.29 are recorded after the product has been washed with copious amounts of methanol, and therefore any resonances present corresponding to TMC (4.2 ppm and 2.1 ppm)[15] are from incorporation into the polymer chain and not unreacted monomer. It can be seen that as the amount of TMC added to the reaction is increased, the resonance at 4.2 ppm shows a slight increase in intensity suggesting that a small amount of TMC is incorporated into the polymeric chain.

## 2.7 Copolymerisation of *rac*-LA and isosorbide

The group (IV) initiators reported in this chapter were also trialled for the production of another set of copolymers produced from the polymerisation of *rac*-LA and isosorbide.

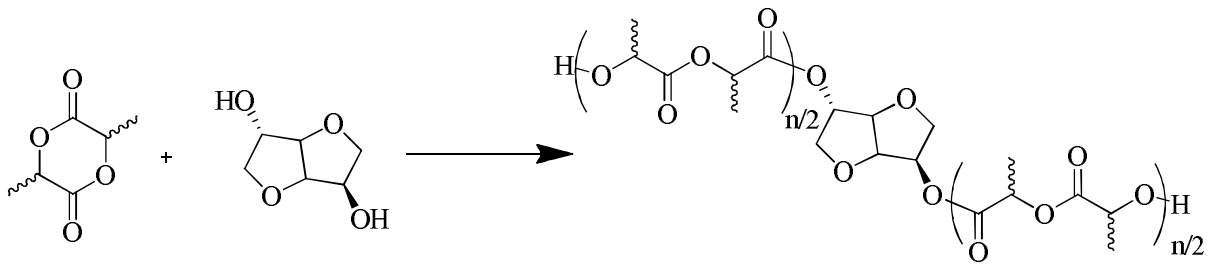


**Figure 2.30**: Preparation of copolymer of LA and TMC

It was hoped that analogous to the incorporation of TMC into the polymer backbone, the physical properties of the resulting polymer would be altered and in the case of *rac*-LA and isosorbide, would enhance the solubility desirable for medical applications, such as water solubility.

The copolymerisaton of *rac*-LA and isosorbide was carried out in the absence of solvent at different ratios of the monomers to initiator analogous to that seen in Section 2.5.2 but for a prolonged reaction time of 2 hours.

| Entry | Initiator | [LA]:[isosorbide]:[initiator] | Yield (%)[a] | $M_n$[b] | $M_w$[b] | PDI[b] |
|---|---|---|---|---|---|---|
| **1** | Ti(**1**)O$^i$Pr | 300:10:1 | 95 | 12050 | 14200 | 1.18 |
| **2** | Ti(**1**)O$^i$Pr | 300:20:1 | 81 | 5300 | 6000 | 1.14 |
| **3** | Ti(**1**)O$^i$Pr | 300:30:1 | 27 | 4700 | 3800 | 1.24 |
| **4** | Ti(**3**)O$^i$Pr | 300:10:1 | 70 | 5500 | 1600 | 1.11 |
| **5** | Ti(**3**)O$^i$Pr | 300:20:1 | 2 | 2900 | 3200 | 1.12 |
| **6** | Ti(**3**)O$^i$Pr | 300:30:1 | 1 | 1800 | 2100 | 1.14 |
| **7** | {Zr(**1**)O$^i$Pr}$_2$ | 300:10:1 | 75 | 6150 | 6950 | 1.13 |
| **8** | {Zr(**1**)O$^i$Pr}$_2$ | 300:20:1 | 37 | 2900 | 3350 | 1.15 |
| **9** | {Zr(**1**)O$^i$Pr}$_2$ | 300:30:1 | 6 | 1850 | 2150 | 1.16 |
| **10** | {Zr(**3**)O$^i$Pr}$_2$ | 300:10:1 | 64 | 6100 | 6650 | 1.09 |
| **11** | {Zr(**3**)O$^i$Pr}$_2$ | 300:20:1 | 37 | 3000 | 3400 | 1.13 |
| **12** | {Zr(**3**)O$^i$Pr}$_2$ | 300:30:1 | 24 | 1600 | 1900 | 1.18 |
| **13** | {Hf(**1**)O$^i$Pr}$_2$ | 300:10:1 | 69 | 5100 | 5550 | 1.09 |
| **14** | {Hf(**1**)O$^i$Pr}$_2$ | 300:20:1 | 60 | 2350 | 2650 | 1.13 |
| **15** | {Hf(**1**)O$^i$Pr}$_2$ | 300:30:1 | 31 | 1450 | 1650 | 1.13 |
| **16** | {Hf(**3**)O$^i$Pr}$_2$ | 300:10:1 | 77 | 6000 | 6450 | 1.08 |
| **17** | {Hf(**3**)O$^i$Pr}$_2$ | 300:20:1 | 34 | 2650 | 2900 | 1.11 |
| **18** | {Hf(**3**)O$^i$Pr}$_2$ | 300:30:1 | 22 | 1650 | 1900 | 1.13 |

**Table 2.18**: ROP results for Ti(**1/3**)O$^i$Pr and {Zr/Hf(**1/3**)O$^i$Pr}$_2$ in the absence of solvent at 130 °C for 2 hours. 2.0 g of *rac*-LA. [a] based on the amount of recovered material, [b] determined from GPC (in THF) referenced to polystyrene.

Analogous to the copolymerisation data in Table 2.17, Section 2.5.2 for the copolymerisation of *rac*-LA and TMC, the yields are based on the amount of recovered material and calculated based on all monomeric units. The results shown in Table 2.18 indicate, that as the amount of isosorbide is increased, the molecular weight of the resulting polymer is reduced, presumably due to the competing reactions of chain-extension *via* isosorbide *vs* the polymerisation reaction. This is also observed in the increase in PDI values as you increase the mass of isosorbide and a decrease in the yields obtained. From the $^1$H NMR (Figure 2.31) of the co-polymeric products, relatively little unreacted lactide monomer was observed, hence the decrease in yield could be due to an increase in the solubility of the polymer in methanol as the amount of isosorbide is increased.

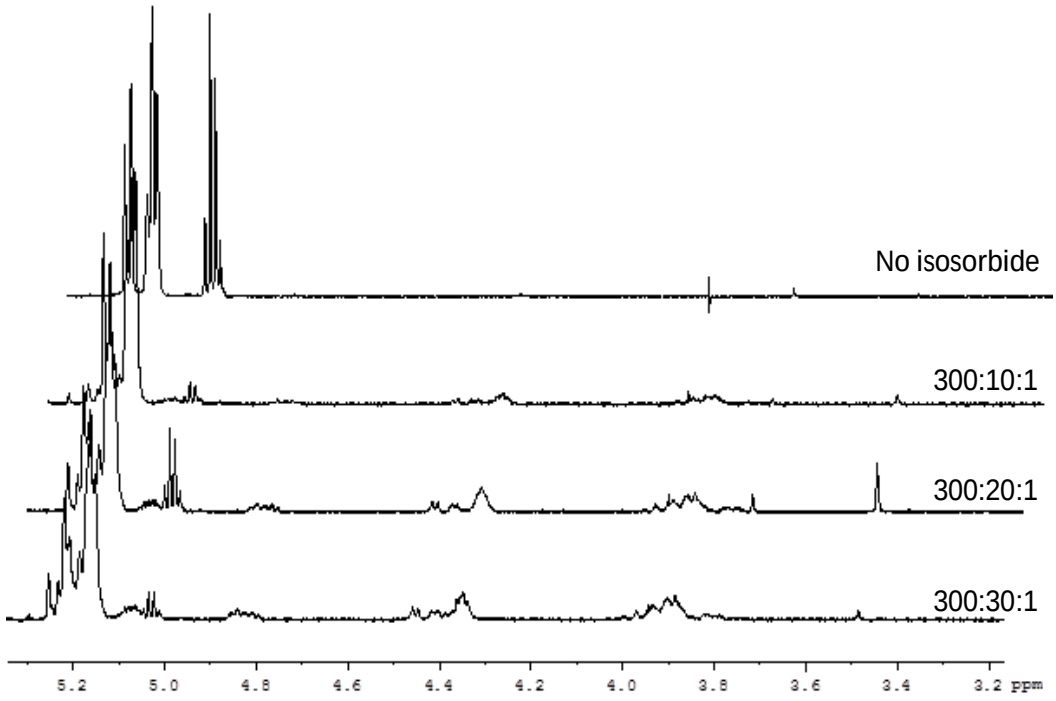


**Figure 2.31**: $^{1}$H NMR of the co-polymeric products formed *via* Ti(**1**)O$^{i}$Pr at different [LA]:[isosorbide]:[initiator] ratios

Isosorbide must be incorporated into the polymeric product as the spectra reported in Figure 2.31 is collected after the polymeric material has been washed with copious amounts of methanol, and peaks corresponding to the isosorbide are still present at around 3.9 ppm and 4.4 ppm. If any unreacted isosorbide was present this would have been removed upon washing the product with methanol. The incorporation of isosorbide into the polymer backbone is further confirmed by analysis of the MALDI-ToF mass spectra which indicates the presence of two –OH end groups, suggesting that isosorbide acts as a spacer in the polymeric chain as not distinction is observed between the two OH groups.

Unlike for the copolymerisation of *rac*-LA and TMC which saw the presence of a bimodal distribution in the GPC spectrum as the amount of the co-monomer was increased, for the polymers obtained in this instance, only monomodal distributions were observed. This can be seen from a comparison in the GPC spectrum of the polymerisations *via* {Hf(**3**)O$^{i}$Pr}$_2$ at a low isosorbide concentration and at a higher isosorbide concentration.

## 2.8 Concluding Remarks

The titanium complexes reported here are monomeric complexes that produce atactic PLA in toluene at 80 °C after 24 hours and under the more industrially preferred solvent-free conditions. Analysis of the MALDI-ToF mass spectrum confirms that the polymerisation is occurring *via* a coordination and insertion mechanism and that the polymerisations do not proceed with a great degree of control from the presence of more than one distribution curve. The zirconium and hafnium complexes are dimeric in the solid-state, however analysis of the $^{1}$H NMR spectrum in $d_8$-THF at 298 K and 230 K indicates a degree of fluxionality is occurring. Both the zirconium and hafnium initiators show higher activity than the titanium counterparts for the ROP of *rac*-LA producing PLA in toluene after 2 hours. Higher $k_{app}$ values are also obtained with the zirconium and hafnium initiators containing **1**H$_3$ and **3**H$_3$, than the analogous titanium initiators. The zirconium and hafnium initiators produce PLA with a slight heterotactic bias in toluene and under solvent-free conditions particularly for those initiators containing ligands **3**H$_3$ and **4**H$_3$.

All group (IV) amine *tris*(phenolate) complexes reported here were active for the ROP of TMC at 80 °C in toluene for 24 hours. Analogous to the ROP of *rac*-LA, the zirconium and hafnium initiators displayed higher activity than the titanium initiators. High PDI values were obtained suggesting that the reaction is not well controlled. The group (IV) complexes containing ligands **1**H$_3$ and **3**H$_3$ were active for the copolymerisation of *rac*-LA and TMC, with Ti(**3**)O$^{i}$Pr showing the lowest activity. As the amount of TMC is increased, the polymerisations occur with less control resulting in higher PDI values and the presence of a bimodal molecular weight distribution. The copolymerisation of *rac*-LA and isosorbide was achieved utilising the initiators containing ligands **1**H$_3$ and **3**H$_3$. It was observed that as the amount of isosorbide was increased, the molecular weight of the polymeric material decreased suggesting that isosorbide acts as a chain terminating moiety.

1. A. J. Chmura, M. G. Davidson, C. J. Frankis, M. D. Jones and M. D. Lunn, *Chem. Commun.*, 2008, 1293-1295.
2. A. J. Chmura, M. G. Davidson, M. D. Jones, M. D. Lunn, M. F. Mahon, A. F. Johnson, P. Khunkamchoo, S. L. Roberts and S. S. F. Wong, *Macromolecules*, 2006, **39**, 7250-7257.
3. L. H. Tong, Y. L. Wong, S. I. Pascu and J. R. Dilworth, *Dalton Trans.*, 2008, 4784-4791.
4. A. Sokolowski, J. Muller, T. Weyhermuller, R. Schnepf, P. Hildebrandt, K. Hildenbrand, E. Bothe and K. Wieghardt, *J. Am. Chem. Soc.*, 1997, **119**, 8889-8900.
5. S. Gendler, S. Segal, I. Goldberg, Z. Goldschmidt and M. Kol, *Inorg. Chem.*, 2006, **45**, 4783-4790.
6. M. Kol, M. Shamis, I. Goldberg, Z. Goldschmidt, S. Alfi and E. Hayut-Salant, *Inorg. Chem. Commun.*, 2001, **4**, 177-179.
7. G. Licini, M. Mba and C. Zonta, *Dalton Trans.*, 2009, 5265-5277.
8. W. O. Appiah, A. D. DeGreeff, G. L. Razidlo, S. J. Spessard, M. Pink, V. G. Young and G. E. Hofmeister, *Inorg. Chem.*, 2002, **41**, 3656-3667.
9. E. Y. Tshuva, I. Goldberg, M. Kol and Z. Goldschmidt, *Inorg. Chem.*, 2001, **40**, 4263-4270.
10. A. J. Chmura, D. M. Cousins, M. G. Davidson, M. D. Jones, M. D. Lunn and M. F. Mahon, *Dalton Trans.*, 2008, 1437-1443.
11. A. J. Chmura, C. J. Chuck, M. G. Davidson, M. D. Jones, M. D. Lunn, S. D. Bull and M. F. Mahon, *Angew. Chem., Int. Ed. Engl.*, 2007, **46**, 2280-2283.
12. K. C. Fortner, J. P. Bigi and S. N. Brown, *Inorg. Chem.*, 2005, **44**, 2803-2814.
13. B. M. Chamberlain, M. Cheng, D. R. Moore, T. M. Ovitt, E. B. Lobkovsky and G. W. Coates, *J. Am. Chem. Soc.*, 2001, **123**, 3229-3238.
14. C. K. A. Gregson, I. J. Blackmore, V. C. Gibson, N. J. Long, E. L. Marshall and A. J. P. White, *Dalton Trans.*, 2006, 3134-3140.
15. J. Y. Liu, C. Zhang and L. J. Liu, *J. Appl. Polym. Sci.*, 2008, **107**, 3275-3279.
16. H. R. Kricheldorf and B. Weegenschulz, *Journal of Polymer Science Part a-Polymer Chemistry*, 1995, **33**, 2193-2201.
17. H. R. Kricheldorf and A. Stricker, *Macromol. Chem. Phys.*, 2000, **201**, 2557-2565.
18. H. R. Kricheldorf and B. Weegenschulz, *Journal of Macromolecular Science-Pure and Applied Chemistry*, 1995, **A32**, 1847-1862.
19. T. Ariga, T. Takata and T. Endo, *Journal of Polymer Science Part a-Polymer Chemistry*, 1993, **31**, 581-584.

# Chapter 3

# Group (IV) Salalen complexes as initiators for the ROP of *rac*-LA and as catalysts for the degradation of PLA

# 3. Group (IV) Salalen complexes as initiators for the ROP of *rac*-LA and as catalysts for the degradation of PLA

## 3.1 Preamble

It was hypothesised that by developing catalysts containing both amine-phenolate and imine-phenolate functionality it could facilitate the production of polylactide with high stereocontrol and activity. Complexes containing two imine-phenolate ligands (Salen ligands) have shown to be highly active for many reactions including living syndiotactic propylene polymerisation.[1, 2] However, Salan ligands complexed to group (IV) metals have produced isotactic polyolefins at room temperature.[3] This is thought to be due to the ability of the Salan ligand to wrap around the metal centre forming octahedral complexes of $C_2$-symmetry, with two labile groups in a *cis*-geometry.[2, 3] It would therefore be of interest to generate a ligand system that incorporates the high activity observed with complexes bearing the Salen ligand and the stereocontrol reported with the Salan ligands. Albeit the examples reported above are not for the production of PLA, it would be of interest to optimise a ligand system that incorporates the high activity observed with Salen complexes with the stereocontrol reported for Salan ligands, and transfer it to the ROP of *rac*-LA.

Salalens are hybrid ligands containing an imine and amine nitrogen centre i.e. they are half Salen/half Salan ligands. An advantage of Salalen ligands is the ability to vary the groups on each phenyl ring as well as the tertiary amine moiety, thus fabricating unsymmetrical ligands.

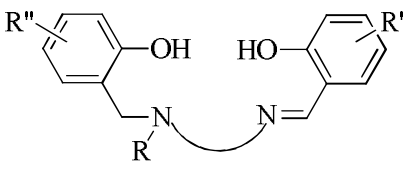


**Figure 3.01**: General structure of Salalen type ligands.[2]

It has been reported that such ligands preferably coordinate to octahedral group (IV) metal centres so that the half Salan donors bind in a *fac* mode and the half

Salen donors bind in a *mer* mode.[4] Kol *et al.* recently reported the use of Salalen titanium complexes for the polymerisation of 1-hexene and propylene in a highly isospecific manner.[4] Other reactions that Salalen ligands have by utilised for include the alternating copolymerisation of cyclohexene oxide and $CO_2$ to produce polycarbonates *via* a chromium catalyst.[5] Aluminium chloro Salalen complexes have be utilised for the hydrophosphonylation of aldehydes[6] as well as being reported to be highly efficient catalysts for the asymmetric oxidation of cyclic dithioacetals[7] and cyclic sulphides.[8] Titanium Salalen complexes containing chiral ligands derived from binaphthol have been reported for the enantioselective epoxidation of olefins, achieving high *ee* values for a range of substrates.[9] Vanadium Salalen catalysts have been shown to active for the preparation of enantioenriched non-protected cyanohydrins, achieving 89 – 95 % *ee* using aliphatic aldehydes.[10]

Both Salan and Salen group (IV) complexes have received an unprecedented amount of interest in the literature for the ROP of *rac*-LA,[11] but no reports have previously utilised Salalen complexes. Developing group (IV) complexes containing Salalen ligands allows unsymmetrical ligand systems to be prepared in which the sterics and electronics of the ligands can be varied in multiple positions. Furthermore, they will formulate $C_1$ symmetric complexes which hitherto have been unexplored for group (IV) complexes for the ROP of *rac*-LA.

Within this chapter, the effect of altering the steric bulk around the metal centre is investigated by changing the substituents of the aromatic ring of the Salen fragment. The steric bulk of the amine substituent has also be varied and the effect such changes have on the rate of polymerisation of *rac*-LA will also be discussed. Furthermore, the use of such Salalen initiators for the degradation of PLA will also be discussed.

## 3.2 Synthesis of ligands

The series of *bis*(phenolate) ligands described above and discussed here in were synthesised as shown in Figure 3.02.

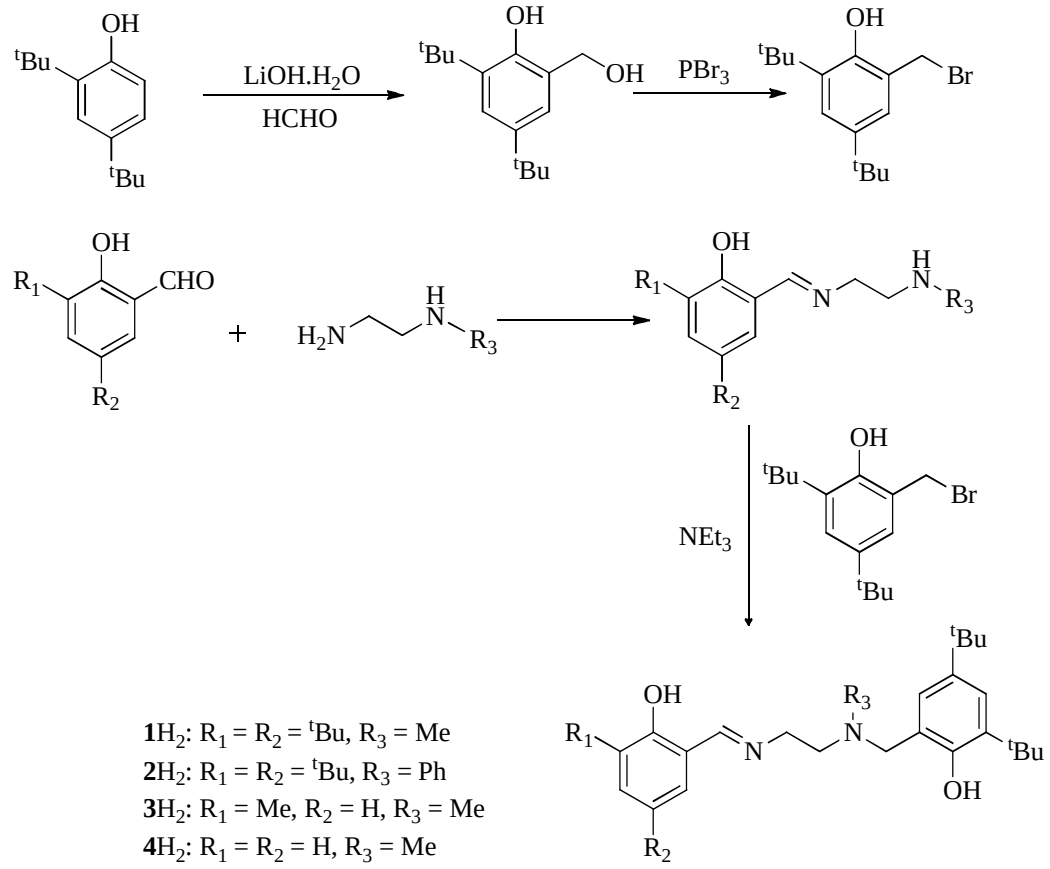


**Figure 3.02**: Synthesis of Salalen Ligands

The first step in the ligand synthesis shown in Figure 3.02, is a modified version of the Mannich reaction to produce the aryl bromide. This is followed by an imine condensation then a $S_N2$ reaction forming the desired ligands. The sterics of the ligands isolated were varied by altering the substituents on the phenolate ring adjacent to the imine centre. In addition to this, the group directly bonded to the amine nitrogen ($R_3$) was varied, being either a methyl or a phenyl group from judicious choice of starting primary amine. It was possible to isolate a single crystal of the more bulky ligand **2**$H_2$ (Figure 3.03). However, further attempts to isolate single crystals of ligands **1**$H_2$, **3**$H_2$ and **4**$H_2$ were unsuccessful. This is presumably due to the unsymmetrical nature of the ligand affecting the packing coupled with their high solubility in common organic solvents. All four ligands were synthesised as indicated in Figure 3.02 and characterised by $^1$H, $^{13}$C{$^1$H} NMR spectroscopy together with high resolution mass spectrometry.

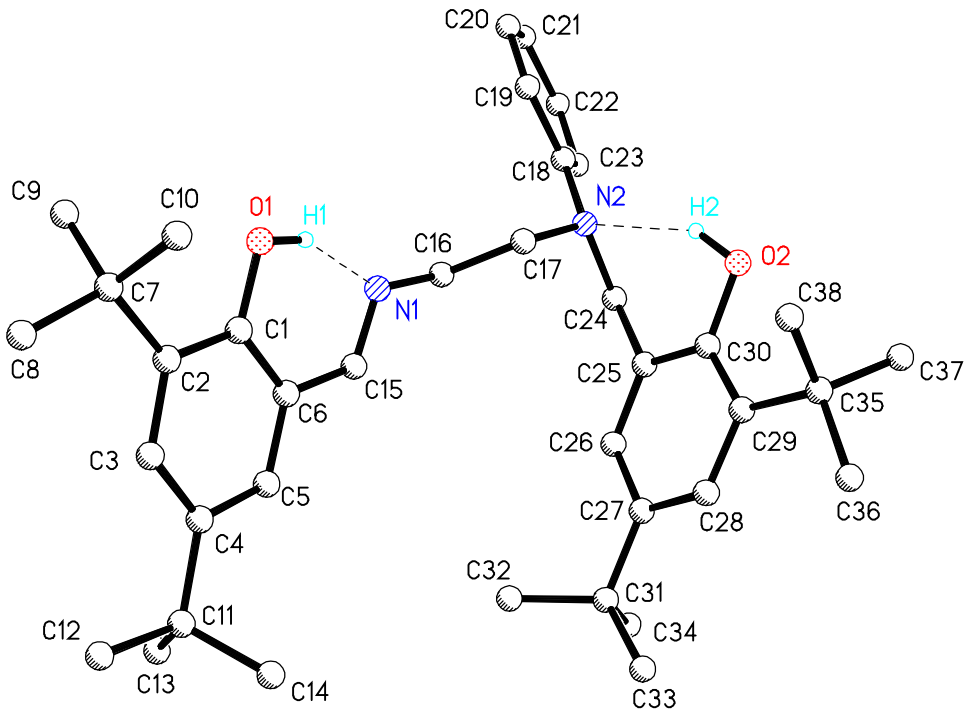


**Figure 3.03**: Solid-state structure of **2**$H_2$ where the H atoms have been removed for clarity except those involved in intramolecular H-bonding. The dashed lines represents the intramolecular H-bonding present.

| H-Bond | D-H (Å) | H···A (Å) | D···A (Å) | D-H-A (°) |
|---|---|---|---|---|
| **O1 H1 N1** | 0.94(2) | 1.74(2) | 2.6059(15) | 152.6(18) |
| **O2 H2 N2** | 0.92(3) | 1.96(3) | 2.7935(16) | 150.0(2) |

**Table 3.01**: Hydrogen bond distances and angles in **2**$H_2$

| | **2**$H_2$ |
|---|---|
| **C15-N1** | 1.2740(17) |
| **C17-N2** | 1.4728(17) |
| **N1-C16** | 1.4533(17) |
| **C24-N2** | 1.4799(17) |

**Table 3.02**: Selected bond lengths (Å) for **2**$H_2$

From Table 3.02 it can be seen that the imine bond length {C(15)-N(1)} is significantly shorter than the amine bond length {C(24)-N(2)} as expected. This highlights the $sp^2$ nature of the imine bond, and the flexibility of the amine bond due to its $sp^3$ hybridization.[12]

## 3.3 Complexing Salalen ligands to group (IV) metals

The ligands prepared in Figure 3.02 were complexed to the group (IV) metals using a 1:1 stoichiometry of the appropriate ligand and metal alkoxide in toluene, as shown in Figure 3.04.[13]

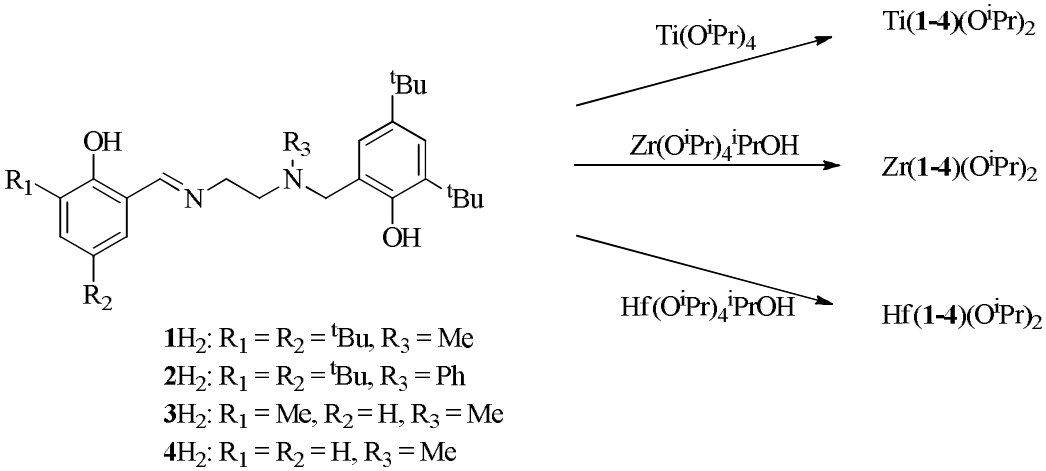


**Figure 3.04**: Complexes prepared using Salalen ligands

Typically the binding modes for Salan and Salen ligands are *fac-fac* and *mer-mer*. However, for such Salalen ligands, it is possible for the ligand to wrap diastereospecifically to produce *fac-fac*, *mer-mer*, *fac-mer or mer-fac* (Figure 3.05). For the complexes mentioned here the geometry observed in the solid state is *fac-mer*, with the Salan fragment *fac* and the Salen fragment *mer*.[2]

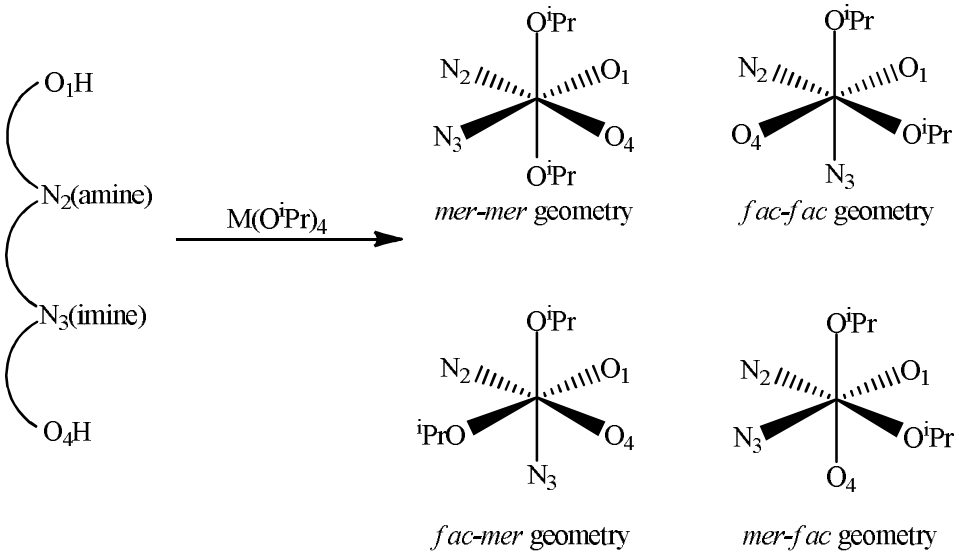


**Figure 3.05**: Possible binding modes of Salalen ligands[2]

All complexes have $C_1$ symmetry with the two isopropoxides being *cis*-orientated {O(1)-M-O(2) = 97.41(10) ° for Zr(**2**)($O^iPr$)$_2$ shown in Figure 3.10}, one being *trans* to the imine with the other *cis* to the amine nitrogen centre, which is in correspondence with literature for similar Salalen complexes.[2]

### 3.3.1 Titanium Initiators

The titanium complexes were characterised by $^1$H NMR, $^{13}$C{$^1$H} NMR spectroscopy and elemental analysis. Titanium complexes containing ligands **1**H$_2$ and **2**H$_2$ were also characterised by single crystal X-ray diffraction. The complexes were shown to be monometallic regardless of the steric bulk on the amine nitrogen centre either being a methyl substituent (Figure 3.06) or a phenyl substituent (Figure 3.07).

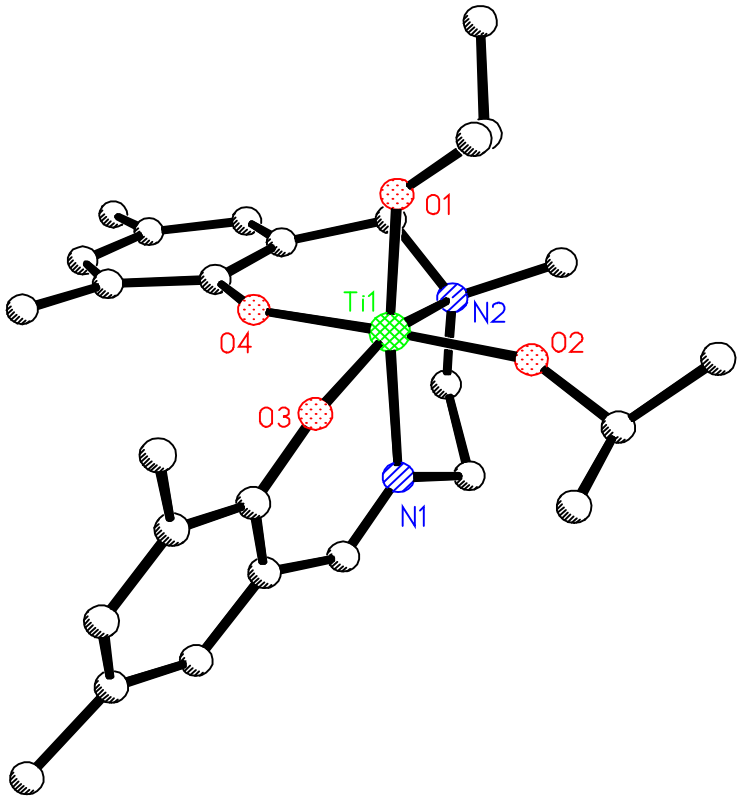


**Figure 3.06**: Solid-state structure of Ti(**1**)($O^iPr$)$_2$ where the methyl groups of the $^t$Bu's have been removed for clarity as have the hydrogen atoms.

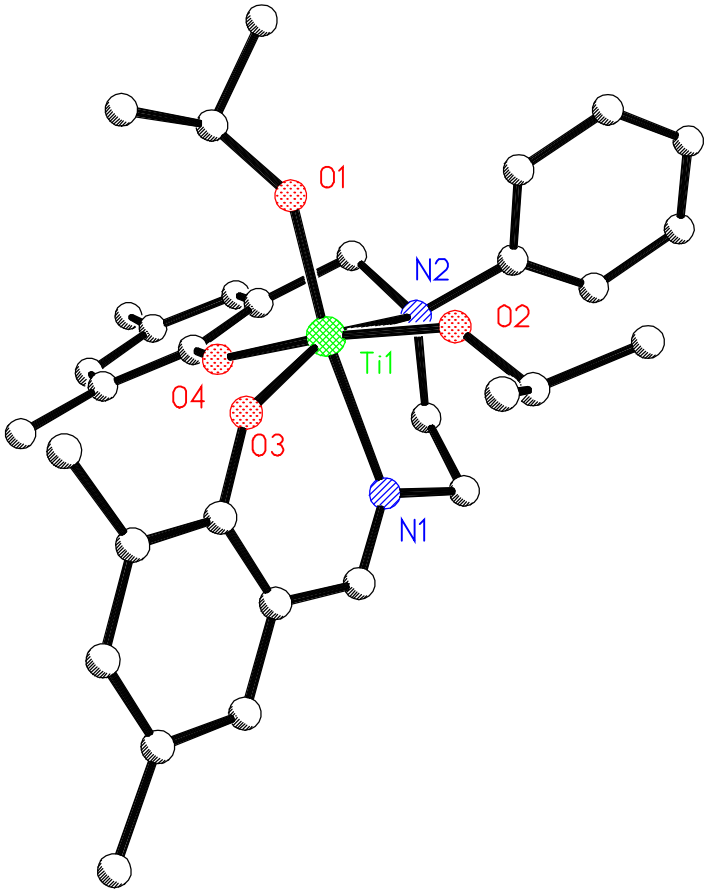


**Figure 3.07**: Solid-state structure of Ti(**2**)($O^iPr$)$_2$ where the methyl groups of the $^t$Bu's have been removed for clarity as have the hydrogen atoms.

| | Ti(1)($O^iPr$)$_2$ | Ti(2)($O^iPr$)$_2$ | [$^t$Bu-salcen-$^t$Bu] Ti($O^iPr$)$_2$[14] | [ONNO]Ti ($O^iPr$)$_2$[15] | Ti(Salalen) ($O^iPr$)$_2$[4] |
|---|---|---|---|---|---|
| **M-O1** | 1.8410(13) | 1.8269(10) | 1.821(4) | 1.806(1) | 1.807(2) |
| **M-O2** | 1.8274(13) | 1.8284(10) | 1.789(4) | 1.819(1) | 1.825(2) |
| **M-O3** | 1.9032(12) | 1.8952(10) | 1.896(4) | 1.939(1) | 1.889(2) |
| **M-O4** | 1.9405(13) | 1.9369(10) | 1.980(4) | 1.921(1) | 2.003(2) |
| **M-N1** | 2.1972(16) | 2.1966(12) | 2.252(4) | 2.325(2) | 2.194(2) |
| **M-N2** | 2.3053(16) | 2.3932(12) | 2.135(5) | 2.309(2) | 2.325(3) |
| **O1-M-N1** | 168.43(6) | 170.62(5) | 82.26(16) | 161.98(11) | 171.79(10) |
| **N1-M-N2** | 74.87(6) | 75.39(4) | 73.04(16) | 75.83(5) | 75.56(9) |
| **C-N imine** | 1.280(2) | 1.283(19) | 1.277(6) & 1.287(6) | - | 1.284(4) |
| **C-N amine** | 1.496(2) | 1.513(3) | - | 1.495(1) & 1.493(1) | 1.491(4) |

**Table 3.03**: Selected bond lengths (Å) and angles (°) for Ti(**1**)($O^iPr$)$_2$, Ti(**2**)($O^iPr$)$_2$ and [$^t$Bu-salcen-$^t$Bu]Ti($O^iPr$)$_2$,[14] [ONNO]Ti($O^iPr$)$_2$[15] and Ti(Salalen)($O^iPr$)$_2$[4] for comparison.

In the solid-state, the titanium centre is seen to adopt a pseudo-octahedral geometry with a {O(1)-Ti-N(1)} bond angle of approximately 170 ° - Table 3.03. The amine and imine bond lengths for Ti(**2**)($O^iPr$)$_2$ shown in Table 3.03 are comparable with the distances reported in the free ligand **2**$H_2$ (C-$N_{amine}$ = 1.4799(17) Å and C-$N_{imine}$ = 1.2740(17) Å - Table 3.02). The data for a Salen complex [$^t$Bu-salcen-$^t$Bu]Ti($O^iPr$)$_2$ (contains ligand **6** in Figure 1.38 of Chapter 1) has also been included in Table 3.03 for comparison with Ti(**1/2**)($O^iPr$)$_2$.[14] The {O(1)-M-N(1)} angle in the [$^t$Bu-salcen-$^t$Bu]Ti($O^iPr$)$_2$ is significantly smaller than that observed for Ti(**1/2**)($O^iPr$)$_2$.[14] This is presumably due to the complex [$^t$Bu-salcen-$^t$Bu]Ti($O^iPr$)$_2$ having *β-cis* geometry with both nitrogen centres equatorial, unlike Ti(**1/2**)($O^iPr$)$_2$ where the imine nitrogen is in an axial position with respect to O(1).[14] All other metric data for Ti(**1/2**)($O^iPr$)$_2$ shown in Table 3.02 are comparable with the example in literature containing a Salcen ligand. [ONNO]Ti($O^iPr$)$_2$ is an example of a titanium complex containing a Salan ligand (Ligand **1c**$H_2$, Figure 1.43, Chapter 1) whose data correlates well with that reported here for Ti(**1/2**)($O^iPr$)$_2$.[15] [ONNO]Ti($O^iPr$)$_2$ is reported to have $C_2$ symmetry in the solid state with both isopropoxide groups being *cis* to each other, and one of the nitrogen centres in an equatorial position analogous to Ti(**1/2**)($O^iPr$)$_2$.[15]

As expected, the M-N(imine) distance is shorter than the M-N(amine) distance for Ti(**1/2**)($O^iPr$)$_2$, which is in correspondence with that observed in the literature for a Ti(Salalen)($O^iPr$)$_2$ complex (Figure 3.08).[4]

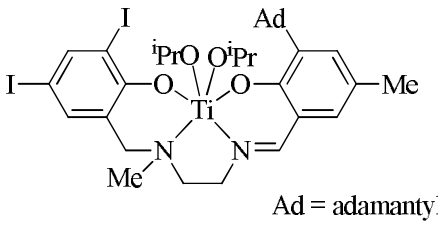


**Figure 3.08**: Ti(Salalen)($O^iPr$)$_2$[4] complex used for comparison with Ti(**1/2**)($O^iPr$)$_2$.

The Ti(Salalen)($O^iPr$)$_2$ complex (Figure 3.08) was reported by Kol *et al.* and shown to display *fac-mer* geometry analogous to that observed for complexes Ti(**1/2**)($O^iPr$)$_2$.[4] All other metric data is consistent with this structure.

The titanium complexes are not fluxional on the NMR timescale and the $^1$H NMR spectra for the compounds have been recorded at 25 °C in $CDCl_3$. The $^1$H NMR spectra has one imine resonance (N=CH) and two septet isopropoxide resonances implying that only one isomer is present in solution – Figure 3.09. Therefore, it is probable that the solid-state structures are maintained in solution.

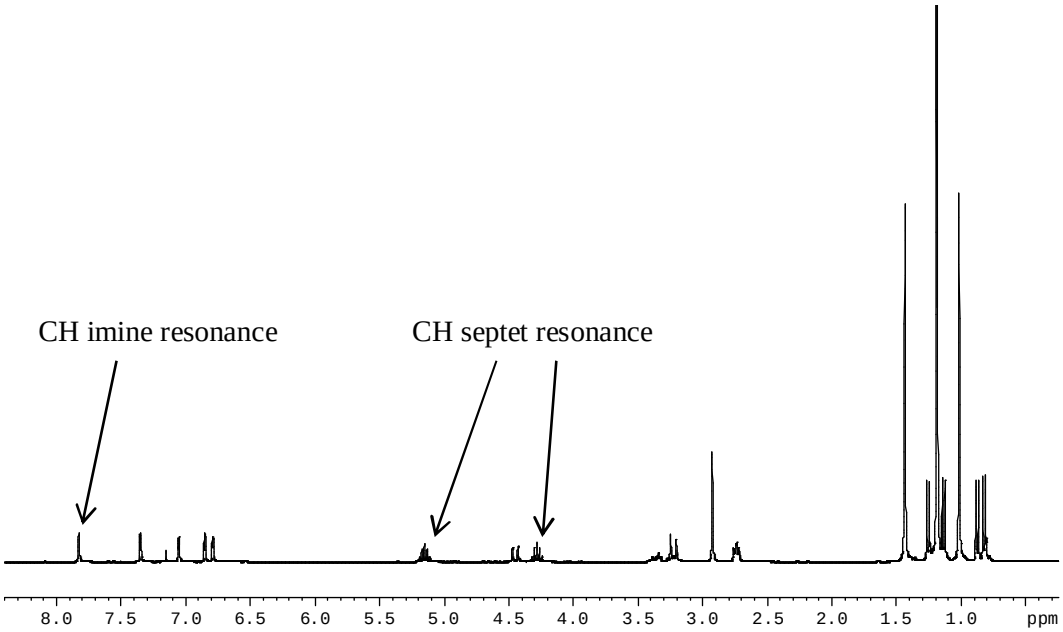


**Figure 3.09:** $^1$H NMR spectrum of Ti(**1**)($O^iPr$)$_2$ in $CDCl_3$ at 298 K

### 3.3.2 Zirconium Initiators

Analogous to the titanium complexes all zirconium complexes were characterised by $^1$H NMR, $^{13}C\{^1H\}$ NMR spectroscopy and elemental analysis. The zirconium complexes containing ligands **1**$H_2$ and **2**$H_2$ were also characterised by single crystal X-ray diffraction – Figures 3.10 and 3.11 respectively.

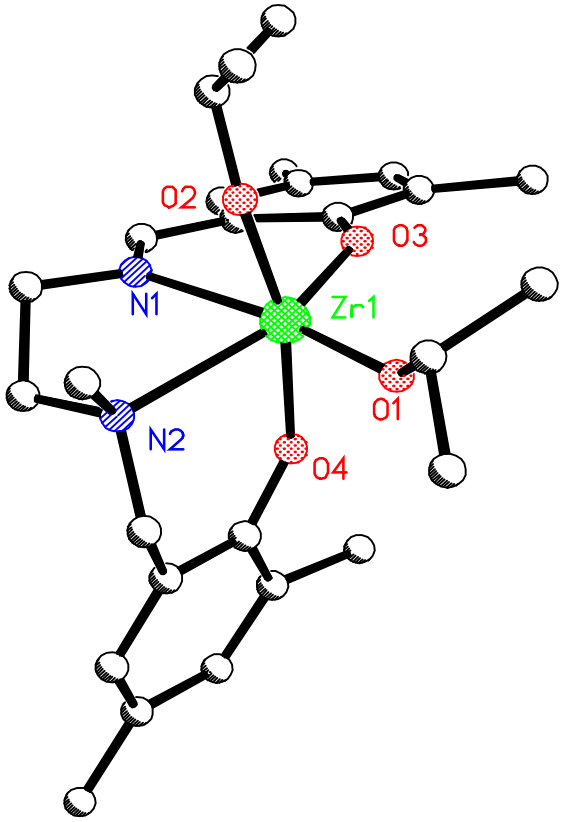


**Figure 3.10**: Solid-state structure of Zr(**1**)($O^iPr$)$_2$ where the methyl groups of the $^t$Bu's have been removed for clarity as have the hydrogen atoms.

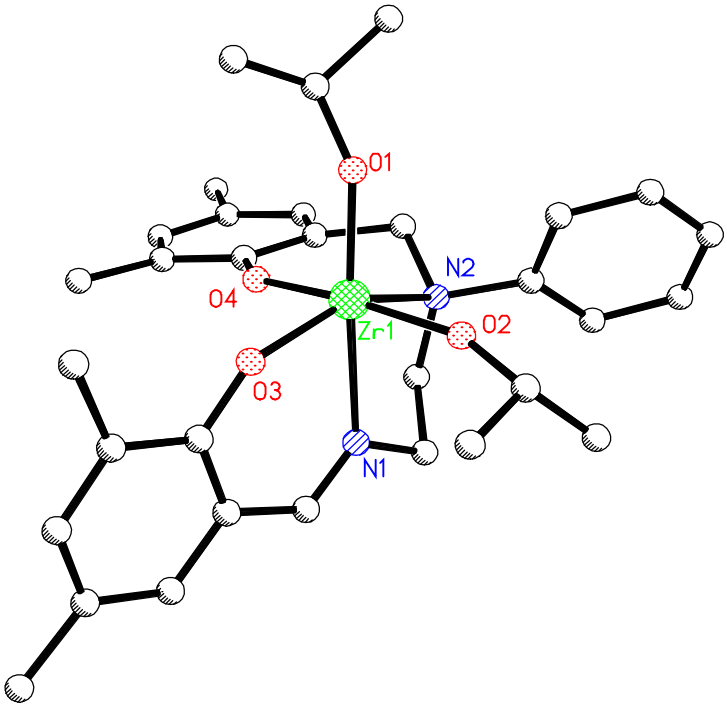


**Figure 3.11**: Solid-state structure of Zr(**2**)($O^iPr$)$_2$ where the methyl groups of the $^t$Bu's have been removed for clarity as have the hydrogen atoms.

| | Zr(1)($O^iPr$)$_2$ | Zr(2)($O^iPr$)$_2$ | [ONNO]Zr$Bn_2$[3] | Zr(Salen)$Cl_2$(THF)[16] | Zr(Salalen)$(NMe_2)_2$[2] |
|---|---|---|---|---|---|
| **M-O1** | 1.9788(12) | 1.963(2) | - | 2.478(2)* | 2.082(2)‡ |
| **M-O2** | 1.9567(12) | 1.949(2) | - | 2.489(2)* | 2.109(2)‡ |
| **M-O3** | 2.0268(11) | 2.016(2) | 2.011(2) | 2.002(4) | 2.026(2) |
| **M-O4** | 2.0534(11) | 2.062(2) | 2.010(2) | 2.024(3) | 2.040(2) |
| **M-N1** | 2.3385(14) | 2.340(2) | 2.509(2) | 2.336(4) | 2.354(2) |
| **M-N2** | 2.4335(14) | 2.487(3) | 2.443(2) | 2.352(4) | 2.493(2) |
| **O1-M-N1** | 168.59(5) | 171.71(10) | 164.75 | - | 174.11(9)‡ |
| **N1-M-N2** | 71.94(5) | 72.74(9) | 70.19(5) | 70.40(2) | 72..09(8) |
| **C-N imine** | 1.281(2) | 1.284(4) | - | 1.282(7) & 1.279(7) | 1.281(4) |
| **C-N amine** | 1.502(2) | 1.518(4) | 1.494 & 1.495 | - | 1.503(4) |

**Table 3.04**: Selected bond lengths (Å) and angles (°) for Zr(**1**)($O^iPr$)$_2$, Zr(**2**)($O^iPr$)$_2$, [ONNO]Zr$Bn_2$[3], Zr(Salen)$Cl_2$(THF)[16] and Zr(Salalen)$(NMe_2)_2$[2]. * M-Cl bond length, ‡ O(1)=N.

The complexes Zr(**1/2**)($O^iPr$)$_2$ were compared with other Salan[3], Salen[16] and Salalen[2] complexes reported in the literature as shown in Table 3.04. [ONNO]Zr$Bn_2$ is an example of a zirconium complex containing a Salan ligand shown in Figure 3.12.

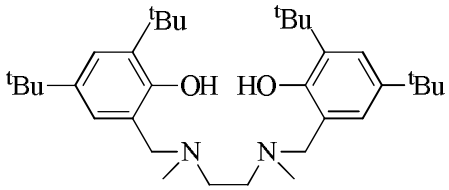


**Figure 3.12**: Salan ligand complexed to zirconium for the production of [ONNO]Zr$Bn_2$[3]

Values for the {M-O(1)} and {M-O(2)} were obviously not obtainable due to the [ONNO]Zr$Bn_2$ complex not containing isopropoxide groups, but benzyl moieties. The [ONNO]Zr$Bn_2$ complex reported by Kol *et al.* displayed $C_2$ symmetry with the benzyl groups being *cis* to each other evident from a C-Zr-C angle of 110.5(11) °.[3] The crystal data obtained for Zr(**1/2**)($O^iPr$)$_2$ correlates well with that reported for [ONNO]Zr$Bn_2$ with a longer {M-N(1)} observed for the Salan complex due to the absence of a imine bond.[3] Zr(Salen)$Cl_2$(THF) is an example of a zirconium complex containing a Salen ligand (Figure 3.13).[16]

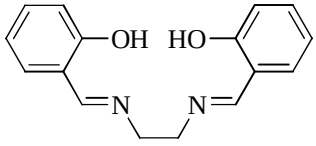


**Figure 3.13**: Salen ligand complexed to zirconium for the production of $Zr(Salen)Cl_2(THF)$[16]

$Zr(Salen)Cl_2(THF)$ is a seven-coordinate zirconium complex in a pseudo-pentagonal bipyramid confirmation with chlorine atoms occupying the axial position and hence *trans* to each other.[16] A {O(1)-M-N(1)} value has not been reported in Table 3.04 for $Zr(Salen)Cl_2(THF)$, due to the two chlorine atoms being in the axial positions with a Cl-Zr-Cl bond angle of 160.24(6) °.[16] The C-N(imine) bond lengths reported for Zr(**1/2**)($O^iPr$)$_2$ are consistent with those reported for corresponding Salen complexes. The values reported for Zr(**1/2**)($O^iPr$)$_2$ in Table 3.04 are in good agreement with the values in the literature for an analogous zirconium complex containing a Salalen ligand (Figure 3.01 where R = Me and R' = $^t$Bu).[2]

All complexes prepared exist as one isomer in solution with the exception of Zr(**3**)($O^iPr$)$_2$, which from $^1$H NMR analysis in $CDCl_3$, showed the presence of more than one structural isomer (Figure 3.14).

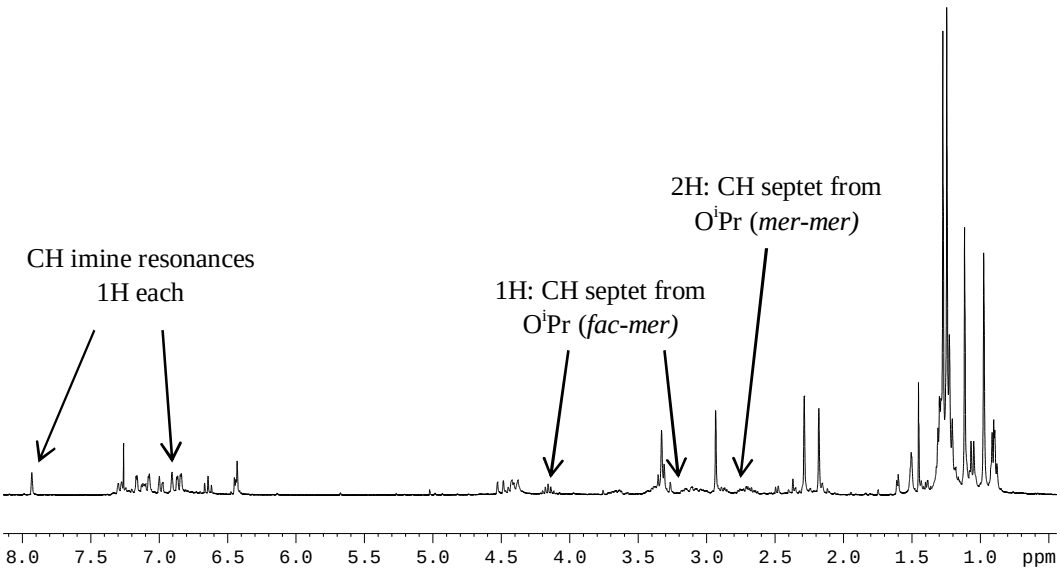


**Figure 3.14**: $^1$H NMR spectrum of Zr(**3**)($O^iPr$)$_2$ in $CDCl_3$ at 298 K

There are two CH imine resonances corresponding to one proton each. One resonance is presumably from the presence of the *fac-mer* isomer in solution and the other from a different structural motif. Due to the presence of a septet of integral 2H present in the $^{1}$H spectrum of Zr(**3**)O$^{i}$Pr)$_2$, it is hypothesised that the *mer-mer* isomer must also be present in solution. If any of the other structural isomers were present then there would be the presence of two isopropoxide septets of 1H integral each due to the different structural environments of the groups. However, only the *mer-mer* isomer can have the two isopropoxide groups in the same environment, producing a septet of integral 2H which is equivalent to that observed in Figure 3.14. The spectrum in Figure 3.14 confirms the presence of two different structural isomers in solution (*fac-mer* and *mer-mer*), in equal proportions. This is also observed when the $^{1}$H NMR spectrum ($CDCl_3$) is recorded at 243 K.

### 3.3.3 Hafnium Initiators

Analogous to the titanium and zirconium complexes all hafnium complexes were characterised by $^{1}$H NMR, $^{13}$C{$^{1}$H} NMR spectroscopy and elemental analysis. The hafnium complexes containing ligands **1**H$_2$, **2**H$_2$ and **3**H$_2$ were also characterised by single crystal X-ray diffraction – Figures 3.15, 3.16 and 3.17 respectively.

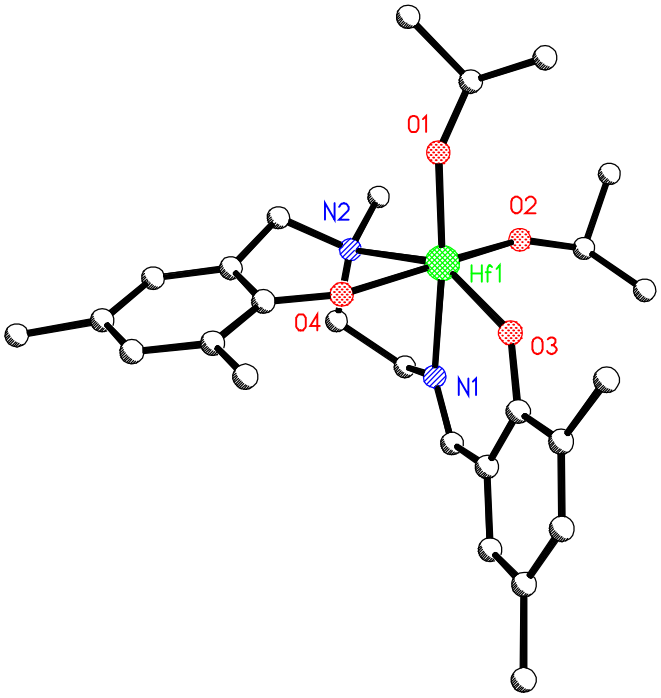


**Figure 3.15**: Solid-state structure of Hf(**1**)($O^iPr$)$_2$ where the methyl groups of the $^t$Bu's have been omitted for clarity, as have the hydrogen atoms.

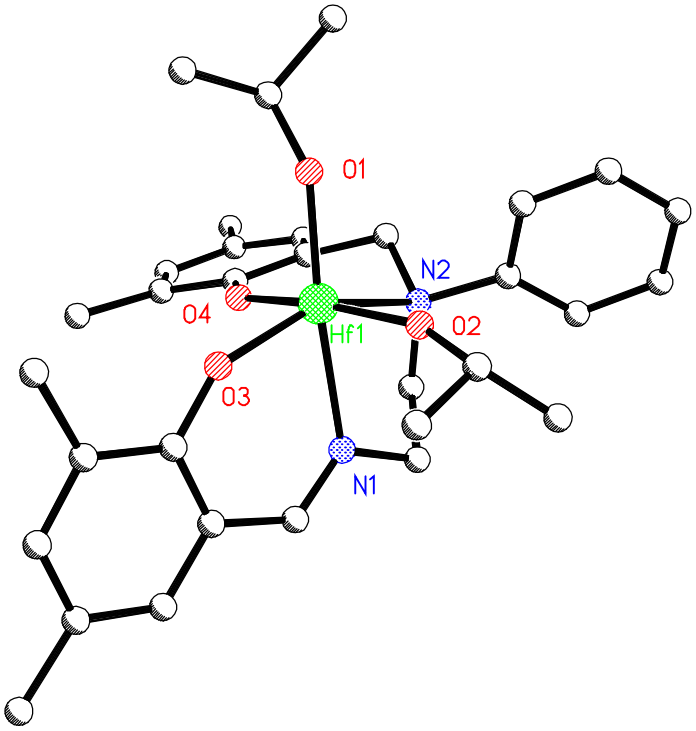


**Figure 3.16**: Solid-state structure of Hf(**2**)($O^iPr$)$_2$ where the methyl groups of the $^t$Bu's have been omitted for clarity, as have the hydrogen atoms.

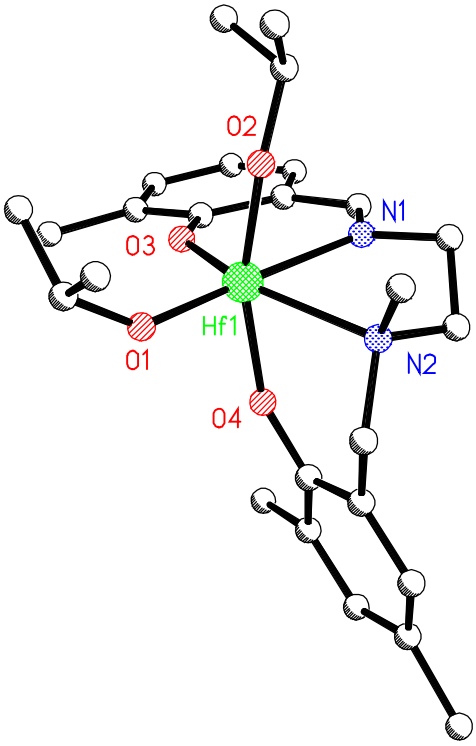


**Figure 3.17**: Solid-state structure of Hf(**3**)($O^iPr$)$_2$ where the hydrogen atoms have been removed for clarity.

Analogous to the titanium and zirconium complexes discussed above, in the solid-state, the hafnium centre is seen to adopt a pseudo-octahedral geometry, Table 3.05. This is exemplified by a {O(1)-M-N(1)} bond angle of approximately 170 ° for Hf(**1/2**)($O^iPr$)$_2$ with an increase in this angle observed for Hf(**3**)($O^iPr$)$_2$ {176.44(10) °}.

| | Hf(1)($O^iPr$)$_2$ | Hf(2)($O^iPr$)$_2$ | Hf(3)($O^iPr$)$_2$ | {$(NO)_2$Hf($O^tBu$)$_2$}[17] | {Hf(Salen)$O^iPr$}$_2$[18] |
|---|---|---|---|---|---|
| **M-O1** | 1.9739(16) | 1.962(2) | 1.964(2) | 1.907(2) | 1.925(5) |
| **M-O2** | 1.9521(17) | 1.944(2) | 1.954(2) | 1.913(2) | 2.193(4)* |
| **M-O3** | 2.0168(16) | 2.007(2) | 2.008(2) | 2.043(2) | 2.099(4) |
| **M-O4** | 2.0471(16) | 2.048(2) | 2.041(2) | 2.059(2) | 2.102(4) |
| **M-N1** | 2.3087(19) | 2.308(3) | 2.327(3) | 2.457(3) | 2.352(5) |
| **M-N2** | 2.399(2) | 2.452(3) | 2.379(3) | 2.554(3) | 2.346(6) |
| **O1-M-N1** | 169.24(7) | 171.58(10) | 176.44(10) | 144.45(8) | 89.92(2) |
| **N1-M-N2** | 72.74(7) | 73.45(8) | 74.19(10) | 84.06(9) | - |
| **C-N imine** | 1.277(3) | 1.283(4) | 1.285(5) | - | 1.277 & 1.293 |
| **C-N amine** | 1.500(3) | 1.523(4) | 1.519(6) | - | - |

**Table 3.05**: Selected bond lengths (Å) and angles (°) for complexes Hf(**1**)($O^iPr$)$_2$, Hf(**2**)($O^iPr$)$_2$, Hf(**3**)($O^iPr$)$_2$, {$(NO)_2$Hf($O^tBu$)$_2$}[17] and {Hf(Salen)$O^iPr$}$_2$[18]. * M-O(2) distance from Hf centre to oxygen of μ-oxo bridge[18]

{$(NO)_2$Hf($O^tBu$)$_2$} is an example of an octahedral group (IV) complex with $C_1$ symmetry (Figure 1.42, Chapter 1).[17] Unlike Hf(**1-3**)($O^iPr$)$_2$, {$(NO)_2$Hf($O^tBu$)$_2$} contains a "half-ligand" with *cis*-N/*trans*-O binding.[17] The geometry observed in {$(NO)_2$Hf($O^tBu$)$_2$} is analogous to that observed in a Salan type complex and therefore has been used for comparison with the Salalen complex reported here.[17] It can be seen in Table 3.05 that the {O(1)-M-N(1)} angle is narrower in {$(NO)_2$Hf($O^tBu$)$_2$} presumably due to the $O^tBu$ labile groups being in a *cis* geometry therefore inflicting a steric repulsion with the "half-ligands".[17] Apart from this exception, the bond lengths and angles reported for Hf(**1-3**)($O^iPr$)$_2$ are consistent with those reported for {$(NO)_2$Hf($O^tBu$)$_2$}. The complex {Hf(Salen)$O^iPr$}$_2$ is a symmetric dimer consisting of two mononuclear hafnium centres containing a Salen ligand (Figure 3.18) joined *via* a dinuclear species with a μ-oxo bridge.[18]

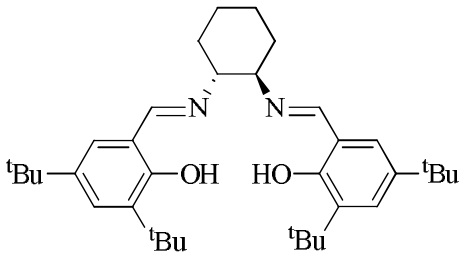


**Figure 3.18**: Salen ligand for the preparation of {Hf(Salen)O$^i$Pr}$_2$[18]

Due to {Hf(Salen)O$^i$Pr}$_2$ being a dimeric complex, the {M-O(2)} distance reported in Table 3.05 is not to a labile isopropoxide group, but to the bridging oxygen between the two metal centres.[18] All values reported for Hf(**1-3**)(O$^i$Pr)$_2$ are consistent with that in the literature for the Salen complex {Hf(Salen)O$^i$Pr}$_2$ with the exception of the {O(1)-M-N(1)} angle which is significantly reduced for the complex containing a Salen ligand. This is presumably due to the Salen complex existing as a dimeric species in the solid-state.[18]

The hafnium complexes isolated are not fluxional on the NMR time-scale and the $^1$H NMR spectra for the compounds have been recorded at 25 °C in $CDCl_3$. Analogous to that observed for the zirconium initiators, all hafnium complexes except Hf(**3**)(O$^i$Pr)$_2$ show only one imine resonance (CH) and two septet isopropoxide resonances in the $^1$H NMR spectrum. This implies that only one isomer is present in solution. Consistent with that observed for Zr(**3**)(O$^i$Pr)$_2$, the $^1$H NMR spectrum of Hf(**3**)(O$^i$Pr)$_2$ contained two imine resonances in the $^1$H NMR spectrum at 7.92 ppm and 6.87 ppm and consequently two imine resonances in the $^{13}$C{$^1$H} NMR spectrum together with 24 aromatic resonances (Figure 3.19 and 3.20).

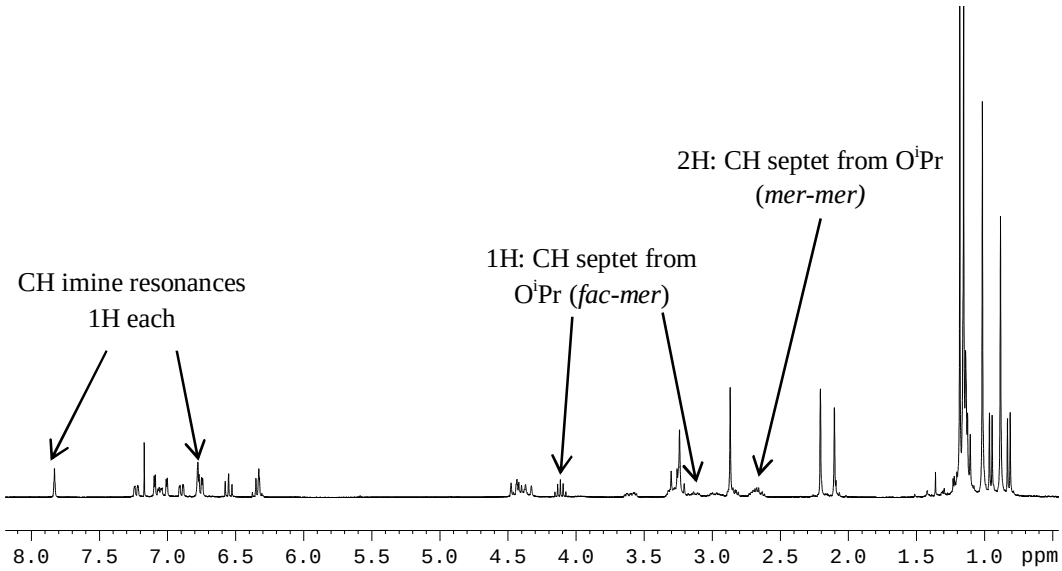


**Figure 3.19**: $^1$H NMR spectrum of complex Hf(**3**)(O$^i$Pr)$_2$ showing two imine peaks and three CH septet resonances.

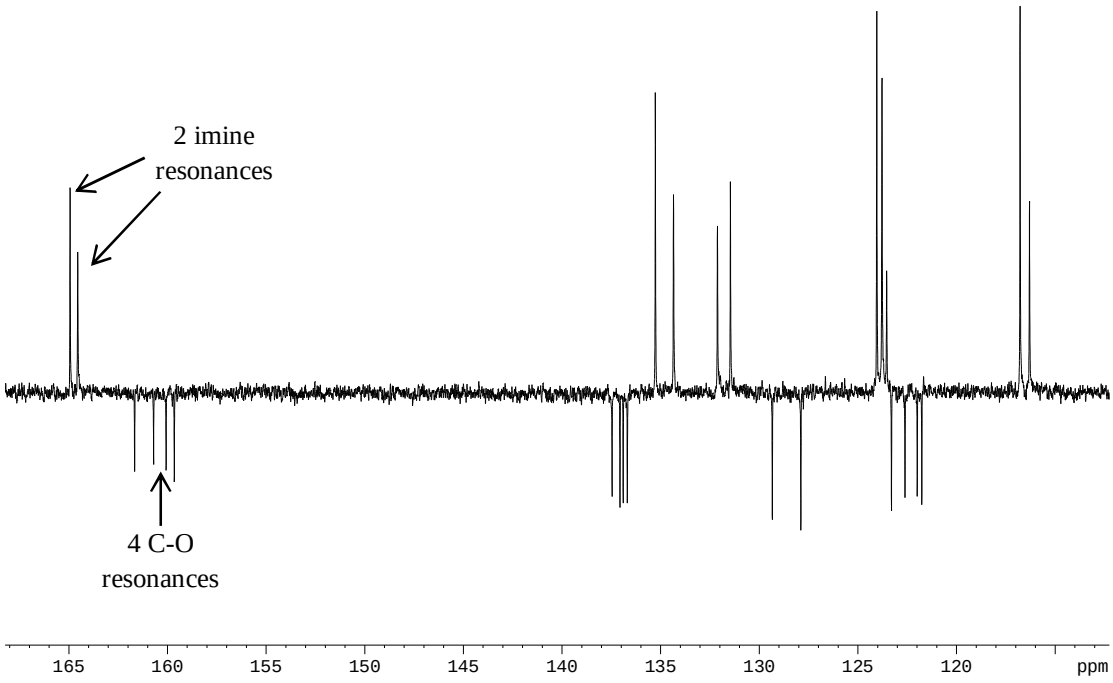


**Figure 3.20**: Aromatic region of $^{13}$C{$^1$H} NMR spectrum of complex Hf(**3**)(O$^i$Pr)$_2$ showing two imine resonances and 24 aromatic resonances.

Analysis of Figure 3.19, shows that there is the presence of more than one structural isomer of complex Hf(**3**)(O$^i$Pr)$_2$. There are two CH imine resonances corresponding to one proton each. One resonance is presumably from the presence of the *fac-mer* isomer in solution and the other from a different structural motif. Due to the presence of a septet of integral 2H present in the $^1$H spectrum of

Hf(**3**)O$^{i}$Pr)$_2$, it is hypothesised that the *mer-mer* isomer must also be present in solution. If any of the other structural isomers were present then there would be the presence of two isopropoxide septets of 1H integral each due to the different structural environments of the groups - Figure 3.05. However, only the *mer-mer* isomer can have the two isopropoxide groups in the same environment producing a septet of integral 2H. The spectra in Figure 3.19 and 3.20 confirm the presence of two different structural isomers in solution (*fac-mer* and *mer-mer*), in equal proportions. This is also observed when the $^{1}$H NMR spectrum ($CDCl_3$) is recorded at 243 K.

## 3.4 Ring-opening Polymerisation of *rac*-LA

As mentioned in Section 3.1, the steric bulk of the ligand and the variation of substituents within the ligand structure can have an effect on the polymerisation. Hence, the initiators shown in Figure 3.04 were trialled for the ROP of *rac*-lactide. All initiators were originally tested in toluene at 80 °C for 2 hours, but the majority of initiators {except the Ti(IV) initiators} failed to produce polymeric material. It was decided to continue with testing all initiators for 24 hours in toluene at 80 °C and under the more industrially preferred melt conditions at 130 °C.

### 3.4.1 Titanium Initiators

All titanium initiators were tested for the ROP of *rac*-LA at 80 °C in toluene for 2 hours and 24 hours (Table 3.06 and Table 3.07) as well as under industrially preferred melt conditions at 130 °C in the absence of solvent (Table 3.08).

| Entry | Initiator | Conversion[a] (%) | $M_n$[b] | $M_w$[b] | $M_n$ (theo.) | PDI[b] | $P_r$[c] |
|---|---|---|---|---|---|---|---|
| **1** | Ti(**1**)($O^iPr$)$_2$ | 98 | 11650 | 16900 | 14150 | 1.45 | 0.5 |
| **2** | Ti(**2**)($O^iPr$)$_2$ | 69 | 8450 | 9950 | 10000 | 1.18 | 0.5 |
| **3** | Ti(**3**)($O^iPr$)$_2$ | 10 | - | - | - | - | - [d] |
| **4** | Ti(**4**)($O^iPr$)$_2$ | 61 | 9300 | 11500 | 8850 | 1.24 | 0.5 |

**Table 3.06**: ROP results for Ti(**1-4**)($O^iPr$)$_2$ in toluene at 80 °C after 2 hours. 0.7 g of *rac*-LA, [LA]/[initiator] = 100. [a] conversion as determined *via* $^1$H NMR, [b] determined from GPC (in THF) referenced to polystyrene, [c] calculated from the $^1$H homonuclear decoupled NMR ($CDCl_3$) analysis, [d] $P_r$ value not obtained.

| Entry | Initiator | Conversion[a] (%) | $M_n$[b] | $M_w$[b] | $M_n$ (theo.) | PDI[b] | $P_r$[c] |
|---|---|---|---|---|---|---|---|
| **1** | Ti(**1**)($O^iPr$)$_2$ | 98 | 9850 | 16000 | 14150 | 1.62 | 0.5 |
| **2** | Ti(**2**)($O^iPr$)$_2$ | 97 | 10100 | 18450 | 14050 | 1.82 | 0.5 |
| **3** | Ti(**3**)($O^iPr$)$_2$ | 91 | 18800 | 26500 | 13150 | 1.41 | 0.5 |
| **4** | Ti(**4**)($O^iPr$)$_2$ | 97 | 12850 | 23750 | 14050 | 1.85 | 0.5 |

**Table 3.07**: ROP results for Ti(**1-4**)($O^iPr$)$_2$ in toluene at 80 °C after 24 hours. 0.7 g of *rac*-LA, [LA]/[initiator] = 100. [a] conversion as determined *via* $^1$H NMR, [b] determined from GPC (in THF) referenced to polystyrene, [c] calculated from the $^1$H homonuclear decoupled NMR ($CDCl_3$) analysis.

| Entry | Initiator | Conversion[a] (%) | $M_n$[b] | $M_w$[b] | $M_n$ (theo.) | PDI[b] | $P_r$[c] |
|---|---|---|---|---|---|---|---|
| **1** | Ti(**1**)($O^iPr$)$_2$ | 89 | 38000 | 54750 | 38500 | 1.44 | 0.5 |
| **2** | Ti(**2**)($O^iPr$)$_2$ | 95 | 43200 | 65450 | 41100 | 1.51 | 0.5 |
| **3** | Ti(**3**)($O^iPr$)$_2$ | 9 | 2700 | 3100 | 3950 | 1.14 | - [d] |
| **4** | Ti(**4**)($O^iPr$)$_2$ | 91 | 48150 | 69750 | 39350 | 1.45 | 0.5 |

**Table 3.08**: ROP results for Ti(**1-4**)($O^iPr$)$_2$ in absence of solvent at 130 °C for 15 minutes. 2 g of *rac*-LA, [LA]/[initiator] = 300. [a] conversion as determined *via* $^1$H NMR, [b] determined from GPC (in THF) referenced to polystyrene, [c] calculated from the $^1$H homonuclear decoupled NMR ($CDCl_3$) analysis, [d] $P_r$ value not obtained

The conversion to polymeric material can be calculated using $^1$H NMR spectroscopy as reported in Chapter 2 for the ROP of *rac*-LA *via* group (IV) amine *tris*(phenolate) complexes. The $M_n$(theo.) values reported in Tables 3.06 - 3.08 were calculated according to Equation 2.03 in Section 2. In most cases there

is good correlation between the theoretical molecular weights and those observed for one polymeric chain per metal centre. Ti(**3**)($O^iPr$)$_2$ in toluene for 2 hours, showed low conversion to polymeric material, therefore it was not possible to analyse any product and hence no values are reported in Table 3.06 for $M_n$, $M_w$, PDI or $P_r$. In the absence of solvent, a low conversion was also seen (9 %) for Ti(**3**)($O^iPr$)$_2$, however, GPC analysis was possible and as expected indicated low molecular weight material was produced. As seen from Tables 3.06 - 3.08 all titanium initiators gave atactic PLA under melt conditions and at 80 °C in toluene, with a $P_r$ value of 0.5. For analogous titanium amine *bis*(phenolate) complexes reported by Davidson *et al.*, atactic PLA was produced, in agreement with the initiators reported here.[15] From the $^1$H homonuclear decoupled NMR spectrum, Figure 3.21, five resonances of 1:1:1:3:2 ratio was observed.

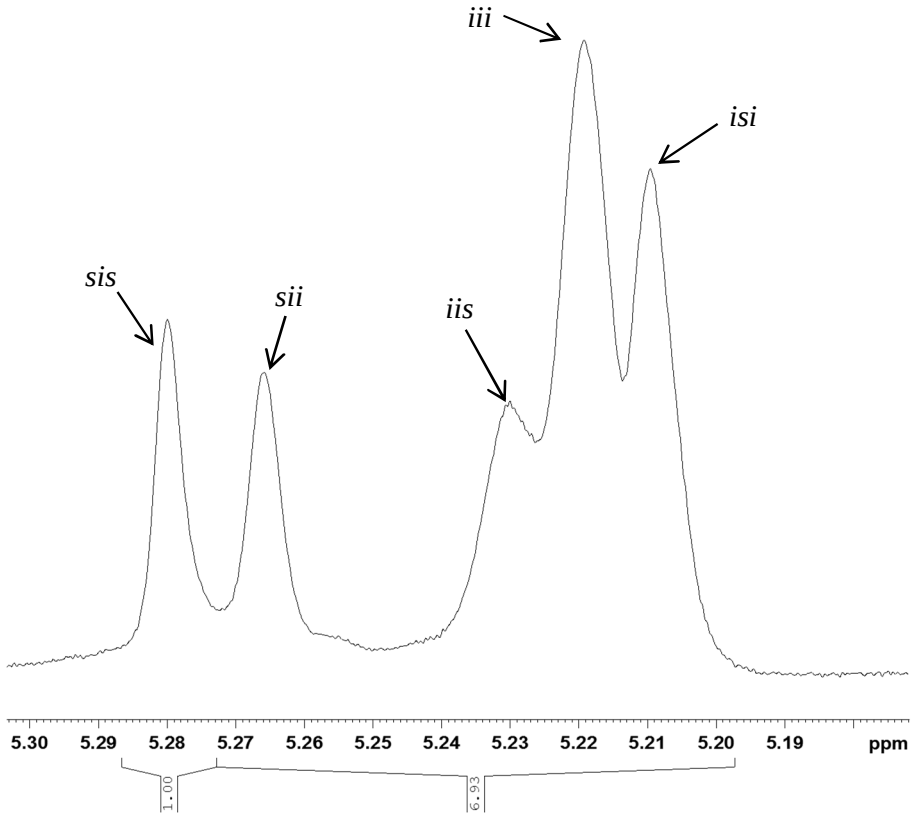


**Figure 3.21**: $^1$H homonuclear decoupled NMR spectrum of polymer produced from Ti(**4**)($O^iPr$)$_2$ in toluene at 80 °C after 24 hours with $P_r$ = 0.5 – entry 4 in Table 3.07

The polymerisation reactions in toluene after 2 hours gave polymeric products with low polydispersity values. However, after a reaction time of 24 hours in toluene, the PDI values were seen to be higher, potentially caused by transesterification after monomer consumption. Under melt conditions or when

the reaction is carried out in toluene for 24 hours, there is very little discrepancy between the theoretical molecular weights and that observed, with all ligands. It does appear however, that Ti(**3**)($O^iPr$)$_2$ is the least active.

To investigate the polymerisation further, MALDI-ToF mass spectrometry was performed on the polymeric products. The MALDI-ToF mass spectrum shows that the polymers contain an isopropoxide end group indicating that the reaction is proceeding *via* a coordination and insertion mechanism. The MALDI-ToF mass spectrum of the polymer obtained using Ti(**4**)($O^iPr$)$_2$ (entry 4, Table 3.07) indicates a separation of repeat units corresponding to 72 gmol$^{-1}$ indicative of transesterification as expected with high PDI values.

### 3.4.2 Zirconium Initiators

All zirconium complexes isolated were trialled for the ROP of *rac*-LA under both solvent (Table 3.09) and solvent-free conditions (Table 3.10). With solvent conditions, the polymerisations were performed in toluene for 2 hours and 24 hours. After 2 hours in toluene at 80 °C, no polymeric material was isolated with initiators Zr(**2/3/4**)($O^iPr$)$_2$. Zr(**1**)($O^iPr$)$_2$ however, gave 91 % conversion to PLA after 2 hours in toluene ($M_n$ = 10,550 gmol$^{-1}$, PDI = 1.13).

| Entry | Initiator | Conversion[a] (%) | $M_n$[b] | $M_w$[b] | $M_n$ (theo.) | PDI[b] | $P_r$[c] |
|---|---|---|---|---|---|---|---|
| **1** | Zr(**1**)($O^iPr$)$_2$ | 99 | 15750 | 22700 | 14300 | 1.44 | 0.56 |
| **2** | Zr(**2**)($O^iPr$)$_2$ | 96 | 10450 | 11300 | 13900 | 1.08 | 0.57 |
| **3** | Zr(**3**)($O^iPr$)$_2$ | 97 | 450 | 500 | 14050 | 1.08 | -[d] |
| **4** | Zr(**4**)($O^iPr$)$_2$ | 99 | 450 | 550 | 14300 | 1.27 | -[d] |

**Table 3.09**: ROP results for Zr(**1-4**)($O^iPr$)$_2$ in toluene at 80 °C for 24 hours. 0.7 g of *rac*-LA, [LA]/[initiator] = 100. [a] conversion as determined *via* $^1$H NMR, [b] determined from GPC (in THF) referenced to polystyrene, [c] calculated from the $^1$H homonuclear decoupled NMR ($CDCl_3$) analysis, [d] $P_r$ value not obtained.

| Entry | Initiator | Conversion[a] (%) | $M_n$[b] | $M_w$[b] | $M_n$ (theo.) | PDI[b] | $P_r$[c] |
|---|---|---|---|---|---|---|---|
| **1** | Zr(**1**)$(O^iPr)_2$ | 98 | 42400 | 50500 | 42400 | 1.19 | 0.57 |
| **2** | Zr(**2**)$(O^iPr)_2$ | 52 | 8700 | 9350 | 22500 | 1.07 | 0.56 |
| **3** | Zr(**3**)$(O^iPr)_2$ | 99 | 1600 | 2050 | 42850 | 1.30 | 0.37 |
| **4** | Zr(**4**)$(O^iPr)_2$ | 99 | 3500 | 5450 | 42850 | 1.56 | 0.52 |

**Table 3.10**: ROP results for Zr(**1-4**)$(O^iPr)_2$ in absence of solvent at 130 °C for 15 minutes. 2 g of *rac*-LA, [LA]/[initiator] = 300. [a] conversion as determined *via* $^1$H NMR, [b] determined from GPC (in THF) referenced to polystyrene, [c] calculated from the $^1$H homonuclear decoupled NMR ($CDCl_3$) analysis.

From Tables 3.09 and 3.10 it can clearly be seen that under both solution and solvent-free conditions, as the steric hindrance around the metal centre is reduced the $M_n$ of the product also decreases. The product is no longer polymeric but oligomeric (entry **3** and **4** in Table 3.09 and Table 3.10). There is a good correlation between the theoretical molecular weights (calculated as for the titanium initiators) and those observed for Zr(**1**)$(O^iPr)_2$ under both solution and solvent-free conditions, for one polymeric chain growing per metal centre. This is further observed when the initiator is Zr(**2**)$(O^iPr)_2$ in solution, however under melt conditions the molecular weights measured are much lower than those expected. In general it can be seen that the zirconium initiators Zr(**1/2**)$(O^iPr)_2$ appear to offer a greater degree of control than the analogous titanium initiators with lower polydispersity indexes observed particularly under melt conditions. For example, when ligand **2**$H_2$ is complexed to Ti(IV) or Zr(IV), the polydispersity index is 1.82 for Ti(IV) in toluene after 24 hrs compared to 1.08 for Zr(IV). Unlike the titanium initiators discussed in Section 3.4.1, which gave all atactic PLA, the zirconium initiators produced PLA with a slight heterotactic bias, except Zr(**3**)$(O^iPr)_2$ where a slight isotactic tendency was observed (entry 3, Table 3.10).

The ability of the zirconium initiators to produce PLA with a heterotactic bias is in correspondence with zirconium complexes reported by Davidson *et al.* using $C_3$-symmetric amine *tris*(phenolate) ligands.[19] However, the initiators reported here do not produce PLA with as high a degree of stereocontrol as that reported by Davidson *et al.* who observed products with $P_r$ values as high as 0.98 in toluene albeit after a longer reaction time of 48 hours or 0.96 under melt conditions.[19] This is in contrast to the tetradentate amine *bis*(phenolate) zirconium

complexes also reported by Davidson *et al.* which were shown to give isotactically enriched PLA under both solution and solvent-free conditions.[15] To study the polymerisation reaction further, Zr(**1**)($O^iPr$)$_2$ was employed as the initiator to investigate how controlled the polymerisation is (Figure 3.22).

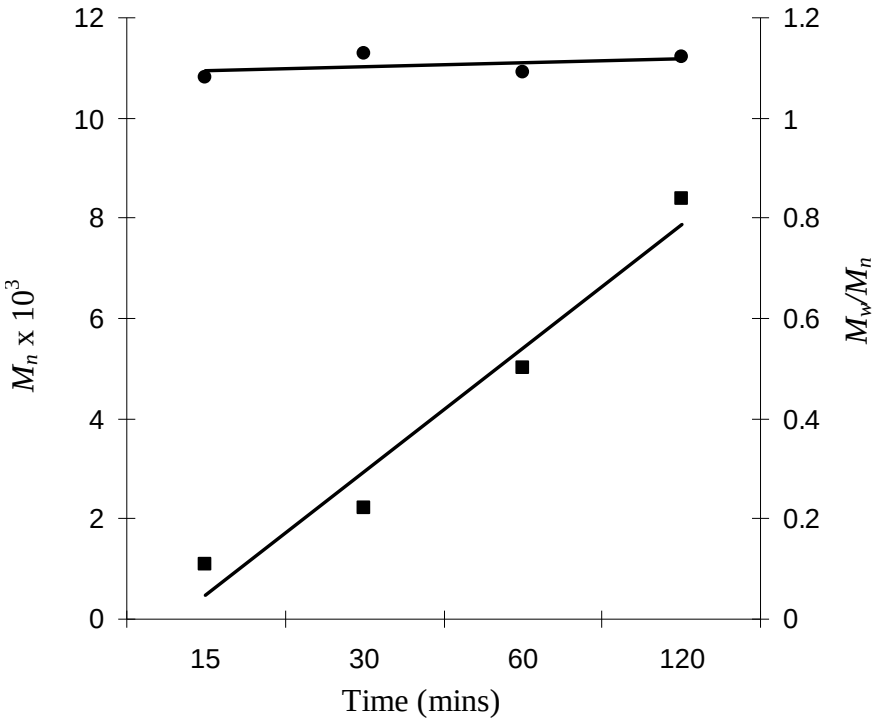


**Figure 3.22**: A plot of $M_n$ (squares) and $M_w/M_n$ (circles) *versus* time for the polymerisation of *rac*-LA initiated with Zr(**1**)($O^iPr$)$_2$ in toluene at 80 °C.

It can be seen that as the time increases the $M_w/M_n$ remains constant whilst the $M_n$ increases linearly with time supporting the idea that a controlled polymerisation is occurring.

### 3.4.3 Hafnium Initiators

Similar to the zirconium initiators, the series of hafnium complexes were trialled for the ROP of *rac*-LA in solution at 80 °C in toluene for 24 hours (Table 3.11).

| Entry | Initiator | Conversion[a] (%) | $M_n$[b] | $M_w$[b] | $M_n$ (theo.) | PDI[b] | $P_r$[c] |
|---|---|---|---|---|---|---|---|
| **1** | Hf(**1**)($O^iPr$)$_2$ | 98 | 8100 | 8750 | 14150 | 1.08 | 0.34 |
| **2** | Hf(**2**)($O^iPr$)$_2$ | 96 | 14300 | 15250 | 13900 | 1.07 | 0.50 |
| **3** | Hf(**3**)($O^iPr$)$_2$ | 99 | 650 | 950 | 14300 | 1.43 | - |
| **4** | Hf(**4**)($O^iPr$)$_2$ | 99 | 2150 | 2650 | 14300 | 1.23 | - |

**Table 3.11**: ROP results for Hf(**1-4**)($O^iPr$)$_2$ in toluene at 80 °C for 24 hours. 0.7 g of *rac*-LA, [LA]/[initiator] = 100. [a] conversion as determined *via* $^1$H NMR, [b] determined from GPC (in THF) referenced to polystyrene, [c] calculated from the $^1$H homonuclear decoupled NMR ($CDCl_3$) analysis.

From Table 3.11, it can be seen that again the polydispersity indices of the polymers produced in toluene *via* Hf(**1/2**)($O^iPr$)$_2$ are lower than those produced from the analogous Ti(IV) initiators. This suggests that Hf(**1/2**)($O^iPr$)$_2$ offer a greater degree of control under solvent conditions than Ti(**1/2**)($O^iPr$)$_2$ and are similar in reactivity to Zr(**1/2**)($O^iPr$)$_2$. The similarity is also observed in that as the steric hinderance of the Hf(IV) complexes is reduced, so too is the molecular weight of the resulting polymer (entries 3 and 4 in Table 3.11). The molecular weights reported in Table 3.11 when Hf(**1**)($O^iPr$)$_2$ or Hf(**2**)($O^iPr$)$_2$ are the initiators, show relatively good correlation with the theoretical molecular weights, calculated in an analogous manner to that for the Ti(IV) and Zr(IV) initiators reported previously in Sections 3.4.1 and 3.4.2. Although not reported, the Hf(IV) complexes were also trialled for the ROP of *rac*-LA in toluene at 80 °C for 2 hours, and although no polymeric material was observed after this time, an oligomeric material could be obtained for all initiators with Hf(**2**)($O^iPr$)$_2$ ($M_n$ = 1,550 gmol$^{-1}$) showing the most stereocontrol giving a $P_r$ value of 0.2 indicative of an isotactic product. However, as shown in Table 3.11 when the reaction time was increased, although the molecular weight of the product increased (entry 2), there is a decrease in the stereoselectivity $P_r$ = 0.5.

The initiators were also trialled for the ROP of *rac*-LA under solvent-free conditions at 130 °C, but unfortunately it was not possible to obtain any polymeric product using initiators Hf(**1**)($O^iPr$)$_2$ and Hf(**2**)($O^iPr$)$_2$ after 15 minutes and hence the reaction time was increased for such initiators. In contrast, with Hf(**4**)($O^iPr$)$_2$ an oligomeric product was obtained after just 6 minutes under melt

conditions, and for Hf(**3**)($O^iPr$)$_2$ after 15 minutes albeit with lower molecular weights than expected (Table 3.12).

| Entry | Initiator | Reaction time (hrs) | Conversion[a] (%) | $M_n$[b] | $M_w$[b] | $M_n$ (theo.) | PDI[b] | $P_r$[c] |
|---|---|---|---|---|---|---|---|---|
| **1** | Hf(**1**)($O^iPr$)$_2$ | 48 | 75 | 24400 | 32250 | 32450 | 1.32 | 0.34 |
| **2** | Hf(**2**)($O^iPr$)$_2$ | 24 | 96 | 46550 | 69400 | 41550 | 1.49 | 0.50 |
| **3** | Hf(**3**)($O^iPr$)$_2$ | 0.25 | 99 | 5300 | 7700 | 42850 | 1.45 | 0.30 |
| **4** | Hf(**4**)($O^iPr$)$_2$ | 0.10 | 99 | 4800 | 8500 | 42850 | 1.76 | 0.40 |

**Table 3.12**: ROP results for Hf(**1-4**)($O^iPr$)$_2$ in the absence of solvent at 130 °C. 2 g of *rac*-LA, [LA]/[initiator] = 300. [a] conversion as determined *via* $^1$H NMR, [b] determined from GPC (in THF) referenced to polystyrene, [c] calculated from the $^1$H homonuclear decoupled NMR ($CDCl_3$) analysis.

Analogous to that observed when the polymerisations were carried out in toluene at 80 °C, Hf(**1/2**)($O^iPr$)$_2$ show good correlation between observed and theoretical molecular weights indicative of one polymeric chain per metal centre. Due to the molecular weight of the resulting polymers produced from Hf(**3**)($O^iPr$)$_2$ and Hf(**4**)($O^iPr$)$_2$ still being lower than expected, even under solvent-free polymerisations conditions, the reactions were repeated in dichloromethane at a lower temperature of 25 °C, in an attempt to improve the molecular weight of the resulting polymer product.

| Entry | Initiator | Reaction time (hrs) | Conversion[a] (%) | $M_n$[b] | $M_w$[b] | $M_n$ (theo.) | PDI[b] | $P_r$[c] |
|---|---|---|---|---|---|---|---|---|
| **1** | Hf(**3**)($O^iPr$)$_2$ | 6 | 99 | 8200 | 10300 | 14300 | 1.25 | 0.25 |
| **3** | Hf(**4**)($O^iPr$)$_2$ | 24 | 99 | 10350 | 16050 | 14300 | 1.55 | 0.31 |

**Table 3.13**: ROP results for Hf(**3-4**)($O^iPr$)$_2$ in dichloromethane at 25 °C. 0.7 g of *rac*-LA, [LA]/[initiator] = 100. [a] conversion as determined *via* $^1$H NMR, [b] determined from GPC (in THF) referenced to polystyrene, [c] calculated from the $^1$H homonuclear decoupled NMR ($CDCl_3$) analysis.

It can be seen in Table 3.13 that a longer reaction time is required for Hf(**4**)($O^iPr$)$_2$ to achieve a polymeric product of molecular weight close to the theoretical weight, for one polymeric chain per metal centre. However, with this increased reaction time, there is also an increase in the polydispersity index suggesting that transesterification could be occurring. The Hf(IV) complexes generate isotactic PLA ($P_r$ = 0.25 – 0.4) in toluene and dichloromethane, with the

exception of Hf(**2**)($O^iPr$)$_2$ which produces atactic PLA. This could be related to the fact that Hf(**2**)($O^iPr$)$_2$ is the only initiator with a phenyl group on the amine nitrogen and hence could inhibit any stereocontrol at the metal centre. By analysis of the methine region of the $^1H$ homonuclear decoupled NMR spectra and $^{13}C\{^1H\}$ NMR spectra (Figure 3.23 and Figure 3.24 respectively) it is clear that there is an enhancement of the *iii* peak indicating that isotactic PLA is indeed produced. In the $^{13}C\{^1H\}$ NMR spectrum (Figure 3.24) an extra resonance is observed, implying transesterification has occurred.

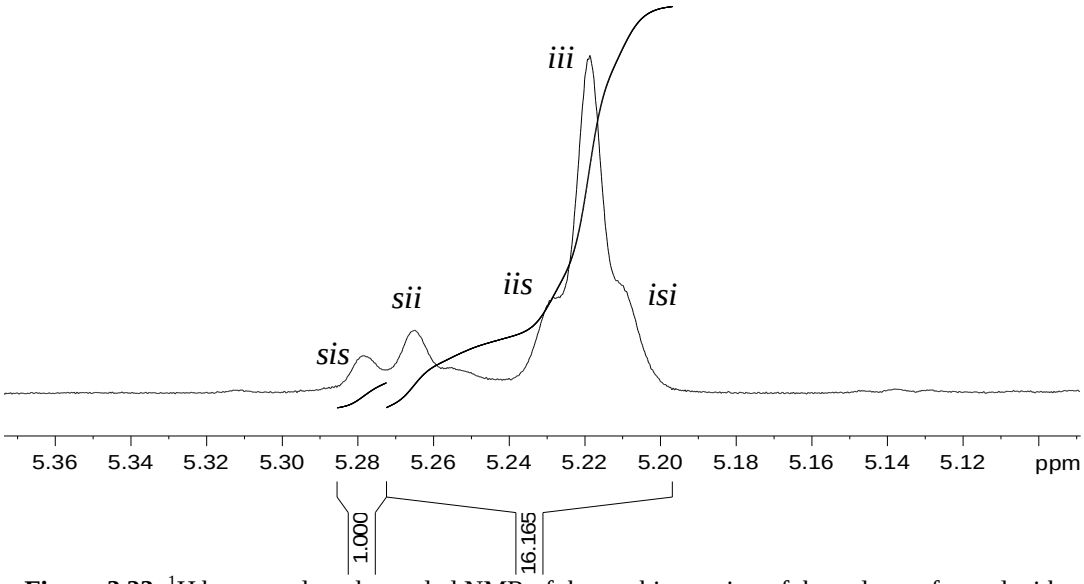


**Figure 3.23**: $^1H$ homonuclear decoupled NMR of the methine region of the polymer formed with Hf(**1**)($O^iPr$)$_2$ polymerisation in toluene at 80 °C for 24 hours showing isotactic bias with $P_r$ = 0.34, entry 1, Table 3.11.

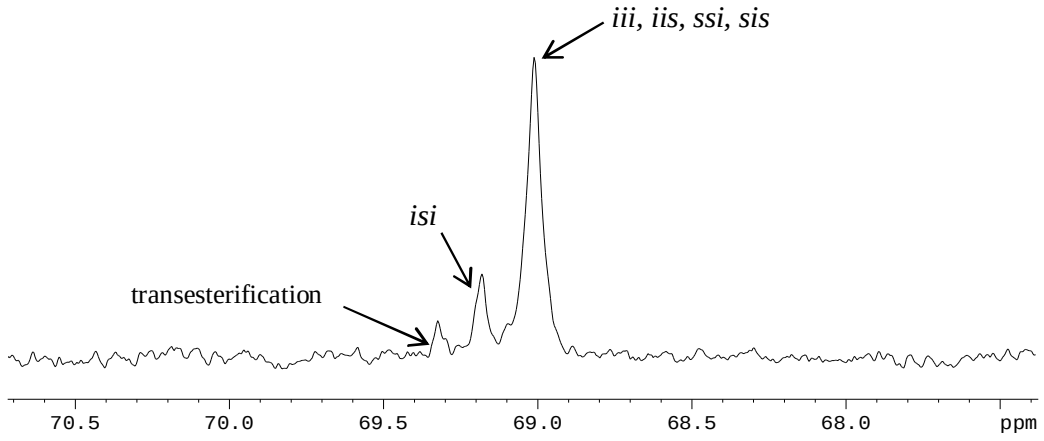


**Figure 3.24**: $^{13}C\{^1H\}$ NMR spectrum of the methine region of the polymer formed with Hf(**1**)($O^iPr$)$_2$ polymerisation in toluene at 80 °C for 24 hours showing isotactic bias with $P_r$ = 0.34, entry 1, Table 3.11.

The polymeric products were also analysed *via* MALDI-ToF mass spectrometry, which indicated that again the end group of the polymer chain is an isopropoxide group confirming that for the hafnium initiators a coordination and insertion mechanism is taking place. It can also be observed that the difference between resonances in the MALDI-ToF mass spectrum is 72 gmol$^{-1}$ indicative of transesterification.

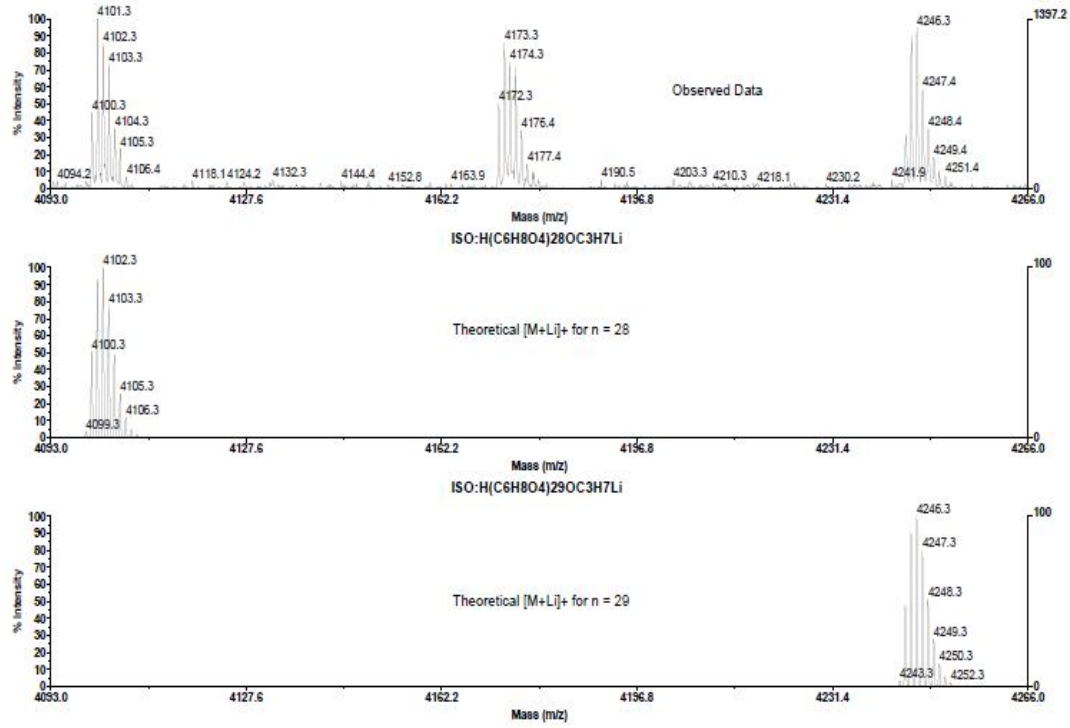


**Figure 3.25**: MALDI-ToF mass spectrum of the polymer obtained using Hf(**1**)($O^iPr$)$_2$ as the initiator in toluene at 80 °C for 24 hours (entry 1, Table 3.11).

## 3.5 Kinetic Studies

Investigation into the reactivity of initiators Ti/Zr/Hf(**1-4**)($O^iPr$)$_2$ was carried out by determining $k_{app}$ for each complex. The polymerisations were all carried out on a NMR scale ensuring that the initial concentration of LA ([LA]$_o$) was consistent for all initiators (0.578 mol dm$^{-3}$) and that all reactions were performed in a similar manner. The apparent rate of propagation ($k_{app}$) was determined from analysis of a semilogarithmic plot of ln{[LA]$_o$/[LA]$_t$} *vs* time where [LA]$_o$ = 0.578 mol dm$^{-3}$ with a monomer: initiator ratio of 100: 1. Initial results were gathered over a 12 hour period at a temperature of 80 °C to mimic

the results in Tables 3.06, 3.07, 3.09 and 3.11 for the solution polymerisations of *rac*-LA. Changes to the ligand and the choice of metal, can play a significant part in the reactivity of the initiator developed. Therefore, the apparent rate of propagation was determined for all of the initiators in Figure 3.04 and the values compared.

### 3.5.1 Ligands **1**$H_2$ and **2**$H_2$

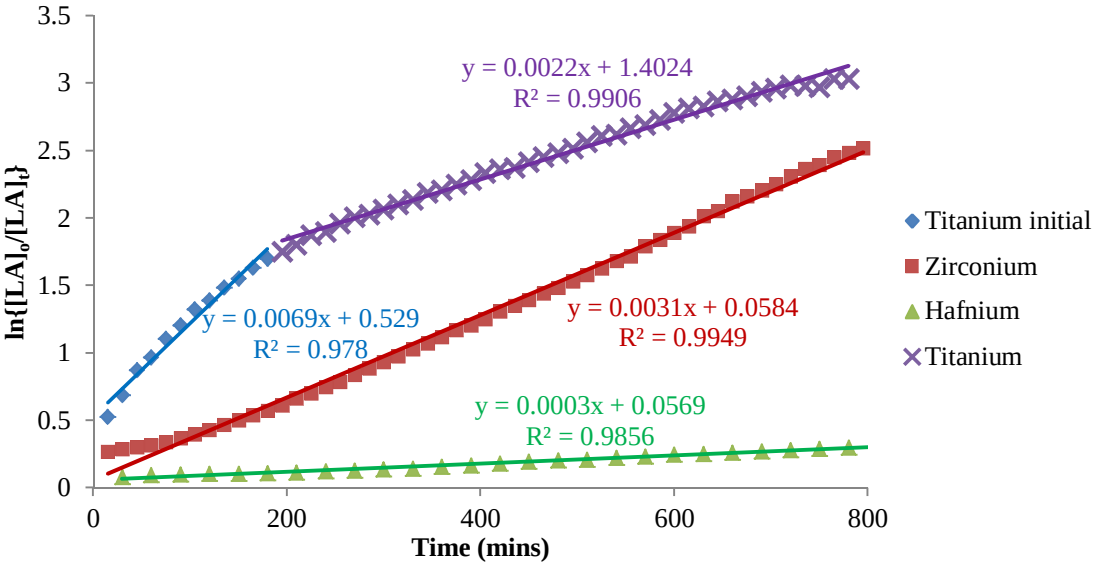


**Figure 3.26**: Semi-logarithmic plots for all metals containing ligand **1**$H_2$ at 80 °C in $C_6D_5CD_3$

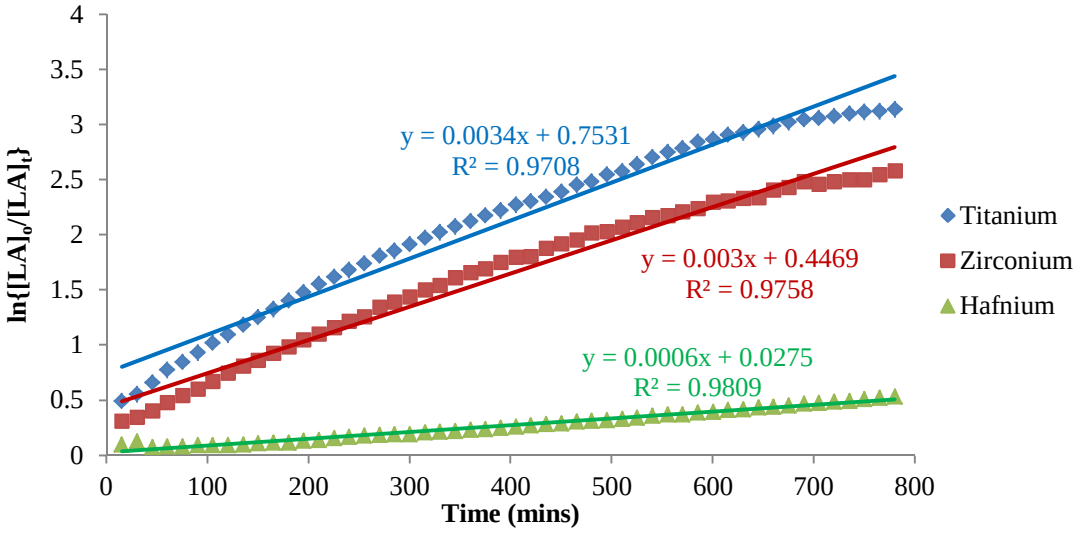


**Figure 3.27**: Semi-logarithmic plots for all metals containing ligand **2**$H_2$ at 80 °C in $C_6D_5CD_3$

| Initiator | $k_{app}$ ($min^{-1}$) | $R^2$ |
|---|---|---|
| **Ti(1)(O$^i$Pr)$_2$** | $6.93 \times 10^{-3}$ | 0.9780 |
| | (initial) | 0.9906 |
| | $2.19 \times 10^{-3}$ | |
| **Ti(2)(O$^i$Pr)$_2$** | $3.44 \times 10^{-3}$ | 0.9708 |
| **Zr(1)(O$^i$Pr)$_2$** | $3.06 \times 10^{-3}$ | 0.9949 |
| **Zr(2)(O$^i$Pr)$_2$** | $3.02 \times 10^{-3}$ | 0.9758 |
| **Hf(1)(O$^i$Pr)$_2$** | $0.30 \times 10^{-3}$ | 0.9856 |
| **Hf(2)(O$^i$Pr)$_2$** | $0.62 \times 10^{-3}$ | 0.9809 |

**Table 3.14**: $k_{app}$ values for Ti/Zr/Hf(**1**/**2**)(O$^i$Pr)$_2$ at 80 °C in $C_6D_5CD_3$

All kinetic experiments shown in Figure 3.24 and 3.25 were recorded in $C_6D_5CD_3$ at 80 °C. Although the data is fitted for a first order rate of reaction, it can be quite clearly seen form Figures 3.26 and 3.27 that the plots are not linear with an intercept through the origin. This suggests that the polymerisation reactions for the group (IV) complexes containing ligands **1**$H_2$ and **2**$H_2$ are more complex than initially anticipated. For Ti(**1**)(O$^i$Pr)$_2$ in can be observed in Figure 3.26 that an initial fast reaction is occurring followed by a consecutive slower process. From Figures 3.26 and 3.27 it can be seen that as you go down the group (IV) metals there is a decrease in the apparent rate of propagation, with relatively similar rates observed for the titanium and zirconium catalysts ($k_{app}$ = ~ $3 \times 10^{-3}$ $min^{-1}$). Changing from a methyl to a phenyl substituent on the amine nitrogen has little effect on the rate of polymerisation for all initiators containing ligands **1**$H_2$ and **2**$H_2$. The apparent rate of propagation for Hf(**1**)(O$^i$Pr)$_2$ and Hf(**2**)(O$^i$Pr)$_2$ are both significantly slower with Hf(**1**)(O$^i$Pr)$_2$ an order of magnitude slower than its titanium and zirconium counterparts.

### 3.5.2 Ligands $3H_2$ and $4H_2$

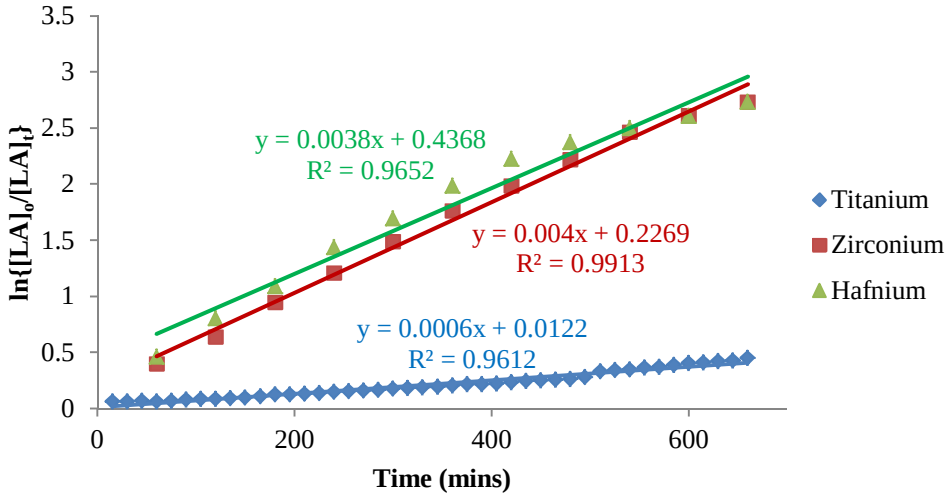


**Figure 3.28**: Semi-logarithmic plots for all metals containing ligand **3**$H_2$ at 80 °C in $C_6D_5CD_3$ for Ti(**3**)($O^iPr$)$_2$ and 25 °C in $CDCl_3$ for Zr(**3**)($O^iPr$)$_2$ and Hf(**3**)($O^iPr$)$_2$

| Initiator | $k_{app}$ ($min^{-1}$) | $R^2$ | Temperature |
|---|---|---|---|
| **Ti(3)($O^iPr$)$_2$** | $0.67 \times 10^{-3}$ | 0.9612 | 80 °C |
| **Zr(3)($O^iPr$)$_2$** | $3.99 \times 10^{-3}$ | 0.9913 | 25 °C |
| **Hf(3)($O^iPr$)$_2$** | $3.82 \times 10^{-3}$ | 0.9652 | 25 °C |

**Table 3.15**: $k_{app}$ values for all initiators containing ligand **3**$H_2$

In contrast to ligands **1**$H_2$ and **2**$H_2$, the semi logarithmic plots for the group (IV) complexes containing **3**$H_2$ show a difference in reactivity such that the titanium complex is now the slowest with a $k_{app}$ of $6.0 \times 10^{-4}$ $min^{-1}$ at 80 °C in $C_6D_5CD_3$. However, when the kinetics were recorded for the zirconium and hafnium complexes, their reactivity at 80 °C was too fast to be monitored accurately. Therefore, the reaction was repeated at room temperature in $CDCl_3$ over 12 hours. It can be seen in Table 3.15 that Zr(**3**)($O^iPr$)$_2$ and Hf(**3**)($O^iPr$)$_2$ have a similar apparent rate of propagation of around $4.0 \times 10^{-3}$ $min^{-1}$ which is consistent with values present in the literature. For example Gibson *et al.* reported their fastest example of a Ti(Salen)($O^iPr$)$_2$ complex[14] with a $k_{app}$ of $3.7 \times 10^{-3}$ $min^{-1}$ for the conversion of *rac*-LA, albeit at 70 °C. The $k_{app}$ value reported for Ti(**3**)($O^iPr$)$_2$ is of the same magnitude to the apparent rate reported by Gibson *et al.* for their slowest example of a Ti(Salen)($O^iPr$)$_2$ complex under

similar conditions.[14] All complexes reported in Table 3.15 show comparable rates to aluminium Salan complexes reported to have $k_{app}$ values between 15.2 × $10^{-4}$ $min^{-1}$ to 10.9 × $10^{-3}$ $min^{-1}$ at 70 °C in toluene.[20]

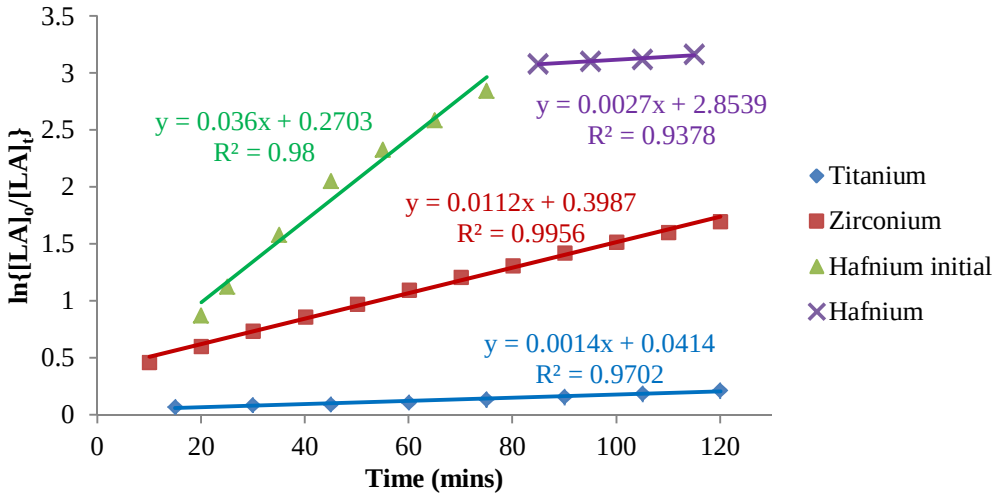


**Figure 3.29**: Semi-logarithmic plots for all metals containing ligand **4**$H_2$ at 80 °C in $C_6D_5CD_3$ for Ti(**4**)($O^iPr$)$_2$ and 25 °C in $CDCl_3$ for Zr(**4**)($O^iPr$)$_2$ and Hf(**4**)($O^iPr$)$_2$

| Initiator | $k_{app}$ ($min^{-1}$) | $R^2$ | Temperature |
|---|---|---|---|
| **Ti(4)($O^iPr$)$_2$** | 1.39 × $10^{-3}$ | 0.9702 | 80 °C |
| **Zr(4)($O^iPr$)$_2$** | 11.2 × $10^{-3}$ | 0.9956 | 25 °C |
| **Hf(4)($O^iPr$)$_2$** | 36.0 × $10^{-3}$(initial) | 0.9800 | 25 °C |
| | 2.67 × $10^{-3}$ | 0.9378 | |

**Table 3.16**: $k_{app}$ values for all initiators containing ligand **4**$H_2$

A similar trend to that observed for **3**$H_2$ is seen for the complexes containing **4**$H_2$, in that titanium shows the lowest rate with a $k_{app}$ = 1.4 × $10^{-3}$ $min^{-1}$ when recorded at 80 °C in $C_6D_5CD_3$. However, zirconium and hafnium complexes are seen to be an order of magnitude faster and hence the kinetics for Zr(**4**)($O^iPr$)$_2$ and Hf(**4**)($O^iPr$)$_2$ were recorded at 25 °C in $CDCl_3$. Unlike with **3**$H_2$, the Zr(IV) and Hf(IV) complexes containing **4**$H_2$ have different rates with the hafnium complex being nearly twice as fast as the zirconium equivalent. For Hf(**4**)($O^iPr$)$_2$ an initial fast rate is observed which after 80 minutes, slows to a rate comparable to that of Ti(**4**)($O^iPr$)$_2$. In comparison to the kinetic plots observed in Section 3.5.1 for ligands **1**$H_2$ and **2**$H_2$, Figures 3.28 and

3.29 show an increase in linearity of the data when fitted to a first order reaction. However, the kinetic plots still do not have an intercept through the origin, and it can therefore be assumed that the polymerisation is still more complex than first anticipated.

Overall, it can be summarised that the choice of metal centre has an effect on the apparent rate of propagation in the production of PLA from *rac*-LA such that for the more sterically hindered ligands **1**$H_2$ and **2**$H_2$, the order of reactivity is titanium > zirconium > hafnium. Whereas, for the least sterically hindered ligands **3**$H_2$ and **4**$H_2$, a change in reactivity occurs resulting in hafnium > zirconium > titanium. It can also be noted that for the latter two ligands, the values of $k_{app}$ shown in Figure 3.28 and Figure 3.29 are some of the fastest reported for group (IV) initiators of this type. The ligand design can also have an important effect on the rate of polymerisation. For example, when the steric hindrance on the phenoxy ring adjacent to the imine nitrogen centre is decreased in the Ti(IV) initiators, there is a decrease in the observed rate of reaction. Furthermore, changing $R^1$ from a bulky $^t$Bu group to a methyl group and $R^2$ to H, the $k_{app}$ value decreases from $2.2 \times 10^{-3}$ $min^{-1}$ for Ti(**1**)($O^iPr$)$_2$ to $0.7 \times 10^{-3}$ $min^{-1}$ for Ti(**3**)($O^iPr$)$_2$. Further decreasing the steric hindrance to no substitution on the phenoxy ring {(Ti(**4**)($O^iPr$)$_2$} increases the rate of polymerisation. This results in the $k_{app}$ value increasing from $0.7 \times 10^{-3}$ $min^{-1}$ for Ti(**3**)($O^iPr$)$_2$ to $1.4 \times 10^{-3}$ $min^{-1}$ for Ti(**4**)($O^iPr$)$_2$, however this value is still lower than that for Ti(**1**)($O^iPr$)$_2$ or Ti(**2**)($O^iPr$)$_2$.

From analysis of the kinetic plots, it can be seen that all initiators show conversion of *rac*-LA to PLA whether it be at room temperature or at 80 °C. Taking this into account it was therefore surprising that when the initiators Zr(**3/4**)($O^iPr$)$_2$ and Hf(**3/4**)($O^iPr$)$_2$ were used for the ROP of *rac*-LA on a larger scale, it was not possible to isolate material of a high molecular weight under the same conditions (See Tables 3.09 and 3.11). It was therefore of interest to investigate further what was causing the formation of low molecular weight PLA.

## 3.6 Degradation Studies

One of the main obstacles in the wider implementation of PLA on an industrial scale is the cost of the platform chemical lactic acid. Lactic acid can be produced from batch fermentation of aqueous glucose under anaerobic conditions, which typically takes between 2 – 4 days.[21, 22] However, this requires calcium hydroxide to be added continuously to maintain pH = 7 resulting in the formation of calcium lactate.[21, 22] To produce crude lactic acid, crystallisation of the calcium lactate is required, followed by acidification with sulphuric acid. In addition to producing crude lactic acid, gypsum {$Ca(OH)_2$} is also produced, and it has been reported that for every ton of lactic acid produced, one ton of gypsum is also formed.[22] Furthermore, the esterification of lactic acid to methyl lactate (an intermediate in LA formation) is often necessary to aid purification before production of PLA can be achieved.

Previous reports have shown that dissolving various sugars in methanol can generate methyl lactate in yields up to 68 %.[21] Another method of producing methyl lactate involves utilising high catalytic amounts (10 mol %) of tin chloride for the isomerisation/esterification of dihydroxyacetone and glyceraldehyde.[22] A recent report by NatureWorks® states that an attractive method of producing methyl lactate without the generation of needless volumes of waste is through the chemical recycling of PLA.[23] The recycling of PLA can be achieved with water at a wide range of temperatures (100 – 250 °C) typically using a catalyst such as a strong inorganic acid.[23] Other methods of recycling or degrading LA have been reported in the literature, for example alcoholysis under microwave irradiation at temperatures in the excess of 130 °C or the use of DMAP as a catalyst under bulk conditions of 135 °C.[24, 25] Phomphrai *et al.* has also shown it is possible to convert LA into alkyl lactyllactates using group (I) metal amides.[26] Analysis of the patent literature has shown that the depolymerisation of PLA has also been reported *via* transesterification using Sn(II) octanoate or triazabicyclodecene.[27] The PLA sample is dissolved in ethyl lactate and ethanol added, heating the reaction to 120 °C for 24 hours.[27] PLA can be depolymerised to methyl lactate at 150 °C, in the presence of $H_2SO_4$.[28]

However, the examples reported above all require elevated temperatures to convert the PLA sample into intermediates of value for recycling methods. It is therefore of interest to develop a less expensive route to the starting materials, specifically methyl lactate, required for PLA production. Due to the formation of low molecular weight PLA when Zr/Hf(**3/4**)($O^iPr$)$_2$ were utilised as initiators for the ROP of *rac*-LA, it was hypothesised that methyl lactate could be forming in such examples which will be discussed further.

### 3.6.1 Investigation into addition of methanol

Further analysis of the low molecular weight PLA produced *via* Zr/Hf(**3/4**)($O^iPr$)$_2$ indicated the presence of additional resonances in the $^1$H NMR spectrum. Such resonances were not however present in analogous $^1$H NMR spectrum for those polymers of high molecular weight – Figure 3.30.

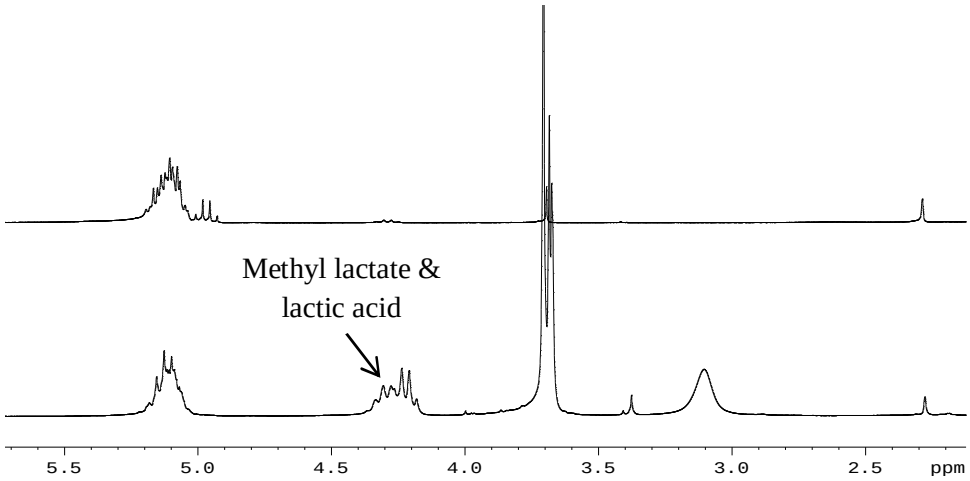


**Figure 3.30**: $^1$H NMR spectra of polymer produced from Ti(**3**)($O^iPr$)$_2$ with $M_n$ = 18,800 gmol$^{-1}$ (entry 3, Table 3.07) – top spectrum, and Zr(**3**)($O^iPr$)$_2$ with $M_n$ = 450 gmol$^{-1}$ (entry 3, Table 3.09) – lower spectrum.

The lower spectrum in Figure 3.30 shows additional resonances around 4.2 ppm which is thought to be attributed to methyl lactate and perhaps even lactic acid. The presence of resonances for methyl lactate indicates that this must be produced upon workup of the polymerisation reaction, as no such resonances were observed in the kinetic spectra obtained using the same initiator. For a general polymerisation reaction, methanol is added after the reaction time to quench the reaction and dichloromethane to dissolve any product formed. After removal of the solvent, a $^1$H NMR spectrum is obtained to calculate the

conversion. The product is then washed with copious amounts of methanol to remove any unreacted monomer. To confirm that methyl lactate is formed from the addition of methanol to quench the reaction, the polymerisation using Hf(**3**)($O^iPr$)$_2$ under melt conditions was repeated quenching the reaction with ethanol instead of methanol. A comparison was made between the two polymerisations as well as the reaction where the polymerisation is quenched by exposure to air, Figure 3.31.

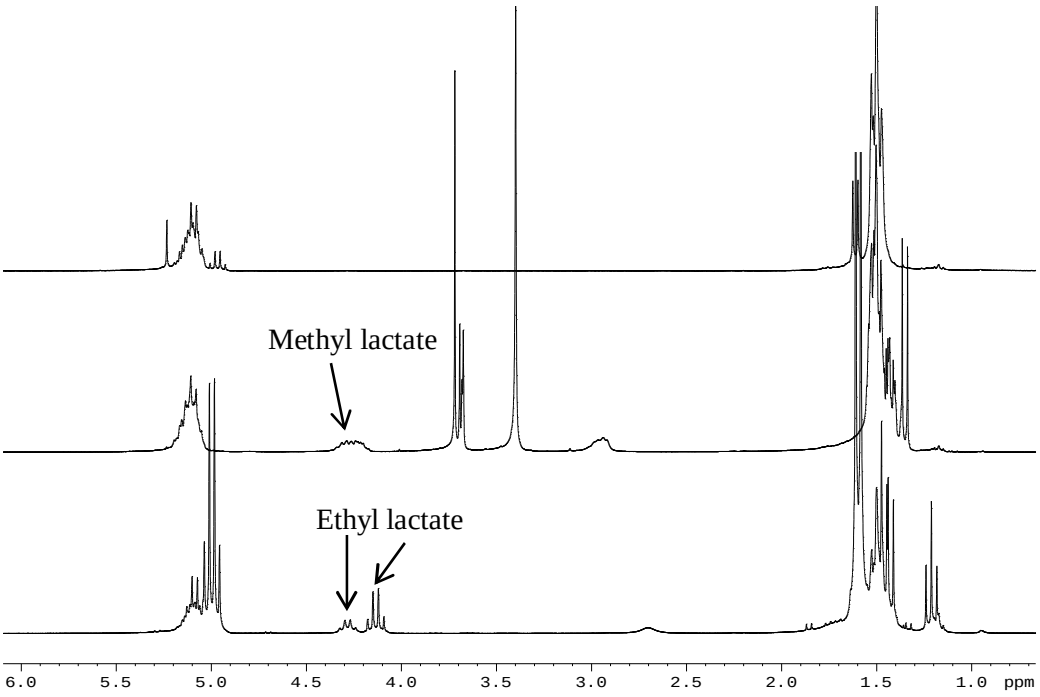


**Figure 3.31**: $^1$H NMR spectrum of polymerisations *via* Hf(**3**)($O^iPr$)$_2$ in the absence of solvent at 130 °C. Top spectrum polymerisation not quenched with solvent; middle spectrum polymerisation quenched with methanol and lower spectrum polymerisation quenched with ethanol.

Figure 3.31 highlights that addition of an alcohol to quench the reaction, either methanol or ethanol, results in the degradation of the polymer product and hence leads to the formation of either methyl lactate or ethyl lactate. The formation of methyl lactate can also be confirmed from analysis of the product produced upon quenching the reaction with methanol *via* GC-MS. From the top spectrum in Figure 3.31, it can be seen that when no alcohol is used to quench the polymerisation reaction, but the reaction quenched in air, the degradation of the polymer peak at 5.1 ppm is inhibited. It was therefore of interest to repeat the polymerisation reactions that afforded low molecular weight products, without the addition of any alcohol to terminate the process. The polymerisations were carried

out in toluene for 2 hours with the zirconium and hafnium initiators containing ligands **3**$H_2$ and **4**$H_2$, after which only dichloromethane was added to dissolve any polymeric material, before removing the solvents *in vacuo*.

| Entry | Initiator | Quenched with MeOH | Conversion[a] (%) | $M_n$[b] | $M_w$[b] | PDI[b] | $P_r$[c] |
|---|---|---|---|---|---|---|---|
| **1** | Zr(**3**)($O^iPr$)$_2$ | ✓ | 99 | 500 | 550 | 1.13 | - |
| **2** | Zr(**3**)($O^iPr$)$_2$ | × | 98 | 32750 | 46700 | 1.43 | 0.27 |
| **3** | Zr(**4**)($O^iPr$)$_2$ | ✓ | 92 | 350 | 450 | 1.17 | - |
| **4** | Zr(**4**)($O^iPr$)$_2$ | × | 98 | 21600 | 35600 | 1.65 | 0.34 |

**Table 3.17:** Polymerisations of *rac*-LA *via* Zr(**3**)($O^iPr$)$_2$ and Zr(**4**)($O^iPr$)$_2$ with and without quenching with methanol in toluene at 80 °C for 2 hours with a 100: 1 ratio of [LA]: [initiator] [a] conversion as determined *via* $^1$H NMR, [b] determined from GPC (in THF) referenced to polystyrene, [c] calculated from the $^1$H homonuclear decoupled NMR ($CDCl_3$) analysis.

| Entry | Initiator | Quenched with MeOH | Conversion[a] (%) | $M_n$[b] | $M_w$[b] | PDI[b] | $P_r$[c] |
|---|---|---|---|---|---|---|---|
| **1** | Hf(**3**)($O^iPr$)$_2$ | ✓ | 99 | 2950 | 4100 | 1.39 | 0.30 |
| **2** | Hf(**3**)($O^iPr$)$_2$ | × | 98 | 15500 | 22650 | 1.46 | 0.34 |
| **3** | Hf(**4**)($O^iPr$)$_2$ | ✓ | 97 | 2150 | 2700 | 1.24 | 0.30 |
| **4** | Hf(**4**)($O^iPr$)$_2$ | × | 99 | 20250 | 32500 | 1.61 | 0.31 |

**Table 3.18**: Polymerisations of *rac*-LA *via* Hf(**3**)($O^iPr$)$_2$ and Hf(**4**)($O^iPr$)$_2$ with and without quenching with methanol in toluene at 80 °C for 2 hours with a 100: 1 ratio of [LA]: [initiator] [a] conversion as determined *via* $^1$H NMR, [b] determined from GPC (in THF) referenced to polystyrene, [c] calculated from the $^1$H homonuclear decoupled NMR ($CDCl_3$) analysis.

It can be seen from Tables 3.17 and 3.18 that the molecular weights are higher for the products obtained without quenching the reaction in methanol. However, high polydispersity indices for the polymers formed without quenching with methanol were observed, although a similar degree of stereocontrol was observed. Interestingly, for Zr(**3**)($O^iPr$)$_2$, the product obtained in entry 2 in Table 3.17 shows the highest degree of stereoselectivity to isotactic PLA with a $P_r$ value of 0.27 and enhancement of the *iii* peak in the $^1$H homonuclear decoupled NMR spectrum, Figure 3.32.

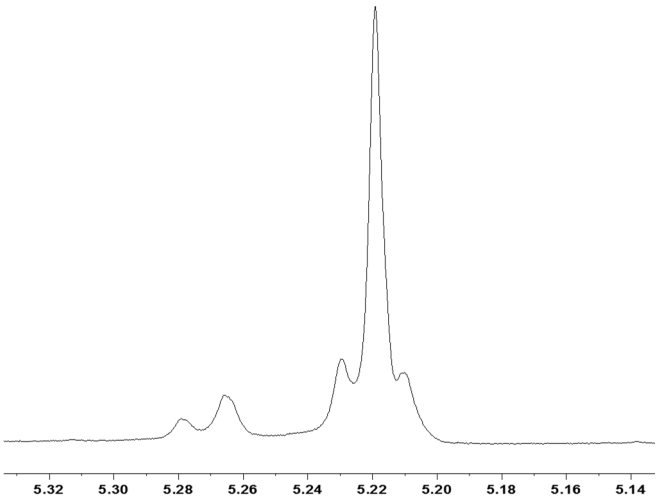


**Figure 3.32**: $^{1}$H homonuclear decoupled NMR spectrum of the polymer from Zr(**3**)($O^{i}Pr$)$_2$ without quenching with methanol, $P_r$ = 0.27 (entry 2 Table 3.17)

Due to the success of producing polymeric material without quenching the reaction at the end with methanol, the polymerisations under melt conditions for Zr(**3**/**4**)($O^{i}Pr$)$_2$ and Hf(**3**/**4**)($O^{i}Pr$)$_2$ were also repeated without termination by alcohol – Tables 3.19 and 3.20.

| Entry | Initiator | Quenched with MeOH | Conversion[a] (%) | $M_n$[b] | $M_w$[b] | PDI[b] | $P_r$[c] |
|---|---|---|---|---|---|---|---|
| **1** | Zr(**3**)($O^{i}Pr$)$_2$ | ✓ | 99 | 1600 | 2050 | 1.30 | 0.37 |
| **2** | Zr(**3**)($O^{i}Pr$)$_2$ | × | 77 | 103500 | 212550 | 2.05 | 0.40 |
| **3** | Zr(**4**)($O^{i}Pr$)$_2$ | ✓ | 99 | 3500 | 5450 | 1.56 | 0.52 |
| **4** | Zr(**4**)($O^{i}Pr$)$_2$ | × | 82 | 368400 | 541950 | 1.47 | 0.47 |

**Table 3.19**: Polymerisations of *rac*-LA *via* Zr(**3**)($O^{i}Pr$)$_2$ and Zr(**4**)($O^{i}Pr$)$_2$ with and without quenching with methanol in the absence of solvent at 130 °C for 15 minutes with a 300: 1 ratio of [LA]: [initiator]. [a] conversion as determined *via* $^{1}$H NMR, [b] determined from GPC (in THF) referenced to polystyrene, [c] calculated from the $^{1}$H homonuclear decoupled NMR ($CDCl_3$) analysis.

| Entry | Initiator | Quenched with MeOH | Conversion[a] (%) | $M_n$[b] | $M_w$[b] | PDI[b] | $P_r$[c] |
|---|---|---|---|---|---|---|---|
| **1** | Hf(**3**)($O^iPr$)$_2$ | ✓ | 99 | 5300 | 7700 | 1.45 | 0.30 |
| **2** | Hf(**3**)($O^iPr$)$_2$ | × | 91 | 50600 | 110950 | 2.19 | 0.43 |
| **3** | Hf(**4**)($O^iPr$)$_2$ | ✓ | 99 | 750 | 800 | 1.05 | 0.30 |
| **4** | Hf(**4**)($O^iPr$)$_2$ | × | 81 | 90550 | 284900 | 3.15 | 0.40 |

**Table 3.20**: Polymerisations of *rac*-LA *via* Hf(**3**)($O^iPr$)$_2$ and Hf(**4**)($O^iPr$)$_2$ with and without quenching with methanol in the absence of solvent at 130 °C for 15 minutes with a 300: 1 ratio of [LA]: [initiator]. [a] conversion as determined *via* $^1$H NMR, [b] determined from GPC (in THF) referenced to polystyrene, [c] calculated from the $^1$H homonuclear decoupled NMR ($CDCl_3$) analysis.

Analogous to the solution polymerisations, when the reactions were repeated without quenching with methanol, polymeric material with a significantly higher molecular weight was produced compared with the polymerisations which were terminated with methanol. As shown in Tables 3.19 and 3.20, the reactions in the absence of solvent at 130 °C without quenching with methanol lead to a highly uncontrolled polymerisation with the resulting polymers having high polydispersity values. With the exception of Zr(**4**)($O^iPr$)$_2$, all polymers produced without quenching with methanol lead to a decrease in the stereoselectivity with an increase in the $P_r$ values obtained towards 0.5. It is hypothesised that for the polymerisations $k_{prop} \gg k_{int}$, which could explain the higher $M_n$ and PDI values observed coupled with transesterification. As observed in solution, the initiators are very active in the absence of solvent. It is hypothesised that upon quenching with methanol, an active M-OMe species is formed (where M = Zr or Hf), which is active for the transesterification of PLA.

To study the formation of methyl lactate further, a kinetic experiment on an NMR scale was set up where the polymerisation of *rac*-LA to PLA *via* Hf(**3**)($O^iPr$)$_2$ and Hf(**4**)($O^iPr$)$_2$ was allowed to proceed until about 30 % conversion. $CD_3OD$ was added after this time. The reaction was allowed to continue, collecting a $^1$H NMR spectrum at regular intervals. From analysis of the methine region of the NMR spectrum, the mole fraction of polymer, monomer and methyl lactate were recorded for both initiators.

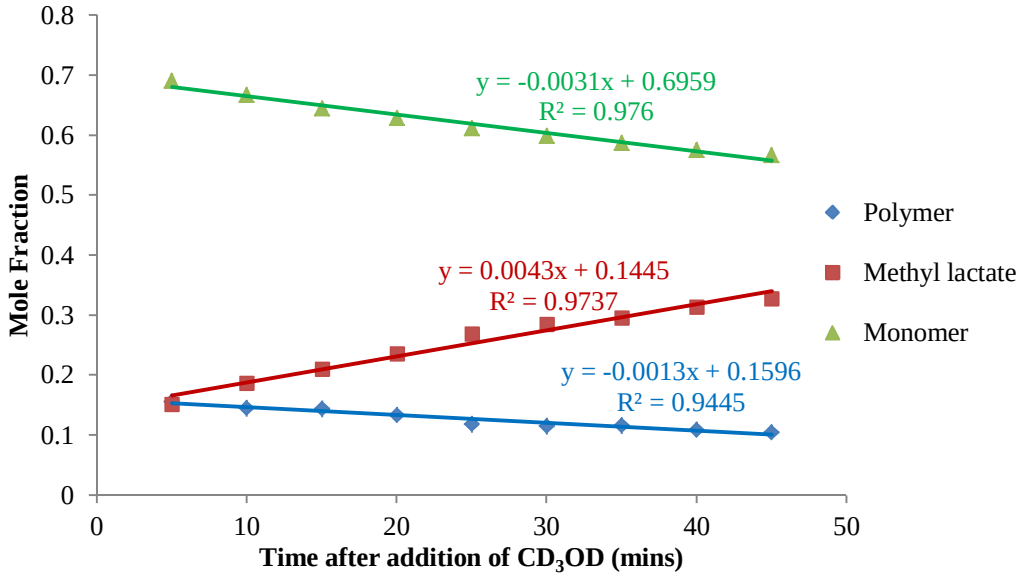


**Figure 3.33**: Mole fractions of polymer, monomer and methyl lactate after addition of $CD_3OD$ to the polymerisation of *rac*-LA *via* Hf(**3**)($O^iPr$)$_2$

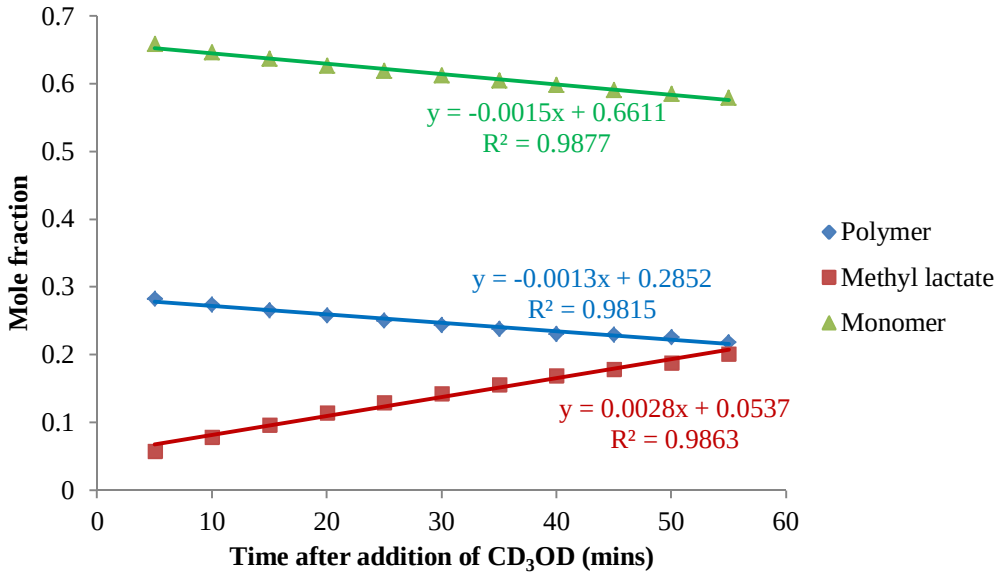


**Figure 3.34**: Mole fractions of polymer, monomer and methyl lactate after addition of $CD_3OD$ to the polymerisation of *rac*-LA *via* Hf(**4**)($O^iPr$)$_2$

From Figure 3.33 and 3.34, it can be seen that upon addition of $CD_3OD$, the mole fraction of the polymer and monomer both decrease, as the mole fraction of methyl lactate increases, suggesting that not only the polymer, but also the monomer is converted to methyl lactate. These results clearly indicate that it is possible to use the zirconium and hafnium initiators containing the less sterically hindered ligands **3**$H_2$ and **4**$H_2$, to not only produce PLA under both solution and

solvent-free conditions without quenching the reaction, with relatively high stereocontrol ($P_r$ = 0.27, entry 2, Table 3.17), but could also have implications for PLA recycling into lactic acid derivatives.

### 3.6.2 Polymer recycling

Section 3.6.1 above shows that it is possible to form methyl lactate from PLA upon addition of methanol. It was therefore of interest to further test if there could be important recycling implications. To investigate this further, PLA produced from Zr(**4**)($O^iPr$)$_2$ in solution at 80 °C for 2 hours (entry 4, Table 3.17) was dissolved in dichloromethane to which Hf(**3**)($O^iPr$)$_2$ and methanol was added and the products analysed by $^1$H NMR spectroscopy, Figure 3.35.

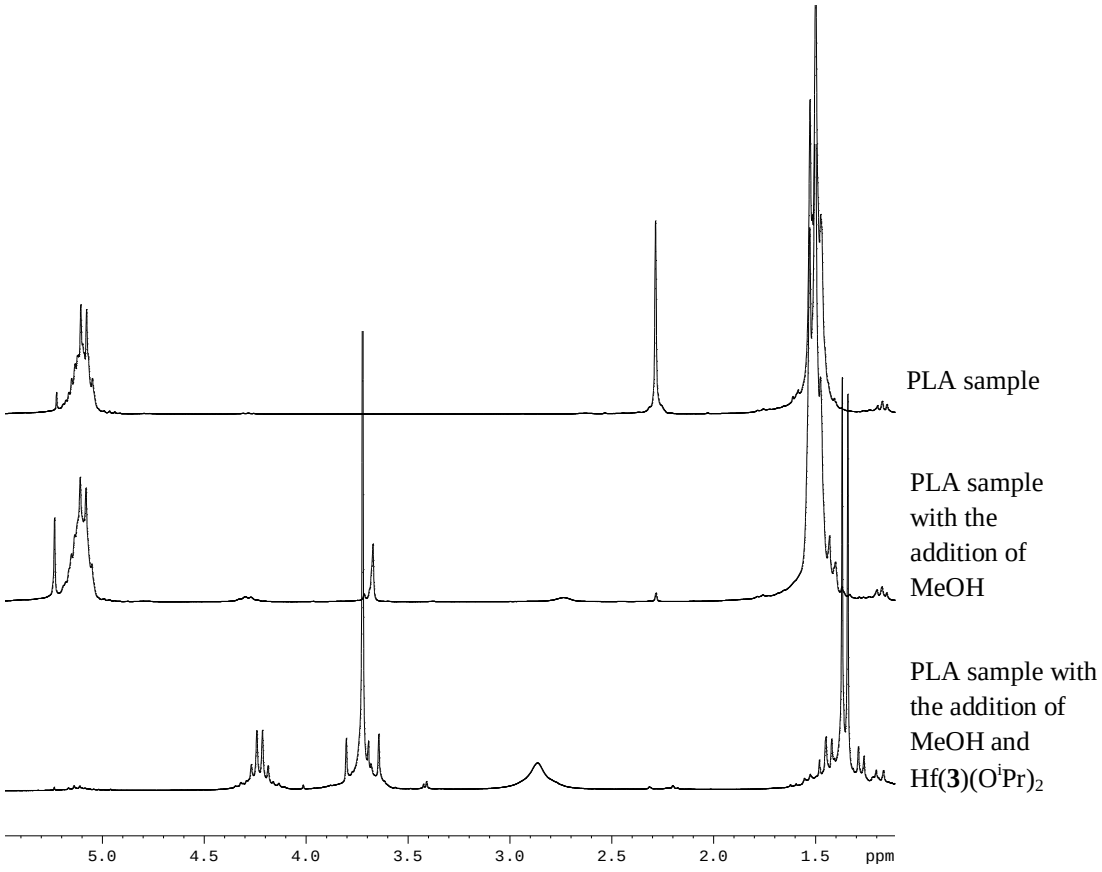


**Figure 3.35**: $^1$H NMR spectra showing polymer produced from Zr(**4**)($O^iPr$)$_2$ (entry 4, Table 3.17) with the addition of methanol and with the addition of methanol and Hf(**3**)($O^iPr$)$_2$

It can be clearly seen from Figure 3.35 that when only methanol is added to the polymer sample dissolved in dichloromethane and stirred for 24 hours, very little, or no change in the $^1$H NMR spectrum is observed. However, when the reaction is repeated adding not only methanol but also Hf(**3**)($O^iPr$)$_2$ in a ratio of

100: 1 of [PLA]: [initiator], and allowed to stir at room temperature for 24 hours, a prominent peak present for methyl lactate in now present in the $^{1}$H NMR spectrum (lower spectrum, Figure 3.35). A resonance for PLA at 5.1 ppm is now not observed. Although Figure 3.35 shows that it is possible to convert already prepared PLA to methyl lactate, it still utilises a polymer sample prepared from a similar Salalen initiator. Therefore, it was investigated if Hf(**3**)($O^{i}Pr$)$_2$ could be utilised to convert PLA prepared from other group (IV) initiators into methyl lactate. A polymer sample prepared *via* a zirconium amine *tris*(phenolate) complex described in Chapter 2, was dissolved in dichloromethane and Hf(**3**)($O^{i}Pr$)$_2$ plus methanol added. The products were analysed by $^{1}$H NMR spectroscopy.

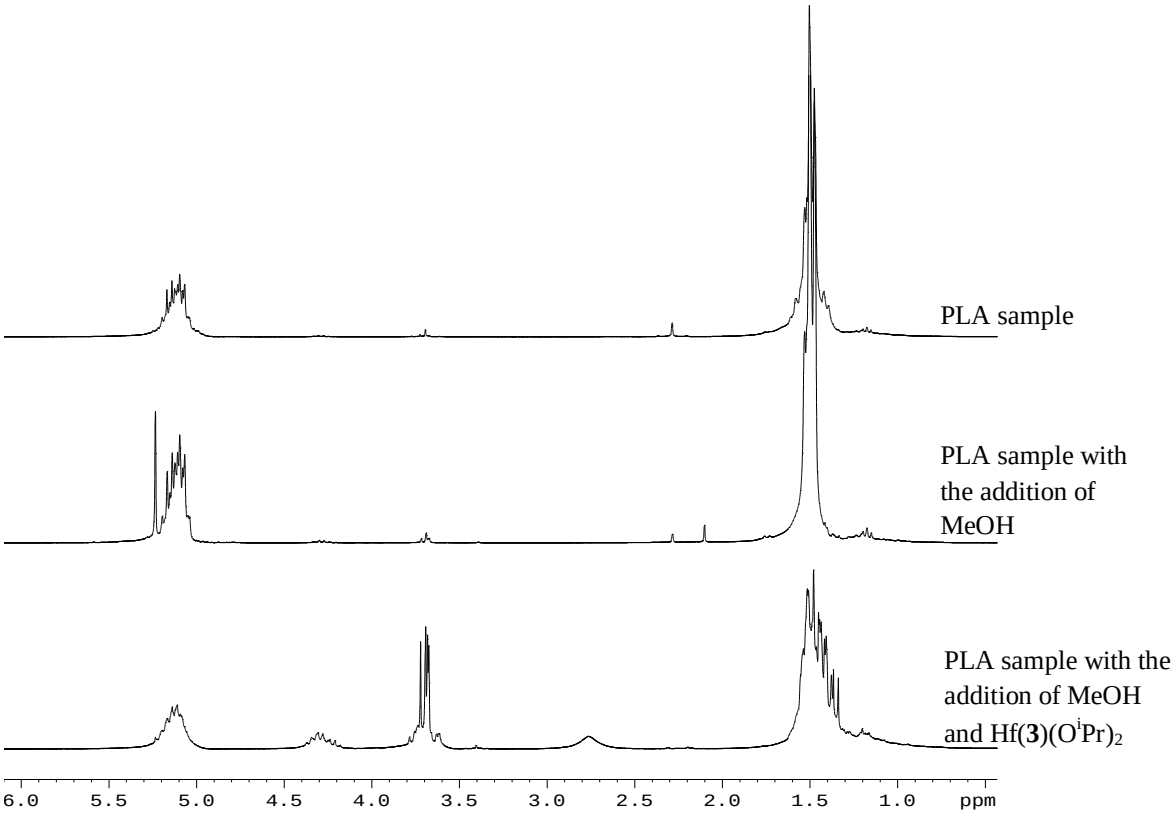


**Figure 3.36**: $^{1}$H NMR spectra showing polymer produced from Zr-$O_3$N (zirconium amine *tris*(phenolate) complex) with the addition of methanol and with the addition of methanol and Hf(**3**)($O^{i}Pr$)$_2$

Figure 3.36 indicates that addition of methanol to the PLA sample dissolved in dichloromethane shows no effect on the polymer sample. However upon addition of Hf(**3**)($O^{i}Pr$)$_2$ and methanol, the $^{1}$H NMR spectrum shows the formation of

methyl lactate albeit to a lesser extent than that observed for a PLA sample prepared using a Salalen catalyst (Figure 3.35).

Having demonstrated that PLA from different sources can successfully be converted to PLA using Hf(**3**)($O^iPr$)$_2$ and methanol, it was then investigated if polymer samples of different molecular weights could be trialled for the degradation into lactic acid derivatives. A series of PLA samples with molecular weights around 10,000 $gmol^{-1}$, 20,000 $gmol^{-1}$, 30,000 $gmol^{-1}$ and 40,000 $gmol^{-1}$ of different stereochemistries and prepared from a range of initiators, were dissolved in dichloromethane to which Hf(**3**)($O^iPr$)$_2$ (17 mg) and methanol were added and the reaction stirred at room temperature for 24 hours. The degradation reactions were carried out using a 100: 1 ratio of [PLA]: [initiator] and 0.1 ml of methanol was added.

| Entry | Type of initiator used to make PLA | Stereochemistry of PLA | Conversion to Methyl Lactate[a] | $M_n$[b] before | $M_n$[b] after |
|---|---|---|---|---|---|
| **1** | Hf(**4**)($O^iPr$)$_2$ | Slightly isotactic | 11 % | 10350 | 2100 |
| **2** | Al Salalen | Atactic | 18 % | 23000 | 2000 |
| **3** | Hf Amine *tris*(phenolate) | Slightly heterotactic | 17 % | 37750 | 18300 |
| **4** | Al Salalen | Atactic | 13 % | 44100 | 1600 |

**Table 3.21**: Results of difference molecular weight PLA samples after addition of Hf(**3**)($O^iPr$)$_2$ and methanol. [a] conversion as determined *via* $^1$H NMR, [b] determined from GPC (in THF) referenced to polystyrene

Table 3.21 shows that regardless of the molecular weight of the PLA used in the degradation study, it is possible to convert the polymeric material to methyl lactate with a dramatic decrease in the molecular weight of the product, after the reaction is stirred for 24 hours at room temperature. This decrease in molecular weight is also seen regardless of the stereochemistry of the initial polymer sample with exception to the heterotactic sample in Table 3.21, entry 3. Although this shows a 17 % conversion to methyl lactate, it does not give as dramatic a decrease in molecular weight as the other samples. For example, only 50 % decrease is observed compared to over 90 % decrease in molecular weight.

To investigate the effect the reaction conditions have on the degradation of PLA samples, the reaction in entry 4 of Table 3.21 was repeated using a 200: 1 ratio of [PLA]: [initiator]. Again the PLA sample prepared using an aluminium

Salalen catalyst was dissolved in dichloromethane, and 0.1 ml of methanol as well as Hf(**3**)($O^iPr$)$_2$ (8.5 mg) was added. Analysis of $^1$H NMR spectrum of the product shows 6 % conversion to methyl lactate which is half that observed when a ratio of 100: 1 of [PLA]: [initiator] was used. From GPC analysis the $M_n$ of the product after being stirred in dichloromethane at room temperature in the presence of Hf(**3**)($O^iPr$)$_2$ and methanol, was reported to be 3,100 gmol$^{-1}$ which is 50 % higher than the $M_n$ value obtained in entry 4 of Table 3.21 when the reaction is carried out with double the amount of Hf(**3**)($O^iPr$)$_2$.

A further reaction condition that was investigated was the effect the amount of methanol being added had on the product obtained. A series of experiments were conducted with PLA samples with molecular weights of 20,000 gmol$^{-1}$ and 40,000 gmol$^{-1}$ and 1 ml of methanol was added instead of 0.1 ml in the case of Table 3.21 above. A PLA sample with a molecular weight of 80,000 gmol$^{-1}$ was also tested to see if it was possible to convert high molecular weight PLA to methyl lactate using Hf(**3**)($O^iPr$)$_2$ in the presence of methanol at room temperature.

| Entry | Type of initiator used to make PLA | Stereochemistry of PLA | Conversion to Methyl Lactate[a] | $M_n$[b] before | $M_n$[b] after |
|---|---|---|---|---|---|
| **1** | Al Salalen | Slightly isotactic | 16 % | 23050 | 3700 |
| **2** | Zr Amine *tris*(phenolate) | Slightly heterotactic | 17 % | 41800 | 4800 |
| **3** | Hf(**4**)($O^iPr$)$_2$ | Slightly isotactic | 12 % | 84750 | 2850 |

**Table 3.22:** Results of difference molecular weight PLA samples after addition of Hf(**3**)($O^iPr$)$_2$ and 1 ml of methanol. [a] conversion as determined *via* $^1$H NMR, [b] determined from GPC (in THF) referenced to polystyrene

Analogous to the results shown in Table 3.21, the PLA samples prepared from various initiators were dissolved in dichloromethane, after which Hf(**3**)($O^iPr$)$_2$ (17 mg) and 1 ml of methanol was added in a 100: 1 ratio of [PLA]: [initiator] and the reactions stirred at room temperature for 24 hours. It can be seen from Table 3.21 and Table 3.22 that no effect is seen on the conversion to methyl lactate upon increasing the amount of methanol present from 0.1 ml to 1 ml. For example a PLA sample with a molecular weight of around 20,000 gmol$^{-1}$, gives 18 % conversion to methyl lactate upon addition of 0.1 ml (entry 2, Table 3.21) and 16 % conversion to methyl lactate when 1 ml of methanol is used (entry 1, Table 3.22). The results in Table 3.22 indicates that

when the higher amount of methanol is added, the molecular weight of the PLA sample does not decrease to the same degree. For example, a PLA sample with an initial $M_n$ = 40,000 gmol$^{-1}$, in the presence of 0.1 ml of methanol results in a product with a $M_n$ = 1,600 gmol$^{-1}$ (entry 4, Table 3.21) compared to a resulting $M_n$ = 4,800 gmol$^{-1}$ when 1 ml of methanol is added (entry 2, Table 3.22). However, the starting PLA samples for the latter comparison have been produced from different initiators and therefore have a different stereochemistry.

Entry 1 in Table 3.21 and entry 1 in Table 3.22 indicates that it is possible to carry out the degradation of isotactic PLA. In these cases the initial PLA samples are only slightly isotactic, however, it was thought that the addition of Hf(**3**)(O$^i$Pr)$_2$ and methanol could be used for a more commercial aspect. Hence, a commercial source of PLA (poly–*L*–LA) was trialled for the production of methyl lactate under similar conditions (room temperature, 100: 1 ratio of [PLA]: [initiator], reaction time of 24 hours) except with an increase in the amount of methanol added (5 ml). Initial GPC analysis before the degradation reaction indicated that the BioWare® cup (the commercial sample) had a $M_n$ = 211,400 gmol$^{-1}$, and from $^1$H NMR analysis after 24 hours at room temperature, showed a 75 % conversion to methyl lactate had occurred.

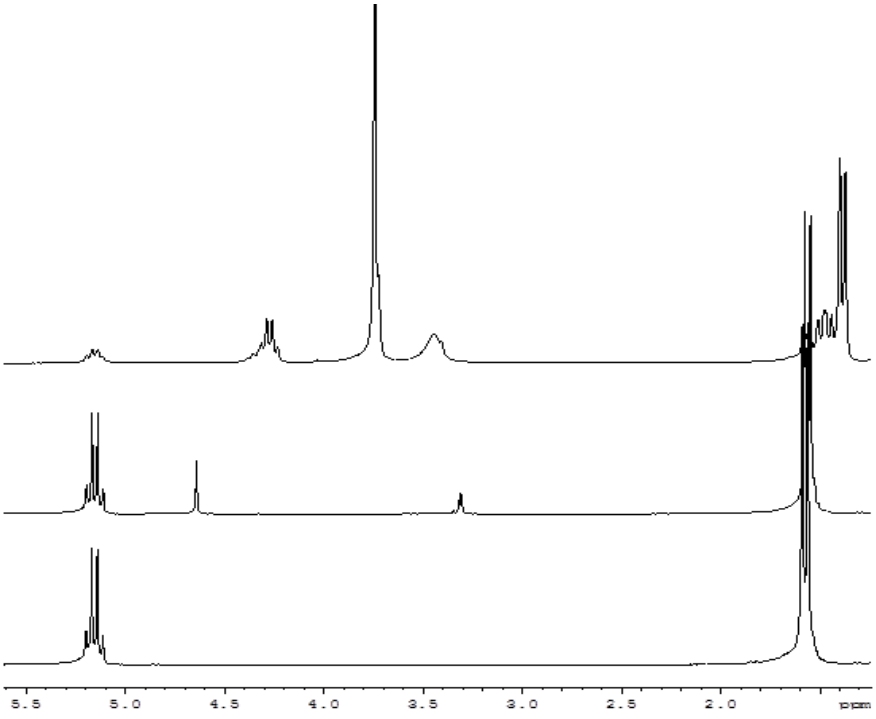


Commercial PLA in DCM and methanol with Hf(**3**)(O$^i$Pr)$_2$

Commercial PLA in DCM and methanol without Hf(**3**)(O$^i$Pr)$_2$

Commercial PLA

**Figure 3.37**: $^{1}$H NMR spectra of commercial PLA sample before degradation reaction and after reaction

It can be seen in Figure 3.37 that the commercial PLA sample is indeed isotactic from the presence of a quartet at around 5.1 ppm in the lower spectrum. The middle spectrum in Figure 3.37 highlights the need for the presence of Hf(**3**)($O^{i}Pr$)$_2$ as when the PLA sample is dissolved in dichloromethane and methanol added without the addition of catalyst, no conversion to methyl lactate is observed with the polymer peak still evident from the $^{1}$H NMR spectrum. Upon addition of Hf(**3**)($O^{i}Pr$)$_2$ (top spectrum in Figure 3.37), there is a significant decrease in the polymeric peak at 5.1 ppm. The formation of methyl lactate at 4.3 ppm can be observed, highlighting that Hf(**3**)($O^{i}Pr$)$_2$ is a successful catalyst for the degradation of PLA at room temperature in the presence of alcohol.

The resulting product from the degradation of the commercial PLA sample gave a $M_n$ = 500 gmol$^{-1}$ indicating that intensive degradation has occurred. The addition of Hf(**3**)($O^{i}Pr$)$_2$ in the presence of methanol can therefore be considered a successful route to the formation of lactic acid derivatives from various PLA samples, even those in the commercial marketplace. More significantly is that the degradation is successful at room temperature, as examples of PLA degradation that have been reported in the literature involve elevated temperatures, and in some cases microwave irradiation.[24-30]

## 3.7 Concluding Remarks

In summary, this chapter reports the first example of group (IV) Salalen complexes for the ROP of *rac*-LA. The monomeric complexes display *fac-mer* geometry in the solid-state with the Salan fragment *fac* and the Salen fragment *mer*. Kinetic studies indicated that the subtle change in the sterics of the complex can have a profound effect on the rate of polymerisation. Complexes containing bulky $^{t}$Bu substituents on the phenoxy rings (**1**H$_2$ and **2**H$_2$) reported a reactivity order of Ti > Zr > Hf. However, decreasing the steric hindrance of the ligand (**3**H$_2$ and **4**H$_2$) displayed a change in reactivity such that Hf > Zr > Ti. The complexes reported for ligands **3**H$_2$ and **4**H$_2$ are some of the fastest group (IV) initiators of

this type. Initial polymerisation studies produced atactic PLA when titanium initiators were employed. Zirconium initiators containing **1**$H_2$ and **2**$H_2$ produced PLA with a heterotactic bias. Zr(**3**)($O^iPr$)$_2$ and Zr(**4**)($O^iPr$)$_2$ produced low molecular weight PLA in toluene and under solvent-free conditions. The hafnium initiators displayed a tendency to produce isotactic PLA in solution and in the absence of solvent. However, analogous to that observed with zirconium counterparts, complexes containing **3**$H_2$ and **4**$H_2$ produced PLA with $M_n$ values lower than the theoretical values. The production of low molecular weight PLA could be attributed to the formation of methyl lactate and lactic acid upon workup. It has been shown that it is possible to produce PLA with higher molecular weight utilising the zirconium and hafnium complexes of **3**$H_2$ and **4**$H_2$, by eliminating the addition of methanol when quenching the polymerisation. The production of methyl lactate and hence the degradation of PLA at room temperature upon addition of methanol and Hf(**3**)($O^iPr$)$_2$ has been demonstrated for a variety of PLA products, including a commercial PLA sample.

1. J. Tian and G. W. Coates, *Angew. Chem., Int. Ed. Engl.*, 2000, **39**, 3626-3629.
2. A. Yeori, S. Gendler, S. Groysman, I. Goldberg and M. Kol, *Inorg. Chem. Commun.*, 2004, **7**, 280-282.
3. E. Y. Tshuva, I. Goldberg and M. Kol, *J. Am. Chem. Soc.*, 2000, **122**, 10706-10707.
4. K. Press, A. Cohen, I. Goldberg, V. Venditto, M. Mazzeo and M. Kol, *Angew. Chem., Int. Ed. Engl.*, 2011, **50**, 3529-3532.
5. K. Nakano, M. Nakamura and K. Nozaki, *Macromolecules*, 2009, **42**, 6972-6980.
6. K. Matsumoto, B. Saito and T. Katsuki, *Chem. Commun.*, 2007, 3619-3627.
7. J. Fujisaki, K. Matsumoto, K. Matsumoto and T. Katsuki, *J. Am. Chem. Soc.*, 2011, **133**, 56-61.
8. K. Matsumoto, T. Yamaguchi and T. Katsuki, *Heterocycles*, 2008, **76**, 191-196.
9. D. Xiong, M. Wu, S. Wang, F. Li, C. Xia and W. Sun, *Tetrahedron-Asymmetry*, 2010, **21**, 374-378.
10. Y. Sakai, J. Mitote, K. Matsumoto and T. Katsuki, *Chem. Commun.*, 2010, **46**, 5787-5789.
11. M. J. Stanford and A. P. Dove, *Chem. Soc. Rev.*, 2010, **39**, 486-494.
12. H. Z. Du, A. H. Velders, P. J. Dijkstra, J. R. Sun, Z. Y. Zhong, X. S. Chen and J. Feijen, *Chem. Eur. J.*, 2009, **15**, 9836-9845.
13. E. L. Whitelaw, M. D. Jones and M. F. Mahon, *Inorg. Chem.*, 2010, **49**, 7176-7181.
14. C. K. A. Gregson, I. J. Blackmore, V. C. Gibson, N. J. Long, E. L. Marshall and A. J. P. White, *Dalton Trans.*, 2006, 3134-3140.
15. A. J. Chmura, M. G. Davidson, M. D. Jones, M. D. Lunn, M. F. Mahon, A. F. Johnson, P. Khunkamchoo, S. L. Roberts and S. S. F. Wong, *Macromolecules*, 2006, **39**, 7250-7257.
16. T. Repo, M. Klinga, P. Pietikainen, M. Leskela, A. M. Uusitalo, T. Pakkanen, K. Hakala, P. Aaltonen and B. Lofgren, *Macromolecules*, 1997, **30**, 171-175.
17. A. Stopper, I. Goldberg and M. Kol, *Inorg. Chem. Commun.*, 2011, **14**, 715-718.
18. T. K. Saha, V. Ramkumar and D. Chakraborty, *Inorg. Chem.*, 2011, **50**, 2720-2722.
19. A. J. Chmura, M. G. Davidson, C. J. Frankis, M. D. Jones and M. D. Lunn, *Chem. Commun.*, 2008, 1293-1295.
20. P. Hormnirun, E. L. Marshall, V. C. Gibson, A. J. P. White and D. J. Williams, *J. Am. Chem. Soc.*, 2004, **126**, 2688-2689.
21. M. S. Holm, S. Saravanamurugan and E. Taarning, *Science*, 2010, **328**, 602-605.
22. R. M. West, M. S. Holm, S. Saravanamurugan, J. Xiong, Z. Beversdorf, E. Taarning and C. H. Christensen, *J. Catal.*, 2010, **269**, 122-130.
23. E. T. H. Vink, K. R. Rabago, D. A. Glassner, B. Springs, R. P. O'Connor, J. Kolstad and P. R. Gruber, *Macromol. Biosci.*, 2004, **4**, 551-564.
24. K. Hirao, Y. Nakatsuchi and H. Ohara, *Polym. Degrad. Stab.*, 2010, **95**, 925-928.
25. F. Nederberg, E. F. Connor, T. Glausser and J. L. Hedrick, *Chem. Commun.*, 2001, 2066-2067.
26. K. Phomphrai, S. Pracha, P. Phonjanthuek and M. Pohmakotr, *Dalton Trans.*, 2008, 3048-3050.
27. P. Coszach and J. Willocq, *WO 2011/029648 A1*, 2011.
28. L. D. Brake, *US 5264617*.
29. K. Odelius, A. Hoglund, S. Kumar, M. Hakkarainen, A. K. Ghosh, N. Bhatnagar and A.-C. Albertsson, *Biomacromolecules*, 2011, **12**, 1250-1258.
30. H. Tsuji, A. Mizuno and Y. Ikada, *J. Appl. Polym. Sci.*, 2000, **77**, 1452-1464.

# Chapter 4

## Salalen Aluminium Complexes and their Exploitation for the ROP of *rac*-LA

# 4. Salalen Aluminium Complexes and their Exploitation for the ROP of *rac*-LA

## 4.1 Preamble

As reported in Chapter 1, Section 1.3.2, one of the earliest examples in the literature utilising aluminium complexes for the ROP of *rac*-LA was by Spassky and co-workers who reported the use of a chiral Schiff base complex based on *R*-(+)-1,1'-binaphthyl-2,2'-diamine, to produce isotactic PLA.[1] Since then, a vast majority of examples utilising aluminium initiators have been reported for the ROP of *rac*-LA, mainly based on Salan[2] or Salen[3, 4] ligands with no examples utilising Al(III) Salalen complexes. However, aluminium Salalen complexes have been utilised in catalysis for the oxidation of sulphides[5-9] and for the hydrophosphonylation of aldehydes.[10-12] Katsuki *et al.* also demonstrated the use of aluminium Salalen complexes as a bifunctional catalyst for the asymmetric Simmons-Smith reaction of *trans*-disubstituted allylic alcohols at room temperature.[13] More recently, the same group utilised such aluminium complexes as highly enantioselective Lewis acid catalysts for the Friedel-Crafts reaction of indole.[14]

Due to the high activity of the group (IV) initiators containing Salalen ligands, developed in Chapter 3 for the ROP of *rac*-LA, it was hypothesised that analogous aluminium initiators would not only have high activity, but also increase the stereocontrol of the reaction, to potentially produce highly stereoblock isotactic PLA. This chapter therefore reports the preparation of a range of aluminium Salalen complexes analogous to those in Chapter 3, and their ability in the ROP of *rac*-LA is investigated. Furthermore, due to the stark change in stereocontrol reported by Gibson *et al.* for aluminium Salan complexes upon addition of chloro substituents,[2] additional complexes have been synthesised containing chloro moieties on the phenoxy ring adjacent to the imine nitrogen centre.

## 4.2 Synthesis of Ligands

The ligands mentioned above and described here in, were synthesised in an identical manner to those Salalen ligands reported in Chapter 3.

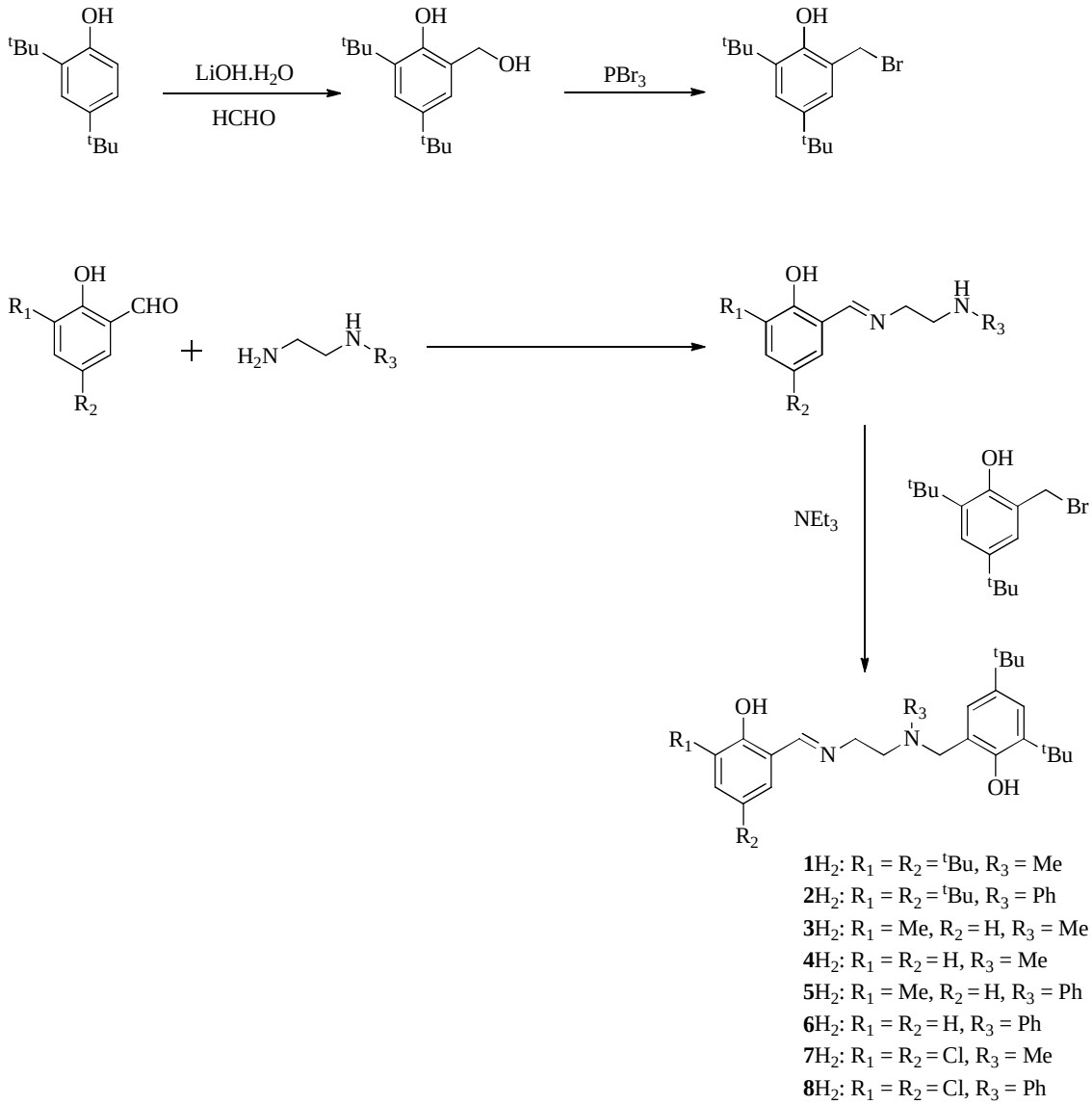


**Figure 4.01**: Synthesis of Salalen ligands

In contrast to the group (IV) complexes discussed in Chapter 3, the ligands in Figure 4.01 and hence the complexes reported here in, not only allow a comparison of the sterics, but also allow an investigation into the effect of varying the electronics of the Salen fragment (**7**$H_2$ and **8**$H_2$). Again for completeness the steric effect of changing the substituent on the amine was also investigated, with the amine substituent being either a methyl or a phenyl group. Unfortunately, apart from the single crystal X-ray diffraction structure obtained for **2**$H_2$, shown

in Figure 3.03, Chapter 3, it was not possible to obtain further X-ray crystal structures of any of the ligands shown in Figure 4.01. This is presumably due to the unsymmetrical nature of the ligand effecting the packing coupled with their high solubility in most common organic solvents. All ligands prepared were characterised by $^{1}H$, $^{13}C\{^{1}H\}$ NMR spectroscopy together with high resolution mass spectrometry.

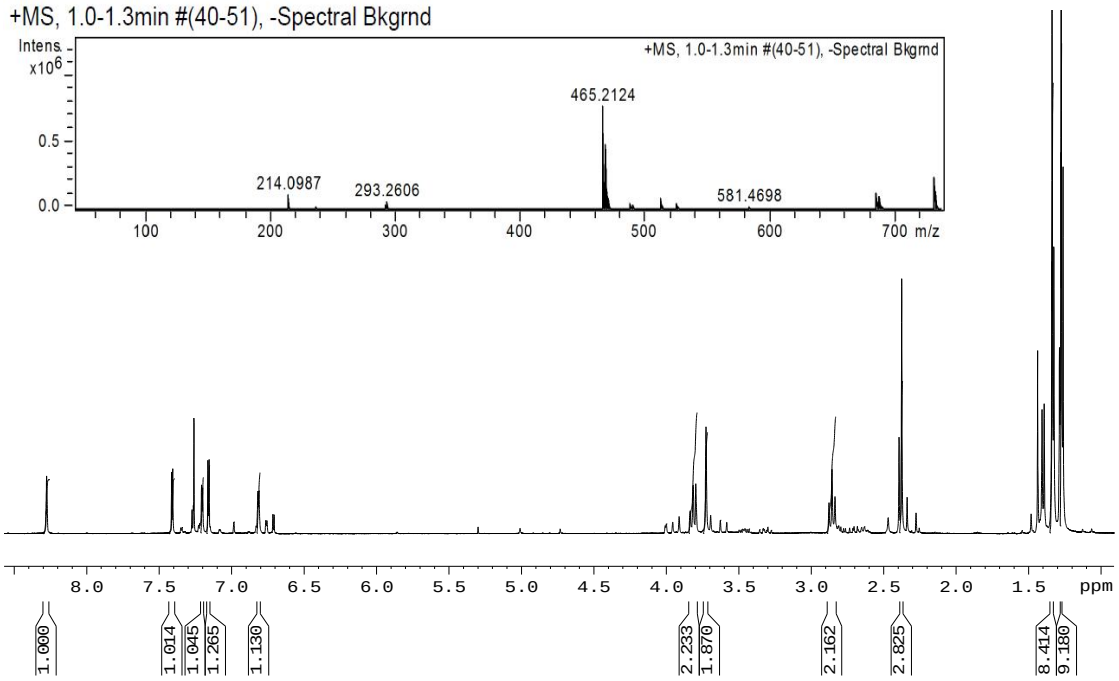


**Figure 4.02**: $^{1}H$ NMR spectrum of **7**$H_2$

Analysis of the spectrum shown in Figure 4.02 shows that ligand **7**$H_2$ was successfully isolated, however, the sample used for analysis is not 100 % pure, with resonances present in the spectrum after flash chromatography, corresponding to starting material. From high resolution mass spectrometry, it can be seen that the desired product is obtained. Although the $^{1}H$ NMR spectrum shows impurities or remaining starting material (*ca.* 25 %), the mass spectrometry together with the dominant peaks in the NMR spectrum, provide suffice evidence that the desired product is present and hence the ligand was further utilised for complexation to aluminium.

## 4.3 Complexing Salalen ligands to Aluminium

The ligands prepared in Figure 4.01 were complexed to aluminium simply by reaction of one equivalent of $AlMe_3$ with one equivalent of the Salalen ligand in toluene, as shown in Figure 4.03.

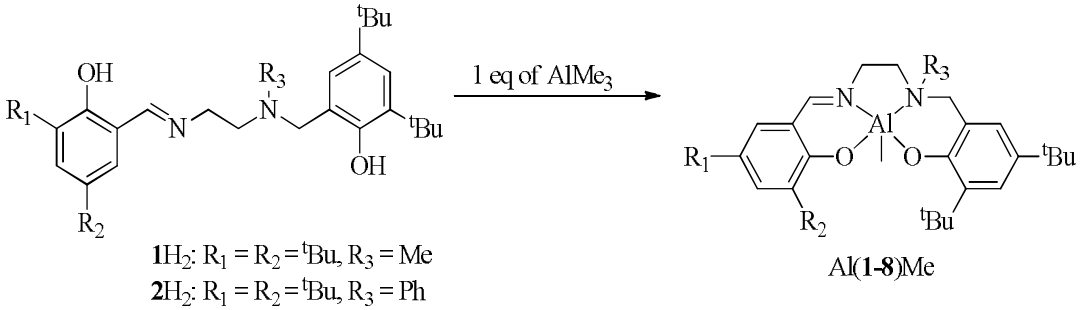


**1**$H_2$: $R_1 = R_2 = {}^tBu$, $R_3 = Me$
**2**$H_2$: $R_1 = R_2 = {}^tBu$, $R_3 = Ph$
**3**$H_2$: $R_1 = Me$, $R_2 = H$, $R_3 = Me$
**4**$H_2$: $R_1 = R_2 = H$, $R_3 = Me$
**5**$H_2$: $R_1 = Me$, $R_2 = H$, $R_3 = Ph$
**6**$H_2$: $R_1 = R_2 = H$, $R_3 = Ph$
**7**$H_2$: $R_1 = R_2 = Cl$, $R_3 = Me$
**8**$H_2$: $R_1 = R_2 = Cl$, $R_3 = Ph$

Al(**1-8**)Me

**Figure 4.03**: Aluminium complexes prepared using Salalen ligands

It was possible to isolate all eight pure aluminium complexes of the ligands in Figure 4.01. For the group (IV) complexes in Chapter 3, due to issues with recrystallistion, it was not possible to isolate cleanly metal complexes of ligands **5**$H_2$, **6**$H_2$, **7**$H_2$ and **8**$H_2$. Due to the unsymmetrical nature of these complexes coupled with their high solubility in common organic solvents, the production of crystals of suitable quality for diffraction studies was challenging, however, complexes based on ligands **2**$H_2$, **3**$H_2$, **7**$H_2$ and **8**$H_2$ were characterised by single crystal X-ray diffraction (Figures 4.04 – 4.07 respectively).

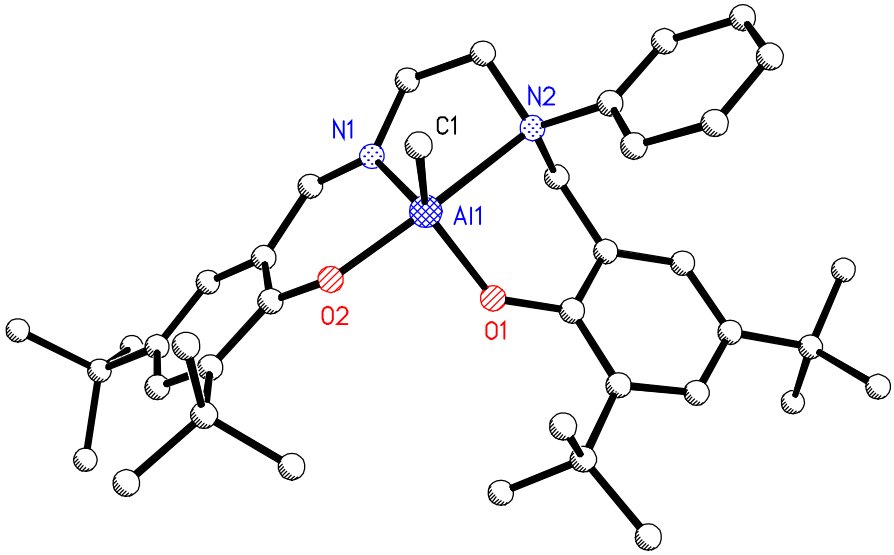


**Figure 4.04**: Solid-state structure of Al(**2**)Me where the hydrogen atoms have been removed for clarity

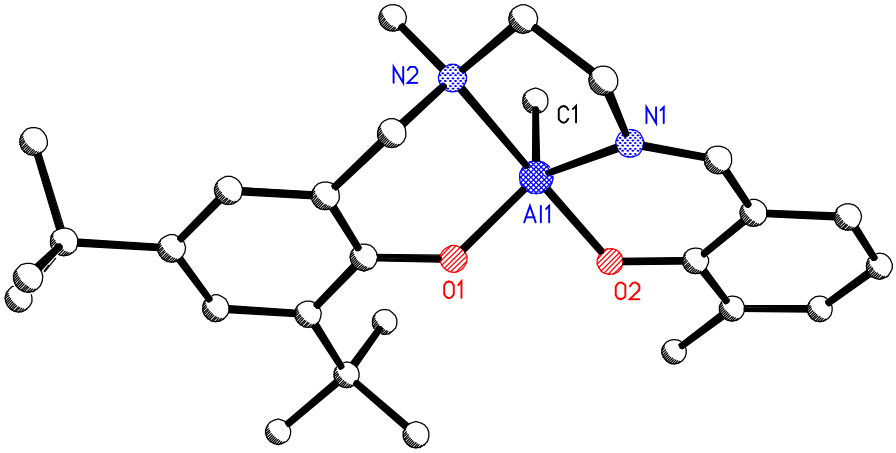


**Figure 4.05**: Solid-state structure of Al(**3**)Me where the hydrogen atoms have been removed for clarity

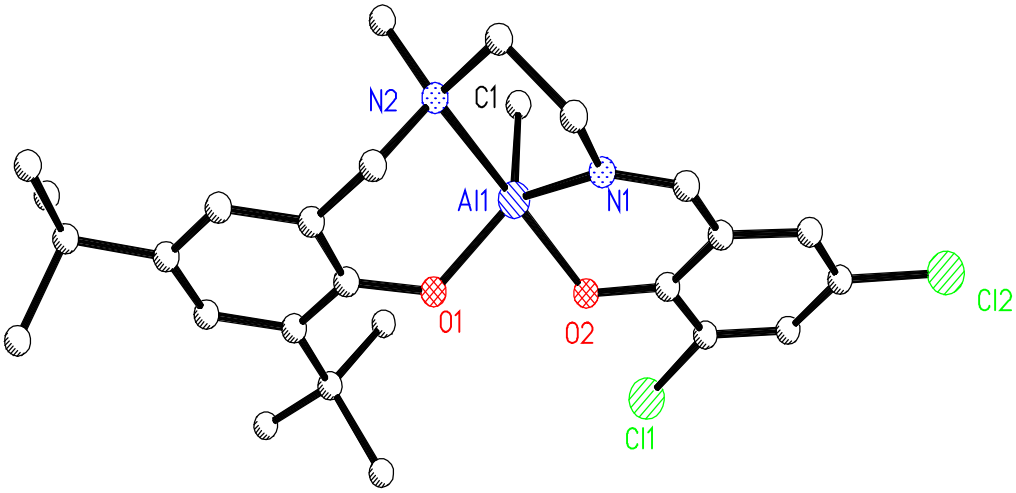


**Figure 4.06**: Solid-state structure of Al(**7**)Me where the hydrogen atoms have been removed for clarity

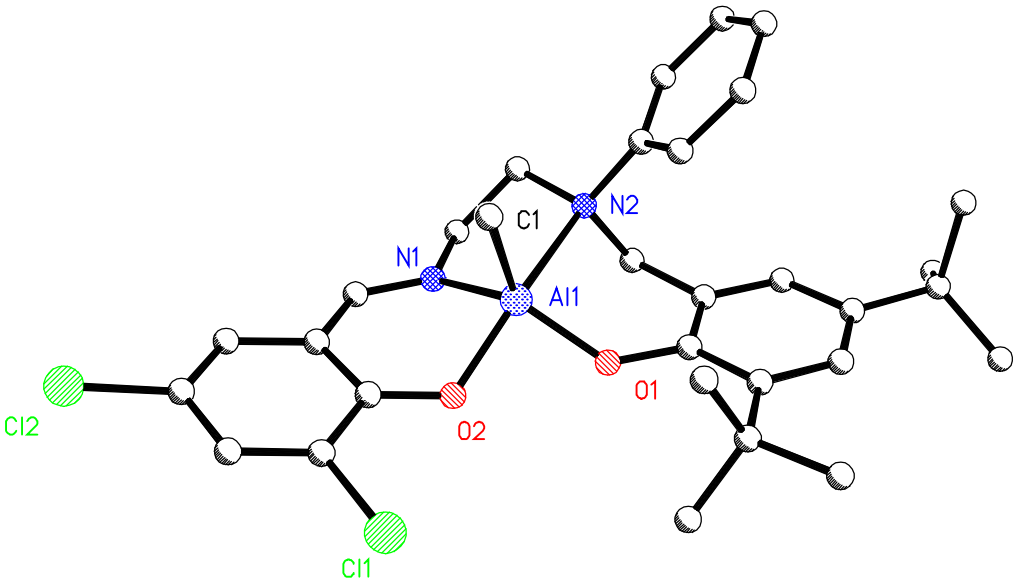


**Figure 4.07**: Solid-state structure of Al(**8**)Me where the hydrogen atoms have been removed for clarity

For the aluminium complexes crystallographically characterised (Figures 4.04 - 4.07) the metal centre is seen to be in a highly distorted trigonal pyramidal geometry. The τ values can be calculated according to literature: $\tau = (\beta - \alpha)/60$ where β is the angle {N(2)-M-O(2)} and α = {N(1)-M-O(1)}. This gives an indication into the structural preference between trigonal bipyramidal when τ = 1 and tetragonal when τ = 0.[15]

| | Al(2)Me | Al(3)Me | Al(7)Me | Al(8)Me |
|---|---|---|---|---|
| **τ** | 0.809 | 0.746 | 0.667 | 0.562 |

**Table 4.01**: τ values for Al(**2**)Me, Al(**3**)Me, Al(**7**)Me and Al(**8**)Me

For the complexes shown in Figures 4.04 – 4.07 the τ values are given in Table 4.01 with the values ranging from 0.56 - 0.80 implying a bias towards the trigonal bipyramidal geometry being closer to 1 than 0.

Selected bond lengths and angles for the aluminium complexes under investigation are shown in Table 4.02.

| | Al(2)Me | Al(3)Me | Al(7)Me | Al(8)Me | Al(Salan)Me[2] | Al(Salen)Et[16] | Al(Salalen)Cl[11] |
|---|---|---|---|---|---|---|---|
| **M-O1** | 1.7701(17) | 1.757(2) | 1.762(2) | 1.751(2) | 1.7570(15) | 1.799(6) | 1.747(2) |
| **M-O2** | 1.8193(18) | 1.827(2) | 1.847(2) | 1.844(2) | 1.7930(16) | 1.816(5) | 1.800(19) |
| **M-N1** | 1.958(2) | 1.979(3) | 2.000(3) | 1.982(3) | 2.0550(18) | 2.015(7) | 1.960(2) |
| **M-N2** | 2.315(2) | 2.266(3) | 2.239(3) | 2.329(3) | 2.4532(19) | 2.046(7) | 2.124(2) |
| **M-C1** | 1.957(3) | 1.960(3) | 1.984(3) | 1.960(3) | 1.955(3) | 1.960(9) | 2.187(10)* |
| **O1-M-N1** | 116.83(9) | 120.70(12) | 123.13(11) | 126.92(12) | 113.86(8) | 141.6(3) | 122.26(9) |
| **N1-M-N2** | 77.25(8) | 79.10(11) | 78.94(10) | 78.20(11) | 77.88(7) | 77.5(3) | 79.34(9) |
| **C1-M-N1** | 114.87(11) | 113.68(13) | 113.62(12) | 106.30(14) | 119.93(12) | 106.8(4) | 120.57(7)* |
| **C1-M-N2** | 94.50(10) | 93.26(13) | 94.82(11) | 96.81(13) | 89.35(10) | 101.8(3) | 91.84(6)* |
| **Cl-M-O1** | 126.88(11) | 124.68(14) | 122.72(13) | 125.90(13) | 122.84(12) | 110.6(4) | 116.52(7)* |
| **C1-M-O2** | 97.56(10) | 99.65(14) | 100.04(12) | 100.55(13) | 100.23(10) | 106.8(3) | 94.72(7)* |
| **C-N imine** | 1.303(3) | 1.296(5) | 1.287(4) | 1.283(4) | - | 1.292(7) & 1.291(7) | 1.292(3) |
| **C-N amine** | 1.503(3) | 1.496(4) | 1.491(4) | 1.515(4) | 1.504(3) & 1.488(3) | - | 1.500(3) |

**Table 4.02**: Selected bond lengths (Å) and angles (°) for complexes Al(**2**)Me, Al(**3**)Me, Al(**7**)Me, Al(**8**)Me, Al(Salan)Me,[2] Al(Salen)Et,[16] and Al(Salalen)Cl[11] for comparison. * denotes C(1) replaced with Cl atom.

The phenoxide {O(1)} *trans* to the imine has the shortest Al-O bond distance in all cases, and as expected the Al-$N_{imine}$ distance {M-N(1)} is considerable shorter than that of the Al-$N_{amine}$ {M-N(2)}. Complexes Al(**2**)Me and Al(**8**)Me which contain a phenyl substituent on the amine nitrogen centre have longer Al-$N_{amine}$ bond lengths than their methyl substituted counterparts, presumably due to the bulk of the substituent. The {C(1)-M-N(1)} angle is considerably larger than the {C(1)-M-N(2)} angle, and the {C(1)-M-O(2)} angle

is considerably smaller than the {C(1)-M-O(1)} angle. It is worth noting that the {C(1)-M-N(1)} angle for Al(**8**)Me is smaller than the other complexes. When the substituents on the phenoxy ring adjacent to the amine nitrogen centre are changed from $^{t}$Bu to Cl groups, there is an increase of around 10 ° in the {O(1)-M-N(1)} angle. The complexes have $C_1$ symmetry and all adopt a *β-cis* configuration in the solid-state. Although the complexes themselves are not chiral, they do contain a chiral nitrogen centre N(2), and therefore it is possible to obtain both the Λ and the Δ form of the complexes. It can be determined that the *S* configuration at N(2) induces the Λ form of the complex and a *R* configuration at N(2) induces the Δ form of the complexes, however both enantiomeric forms of the complexes are produced as the complexes crystallise in a centrosymmetric space group.

The aluminium Salan complex reported in Table 4.02 was reported by Gibson *et al.* and displays an analogous structure to the compound shown in Figure 1.28 in Chapter 1. However, in the example discussed here, both the substituents on the phenoxy ring and the amine nitrogen centres are methyl groups.[2] The Salan complex shows comparable data with Al(**2,3,7,8**)Me and with the free ligand **2**$H_2$ which is reported to have a C-$N_{imine}$ and C-$N_{amine}$ bond lengths of 1.2740(17) Å and 1.4799(17) Å respectively.

The data for an aluminium complex containing a Salen ligand (Figure 4.08) has also been reported in Table 4.02 for comparison.[16]

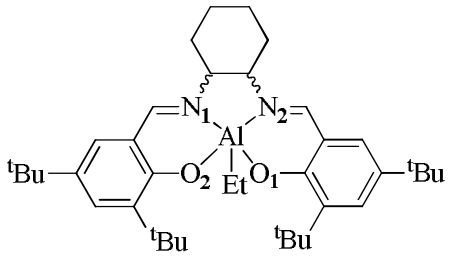


**Figure 4.08**: Salen aluminium complex reported by Darensbourg *et al.*[16]

The aluminium complex shown in Figure 4.08, affords crystallographic data in comparison with the complexes Al(**2,3,7,8**)Me. However, the {O(1)-M-N(1)} angle is statistically larger for the Salen complex than the Salalen complexes reported here.[16] This is presumably due to the presence of the bridging

cyclohexane ring. It can also be observed in Table 4.02 that the {C(1)-M-O(1)} angle is statistically smaller in the Salen complex than for Al(**2,3,7,8**)Me. This could be contributed to the complexes displaying square pyramidal geometry.[16]

The Salalen complex reported by Katsuki *et al.* (Figure 4.09) has been included in Table 4.02 for comparison with the Salalen complexes prepared here.[11]

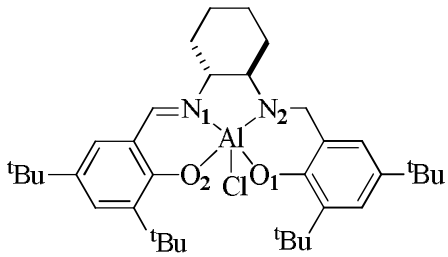


**Figure 4.09**: Aluminium Salalen complex reported by Katsuki *et al.*.[11]

It can be observed that in general the complexes Al(**2,3,7,8**)Me show data consistent with that reported in the literature for analogous Salalen complexes, albeit the example shown here contains a labile chloro group instead of a methyl group.[11]

The $^{1}$H NMR spectra for all complexes prepared in this study are in agreement with the solid-state structures being maintained in solution, with a resonance at *ca.* -0.5 ppm for the methyl group and a resonance at *ca.* 7.4 ppm for the imine proton. It can be seen from $^{1}$H NMR analysis that the $CH_2$ groups are now diastereotopic indicating that the ligand is “locked” in position once coordinated to aluminium.

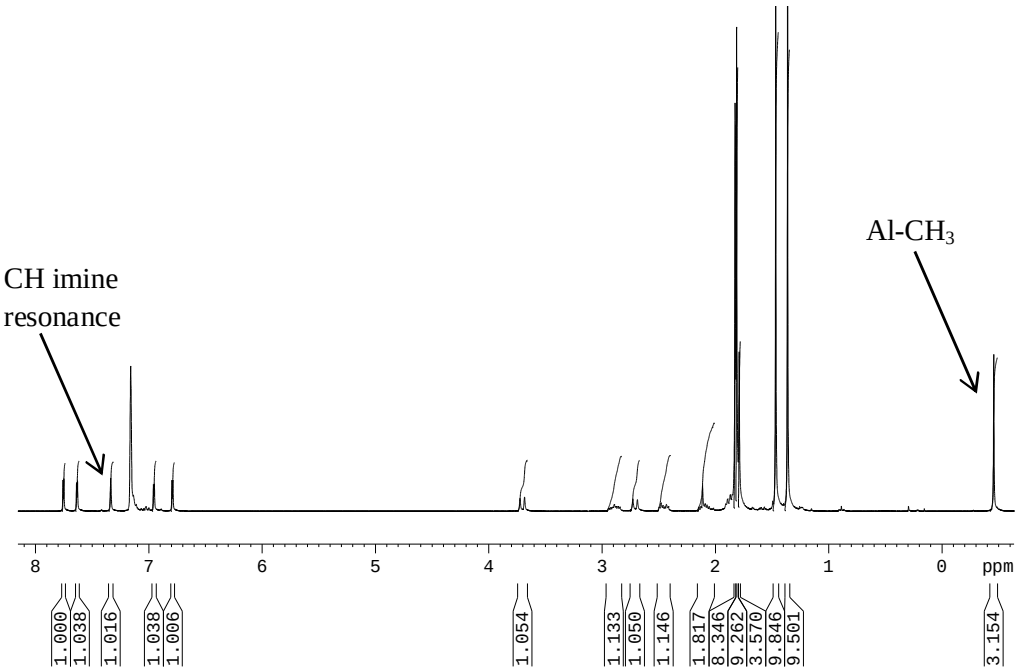


**Figure 4.10**: $^{1}$H NMR spectrum of Al(**1**)Me

Figure 4.10 is representative of all of the complexes under investigation within this chapter, and signifies that the desired complex is prepared.

Interestingly when the complexation of ligand **3**$H_2$ was repeated at a lower concentration in toluene, a second product was observed that could be analysed by single crystal X-ray diffraction, Figure 4.11.

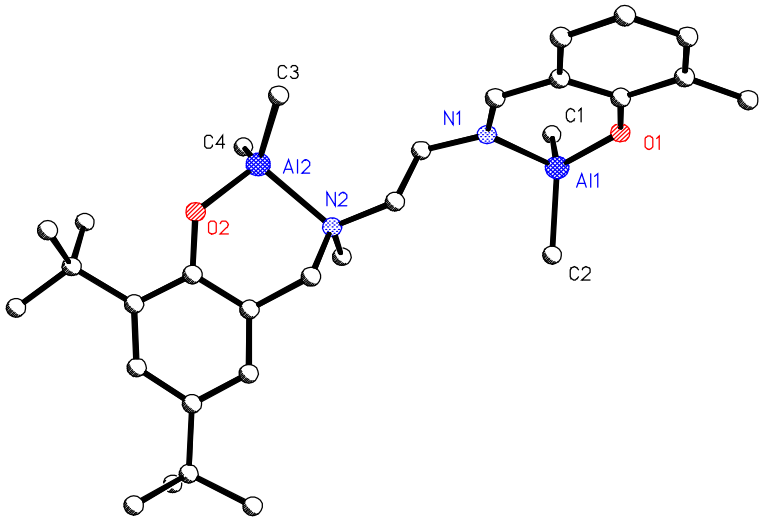


**Figure 4.11**: Solid-state structure of $Al_2$(**3**)$Me_4$ where the hydrogen atoms have been removed for clarity

The structure shown in Figure 4.11 again demonstrates $C_1$ symmetry, however, unlike the monometallic form Al(**3**)Me (Figure 4.05), the aluminium centres are now tetrahedral in geometry, with the ligand reacting with two equivalents of $AlMe_3$.

| | **$Al_2$(3)$Me_4$** | **Al(3)Me** |
|---|---|---|
| **M1-O1** | 1.7750(13) | 1.757(2) |
| **M2-O2** | 1.7638(13) | - |
| **M1-N1** | 1.9613(15) | 1.979(3) |
| **M2-N2** | 2.0577(15) | - |
| **M1-C1** | 1.9624(19) | 1.960(3) |
| **M1-C2** | 1.952(2) | - |
| **M2-C3** | 1.950(2) | - |
| **M2-C4** | 1.957(2) | - |
| **O1-M1-N1** | 95.00(6) | 120.70(12) |
| **O2-M2-N2** | 97.96(6) | - |
| **C1-M1-N1** | 109.22(8) | 113.68(13) |
| **C2-M1-N1** | 105.89(8) | - |
| **C3-M2-N2** | 106.86(8) | - |
| **C4-M2-N2** | 108.83(9) | - |
| **C1-M1-O1** | 111.74(7) | 124.68(14) |
| **C2-M1-O1** | 114.01(8) | - |
| **C3-M2-O2** | 109.84(8) | - |
| **C4-M2-O2** | 111.27(9) | - |
| **C1-M1-C2** | 118.11(9) | - |
| **C3-M2-C4** | 119.75(12) | - |
| **C-N imine** | 1.292(2) | 1.296(5) |
| **C-N amine** | 1.521(2) | 1.496(4) |

**Table 4.03**: Selected bond lengths (Å) and angles (°) for complexes $Al_2$(**3**)$Me_4$.

The values reported in Table 4.03 are in general in agreement with the monometallic aluminium complexes containing the Salalen ligands. However, the O-M-N angle at both metal centres is smaller in the bimetallic form {95.00(6) ° and 97.96(6) °} than in the monometallic form Al(**3**)Me {120.70(12) °}. The {C(1)-M(1)-C(2)} and {C(3)-M(2)-C(4)} angles are in agreement with literature values for other reported bimetallic aluminium Salan complexes for example a piperazine-based aluminium Salan system which reports a C-M-C angle of 115.30(8) °.[17]

For complex $Al_2$(**3**)$Me_4$, the Salalen ligand has reacted with two equivalents of $AlMe_3$ and under these dilution conditions, both the 1:1 and 1:2 species are both produced which can be evident from analysis of multiple peaks present for Al-$CH_3$ groups in the $^1$H NMR spectrum.

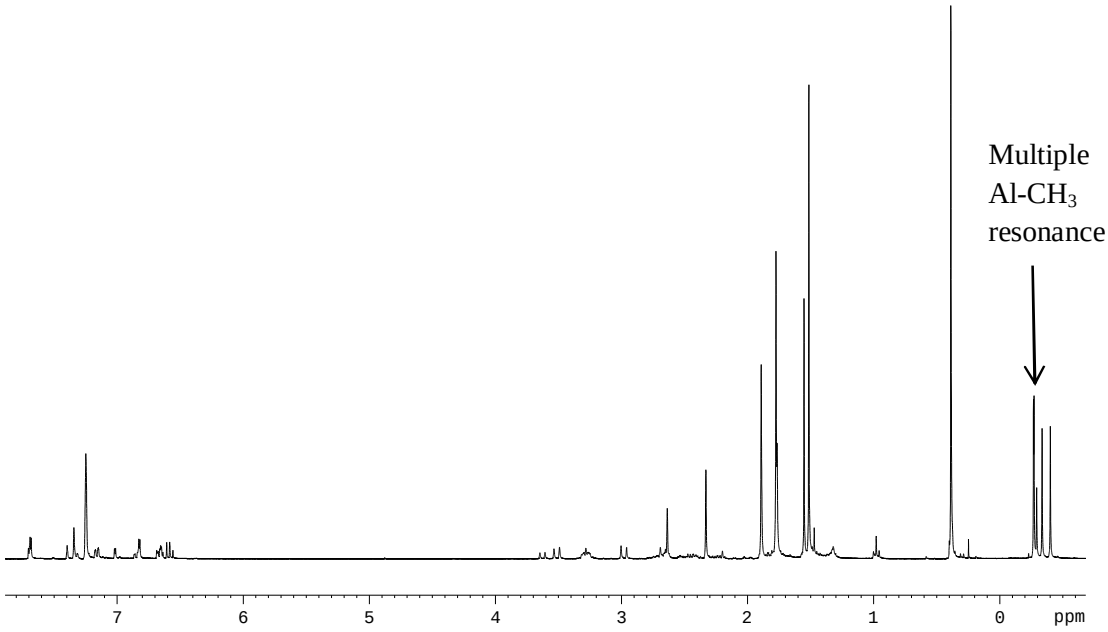


**Figure 4.12**: $^1$H NMR spectrum of $Al_2$(**3**)$Me_4$

At low concentration levels, it proved troublesome to separate the two forms of the complexes, and hence it was necessary to prepare all aluminium Salalen complexes reported here under more concentrated conditions to achieve the 1:1 complexes in high purity.

## 4.4 Ring-opening Polymerisation of *rac*-LA

The monometallic complexes Al(**1-8**)Me were trialled for the ROP of *rac*-LA under both solution and solvent-free conditions. Unlike the group (IV) complexes in Chapter 3, it was necessary to add one equivalent of benzyl alcohol (BnOH) as a co-initiator to generate the alkoxide *in-situ* for the polymerisation to proceed.

### 4.4.1 Solution Polymerisation at 80 °C

Although the group (IV) initiators containing the same Salalen ligands were tested for the ROP in toluene after both 2 hours and 24 hours, the aluminium initiators investigated in this chapter initially showed slower reactivity when the reaction was carried out for 24 hours. Therefore, the ROP was not carried out for 2 hours. The polymerisation reactions were carried out in toluene at 80 °C in a ratio of 100: 1: 1 of monomer to initiator to benzyl alcohol, and the results shown in Table 4.04.

| Entry | Initiator | Conversion[a] (%) | $M_n$[b] | $M_w$[b] | $M_n$ (theo.) | PDI[b] | $P_r$[c] |
|---|---|---|---|---|---|---|---|
| **1** | Al(**1**)Me | 32 | 9400 | 10100 | 4700 | 1.08 | 0.48 |
| **2** | Al(**2**)Me | 96 | 11950 | 13200 | 13950 | 1.11 | 0.43 |
| **3** | Al(**3**)Me | 26 | 7400 | 7700 | 3850 | 1.04 | 0.72 |
| **4** | Al(**4**)Me | 95 | 14200 | 16050 | 13800 | 1.13 | 0.60 |
| **5** | Al(**5**)Me | 96 | 10450 | 17200 | 13950 | 1.65 | 0.42 |
| **6** | Al(**6**)Me | 98 | 9050 | 12600 | 14250 | 1.39 | 0.45 |
| **7** | Al(**7**)Me | 96 | 8600 | 9450 | 13950 | 1.10 | 0.63 |
| **8** | Al(**8**)Me | 69 | 7950 | 8600 | 10050 | 1.08 | 0.48 |

**Table 4.04**: ROP results for Al(**1**-**8**)Me in toluene at 80 °C for 24 hours. 0.7 g of *rac*-LA, [LA]:[benzyl alcohol]:[initiator] = 100:1:1. [a] conversion as determined *via* $^1$H NMR, [b] determined from GPC (in THF) referenced to polystyrene, [c] calculated from the $^1$H homonuclear decoupled NMR ($CDCl_3$) analysis.

The $M_n$(theo.) values reported in Table 4.04 were calculated according to Equation 2.03 in Section 2, where the end group is now a benzyl alcohol group. In general, the initiators generated PLA with reasonable correlation between measured and theoretical molecular weights, with the exception of Al(**1**)Me and Al(**3**)Me which afforded low conversions after 24 hours. From comparison of the $P_r$ values in Table 4.04, it can be seen that when the substituent on the amine nitrogen centre is the less bulky methyl substituent, PLA with a heterotactic bias is produced (entries 3, 5 and 7). The degree of heterotacticity can be observed from an enhancement in the *sis* peak in the $^1$H homonuclear decoupled NMR spectrum (Figure 4.13).

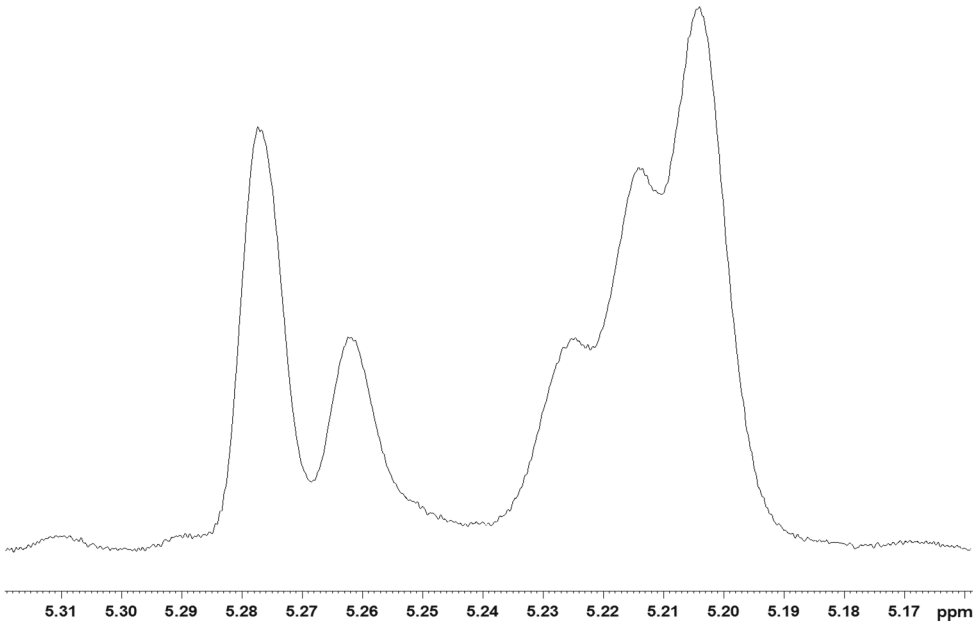


**Figure 4.13**: $^{1}$H homonuclear decoupled NMR spectrum of the product obtained *via* Al(**7**)Me at 80 °C for 24 hours in toluene with $P_r$ = 0.63 – entry 7, Table 4.04.

Interestingly this trend is not transferrable to Al(**1**)Me which too contains a methyl group on the amine centre, but produces PLA with a slight isotactic bias. This may be due to the steric bulk present from the $^{t}$Bu substituents on both phenoxy rings, as when the amine substituent is a more bulky phenyl ring, the products are of an isotactic nature, entries 2, 4, 6 and 8 in Table 3.04 (Figure 3.16).

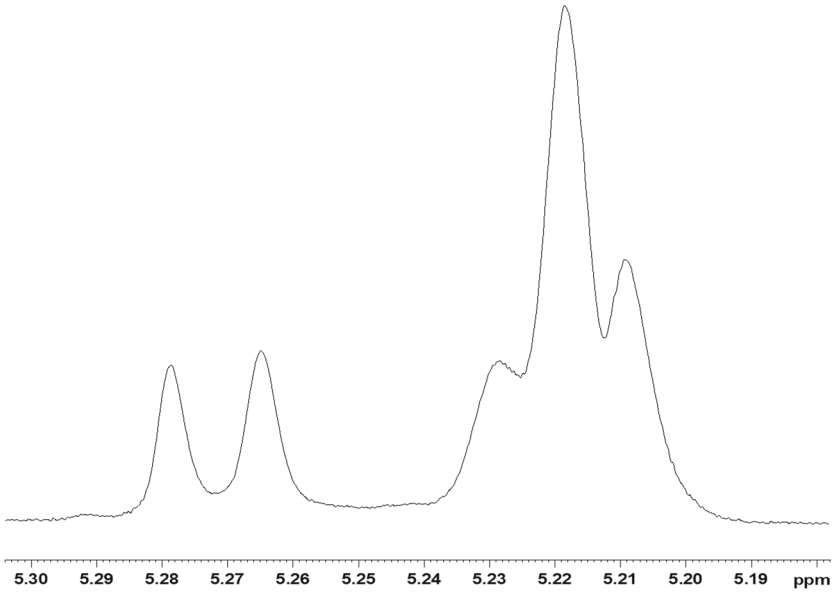


**Figure 4.14**: $^{1}$H homonuclear decoupled NMR spectrum of the product obtained *via* Al(**2**)Me at 80 °C for 24 hours in toluene with $P_r$ = 0.43– entry 2, Table 4.04.

The polymerisations are well controlled with narrow PDI values observed from GPC analysis (Figure 4.15) for all initiators with the exception of Al(**5**)Me which gave a PDI value of 1.65 (entry 5, Table 4.04).

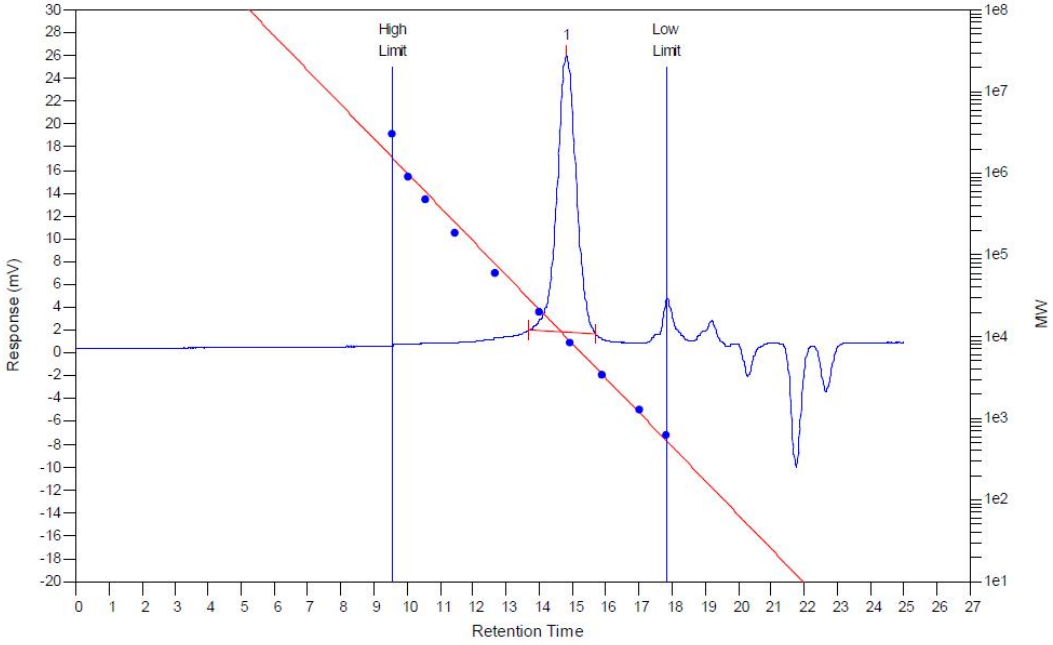


**Figure 4.15**: GPC spectrum of the product obtained from the ROP of *rac*-LA *via* Al(**1**)Me – entry 1, Table 4.04.

From Table 4.04 it can be seen that for some initiators, the reactivity after 24 hours was low, only achieving 32 % conversion for Al(**1**)Me. Therefore, the polymerisation reactions were repeated for a reaction time of 72 hours to achieve higher conversions – Table 4.05.

| Entry | Initiator | Conversion[a] (%) | $M_n$[b] | $M_w$[b] | $M_n$ (theo.) | PDI[b] | $P_r$[c] |
|---|---|---|---|---|---|---|---|
| **1** | Al(**1**)Me | 73 | 11900 | 12500 | 10650 | 1.05 | 0.39 |
| **2** | Al(**2**)Me | 97 | 8100 | 8700 | 14100 | 1.08 | 0.43 |
| **3** | Al(**3**)Me | 98 | 4950 | 5350 | 14250 | 1.08 | - [d] |
| **4** | Al(**4**)Me | 86 | 6600 | 7050 | 12500 | 1.07 | 0.74 |
| **5** | Al(**5**)Me | 99 | 7550 | 12700 | 14400 | 1.68 | 0.41 |
| **6** | Al(**6**)Me | 98 | 14950 | 23000 | 14250 | 1.54 | 0.46 |
| **7** | Al(**7**)Me | 97 | 16150 | 18500 | 14100 | 1.14 | 0.66 |
| **8** | Al(**8**)Me | 99 | 23000 | 28000 | 14400 | 1.22 | 0.48 |

**Table 4.05**: ROP results for Al(**1-8**)Me in toluene at 80 °C for 72 hours. 0.7 g of *rac*-LA, [LA]:[benzyl alcohol]:[initiator] = 100:1:1. [a] conversion as determined *via* $^1$H NMR, [b] determined from GPC (in THF) referenced to polystyrene, [c] calculated from the $^1$H homonuclear decoupled NMR ($CDCl_3$) analysis, [d] $P_r$ value not obtained.

Analogous to the polymerisations carried out at 80 °C for 24 hours in Table 4.04, one equivalent of benzyl alcohol is added to generate the alkoxide initiator *in situ*. After 72 hours the polymerisation *via* Al(**3**)Me showed higher conversion to PLA. However, the product obtained was of low molecular weight and therefore it was not possible to obtain a $P_r$ value for this sample. Again it can be seen that the initiators containing a methyl substituent on the amine nitrogen centre, with the exception of Al(**1**)Me, all afforded PLA with a heterotactic enrichment – entries 3, 5 and 7. An increase in the degree of heterotacticity can be seen from the *sis* peak in the $^1$H homonuclear decoupled NMR for reactions with a longer reaction time of 72 hours, with $P_r$ values around 0.7 compared to $P_r$ values of around 0.6 for a reaction time of 24 hours. All other initiators produce PLA with $P_r$ values similar to those obtained in Table 4.04 for a reaction time of 24 hours, with the exception of Al(**1**)Me which showed an increase in the degree of stereocontrol achieving a $P_r$ value = 0.39 (Figure 4.16).

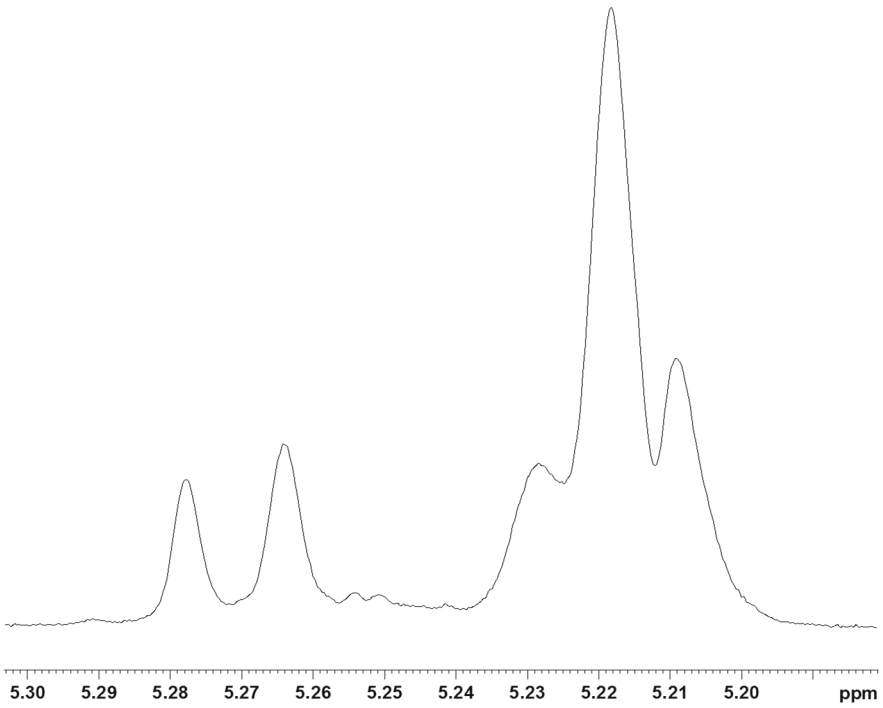


**Figure 4.16**: $^1$H homonuclear decoupled NMR spectrum of the product obtained *via* Al(**1**)Me at 80 °C for 72 hours in toluene with $P_r$ = 0.39 – entry 1, Table 4.05.

Again all polymerisations occur with a good degree of control, with the exception of Al(**5**)Me which showed the highest polydispersity value of 1.68. MALDI-ToF mass spectrometry analysis of the polymer produced *via* Al(**3**)Me

after 72 hours indicated the presence of the benzyl alcohol end group suggesting a coordination and insertion mechanism is occurring.

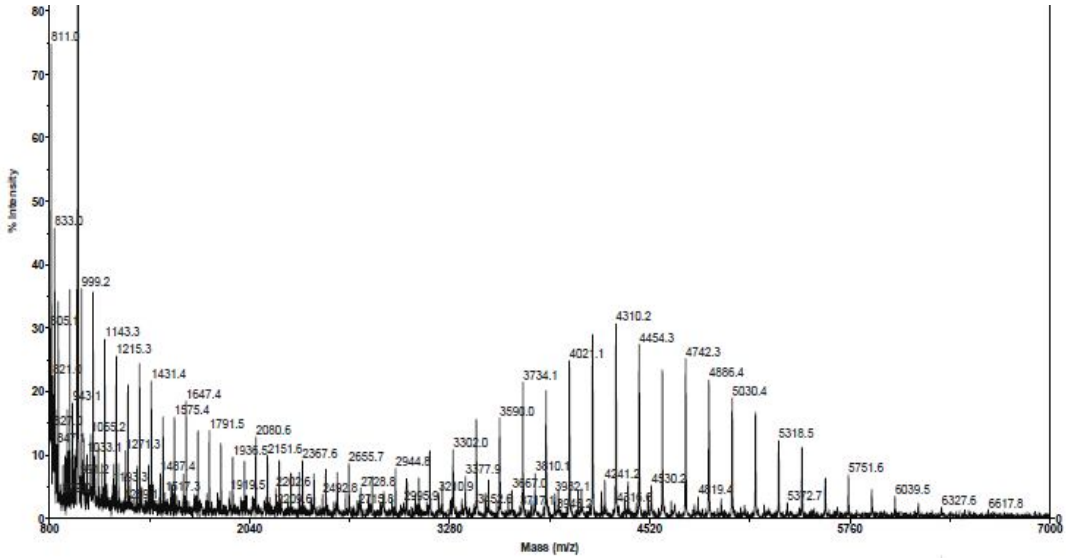


**Figure 4.17**: MALDI-ToF mass spectrum of PLA sample prepared *via* Al(**3**)Me after 72 hours in toluene at 80 °C – entry 3, Table 4.05.

Figure 4.17 shows a polymer weight curve distribution, and it can be observed that although there is more than one distribution curve present, the principle distribution shows a difference of 144 $gmol^{-1}$ indicating a difference of one lactide unit and hence little transesterification is occurring in the reaction.

### 4.4.2 Solution Polymerisation at 100 °C

The ROP of *rac*-LA was also investigated at 100 °C for 24 hours and 72 hours. In an analogous manner, one equivalent of benzyl alcohol was added to the polymerisation to generate the active initiator *in situ*.

| Entry | Initiator | Conversion[a] (%) | $M_n$[b] | $M_w$[b] | $M_n$ (theo.) | PDI[b] | $P_r$[c] |
|---|---|---|---|---|---|---|---|
| **1** | Al(**1**)Me | 72 | 23900 | 28750 | 14400 | 1.20 | 0.40 |
| **2** | Al(**2**)Me | 99 | 12050 | 15250 | 14400 | 1.27 | 0.46 |
| **3** | Al(**3**)Me | 54 | 4800 | 5100 | 7900 | 1.06 | - [d] |
| **4** | Al(**4**)Me | 99 | 7700 | 8350 | 14400 | 1.09 | 0.66 |
| **5** | Al(**5**)Me | 98 | 7400 | 12050 | 14250 | 1.62 | 0.41 |
| **6** | Al(**6**)Me | 89 | 14650 | 22400 | 12950 | 1.53 | 0.46 |
| **7** | Al(**7**)Me | 97 | 7600 | 9300 | 14100 | 1.23 | 0.59 |
| **8** | Al(**8**)Me | 98 | 24150 | 29150 | 14250 | 1.21 | 0.52 |

**Table 4.06**: ROP results for Al(**1-8**)Me in toluene at 100 °C for 24 hours. 0.7 g of *rac*-LA, [LA]:[benzyl alcohol]:[initiator] = 100:1:1. [a] conversion as determined *via* $^1$H NMR, [b] determined from GPC (in THF) referenced to polystyrene, [c] calculated from the $^1$H homonuclear decoupled NMR ($CDCl_3$) analysis, [d] $P_r$ value not obtained.

The results shown in Table 4.06 are comparable with those achieved for the ROP of *rac*-LA at 80 °C for 24 hours (Table 4.04), achieving greater than 72 % conversion for all initiators except Al(**3**)Me. The correlation between measured and theoretical molecular weights at 100 °C (Table 4.06) is not as good as that observed at 80 °C (Table 4.04). The polydispersity indices in general are higher than at 80 °C, suggesting that at the higher temperature of 100 °C the polymerisations are less controlled. For example, Al(**1**)Me at 80 °C gives a PDI value of 1.08 (entry 1, Table 4.04) compared to 1.20 at 100 °C (entry 1, Table 4.06).

All initiators at 100 °C still show the same trends in stereocontrol with those initiators containing a phenyl substituent on the amine nitrogen centre producing isotactically enriched PLA with the exception of Al(**8**)Me which gave atactic PLA. The extent of isotactic enrichment occurs to a lesser extent at 100 °C, suggesting a decrease in the stereocontrol at an elevated temperature. Al(**1**)Me although not containing a phenyl substituent on the amine nitrogen centre, again produces moderately isotactic PLA after 24 hours to a higher degree at 100 °C than at 80 °C. Those initiators containing a methyl substituent on the amine nitrogen centre all produce PLA with a heterotactic bias at 100 °C (entries 3, 5 and 7 in Table 4.06) analogous to the results achieved at 80 °C.

Analogous to the polymerisations at 80 °C the initiators are seen to produce PLA *via* a coordination and insertion mechanism from analysis of MALDI-ToF mass spectrometry which indicates the presence of a benzyl alcohol end group. The MALDI-ToF mass spectrum for the polymer obtain in entry 3, Table 4.06 also demonstrates that very little transesterification is occurring in the polymerisation at 100 °C after 24 hours *via* Al(**3**)Me with a repeating unit of the polymer being 144 $gmol^{-1}$.

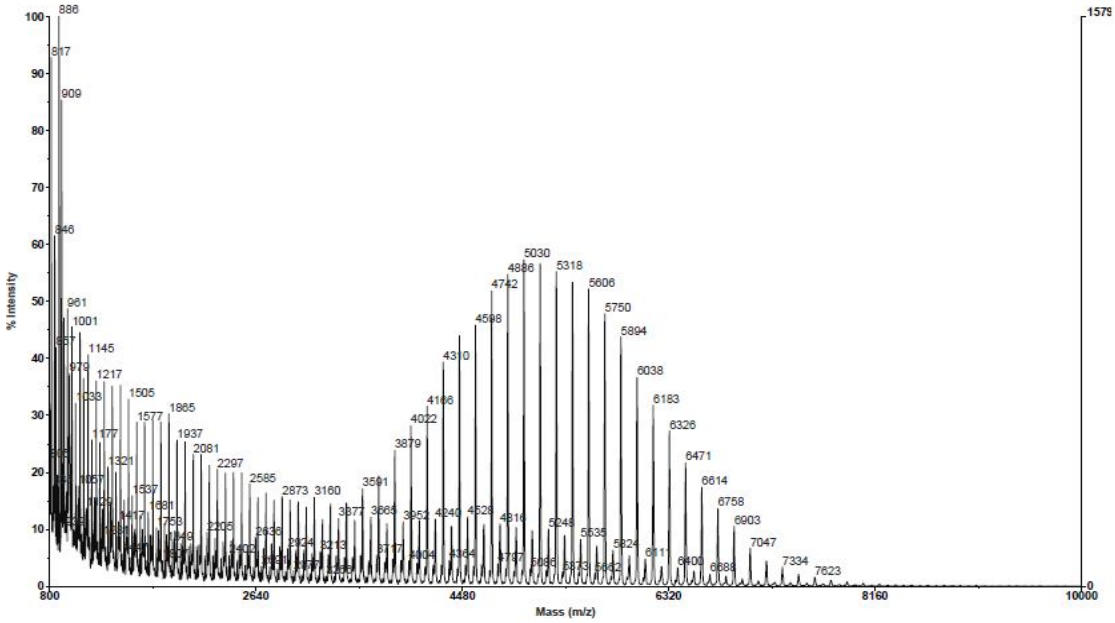


**Figure 4.18**: MALDI-ToF mass spectrum of PLA sample prepared *via* Al(**3**)Me after 24 hours in toluene at 100 °C – entry 3, Table 4.06.

For completeness the reactions in Table 4.06 were repeated for a prolonged reaction time of 72 hours to try and improve the degree of stereocontrol occurring as previously observed for the reactions at 80 °C (Section 4.4.1).

| Entry | Initiator | Conversion[a] (%) | $M_n$[b] | $M_w$[b] | $M_n$ (theo.) | PDI[b] | $P_r$[c] |
|---|---|---|---|---|---|---|---|
| **1** | Al(**1**)Me | 82 | 5600 | 6250 | 11950 | 1.12 | 0.40 |
| **2** | Al(**2**)Me | 99 | 10100 | 11200 | 14400 | 1.11 | 0.44 |
| **3** | Al(**3**)Me | 80 | 8700 | 9350 | 11650 | 1.07 | 0.68 |
| **4** | Al(**4**)Me | 98 | 10450 | 13400 | 14250 | 1.28 | 0.66 |
| **5** | Al(**5**)Me | 97 | 6750 | 10300 | 14100 | 1.53 | 0.42 |
| **6** | Al(**6**)Me | 98 | 12650 | 17450 | 14250 | 1.38 | 0.44 |
| **7** | Al(**7**)Me | 98 | 11550 | 16700 | 14250 | 1.44 | 0.57 |
| **8** | Al(**8**)Me | 99 | 16600 | 28400 | 14400 | 1.71 | 0.46 |

**Table 4.07**: ROP results for Al(**1-8**)Me in toluene at 100 °C for 72 hours. 0.7 g of *rac*-LA, [LA]:[benzyl alcohol]:[initiator] = 100;1:1. [a] conversion as determined *via* $^1$H NMR, [b] determined from GPC (in THF) referenced to polystyrene, [c] calculated from the $^1$H homonuclear decoupled NMR ($CDCl_3$) analysis.

The molecular weights obtained at 100 °C after 72 hours have in general a good correlation with the theoretical weights, albeit the $M_n$ observed when Al(**1**)Me and Al(**5**)Me are the initiators is lower than expected. With the exception of Al(**8**)Me, the polymerisations in Table 4.07 occur with the same degree of control as those reactions after 24 hours. There is very little, if any increase in stereocontrol observed when the polymerisations are repeated for a prolonged length of time, which is in contrast to that seen for the reactions at 80 °C which demonstrated an increase in isotacticity for the Al(**1**)Me.

## 4.5 Kinetic Studies

Kinetic studies for initiators Al(**1**)Me, Al(**3**)Me and Al(**4**)Me were carried out at 80 °C and $k_{app}$ values obtained for the ROP of *L*-LA, *D*-LA and *rac*-LA. It was hypothesised that this would aid the understanding of the polymerisation process. All kinetic studies for these initiators were performed in a stock solution of benzyl alcohol and $C_6D_5CD_3$ to provide one equivalent of the co-initiator to generate the alkoxide *in situ*. A spectrum was recorded every 15 minutes over a period of 1400 minutes. A plot of $\ln\{[LA]_o/[LA]_t\}$ *vs* time was drawn and $k_{app}$ values for each monomer with initiators Al(**1**/**3**/**4**)Me were determined.

### 4.5.1 Investigation of Initiator Al(1)Me

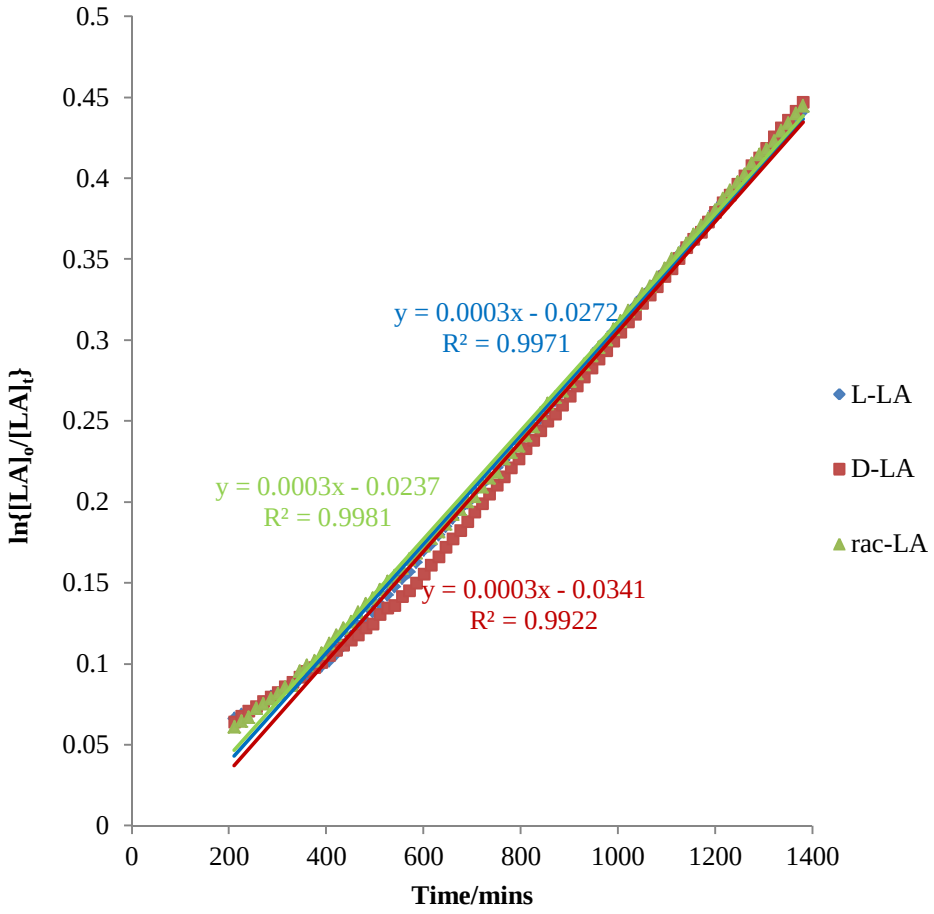


**Figure 4.19**: Semi-logarithmic plots for *L*-LA, *D*-LA and *rac*-LA *via* Al(**1**)Me at 80 °C in $C_6D_5CD_3$.

| Monomer | $k_{app}$ ( × $10^{-5}$ $min^{-1}$) | $R^2$ |
|---|---|---|
| ***D*-LA** | 34.0 | 0.9922 |
| ***L*-LA** | 34.0 | 0.9971 |
| ***rac*-LA** | 33.5 | 0.9981 |

**Table 4.09**: $k_{app}$ values for all monomers *via* Al(**1**)Me

It can be seen from Figure 4.19 that the $k_{app}$ values obtained for all three monomers (*L*-LA, *D*-LA and *rac*-LA) are comparable and hence explains why at 80 °C after 24 hours atactic PLA is obtained from the ROP of *rac*-LA – Entry 1, Table 4.04. The $k_{app}$ values shown in Figure 4.19 and Table 4.09 are an order of magnitude slower than the $k_{app}$ values reported by Gibson *et al.* for analogous

Salan aluminium complexes for the ROP of *rac*-LA (Figure 1.28, Chapter 1).[2] Such Salan complexes contain H, Me or Cl substituents on the phenoxy rings and a methyl group or $CH_2Ph$ on the amine nitrogen and were reported to give $k_{app}$ values between 15.2 × $10^{-4}$ $min^{-1}$ and 109.2 × $10^{-4}$ $min^{-1}$ when carried out at 70 °C in toluene.[2] However, an analogous complex where $^{t}$Bu substituents were present on the phenoxy rings and a benzyl group on the amine substituent demonstrated a comparable rate to the Al(**1**)Me with a $k_{app}$ = 20.4 × $10^{-5}$ $min^{-1}$.[2]

### 4.5.2 Investigation of Initiator Al(3)Me

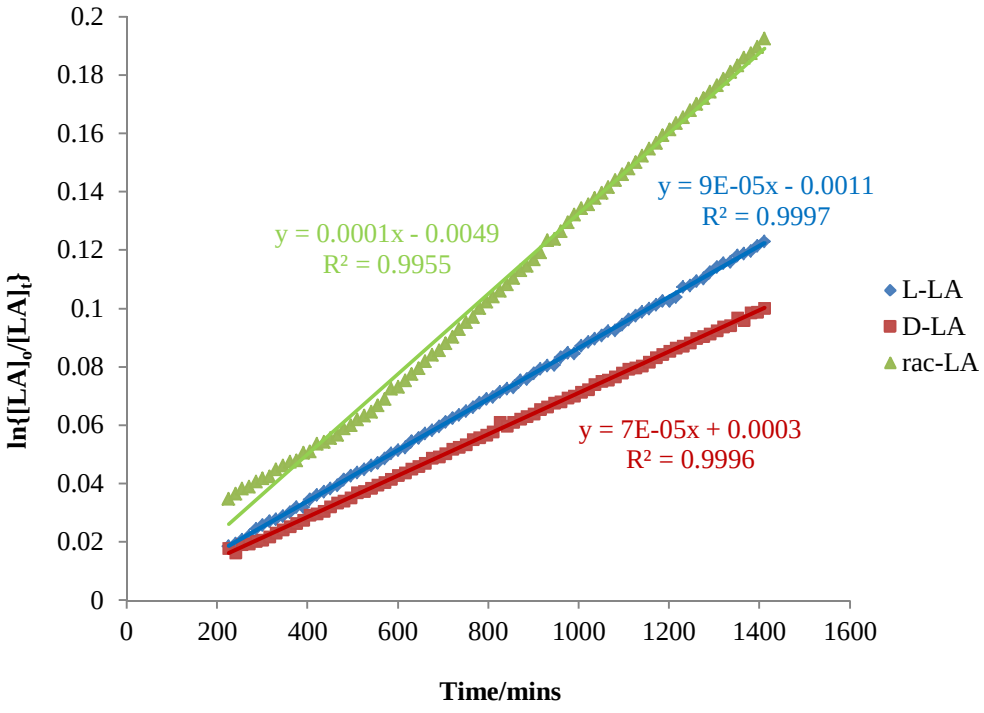


**Figure 4.20**: Semi-logarithmic plots for *L*-LA, *D*-LA and *rac*-LA *via* Al(**3**)Me at 80 °C in $C_6D_5CD_3$.

| Monomer | $k_{app}$ ( × $10^{-5}$ $min^{-1}$) | $R^2$ |
|---|---|---|
| ***D*-LA** | 7.09 | 0.9996 |
| ***L*-LA** | 8.77 | 0.9997 |
| ***rac*-LA** | 13.8 | 0.9955 |

**Table 4.10**: $k_{app}$ values for all monomers *via* Al(**3**)Me

Figure 4.20 shows a difference in apparent rate constants between the different monomers such that Al(**3**)Me polymerises *rac*-LA at a faster rate than

*L*-LA which is slightly faster than *D*-LA. This means that it is preferable to insert a monomer of a different stereochemistry to that previously inserted into the growing polymer chain than it is to insert a monomer of the same stereochemistry as that previously inserted. The significance of this deviation between *rac*-LA and *D* or *L*-LA, accounts for the heterotacticity observed in the polymerisations at 80 °C in toluene. Furthermore, the $k_{app}$ values obtained for Al(**3**)Me are lower than those observed for Al(**1**)Me which is in agreement with the lower conversions observed with Al(**3**)Me than Al(**1**)Me for the ROP of *rac*-LA – entries 1 and 3, Table 4.05.

### 4.5.3 Investigation of Initiator Al(4)Me

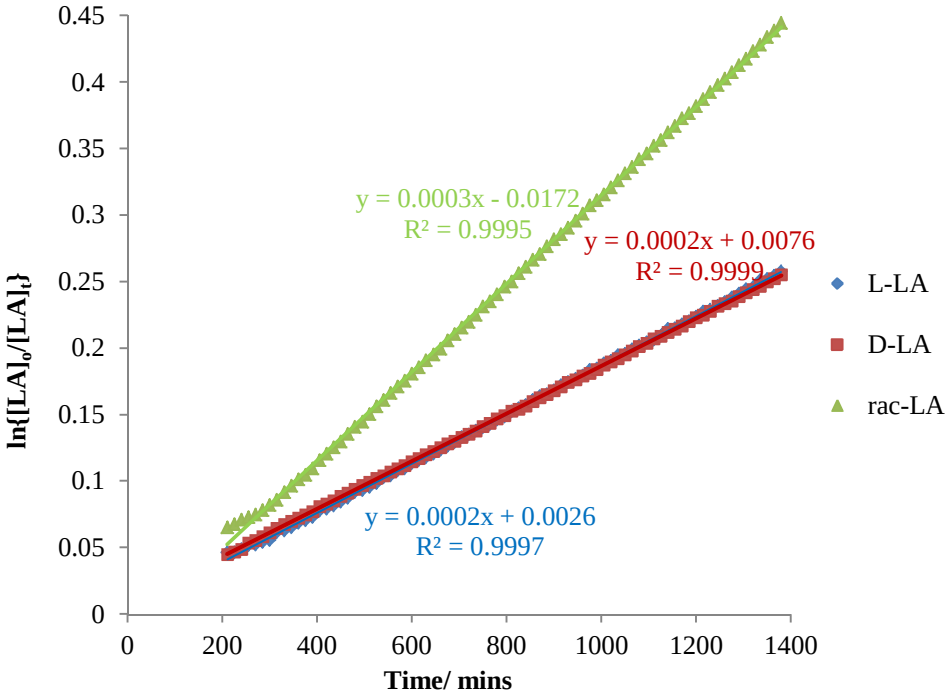


**Figure 4.21**: Semi-logarithmic plots for *L*-LA, *D*-LA and *rac*-LA *via* Al(**4**)Me at 80 °C in $C_6D_5CD_3$.

| Monomer | $k_{app}$ ( $\times 10^{-5}$ $min^{-1}$) | $R^2$ |
|---|---|---|
| ***D*-LA** | 17.9 | 0.9999 |
| ***L*-LA** | 18.4 | 0.9997 |
| ***rac*-LA** | 33.2 | 0.9995 |

**Table 4.11**: $k_{app}$ values for all monomers *via* Al(**4**)Me

Analogous to that observed in Section 4.5.2 for Al(**3**)Me, the $k_{app}$ values obtained when the initiator is Al(**4**)Me shows a discrepancy in the rates between the different forms of the monomer. It can be seen that the $k_{app}$ obtained for the ROP of *rac*-LA is nearly twice as fast as that observed for the ROP of either *D*-LA or *L*-LA. Consistent with this observation is the production of heterotactically enriched PLA for the ROP of *rac*-LA in toluene at 80 °C with $P_r$ = 0.60 after 24 hours (entry 4, Table 4.04) and $P_r$ = 0.74 after 72 hours (entry 4, Table 4.05). The ROP of *rac*-LA is therefore exhibiting a chain-end control mechanism with preference for the next approaching monomer to have a different stereochemistry to that of the polymer chain end. The $k_{app}$ value obtained for *rac*-LA *via* Al(**4**)Me is comparable with that reported for Al(**1**)Me, with the rate recorded for *D*-LA and *L*-LA *via* Al(**4**)Me being approximately 50 % slower.

## 4.6 Concluding Remarks

The complexes reported in this chapter are seen to be active for the ROP of *rac*-LA in toluene at 80 °C and 100 °C. Higher polydispersity indices are obtained at the elevated temperature of 100 °C than at 80 °C. A reaction time of 24 hours, and in some cases, for example Al(**1**)Me, 72 hours is required to achieve high conversion to PLA. At both temperatures, the polymerisations are seen to proceed *via* a coordination and insertion mechanism with little transesterification occurring. The initiators containing a phenyl substituent on the amine nitrogen centre, and Al(**1**)Me produce isotactically enriched PLA. However, the initiators containing a methyl substituent on the amine nitrogen centre are seen to produce PLA with a slight heterotactic bias. This preference can be emphasised by comparison of the $k_{app}$ values for *L*-LA, *D*-LA and *rac*-LA *via* such initiators (Al(**3**/**4**)Me). It has been shown that such initiators give a higher $k_{app}$ value for the ROP of *rac*-LA than the other two monomers and hence a chain end control mechanism is occurring. Varying the substituents on the phenoxy rings, showed slight differences in the stereocontrol for the ROP of *rac*-LA, however to a lesser extent than that observed by Gibson *et al.* for analogous Salan complexes.[2]

1. N. Spassky, M. Wisniewski, C. Pluta and A. LeBorgne, *Macromol. Chem. Phys.*, 1996, **197**, 2627-2637.
2. P. Hormnirun, E. L. Marshall, V. C. Gibson, A. J. P. White and D. J. Williams, *J. Am. Chem. Soc.*, 2004, **126**, 2688-2689.
3. Z. Y. Zhong, P. J. Dijkstra and J. Feijen, *Angew. Chem., Int. Ed. Engl.*, 2002, **41**, 4510-4513.
4. Z. Y. Zhong, P. J. Dijkstra and J. Feijen, *J. Am. Chem. Soc.*, 2003, **125**, 11291-11298.
5. J. Fujisaki, K. Matsumoto, K. Matsumoto and T. Katsuki, *J. Am. Chem. Soc.*, 2011, **133**, 56-61.
6. K. Matsumoto, T. Yamaguchi and T. Katsuki, *Chem. Commun.*, 2008, 1704-1706.
7. K. Matsumoto, T. Yamaguchi and T. Katsuki, *Heterocycles*, 2008, **76**, 191-196.
8. T. Yamaguchi, K. Matsumoto, B. Saito and T. Katsuki, *Angew. Chem., Int. Ed. Engl.*, 2007, **46**, 4729-4731.
9. K. Matsumoto, T. Yamaguchi, J. Fujisaki, B. Saito and T. Katsuki, *Chem. Asian J.*, 2008, **3**, 351-358.
10. K. Suyama, Y. Sakai, K. Matsumoto, B. Saito and T. Katsuki, *Angew. Chem., Int. Ed. Engl.*, 2010, **49**, 797-799.
11. B. Saito, H. Egami and T. Katsuki, *J. Am. Chem. Soc.*, 2007, **129**, 1978-1986.
12. B. Saito and T. Katsuki, *Angew. Chem., Int. Ed. Engl.*, 2005, **44**, 4600-4602.
13. H. Shitama and T. Katsuki, *Angew. Chem., Int. Ed. Engl.*, 2008, **47**, 2450-2453.
14. K. Suyama, K. Matsumoto and T. Katsuki, *Heterocycles*, 2009, **77**, 817-824.
15. A. W. Addison, T. N. Rao, J. Reedijk, J. Vanrijn and G. C. Verschoor, *J. Chem. Soc., Dalton Trans.,* 1984, 1349-1356.
16. D. J. Darensbourg and D. R. Billodeaux, *Inorg. Chem.*, 2005, **44**, 1433-1442.
17. N. C. Johnstone, E. S. Aazam, P. B. Hitchcock and J. R. Fulton, *J. Organomet. Chem.*, 2010, **695**, 170-176.

# Chapter 5

# Experimental

# 5 Experimental

## 5.1 General considerations

All manipulations involving metal complexes were carried out under an atmosphere of dry argon using standard Schlenk and glove-box techniques. Solvents were purified by a MBraun SPS solvent system. $Ti(O^iPr)_4$ (97 %, Aldrich) was purified by vacuum distillation prior to use, $Zr(O^iPr)_4{}^iPrOH$ (99.9 %, Aldrich), $Hf(O^iPr)_4{}^iPrOH$ (Alfa Aesar) and $AlMe_3$ (2.0 M solution in hexanes, Aldrich) were used without further purification. *rac*-LA (Aldrich) was recrystallised from dry toluene and sublimed twice prior to use in polymerisation reactions. All other starting materials were used as received and purchased from Aldrich, Acros Organics or Lancaster. Solution $^1H$ and $^{13}C\{^1H\}$ NMR experiments were performed at ambient temperature unless otherwise stated using a Bruker Advance-300, Bruker DRX400 or Bruker DRX500 MHz FT-NMR spectrometer with samples dissolved in $CDCl_3$, $C_4D_8O$, $C_6D_5CD_3$ or $C_6D_6$. $CDCl_3$ for analysis of metal complexes was distilled from calcium hydride prior to use. Coupling constants are given in Hertz. Wilmad 5 mm NMR tubes were used for ligand and polymer characterisation, while NMR tubes fitted with Young's taps were used for metal complexes and kinetic experiments. All chemical shifts are quoted as δ values in ppm relative to residual protio solvent resonances and all coupling constants are given in Hertz.

High resonance mass spectrometry of ligands was recorded on a micrOTOFQ electrospray quadrupole time-of-flight (ESI-TOF) spectrometer. The samples were dissolved in methanol and the spectra recorded in positive mode. MALDI-TOF Mass Spectra of polymeric products were recorded at the EPSRC National Mass Spectrometry Service Centre, Swansea, UK. The samples were solubilised in THF and analysed by positive MALDI in linear and reflectron modes using Dithranol matrix with LiCl as an additive to promote $[M^+Li]^+$ or NaOAc. GPC analyses were performed on a Polymer Laboratories PL-GPC 50 integrated system using a PLgel 5 μm MIXED-D 300 x 7.5 mm column at 35 °C, using THF as the solvent at a flow rate of 1.0 ML/min. The polydispersity

index (PDI) was determined from $M_w/M_n$, where $M_n$ is the number average molecular weight and $M_w$ is the weight average molecular weight. The polymers were referenced to 10 narrow molecular weight polystyrene standards with a range of $M_w$ 580 – 6035000 Da. The equations used to calculate $P_r$ are given by Coates *et al.*.[1] In the case where $P_r \neq 0.5$, the tacticity was also confirmed by $^{13}C\{^1H\}$ NMR ($CDCl_3$) by analysis of the methine region.

X-ray crystallographic analysis were carried out at 150 K on a Nonius Kappa or Nonius Helix X-ray diffractometer using Mo-Kα radiation (λ = 0.71073 Å) at the University of Bath. All structures were solved by direct methods and refined on all $F^2$ data using SHELXL-97 suite of programs, with hydrogen atoms included in idealized positions and refined using the riding model.[2] Elemental analysis was performed by Mr. A. K. Carver at the Department of Chemistry, University of Bath, on an Exeter Analytical CE440 Elemental Analyzer. It should be noted that elemental analysis is not reported for all complexes, and in the instances where it is reported, values are not as accurate to the theoretical values as anticipated. This is due to the elemental analysis not being performed under rigorous conditions and hence not precise. However, for such complexes, detailed analysis *via* $^1H$ and $^{13}C\{^1H\}$ NMR was carried out.

## 5.2 Synthetic Procedures

### 5.2.1 Synthesis of starting materials

**Preparation of 3,5-di-*tert*-butyl-2-hydroxybenzyl alcohol[3]:** To a solution of 2,4-di-*tert*-butylphenol (60 g, 0.29 mol) in methanol (80 ML), was added dropwise with stirring at room temperature a suspension of paraformaldehyde (9 g, 0.3 mol) and $LiOH.H_2O$ (1 g, 0.024 mol) in methanol (80 ML). The mixture was heated to reflux for 6 hours after which the solvent was removed by rotary evaporation and the orange-brown viscous residue was dissolved in hexane (40 ML). Upon filtration and storage of the solution at -20 $^oC$ for 2 days, a colourless precipitate of 3,5-di-*tert*-butyl-2-hydroxybenzyl alcohol formed (24.54 g, 35.9 %), when washed with copious amounts of hexane. **$^1H$ NMR** ($CDCl_3$) 1.29 (9H,

s, $C(CH_3)_3$), 1.44 (9H, s, $C(CH_3)_3$), 4.85 (2H, d J = 6Hz, $CH_2$), 6.90 (1H, d J = 2.5 Hz, Ar-H), 7.29 (1H, d J = 2.5 Hz, Ar-H), 7.57 (1H, s, OH). **$^{13}C\{^1H\}$ NMR** ($CDCl_3$) 29.7, 31.6, ($C(CH_3)_3$), 34.2, 34.9, ($C(CH_3)_3$), 65.9 ($CH_2$), 122.6, (Ar-CH), 124.0 (Ar-C), 124.1 (Ar-CH), 136.5, 141.6 (Ar-C), 153.1 (Ar-O).

**Preparation of 3,5-di-*tert*-butyl-2-hydroxybenzyl bromide[3]:** 3,5-di-*tert*-butyl-2-hydroxybenzyl alcohol (**1**) (24.54 g, 0.104 mol) was dissolved in chloroform (170 ML), to which a solution of $PBr_3$ (11.38 g, 3.95 ML, 0.04 mol) in chloroform (100 ML) was added dropwise. After stirring the solution for 1 hour at room temperature, water (100 ML) was added. The organic phase was quickly washed three times with water, dried over $MgSO_4$, filtered, and the solvent removed by rotary evaporation. Any residual solvent was removed under reduced pressure and the product isolated upon storage at -20 $^oC$ overnight (22.31 g, 71.7 %). **$^1H$ NMR** ($CDCl_3$) 1.35 (9H, s, $C(CH_3)_3$), 1.49 (9H, s, $C(CH_3)_3$), 4.63 (2H, s, $CH_2$), 7.16 (1H, d J = 2.5 Hz, Ar-H), 7.39 (1H, d J = 2.5 Hz). **$^{13}C\{^1H\}$ NMR** ($CDCl_3$) 30.2, 31.9, ($C(CH_3)_3$), 34.7, 35.3, ($C(CH_3)_3$), 71.7 ($CH_2$), 123.6 (Ar-C), 125.0, 126.0 (Ar-CH), 137.5, 143.3 (Ar-C), 152.0 (Ar-O).

**Preparation of trimethylene carbonate (TMC)[4]:** A solution of 1,3-propanediol (3.4 g, 3.22 ML, 0.0446 mol), ethyl chloroformate (28.50 g, 25.08 ML, 0.2623 mol) in THF (670 ML) was prepared. Triethylamine (28 g, 40.0 ML, 0.277 mol) was added dropwise with stirring. The mixture was stirred for 2 hours at room temperature, after which time, the solution was filtered and the solvent removed via rotary evaporation. The oily residue was recrystallised from diethyl ether (20 ML) and stored at -20 $^oC$ overnight, to yield a microcrystalline solid (1.76 g, 38.7 %). **$^1H$ NMR** ($CDCl_3$) 2.13 (2H, quintet J = 6 Hz, $CH_2$), 4.44 (4H, t J = 6 Hz, $CH_2$). **$^{13}C\{^1H\}$ NMR** ($CDCl_3$) 21.7 ($CH_2$), 67.9 ($CH_2$), 148.4 (CO).

### 5.2.2 Experimental for Chapter 2

**Preparation of 1$H_3$:** 2-hydroxyaniline (1 g, 9.16 mmol) was dissolved in THF (20 $cm^3$), to which a solution of 3,5-di-*tert*-butyl-2-hydroxybenzyl bromide (5.49 g, 18.35 mmol) in THF (20 $cm^3$) was added. Triethylamine (1.86 g, 3 ML, 18.35 mmol) was added and the mixture stirred at 80 $^oC$ for three hours. The white

precipitate was filtered and the solvent removed under reduced pressure. The product was isolated *via* flash chromatography to obtain the product (3.82 g, 76.0 %). **$^1$H NMR** ($CDCl_3$) 1.28 (18H, s, $C(CH_3)_3$), 1.40 (18H, s, $C(CH_3)_3$), 4.14 (4H, s, $CH_2$), 6.82 – 6.87 (2H, m, Ar-H), 6.97 (3H, d J = 2.5 Hz, Ar-H), 7.20 (2H, d J = 2.5 Hz, Ar-H) and 7.24 (1H, d J = 1.5 Hz, Ar-H). **$^{13}$C{$^1$H} NMR** ($CDCl_3$) 29.8, 31.6 ($C(CH_3)_3$), 34.1, 34.6 ($C(CH_3)_3$), 56.4 ($CH_2$), 114.7, 116.1, 120.6 (Ar-CH), 121.8 (Ar-C), 122.1, 123.5, 125.8 (Ar-CH), 135.5, 135.6, 141.7 (Ar-C), 151.3, 152.1 (Ar-O). **m/z** calc. $C_{36}H_{51}NO_3^+$ 546.3947, found 546.3985.

**Preparation of 2**$H_3$**:** 2-amino-*p*-cresol (1 g, 8.12 mmol) was dissolved in THF (20 $cm^3$), to which a solution of 3,5-di-*tert*-butyl-2-hydroxybenzyl bromide (4.84 g, 16.17 mmol) in THF (20 $cm^3$) was added. Triethylamine (1.64 g, 2.5 ML, 16.17 mmol) was added and the mixture stirred at 80 $^o$C for three hours. The white precipitate was filtered and the solvent removed under reduced pressure. The product was isolated *via* flash chromatography to obtain the product (3.46 g, 76.1 %). **$^1$H NMR** ($CDCl_3$) 1.29 (18H, s, $C(CH_3)_3$), 1.40 (18H, s, $C(CH_3)_3$), 2.23 (3H, s, $CH_3$), 4.13 (4H, s, $CH_2$), 6.71 – 6.75 (2H, m, Ar-H), 7.00 (2H, d J = 2.5 Hz, Ar-H), 7.04 (1H, d J = 1.5 Hz, Ar-H) and 7.20 (2H, d J = 2.5 Hz, Ar-H). **$^{13}$C{$^1$H} NMR** ($CDCl_3$) 20.7 ($CH_3$), 29.7, 31.6 ($C(CH_3)_3$), 34.1, 34.6 ($C(CH_3)_3$), 56.3 ($CH_2$), 114.6, 115.7, 120.7 (Ar-CH), 121.7 (Ar-C), 123.4, 125.8 (Ar-CH), 129.8, 135.2, 135.6, 141.5 (Ar-C), 148.6, 152.2 (Ar-O). **m/z calc**. $C_{37}H_{53}NO_3Na$ 582.3923, found 582.3913.

**Preparation of 3**$H_3$**:** 2-amino-4-tert-butylphenol (1 g, 8.12 mmol) was dissolved in THF (20 $cm^3$), to which a solution of 3,5-di-*tert*-butyl-2-hydroxybenzyl bromide (3.62 g, 12.10 mmol) in THF (20 $cm^3$) was added. Triethylamine (1.23 g, 2 ML, 12.10 mmol) was added and the mixture stirred at 80 $^o$C for three hours. The white precipitate was filtered and the solvent removed under reduced pressure. The product was isolated *via* flash chromatography to obtain the product (2.12 g, 58.3 %). **$^1$H NMR** ($CDCl_3$) 1.28 (9H, s, $C(CH_3)_3$), 1.30 (18H, s, $C(CH_3)_3$), 1.42 (18H, s, $C(CH_3)_3$), 4.19 (4H, s, $CH_2$), 6.79 (1H, d J = 8.5 Hz, Ar-H), 6.99 (1H, d J = 8.5 Hz, Ar-H), 7.03 (2H, d J = 1.5 Hz, Ar-H), 7.22 (2H, d J = 1.5 Hz, Ar-H), 7.31 (1H, s, Ar-H). **$^{13}$C{$^1$H} NMR** ($CDCl_3$) 29.8, 31.5, 31.6 ($C(CH_3)_3$), 34.1, 34.3, 34.6 ($C(CH_3)_3$), 56.4 ($CH_2$), 115.3, 119.2, (Ar-CH), 121.8

(Ar-C), 122.2, 123.5, 125.6 (Ar-CH), 134.7, 135.6, 141.5, 143.3 (Ar-C), 148.5, 152.2 (Ar-O). **m/z** calc. $C_{40}H_{59}NO_3^+$ = 602.4573, found 602.4620.

**Preparation of 4**$H_3$**:** 2-amino-4-chlorophenol (1 g, 6.97 mmol) was dissolved in THF (20 $cm^3$), to which a solution of 3,5-di-*tert*-butyl-2-hydroxybenzyl bromide (4.17 g, 13.94 mmol) in THF (20 $cm^3$) was added. Triethylamine (1.41 g, 2 ML, 13.94 mmol) was added and the mixture stirred at 80 $^oC$ for three hours. The white precipitate was filtered and the solvent removed under reduced pressure. The product was isolated *via* flash chromatography to obtain the product (2.30 g, 56.9 %). **$^1$H NMR** ($CDCl_3$) 1.30 (18H, s, $C(CH_3)_3$), 1.41 (18H, s, $C(CH_3)_3$), 4.12 (4H, s, $CH_2$), 6.76 (1H, d J = 8.5 Hz, Ar-H), 6.91 (1H, dd J = 8.5 Hz, 2.5 Hz, Ar-H), 7.01 (2H, d J = 2.5 Hz, Ar-H), 7.20 (1H, d J=2.5 Hz, Ar-H), 7.22 (2H, d J = 2.5 Hz, Ar-H). **$^{13}$C{$^1$H} NMR** ($CDCl_3$) 29.7, 31.6 ($C(CH_3)_3$), 34.1, 34.6 ($C(CH_3)_3$), 56.1 ($CH_2$), 116.8, (Ar-CH), 121.4 (Ar-C), 122.7, 123.6 (Ar-CH), 124.9 (Ar-C), 125.3, 126.0 (Ar-CH) 135.6, 136.6, 141.8 (Ar-C), 150.0, 152.0 (Ar-O). **m/z** calc. $C_{36}H_{50}NO_3Cl^+$ = 580.3557, found 580.3523.

**Preparation of Ti(1)(O$^i$Pr):** **1**$H_3$ (0.70 g, 1.28 mmol) was dissolved in toluene (20 $cm^3$) to which $Ti(O^iPr)_4$ (0.40 ML, 1.28 mmol) was added. This was stirred for 2 hours, after which time the solvent was removed *in-vacuo* and the product was recrystallised in hexane. After 1 day at – 20 ºC a crop of crystals were obtained which were filtered and dried. **$^1$H NMR** ($CDCl_3$) 1.30 (18H, s, $C(CH_3)_3$), 1.47 (18H, s, $C(CH_3)_3$), 1.56 (6H, d J = 6 Hz, $CH_3$ isopropoxide), 3.97 (2H, d J = 13.5 Hz, $CH_2$), 4.20 (2H, d J = 13.5 Hz, $CH_2$), 5.17 (1H, sept J = 6 Hz, CH isopropoxide), 6.61 (1H, dd J = 8 Hz, 1.5 Hz, Ar-H), 6.81 (1H, m, Ar-H), 7.01 (2H, d J = 2.5 Hz, Ar-H), 7.06 (1H, m, Ar-H), 7.22 (2H, d J = 2.5 Hz, Ar-H), 7.26 (1H, d J = 8 Hz, Ar-H). **$^{13}$C{$^1$H} NMR** ($CDCl_3$) 25.9 ($CH_3$ isopropoxide), 29.6, 31.6 ($C(CH_3)_3$), 34.3, 34.9 ($C(CH_3)_3$), 59.6 ($CH_2$) 80.3 (C-H isopropoxide), 115.4, 119.9, 121.5 (Ar-CH), 123.2 (Ar-C), 123.5, 124.6, 128.5 (Ar-CH), 135.2, 137.9, 142.7 (Ar-C), 159.1, 161.1 (Ar-O). **Anal**: Calc for $C_{39}H_{55}NO_4Ti$ C, 72.1; H, 8.53; N, 2.16. Found: C, 71.0; H, 8.41; N, 2.08.

**Preparation of Ti(2)(O$^i$Pr):** **2**$H_3$ (0.72 g, 1.28 mmol) was dissolved in toluene (20 $cm^3$) to which $Ti(O^iPr)_4$ (0.40 ML, 1.28 mmol) was added. This was stirred for 2 hours, after which time the solvent was removed *in-vacuo* and the product

was recrystallised in hexane. After 3 days at – 20 ºC a crop of crystals were obtained which were filtered and dried. **$^{1}$H NMR** ($CDCl_3$) 1.20 (18H, s, C(C*H*$_3$)$_3$), 1.42 (18H, s, C(C*H*$_3$)$_3$), 1.50 (6H, d J = 6 Hz, $CH_3$ isopropoxide), 2.21 (3H, s, $CH_3$), 3.91 (2H, d J = 13.5 Hz, $CH_2$), 4.15 (2H, d J = 13.5 Hz, $CH_2$), 5.11 (1H, sept J = 6 Hz, CH isopropoxide), 6.44 (1H, d J = 8.0 Hz, Ar-H), 6.80 (1H, m, Ar-H), 6.99 (3H, m, Ar-H), 7.17 (2H, d J = 2.5 Hz, Ar-H). **$^{13}$C{$^{1}$H} NMR** ($CDCl_3$) 20.7 ($CH_3$) 25.9 ($CH_3$ isopropoxide), 29.6, 31.6 (C(*C*H$_3$)$_3$), 34.3, 34.9 (*C*(CH$_3$)$_3$), 59.6 ($CH_2$), 80.2 (CH isopropoxide), 114.7, 122.3 (Ar-CH), 123.3 (Ar-C), 123.4, 124.7 (Ar-CH), 128.9 (Ar-CH), 129.2, 135.2, 137.5, 142.6 (Ar-C), 158.8, 159.1 (Ar-O). **Anal**: Calc for $C_{40}H_{57}NO_4Ti$ C, 72.4; H, 8.66; N, 2.11. Found: C, 70.9; H, 8.62; N, 2.26.

**Preparation of Ti(3)(O$^{i}$Pr):** **3**$H_3$ (0.77 g, 1.28 mmol) was dissolved in toluene (20 cm$^3$) to which Ti(O$^{i}$Pr)$_4$ (0.40 ML, 1.28 mmol) was added. This was stirred for 2 hours, after which time the solvent was removed *in-vacuo* and the product was recrystallised in hexane. After 7 days at – 20 ºC a crop of crystals were obtained which were filtered and dried. **$^{1}$H NMR** ($CDCl_3$) 1.25 (18H, s, C(C*H*$_3$)$_3$), 1.26 (9H, s, C(C*H*$_3$)$_3$), 1.43 (18H, s, C(C*H*$_3$)$_3$), 1.51 (6H, d J = 6 Hz, $CH_3$ isopropoxide), 3.91 (2H, d J = 13.5 Hz, $CH_2$), 4.16 (2H, d J = 13.5 Hz, $CH_2$), 5.12 (1H, sept J = 6 Hz, CH isopropoxide), 6.46 (1H, d J = 8.5 Hz, Ar-H), 6.98 – 7.03 (3H, m, Ar-H), 7.17 (2H, d J = 2.5 Hz, Ar-H), 7.23 (1H, d J = 2.5Hz, Ar-H). **$^{13}$C{$^{1}$H}NMR** ($CDCl_3$) 25.9 ($CH_3$ isopropoxide), 29.6, 31.6 (C(*C*H$_3$)$_3$), 34.3, 34.9 (*C*(CH$_3$)$_3$), 59.6 ($CH_2$), 80.2 (CH isopropoxide), 114.2, 118.5 (Ar-CH), 123.3 (Ar-C), 123.5, 124.5, 125.0 (Ar-CH), 135.3, 137.0, 142.5, 142.8 (Ar-C), 158.7, 159.2 (Ar-O). **Anal**: Calc for $C_{43}H_{63}NO_4Ti$ C, 73.17; H, 9.00; N, 1.98. Found: C, 72.7; H, 8.95; N, 2.16.

**Preparation of Ti(4)(O$^{i}$Pr):** **4**$H_3$ (0.74 g, 1.28 mmol) was dissolved in toluene (20 cm$^3$) to which Ti(O$^{i}$Pr)$_4$ (0.40 ML, 1.28 mmol) was added. This was stirred for 2 hours, after which time the solvent was removed *in-vacuo* and the product was recrystallised in hexane. After 2 days at – 20 ºC a crop of crystals were obtained which were filtered and dried. **$^{1}$H NMR** ($CDCl_3$) 1.28 (18H, s, C(C*H*$_3$)$_3$), 1.44 (18H, s, C(C*H*$_3$)$_3$), 1.52 (6H, d J = 6 Hz, $CH_3$ isopropoxide), 2.21 (3H, s, $CH_3$), 3.94 (2H, d J = 13.5 Hz, $CH_2$), 4.14 (2H, d J = 13.5 Hz, $CH_2$), 5.13 (1H,

sept J = 6 Hz, CH isopropoxide), 6.50 (1H, d J = 8.5 Hz, Ar-H), 6.96 – 7.01 (3H, m, Ar-H), 7.21 (3H, m, Ar-H). **$^{13}$C{$^{1}$H} NMR** ($CDCl_3$) 25.8 ($CH_3$ isopropoxide), 29.6, 31.6 (C($CH_3$)$_3$), 34.3, 34.9 ($C$($CH_3$)$_3$), 59.5 ($CH_2$), 80.7 (CH isopropoxide), 116.3, 122.4 (Ar-CH), 122.8 (Ar-C), 123.6, (Ar-CH), 124.2 (Ar-C), 124.7, 128.6 (Ar-CH) 135.2, 138.6, 143.0 (Ar-C), 159.1, 159.8 (Ar-O). **Anal**: Calc for $C_{39}H_{54}NO_4TiCl$ C, 68.47; H, 7.96; N, 2.05. Found: C, 61.7; H, 7.71; N, 1.95.

**Preparation of {Zr(1)(O$^{i}$Pr)}$_2$:** Zr(O$^{i}$Pr)$_2$$^{i}$PrOH (0.5 g, 1.5 mmol) was dissolved in toluene (20 cm$^3$) to which **1**$H_3$ (0.70 g, 1.28 mmol)) was added. This was stirred for 2 hours, after which time the solvent was removed *in-vacuo* and the product was recrystallised in hexane. After 1 day at – 20 ºC a crop of crystals were obtained which were filtered and dried. **$^{1}$H NMR** ($d_8$-THF) 1.19 (36H, s, C(C$H_3$)$_3$), 1.34 (12H, d J = 6 Hz, $CH_3$ isopropoxide), 1.47 (36H, s, C(C$H_3$)$_3$), 3.81 (4H, d J = 12.5 Hz, $CH_2$), 4.06 (4H, d J = 12.5 Hz, $CH_2$), 4.56 (2H, sept J = 6 Hz, CH isopropoxide), 6.31 (2H, dd J = 8.0 Hz, 1.5 Hz, Ar-H), 6.63 (2H, m, Ar-H), 6.82 (4H, m, Ar-H), 7.05 – 7.21 (4H, m, Ar-H), 7.46 (2H, dd J = 8.0 Hz, 1.5 Hz, Ar-H). **$^{13}$C{$^{1}$H} NMR** ($d_8$-THF) 28.1 ($CH_3$ isopropoxide), 30.6, 32.3 (C($C$H$_3$)$_3$), 34.8, 35.9 ($C$($CH_3$)$_3$), 62.2 ($CH_2$), 72.7 (CH isopropoxide), 118.2, 118.5, 123.9 (Ar-CH), 125.4 (Ar-C), 126.1, 126.5, 129.0 (Ar-CH), 136.6, 140.4, 140.8 (Ar-C), 158.6, 162.8 (Ar-O). **Anal**: Calc for $C_{39}H_{55}NO_4Zr$ C, 67.6; H, 8.00; N, 2.02. Found: C, 68.1; H, 7.85; N, 1.96.

**Preparation of {Zr(2)(O$^{i}$Pr)}$_2$:** Zr(O$^{i}$Pr)$_2$$^{i}$PrOH (0.5 g, 1.5 mmol) was dissolved in toluene (20 cm$^3$) to which **2**$H_3$ (0.72 g, 1.28 mmol)) was added. This was stirred for 2 hours, after which time the solvent was removed *in-vacuo* and the product was recrystallised in hexane. After 7 days at – 20 ºC a crop of crystals were obtained which were filtered and dried. **$^{1}$H NMR** ($d_8$-THF) 1.20 (36H, s, C(C$H_3$)$_3$), 1.37 (12H, d J = 6 Hz, $CH_3$ isopropoxide), 1.47 (36H, s, C(C$H_3$)$_3$), 2.21 (6H, s, $CH_3$), 3.81 (4H, d J = 12.5 Hz, $CH_2$), 4.04 (4H, d J = 12.5 Hz, $CH_2$), 4.56 (2H, sept J = 6 Hz, CH isopropoxide), 6.18 (2H, d J = 8.0 Hz, Ar-H), 6.63 (2H, dd J = 8.0 Hz, 2 Hz, Ar-H), 6.86 (4H, m, Ar-H), 7.13 (4H, m, Ar-H), 7.28 (2H, d J = 2H, Ar-H). **$^{13}$C{$^{1}$H} NMR** ($d_8$-THF) 20.9 ($CH_3$) 28.1 ($CH_3$ isopropoxide), 30.6, 32.3 (C($C$H$_3$)$_3$), 34.8, 35.9 ($C$($CH_3$)$_3$), 61.9 ($CH_2$), 72.6 (CH isopropoxide), 117.7, 123.8, 124.4 (Ar-CH), 125.4, 125.9 (Ar-C), 126.6 (Ar-CH), 127.4 (Ar-C),

129.5 (Ar-CH), 136.6, 140.3 (Ar-C), 158.6, 160.4 (Ar-O). **Anal:** Calc for $C_{40}H_{57}NO_4Zr$ C, 67.94; H, 8.12; N, 1.98. Found: C, 63.2; H, 8.08; N, 1.88.

**Preparation of {Zr(3)(O$^i$Pr)}$_2$:** $Zr(O^iPr)_2{}^iPrOH$ (0.5 g, 1.5 mmol) was dissolved in toluene (20 cm$^3$) to which **3**$H_3$ (0.77 g, 1.28 mmol)) was added. This was stirred for 2 hours, after which time the solvent was removed *in-vacuo* and the product was recrystallised in hexane. After 4 days at – 20 ºC a crop of crystals were obtained which were filtered and dried. **$^1$H NMR** ($d_8$-THF) 1.96 (36H, s, $C(CH_3)_3$), 1.29 (9H, s, $C(CH_3)_3$), 1.37 (12H, d J = 6 Hz, $CH_3$ isopropoxide), 1.47 (36H, s, $C(CH_3)_3$), 3.83 (4H, d J = 12.5 Hz, $CH_2$), 4.05 (4H, d J = 12.5 Hz, $CH_2$), 4.57 (2H, sept J = 6 Hz, CH isopropoxide), 6.24 (2H, d J = 8.5 Hz, Ar-H), 6.86 – 6.96 (6H, m, Ar-H), 7.14 (4H, m, Ar-H), 7.47 (2H, d J = 2H, Ar-H). **$^{13}$C{$^1$H} NMR** ($d_8$-THF) 28.1 ($CH_3$ isopropoxide), 30.5, 32.3 ($C(CH_3)_3$), 34.8, 35.8 ($C(CH_3)_3$), 62.1 ($CH_2$), 72.6 (CH isopropoxide), 117.2, 120.5, 123.9, 125.4 (Ar-CH), 125.7 (Ar-C), 126.4 (Ar-CH), 136.6, 139.7, 140.2, 141.2 (Ar-C), 158.6, 160.2 (Ar-O). **Anal**: Calc for $C_{43}H_{63}NO_4Zr$ C, 68.94; H, 8.48; N, 1.87. Found: C, 68.70; H, 9.04; N, 1.67.

**Preparation of {Zr(4)(O$^i$Pr)}$_2$:** $Zr(O^iPr)_2{}^iPrOH$ (0.5 g, 1.5 mmol) was dissolved in toluene (20 cm$^3$) to which **4**$H_3$ (0.74 g, 1.28 mmol)) was added. This was stirred for 2 hours, after which time the solvent was removed *in-vacuo* and the product was recrystallised in hexane. After 5 days at – 20 ºC a crop of crystals were obtained which were filtered and dried. **$^1$H NMR** ($d_8$-THF) 1.21 (36H, s, $C(CH_3)_3$), 1.30 (12H, s, $CH_3$ isopropoxide), 1.37 (12H, d J = 6 Hz, $CH_3$ isopropoxide) 1.47 (36H, s, $C(CH_3)_3$), 3.82 (4H, s, $CH_2$), 4.07 (4H, d J = 12.5 Hz, $CH_2$), 4.57 (2H, sept J = 6 Hz, CH isopropoxide), 6.26 (2H, d J = 8.5 Hz, Ar-H), 6.78 – 6.82 (2H, dd J = 8.5 Hz, 2.5 Hz, Ar-H), 6.89 – 7.00 (4H, m, Ar-H), 7.06 – 7.21 (6H, m, Ar-H), 7.54 (2H, d J = 2.5 Hz, Ar-H). **$^{13}$C{$^1$H} NMR** ($d_8$-THF) 28.0 ($CH_3$ isopropoxide), 30.5, 32.2 ($C(CH_3)_3$), 34.8, 35.8 ($C(CH_3)_3$), 61.9 ($CH_2$), 72.8 (CH isopropoxide), 119.0 (Ar-CH), 122.6 (Ar-C), 124.0, 124.8 (Ar-CH), 125.1 (Ar-C), 126.6, 129.0 (Ar-CH), 136.7, 140.6, 141.7 (Ar-C), 158.4, 161.7 (Ar-O). **Anal**: Calc for $C_{39}H_{54}NO_4ZrCl$ C, 64.39; H, 7.48; N, 1.93. Found: C, 62.4; H, 7.44; N, 1.77.

**Preparation of {Hf(1)(O$^i$Pr)}$_2$:** Hf(O$^i$Pr)$_4$.$^i$PrOH (0.5 g, 1.05 mmol) was dissolved in toluene (20 cm$^3$) to which **1**H$_3$ (0.57 g, 1.05 mmol) was added. The solution was stirred for 2 hours, after which time the solvent was removed *in-vacuo* and the product was recrystallised in hexane. After 4 days at -20 °C a crop of crystals were obtained which were filtered and dried. **$^1$H NMR** ($d_8$-THF) 1.20 (36H, s, C(*CH*$_3$)$_3$), 1.38 (12H, d J = 6 Hz, CH$_3$ isopropoxide), 1.48 (36H, s, C(*CH*$_3$)$_3$), 3.82 (4H, br s, CH$_2$), 4.12 (4H, d J = 12.5 Hz, CH$_2$), 4.67 (2H, sept J = 6 Hz, CH isopropoxide), 6.33 (2H, dd J = 1.5 Hz, 8.0 Hz, Ar-H), 6.62 (2H, td J = 1.5 Hz, 8.0 Hz, Ar-H), 6.84 (4H, td J = 1.5 Hz, 8.0 Hz, Ar-H), 7.13 – 7.19 (6H, m, Ar-H), 7.47 (2H, dd J = 1.5 Hz, 8.0 Hz, Ar-H). **$^{13}$C{$^1$H} NMR** ($d_8$-THF) 28.3 (CH$_3$ isopropoxide), 32.2 (C(*C*H$_3$)$_3$), 34.7, 35.7 (*C*(CH$_3$)$_3$), 60.0 (CH$_2$), 72.4 (CH isopropoxide), 118.2, 119.0, 123.9 (Ar-CH), 125.1 (Ar-C), 126.3, 129.1, 129.7 (Ar-CH), 137.1, 140.2, 140.4 (Ar-C), 132.8, 163.0 (Ar-O). **Anal**: Calc for C$_{39}$H$_{55}$NO$_4$Hf C, 60.03; H, 7.10; N, 1.79. Found: C, 60.7; H, 7.41; N, 1.69.

**Preparation of {Hf(2)(O$^i$Pr)}$_2$:** Hf(O$^i$Pr)$_4$.$^i$PrOH (0.5 g, 1.05 mmol) was dissolved in toluene (20 cm$^3$) to which **2**H$_3$ (0.59 g, 1.05 mmol) was added. The solution was stirred for 2 hours, after which time the solvent was removed *in-vacuo* and the product was recrystallised in hexane. After 7 days at -20 °C a crop of crystals were obtained which were filtered and dried. **$^1$H NMR** ($d_8$-THF) 1.20 (36H, s, C(*CH*$_3$)$_3$), 1.37 (12H, d J = 6 Hz, CH$_3$ isopropoxide), 1.48 (36H, s, C(*CH*$_3$)$_3$), 2.23 (3H, s, CH$_3$), 3.84 (4H, br s, CH$_2$), 4.10 (4H, d J = 12.5 Hz, CH$_2$), 4.66 (2H, sept J = 6.0 Hz, CH isopropoxide), 6.21 (2H, d J = 8.0 Hz, Ar-H), 6.62 (2H, dd J = 2.0 Hz, 8.5 Hz, Ar-H), 6.77 – 6.95 (4H, m, Ar-H), 7.14 – 7.23 (4H, m, Ar-H), 7.28 (2H, d J = 2.0 Hz, Ar-H). **$^{13}$C{$^1$H} NMR** ($d_8$-THF) 20.9 (CH$_3$), 29.4 (CH$_3$ isopropoxide), 32.3 (C(*C*H$_3$)$_3$), 34.8, 35.8 (*C*(CH$_3$)$_3$), 63.8 (CH$_2$), 72.4 (CH isopropoxide), 118.6, 123.9, 124.2 (Ar-CH), 125.3 (Ar-C), 126.4, 129.7 (Ar-CH), 137.2, 139.9, 140.2 (Ar-C), 158.6, 160.7 (Ar-O). **Anal**: Calc for C$_{40}$H$_{57}$NO$_4$Hf C, 60.48; H, 7.23; N, 1.76. Found: C, 59.4; H, 7.17; N, 1.74.

**Preparation of {Hf(3)(O$^i$Pr)}$_2$:** Hf(O$^i$Pr)$_4$.$^i$PrOH (0.5 g, 1.05 mmol) was dissolved in toluene (20 cm$^3$) to which **3**H$_3$ (0.63 g, 1.05 mmol) was added. The solution was stirred for 2 hours, after which time the solvent was removed *in-vacuo* and the product was recrystallised in hexane. After 2 days at -20 °C a crop

of crystals were obtained which were filtered and dried. **$^1$H NMR** ($d_8$-THF) 1.20 (18H, s, C($CH_3$)$_3$), 1.30 (36H, s, C($CH_3$)$_3$), 1.37 (12H, d J = 6 Hz, $CH_3$ isopropoxide), 1.47 (36H, s, C($CH_3$)$_3$), 3.90 (4H, br s, $CH_2$), 4.11 (4H, d J = 12.5 Hz, $CH_2$), 4.66 (2H, sept J = 6 Hz, CH isopropoxide), 6.26 (2H, d J = 8.5 Hz, Ar-H), 6.90 (4H, dd J = 2.0 Hz, 8.5 Hz, Ar-H), 7.04 – 7.29 (6H, m, Ar-H), 7.46 (2H, d J = 2.0 Hz, Ar-H). **$^{13}$C{$^1$H} NMR** ($d_8$-THF) 26.1 ($CH_3$ isopropoxide), 32.3, 32.4 (C($CH_3$)$_3$), 34.8, 35.0, 35.8 ($C$($CH_3$)$_3$), 64.6 ($CH_2$), 72.4 (CH isopropoxide), 118.2, 120.5, 124.0 (Ar-CH), 125.3 (Ar-C), 125.9, 126.3 (Ar-CH), 135.0, 137.2, 139.5, 141.1 (Ar-C), 158.7, 160.6 (Ar-O). **Anal**: Calc for $C_{43}H_{63}NO_4Hf$ C, 61.74; H, 7.59; N, 1.67. Found: C, 60.3; H, 7.83; N, 1.52.

**Preparation of {Hf(4)(O$^i$Pr)}$_2$:** Hf(O$^i$Pr)$_4$.$^i$PrOH (0.5 g, 1.05 mmol) was dissolved in toluene (20 cm$^3$) to which **5**$H_3$ (0.61 g, 1.05 mmol) was added. The solution was stirred for 2 hours, after which time the solvent was removed *in-vacuo* and the product was recrystallised in hexane. After 20 days at -20 °C a crop of crystals were obtained which were filtered and dried. **$^1$H NMR** ($d_8$-THF) 1.08 (12H, d J = 6 Hz, $CH_3$ isopropoxide), 1.21 (36H, s, C($CH_3$)$_3$), 1.37 (12H, d J = 6 Hz, $CH_3$ isopropoxide), 1.47 (36H, s, C($CH_3$)$_3$), 3.84 (4H, br s, $CH_2$), 4.11 (4H, dd J = 6.5 Hz, 12.5 Hz, $CH_2$), 4.65 (2H, sept J = 6 Hz, CH isopropoxide), 6.28 (2H, dd J = 2.5 Hz, 8.5 Hz, Ar-H), 6.84 (4H, td J = 2.5 Hz, 8.5 Hz, Ar-H), 7.15 – 7.23 (4H, m, Ar-H), 7.53 (2H, d J = 2.5 Hz, Ar-H), 7.59 (2H, d J = 2.5 Hz, Ar-H). **$^{13}$C{$^1$H} NMR** ($d_8$-THF) 26.1 ($CH_3$ isopropoxide), 28.2, 30.8 ($C$($CH_3$)$_3$), 32.2, 32.3 (C($CH_3$)$_3$), 34.8, 35.8 ($C$($CH_3$)$_3$), 61.9 ($CH_2$), 72.6 (CH isopropoxide), 119.9 (Ar-CH), 122.5, 123.0 (Ar-C), 124.1, 124.9 (Ar-CH), 125.0 (Ar-C), 126.5, 129.1 (Ar-CH), 137.4, 140.5 (Ar-C), 162.1, 162.3 (Ar-O). **Anal**: Calc for $C_{39}H_{54}NO_4HfCl$ C, 57.49; H, 6.68; N, 1.72. Found: C, 57.57; H, 6.77; N, 1.70.

### 5.2.3 Experimental for Chapter 3

**Preparation of 1**$H_2$**:** A solution of 3,5-di-*tert*-butyl-2-hydroxybenzaldehyde (3.228 g, 0.014 mol) and methylethylene diamine (1.02 g, 1.2 ML, 0.014 mol) in methanol (20 ML) was prepared. The solution was stirred until a clear solution was observed, and left to stand for 24 hours to yield a yellow oil which was collected and dried (2.68 g, 65.9 %). **$^1$H NMR** ($CDCl_3$) 1.31 (9H, s, C($CH_3$)$_3$), 1.45 (9H, s, C($CH_3$)$_3$), 2.47 (3H, s, $CH_3$), 2.92 (2H, t J = 6 Hz, $CH_2$), 3.73 (2H, t J

= 6 Hz, $CH_2$), 7.09 (1H, d J = 2.5 Hz, Ar-H), 7.39 (1H, d J = 2.5 Hz, Ar-H), 8.40 (1H, s, CH). **$^{13}C\{^1H\}$ NMR** ($CDCl_3$) 29.8, 31.8 ($C(CH_3)_3$), 34.4, 35.3 ($C(CH_3)_3$), 36.6 ($CH_3$), 52.2, 59.8 ($CH_2$), 118.1, (Ar-C), 126.3, 127.3 (Ar-CH), 137.0, 140.5 (Ar-C), 158.3 (Ar-O), 167.5 (CH). **m/z** calc. $C_{18}H_{31}N_2O$ = 291.2437, found 291.2267. The yellow oil (1 g, 3.44 mmol) was dissolved in THF (20 $cm^3$), to which a solution of 3,5-di-tert-2-hydroxybenzyl bromide (1.029 g, 3.44 mmol) in THF (20 $cm^3$) was added. Triethylamine (0.35 g, 0.48 ML, 3.44 mmol) was added and the mixture stirred at 80 $^oC$ for three hours. The white precipitate was filtered and the solvent removed under reduced pressure. The product was isolated *via* flash chromatography to obtain the product (1.33 g, 76.2 %). **$^1H$ NMR** ($CDCl_3$) 1.29 (9H, s, $C(CH_3)_3$), 1.32 (9H, s, $C(CH_3)_3$), 1.39 (9H, s, $C(CH_3)_3$), 1.46 (9H, s, $C(CH_3)_3$), 2.40 (3H, s, $CH_3$), 2.85 (2H, t J = 6.5 Hz, $CH_2$), 3.76 (2H, s, $CH_2$), 3.78 (2H, t J = 6.5 Hz, $CH_2$), 6.84 (1H, d J = 2.5 Hz, Ar-H), 7.09 (1H, d J = 2.5 Hz, Ar-H), 7.22 (1H, d J = 2.5 Hz, Ar-H), 7.40 (1H, d J = 2.5 Hz, Ar-H), 8.39 (1H, s, CH). **$^{13}C\{^1H\}$ NMR** ($CDCl_3$) 29.4, 29.4, 31.5, 31.7 ($C(CH_3)_3$), 34.1, 35.0 ($C(CH_3)_3$), 41.9 ($CH_3$), 57.1, 57.3, 62.2 ($CH_2$), 117.8, 120.9, (Ar-C), 122.9, 123.2, 125.9, 127.0 (Ar-CH), 135.6, 136.6, 140.1, 140.4 (Ar-C), 154.3, 158.0 (Ar-O), 167.3 (CH). **m/z** calc. $C_{33}H_{53}N_2O_2$ = 509.4107, found 509.4145.

**Preparation of 2$H_2$:** A solution of 3,5-di-*tert*-butyl-2-hydroxybenzaldehyde (3.228 g, 0.014 mol) and phenylethylene diamine (1.91 g, 1.83 ML, 0.014 mol) in methanol (20 ML) was prepared. The solution was stirred until a clear solution was observed, and left to stand for 24 hours to yield a yellow powder which was collected and dried. **$^1H$ NMR** ($CDCl_3$) 1.31 (9H, s, $C(CH_3)_3$), 1.46 (9H, s, $C(CH_3)_3$), 3.52 (2H, t J = 6 Hz, $CH_2$), 3.81 (2H, t J = 5.5 Hz, $CH_2$), 6.66 (2H, d J = 8 Hz, Ar-H), 6.73 (1H, t J = 7.5 Hz, Ar-H), 7.08 (1H, d J = 2.5 Hz, Ar-H), 7.19 (2H, t, J = 8 Hz, Ar-H), 7.40 (1H, d J = 2.5 Hz, Ar-H), 8.35 (1H, s, CH). **$^{13}C\{^1H\}$ NMR** ($CDCl_3$) 29.7, 31.8 ($C(CH_3)_3$), 34.4, 35.3 ($C(CH_3)_3$), 44.5, 58.7 ($CH_2$), 113.5, 118.0, 126.3, 127.5, 129.6 (Ar-CH), 137.0, 140.5, 147.9 (Ar-C), 158.3 (Ar-O), 168.0 (CH). **m/z** calc. $C_{23}H_{33}N_2O$ = 353.2593, found 353.2569. The yellow powder (1 g, 2.84 mmol) was dissolved in THF (20 $cm^3$), to which a solution of 3,5-di-tert-2-hydroxybenzyl bromide (0.85 g, 2.84 mmol) in THF (20 $cm^3$) was added. Triethylamine (0.29 g, 0.4 ML, 2.84 mmol) was added and the mixture stirred at 80 $^oC$ for three hours. The white precipitate was filtered and the solvent

removed under reduced pressure. The product was isolated *via* flash chromatography to obtain the product (0.96 g, 59.2 %). **$^{1}$H NMR** ($CDCl_3$) 1.19 (9H, s, $C(CH_3)_3$), 1.21 (9H, s, $C(CH_3)_3$), 1.32 (9H, s, $C(CH_3)_3$), 1.36 (9H, s, $C(CH_3)_3$), 3.42 (2H, t J = 6.5 Hz, $CH_2$), 3.58 (2H, t J = 6.5 Hz, $CH_2$), 4.32 (2H, s, CH2), 6.87 (1H, d J = 2.5 Hz, Ar-H), 6.90 (1H, d J = 2.5 Hz, Ar-H), 6.93 – 6.99 (1H, m, Ar-H), 7.09 – 7.16 (3H, m, Ar-H), 7.21 – 7.27 (2H, m, Ar-H), 7.29 (1H, d J =2.5 Hz, Ar-H), 8.07 (1H, s, CH). **$^{13}$C{$^{1}$H} NMR** ($CDCl_3$) 29.8, 30.0, 31.8, 32.0 ($C(CH_3)_3$), 34.4, 34.5, 35.2, 35.4 ($C(CH_3)_3$), 52.8, 56.9, 57.9 ($CH_2$), 118.1 (Ar-C), 121.0, (Ar-CH), 121.5 (Ar-C), 123.4, 123.7, 124.3, 126.2, 127.4, 129.7 (Ar-CH), 136.2, 137.0, 140.5, 141.7, 149.2 (Ar-C), 154.0, 158.3 (Ar-O), 167.9 (CH). **m/z** calc. $C_{38}H_{54}N_2O_2^+$ = 571.4264, found 571.4270.

**Preparation of 3**$H_2$**:** A solution of 2-hyrdroxy-3-methylbenzaldehyde (0.75 g, 0.66 ML, 5.51 mmol) and methylethylene diamine (0.41 g, 0.48 ML, 5.51 mol) in methanol (10 ML) was prepared. The solution was stirred until a clear solution was observed, and left to stand for 24 hours to yield a yellow oil which was collected and dried (0.83 g, 78.0 %). **$^{1}$H NMR** ($CDCl_3$) 2.21 (3H, s, $CH_3$), 2.39 (3H, s, $CH_3$), 2.83 (2H, t J = 5.5 Hz, $CH_2$), 3.64 (2H, t J = 5.5 Hz, $CH_2$), 6.72 (1H, t J = 7.5 Hz, Ar-H), 7.03 (1H, d J = 7.5 Hz, Ar-H), 7.11 (1H, d J = 7.0 Hz, Ar-H), 8.28 (1H, s, CH). **$^{13}$C{$^{1}$H} NMR** ($CDCl_3$) 15.6, 36.4 ($CH_3$), 51.9, 59.4 ($CH_2$), 117.9 (Ar-C), 118.2 (Ar-CH), 125.9 (Ar-C), 129.1, 133.3 (Ar-CH), 159.4 (Ar-O), 166.2 (CH). **m/z** calc. $C_{11}H_{17}N_2O$ = 193.1341, found 193.1352. The yellow oil (0.79 g, 4.08 mmol) was dissolved in THF (30 $cm^3$), to which a solution of 3,5-di-*tert*-2-hydroxybenzyl bromide (1.22 g, 4.08 mmol) in THF (30 $cm^3$) was added. Triethylamine (0.41 g, 0.57 ML, 4.08 mmol) was added and the mixture stirred at 80 $^{o}$C for three hours. The white precipitate was filtered and the solvent removed under reduced pressure. The product was isolated *via* flash chromatography to obtain the product (0.21 g, 13.0 %). **$^{1}$H NMR** ($CDCl_3$) 1.31 (9H, s, $C(CH_3)_3$), 1.40 (9H, s, $C(CH_3)_3$), 2.30 (3H, s, $CH_3$), 2.41 (3H, s, $CH_3$), 2.86 (2H, t J = 6.5 Hz, $CH_2$), 3.76 (2H, s, $CH_2$), 3.79 (2H, t J = 6.5 Hz, $CH_2$), 6.80 (1H, t J = 7.5 Hz, Ar-H), 6.85 (1H, d J = 2.5 Hz, Ar-H), 7.11 (1H, d J = 7.5 Hz, Ar-H), 7.20 (1H, d J = 7.5 Hz, Ar-H), 7.24 (1H, d J = 2.5 Hz, Ar-H), 8.37 (1H, s, CH). **$^{13}$C{$^{1}$H} NMR** ($CDCl_3$) 15.8 ($CH_3$), 29.9, 30.7 ($C(CH_3)_3$), 31.9, 32.0 ($C(CH_3)_3$), 34.5, 35.2 ($C(CH_3)_3$), 42.3 ($CH_3$), 57.3, 57.8, 62.6 ($CH_2$), 118.3 (Ar-C), 118.5 (Ar-CH),

121.3 (Ar-C), 123.3, 123.6 (Ar-CH), 126.2 (Ar-C), 129.4, 133.7 (Ar-CH), 136.0, 140.8 (Ar-C), 154.6, 159.6 (Ar-O), 166.8 (CH). **m/z** calc. $C_{26}H_{39}N_2O_2$ = 411.3012, found 411.2993.

**Preparation of 4**$H_2$**:** A solution of salicylaldehyde (2.74 g, 2.39 ML, 0.02 mol) and methylethylene diamine (1.66 g, 1.96 ML, 0.02 mol) in methanol (20 ML) was prepared. The solution was stirred until a clear solution was observed, and left to stand for 24 hours to yield a yellow oil which was collected and dried (3.34 g, 84.0 %). **$^1$H NMR** ($CDCl_3$) 2.36 (3H, s, $CH_3$), 2.81 (2H, s(br), $CH_2$), 3.62 (2H, s(br), $CH_2$), 6.76 – 6.87 (2H, m, Ar-H), 7.14 – 7.20 (2H, m, Ar-H), 8.28 (1H, s, CH). **$^{13}$C{$^1$H} NMR** ($CDCl_3$) 36.4 ($CH_3$), 51.9, 59.5 ($CH_2$), 117.0, 118.7, 131.4, 132.3 (Ar-CH), 138.7 (Ar-C), 161.4 (Ar-O), 166.0 (CH). **m/z** calc. $C_{10}H_{14}N_2O$ = 179.1184, found 179.1177. The yellow oil (2.58 g, 0.014 mol) was dissolved in THF (60 $cm^3$), to which a solution of 3,5-di-*tert*-2-hydroxybenzyl bromide (4.33 g, 0.014 mol) in THF (60 $cm^3$) was added. Triethylamine (1.46 g, 2.01 ML, 0.014 mol) was added and the mixture stirred at 80 $^oC$ for three hours. The white precipitate was filtered and the solvent removed under reduced pressure. The product was isolated *via* flash chromatography to obtain the product (3.20 g, 56.0 %). **$^1$H NMR** ($CDCl_3$) 1.31 (9H, s, $C(CH_3)_3$), 1.40 (9H, s, $C(CH_3)_3$), 2.40 (3H, s, $CH_3$), 3.74 – 3.82 (6H, m, $CH_2$), 6.85 (1H, d J = 2.5 Hz, Ar-H), 6.89 (1H, td J = 7 Hz, 1 Hz, Ar-H), 6.98 (1H, d J = 8 Hz, Ar-H), 7.23 – 7.25 (2H, m, Ar-H), 7.29 – 7.35 (1H, m, Ar-H), 8.38 (1H, s, CH). **$^{13}$C{$^1$H} NMR** ($CDCl_3$) 29.9, 32.0 ($C(CH_3)_3$), 34.4, 35.1 ($C(CH_3)_3$), 42.3 ($CH_3$), 57.3, 57.9, 62.5 ($CH_2$), 117.2, 118.9 (Ar-CH), 119.0, 121.2 (Ar-C), 122.3, 123.6, 131.7, 132.6 (Ar-CH), 135.9, 140.8 (Ar-C), 154.6, 161.3 (Ar-O), 166.6 (CH). **m/z** calc. $C_{25}H_{36}N_2O_2Na$ = 419.2674, found 419.2637.

**Preparation of Ti(1)(O$^i$Pr)$_2$:** **1**$H_2$ (0.6513 g, 1.28 mmol) was dissolved in toluene (20 $cm^3$) to which $Ti(O^iPr)_4$ (0.4 ML, 1.28 mmol) was added. This was stirred for 2 hours, after which time the solvent was removed *in-vacuo* and the product was recrystallised in hexane. After 5 days at – 20 ºC a crop of crystals were obtained which were filtered and dried. **$^1$H NMR** ($CDCl_3$) 0.91 (3H, d J = 6 Hz, $CH_3$ isopropoxide), 0.97 (3H, d J = 6 Hz, $CH_3$ isopropoxide), 1.10 (9H, s, $C(CH_3)_3$), 1.23 (3H, d J = 6 Hz, $CH_3$ isopropoxide), 1.27 (18H, s, $C(CH_3)_3$), 1.35

(3H, d J = 6 Hz, $CH_3$ isopropoxide),1.52 (9H, s, C(C*H*$_3$)$_3$), 2.08 – 2.87 (2H, m, $CH_2$), 3.02 (3H, s, $CH_3$), 3.26 – 3.38 (2H, m, $CH_2$), 4.38 (1H, sept J = 6 Hz, CH isopropoxide), 4.46 – 4.58 (2H, m, $CH_2$), 5.24 (1H, sept J = 6 Hz, CH isopropoxide), 6.88 (1H, d J = 2.5 Hz, Ar-H), 6.94 (1H, d J = 2.5 Hz, Ar-H), 7.14 (1H, d J = 2.5 Hz, Ar-H), 7.44 (1H, d J = 2.5 Hz, Ar-H), 7.92 (1H, s, CH). **$^{13}$C{$^1$H} NMR** ($CDCl_3$) 26.3, 26.4, 26.6, 26.9 ($CH_3$ isopropoxide), 29.9, 30.1, 31.8, 32.2 (C(*C*H$_3$)$_3$), 34.4, 35.0, 35.4, 35.7 (*C*(CH$_3$)$_3$), 52.3 ($CH_3$), 58.6, 58.9, 66.6 ($CH_2$), 75.1, 77.1 (CH isopropoxide), 122.3 (Ar-C), 123.5 (Ar-CH), 123.6 (Ar-C), 123.9 (Ar-CH), 127.9, 129.3 (Ar-CH), 136.5, 137.2, 137.9, 139.3 (Ar-C), 161.2, 161.6 (Ar-O), 163.0 (CH). **Anal:** Calc for $C_{39}H_{64}N_2O_4Ti$ C, 69.62, H 9.59, N 4.16. Found C 68.6, H 9.79, N 4.09.

**Preparation of Ti(2)(O$^i$Pr)$_2$: 2**$H_2$ (0.2191 g, 0.38 mmol) was dissolved in toluene (10 cm$^3$) to which Ti(O$^i$Pr)$_4$ (0.1 ML, 1.28 mmol) was added. This was stirred for 2 hours, after which time the solvent was removed *in-vacuo* and the product was recrystallised in hexane. After 5 days at – 20 ºC a crop of crystals were obtained which were filtered and dried. **$^1$H NMR** ($CDCl_3$) 0.30 – 0.71 (6H, br s, $CH_3$ isopropoxide), 1.20 (9H, s, C(C*H*$_3$)$_3$), 1.26 (6H, s, $CH_3$ isopropoxide), 1.28 (9H, s, C(C*H*$_3$)$_3$), 1.29 (9H, s, C(C*H*$_3$)$_3$), 1.52 (9H, s, C(C*H*$_3$)$_3$), 3.43 (2H, t J = 5 Hz, $CH_2$), 3.66 (2H, br s, $CH_2$), 3.88 (1H, sept J = 6 Hz, CH isopropoxide), 4.51 (1H, sept J = 6 Hz, CH isopropoxide), 5.13 (2H, br s, $CH_2$), 6.83 (1H, d J = 2.5 Hz, Ar-H), 6.98 (1H, d J = 2.5 Hz, Ar-H), 7.17 – 7.22 (2H, m, Ar-H), 7.40 (2H, t J = 8 Hz, Ar-H), 7.45 (1H, d J = 2.5 Hz, Ar-H), 7.92 (2H, d J = 8 Hz, Ar-H), 7.97 (1H, s, CH). **$^{13}$C{$^1$H} NMR** ($CDCl_3$) 26.9 ($CH_3$ isopropoxide), 30.0, 31.8, 32.2 (C(*C*H$_3$)$_3$), 34.4, 35.1, 35.7 (*C*(CH$_3$)$_3$), 53.1, 59.2, 69.2 ($CH_2$), 76.6 (CH isopropoxide), 122.1 (Ar-C), 123.5, 123.9, 124.3, 125.2, 127.6, 128.8, 129.3 (Ar-CH), 136.6, 137.4, 138.1, 139.5 (Ar-C) 154.4 (C-N), 160.9, 161.8 (Ar-O), 162.8 (CH). **Anal:** Calc for $C_{44}H_{66}N_2O_4Ti$ C, 71.91, H 9.05, N 3.81. Found C 70.5, H 8.92, N 3.66.

**Preparation of Ti(3)(O$^i$Pr)$_2$: 3**$H_2$ (0.4334 g, 1.07 mmol) was dissolved in toluene (20 cm$^3$) to which Ti(O$^i$Pr)$_4$ (0.3 ML, 1.07 mmol) was added. This was stirred for 2 hours, after which time the solvent was removed *in-vacuo* and the product was recrystallised in hexane. After 20 days at – 20 ºC a crop of crystals

were obtained which were filtered and dried. **$^1$H NMR** ($CDCl_3$) 0.99 (3H, d J = 6 Hz, $CH_3$ isopropoxide), 1.02 (3H, d J = 6 Hz, $CH_3$ isopropoxide), 1.07 (9H, s, C(C*H*$_3$)$_3$), 1.17 (3H, d J = 6 Hz, $CH_3$ isopropoxide), 1.26 (9H, s, C(C*H*$_3$)$_3$), 1.29 (3H, d J = 6 Hz, $CH_3$ isopropoxide), 2.26 (3H, s, $CH_3$), 2.63 - 2.74 (1H, m, $CH_2$), 2.86 – 2.96 (1H, m $CH_2$), 3.00 (3H, s, $CH_3$), 3.32 – 3.42 (2H, m, CH2), 3.67 – 3.80 (1H, m, CH2), 4.42 (1H, sept J = 6.0 Hz, CH isopropoxide), 4.50 (1H, d J = 13 Hz, CH2), 5.09 (1H, sept J = 6.0 Hz, CH isopropoxide), 6.65 (1H, t J = 7.5 Hz, Ar-H), 6.84 (1H, d J = 2.5 Hz, Ar-H), 7.00 (1H, dd J = 7.5, 1.5 Hz, Ar-H), 7.13 (1H, d J = 2.5 Hz, Ar-H), 7.26 – 7.30 (1H, m, Ar-H), 7.93 (1H, s, CH). **$^{13}$C{$^1$H} NMR** ($CDCl_3$) 17.0 ($CH_3$), 25.7, 25.9, 26.1, 26.3 ($CH_3$ isopropoxide), 29.7, 32.2 (C(*C*H$_3$)$_3$), 34.4, 34.9 (*C*(CH$_3$)$_3$), 51.5 ($CH_3$), 57.7, 58.0, 66.4 ($CH_2$), 77.2, 75.3 (CH isopropoxide), 117.2 (Ar-CH), 121.9, 122.9 (Ar-C), 123.7 (Ar-CH), 127.7 (Ar-C), 131.2, 134.7, 135.0 (Ar-CH), 136.3, 138.0 (Ar-C), 160.6 (Ar-O), 162.0 (CH), 162.7 (Ar-O). **Anal:** Calc for $C_{32}H_{50}N_2O_4Ti$ C, 66.89, H 8.77, N 4.87. Found C 65.9, H 8.73, N 4.57.

**Preparation of Ti(4)(O$^i$Pr)$_2$:** **4**$H_2$ (0.5076 g, 1.28 mmol) was dissolved in toluene (20 ML) to which Ti(O$^i$Pr)$_4$ (0.4 ML, 1.28 mmol) was added. This was stirred for 2 hours, after which time the solvent was removed *in-vacuo* and the product was recrystallised in hexane. After 20 days at – 20 ºC a crop of crystals were obtained which were filtered and dried. **$^1$H NMR** ($CDCl_3$) 1.01 (6H, t J = 6 Hz, $CH_3$ isopropoxide), 1.10 (9H, s, C(C*H*$_3$)$_3$), 1.18 (3H, d J = 6 Hz, $CH_3$ isopropoxide), 1.27 (9H, s, C(C*H*$_3$)$_3$), 1.30 (3H, d J = 6 Hz, $CH_3$ isopropoxide), 2.68 – 2.79 (1H, m, $CH_2$), 2.84 – 2.94 (1H, m, $CH_2$), 2.99 (3H, s, $CH_3$), 3.30 – 3.41 (2H, m, $CH_2$), 3.60 – 3.72 (1H, m, $CH_2$), 4.44 (1H, sept J = 6 Hz, CH isopropoxide), 4.51 (1H, d J = 13 Hz, $CH_2$), 5.09 (1H, sept J = 6 Hz, CH isopropoxide), 6.72 (1H, td J = 6.5 Hz, J = 1.5 Hz, Ar-H), 6.78 (1H, d J = 8.5 Hz, Ar-H), 6.85 (1H, d J = 2.5 Hz, Ar-H), 7.12 – 7.16 (2H, m, Ar-H), 7.36 (1H, td J = 7 Hz, J = 2 Hz, Ar-H), 7.92 (1H, s, CH). **$^{13}$C{$^1$H} NMR** ($CDCl_3$) 25.5, 26.0, 26.2, 26.4 ($CH_3$ isopropoxide), 29.8, 32.2 (C(*C*H$_3$)$_3$), 34.4, 34.9 (*C*(CH$_3$)$_3$), 51.7 ($CH_3$), 57.9, 58.2, 66.4 ($CH_2$), 75.4, 77.3 (CH isopropoxide), 117.5, 119.1 (Ar-CH), 122.7, 123.0 (Ar-C), 123.7, 123.8, 133.4, 134.6 (Ar-CH), 136.4, 138.1 (Ar-C), 160.8, 161.8 (Ar-O), 164.8 (CH). **Anal**: Calc for $C_{31}H_{48}N_2O_4Ti$ C, 66.42, H 8.63, N 5.00. Found C 64.40, H 8.46, N 4.99.

**Preparation of Zr(1)($O^iPr$)$_2$:** Zr($O^iPr$)$_2$$^i$PrOH (0.5 g, 1.28 mmol) was dissolved in toluene (20 cm$^3$) to which **1**$H_2$ (0.6513 g, 1.28 mmol)) was added. This was stirred for 2 hours, after which time the solvent was removed *in-vacuo* and the product was recrystallised in hexane. After 4 days at – 20 ºC a crop of crystals were obtained which were filtered and dried. **$^1$H NMR** ($CDCl_3$) 0.87 (3H, d J = 6.0 Hz, $CH_3$ isopropoxide), 1.04 (3H, d J = 6.0 Hz, $CH_3$ isopropoxide), 1.11 (9H, s, C(C*H*$_3$)$_3$), 1.22 – 1.23 (6H, m, $CH_3$ isopropoxide), 1.26 (18H, d J = 2.5 Hz, C(C*H*$_3$)$_3$, 1.51 (9H, s, C(C*H*$_3$)$_3$), 2.65 – 2.74 (1H, m, $CH_2$), 2.92 (3H, s, $CH_3$), 3.31 (2H, d J = 13.0 Hz, $CH_2$), 3.30 – 3.38 (1H, m, $CH_2$), 3.56 – 3.65 (1H, m, $CH_2$), 4.14 (1H, sept J = 6.0 Hz, CH isopropoxide), 4.41 (1H, sept J = 6.0 Hz, CH isopropoxide), 4.47 (1H, d J = 12.5 Hz, $CH_2$), 6.85 (1H, d J = 2.5 Hz, Ar-H), 6.92 (1H, d J = 2.5 Hz, Ar-H), 7.15 (1H, d J = 2.5 Hz, Ar-H), 7.44 (1H, d J = 2.5 Hz, Ar-H), 7.92 (1H, s, CH). **$^{13}$C{$^1$H} NMR** ($CDCl_3$) 27.4, 27.7 ($CH_3$ isopropoxide), 29.7, 30.0, 31.8, 32.2 (C(*C*H$_3$)$_3$), 34.3, 35.1 (*C*(CH$_3$)$_3$), 49.8 ($CH_3$), 57.7, 58.2, 66.0 ($CH_2$), 70.2, 70.9 (CH isopropoxide), 122.2, 123.1 (Ar-C), 124.1, 124.2, 128.4, 129.5 (Ar-CH), 136.9, 137.6, 138.6, 138.9 (Ar-C), 159.9, 160.0 (Ar-O), 165.7 (CH). **Anal:** Calc for $C_{39}H_{64}N_2O_4Zr$ C, 64.41, H 9.01, N 3.91. Found C 63.4, H 8.73, N 3.76.

**Preparation of Zr(2)($O^iPr$)$_2$:** Zr($O^iPr$)$_2$$^i$PrOH (0.5 g, 1.5 mmol) was dissolved in toluene (20 cm$^3$) to which **2**$H_2$ (0.731 g, 1.28 mmol)) was added. This was stirred for 2 hours, after which time the solvent was removed *in-vacuo* and the product was recrystallised in hexane. After 4 days at – 20 ºC a crop of crystals were obtained which were filtered and dried. **$^1$H NMR** ($CDCl_3$) 0.43 (3H, d J = 5 Hz, $CH_3$ isopropoxide), 0.51 (3H, d J = 5 Hz, $CH_3$ isopropoxide), 1.19 (9H, s, C(C*H*$_3$)$_3$), 1.25 – 1.30 (18H, m, C(C*H*$_3$)$_3$), 1.30 – 1.35 (6H, m, $CH_3$ isopropoxide), 1.53 (9H, s, C(C*H*$_3$)$_3$), 3.26 (1H, sept J = 5.5 Hz, CH isopropoxide), 3.38 (1H, t J = 11 Hz, $CH_2$), 3.44 (1H, m, $CH_2$), 3.64 (1H, d J = 13 Hz, $CH_2$), 3.79 (1H, t J = 11 Hz, $CH_2$), 4.60 (1H, sept J = 5.5 Hz, CH isopropoxide), 5.09 (1H, d J = 13 Hz, $CH_2$), 6.83 (1H, s, Ar-H), 6.95 (1H, s, Ar-H), 7.19 – 7.24 (2H, m, Ar-H), 7.40 – 7.49 (3H, m, Ar-H), 7.72 (2H, d J = 8 Hz, Ar-H), 7.97 (1H, s, CH). **$^{13}$C{$^1$H} NMR** ($CDCl_3$) 26.3, 27.3 ($CH_3$ isopropoxide), 29.3, 29.6, 31.5, 31.8 (C(*C*H$_3$)$_3$), 33.9, 34.0, 34.8, 35.3 (*C*(CH$_3$)$_3$), 52.2, 58.2, 68.6 ($CH_2$), 69.6, 70.8 (CH isopropoxide), 121.5 (Ar-C), 122.0 (Ar-CH), 123.1 (Ar-C), 123.9, 124.0, 125.2,

127.8, 128.9, 129.2 (Ar-CH), 136.7, 137.6, 138.4, 138.6, 152.3 (Ar-C), 159.4, 159.8 (Ar-O), 165.2 (CH). **Anal:** Calc for $C_{44}H_{66}N_2O_4Zr$ C, 67.90, H 8.55, N 3.60. Found C 67.1, H 8.57, N 3.56.

**Preparation of Zr(3)($O^iPr$)$_2$: 3**$H_2$ (0.52 g, 1.28 mmol) was dissolved in toluene (20 $cm^3$) to which $Zr(O^iPr)_4.{}^iPrOH$ (0.5 g, 1.28 mmol) was added. This was stirred for 2 hours, after which time the solvent was removed *in-vacuo* and the product was recrystallised in hexane. After 30 days at – 20 ºC a crop of crystals were obtained which were filtered and dried. **$^1$H NMR** ($CDCl_3$) 0.90 (3H, d J = 6 Hz, $CH_3$ isopropoxide), 0.97 (9H, s, $CH_3$ isopropoxide), 1.06 (3H, d J = 6 Hz, $CH_3$ isopropoxide), 1.12 (9H, s, $CH_3$ isopropoxide), 1.25 (18H, s, C($CH_3$)$_3$), 1.27 (18H, s, C($CH_3$)$_3$), 2.18 (3H, s, $CH_3$), 2.29 (3H, s, $CH_3$), 2.70 (2H, sept J = 6.0 Hz, CH isopropoxide), 2.84 – 2.91 (1H, m, $CH_2$), 2.93 (3H, s, $CH_3$), 2.99 – 3.20 (3H, m, $CH_2$), 3.25 – 3.32 (2H, m, $CH_2$), 3.33 (3H, s, $CH_3$), 3.35 – 3.42 (2H, m, $CH_2$), 3.66 (1H, sept J = 6.0 Hz, CH isopropoxide), 4.16 (1H, sept J = 6.0 Hz, CH isopropoxide), 4.34 – 4.45 (3H, m, $CH_2$), 4.51 (1H, d J = 13.0 Hz, $CH_2$), 6.40 – 6.46 (2H, m, Ar-H), 6.64 (1H, t J = 7.5 Hz, Ar-H), 6.86 (2H, dd J = 8.0, 2.5 Hz, Ar-H), 6.91 (1H, s, CH), 6.99 (1H, dd J = 7.5, 1.0 Hz, Ar-H), 7.08 (1H, d J = 2.5 Hz, Ar-H), 7.10 – 7.13 (1H, m, Ar-H), 7.16 (1H, d J = 2.5 Hz, Ar-H), 7.27 – 7.30 (1H, m, Ar-H), 7.93 (1H, s, CH). **$^{13}$C{$^1$H} NMR** ($CDCl_3$) 16.6, 16.7 ($CH_3$), 27.2, 27.3, 27.5, 27.6 ($CH_3$ isopropoxide), 29.5, 29.6, 32.2 (C($CH_3$)$_3$), 34.3, 34.4, 34.7, 34.9 ($C$($CH_3$)$_3$), 49.7, 50.4 ($CH_3$), 57.5, 57.6, 58.1, 58.2, 66.0, 66.2 ($CH_2$), 70.1, 70.2, 70.4, 70.5 (CH isopropoxide), 116.6, 116.9 (Ar-CH), 121.8, 122.0, 122.9, 123.5 (Ar-C), 123.8, 123.9, 124.1, 124.2 (Ar-CH), 127.6, 129.0 (Ar-C), 131.7, 132.3, 134.4, 135.3 (Ar-CH), 136.5, 136.9, 137.3, 137.8 (Ar-C), 159.7, 160.0, 160.5, 161.6 (Ar-O), 164.4, 164.7 (CH). **Anal:** Calc for $C_{32}H_{50}N_2O_4Zr$ C, 60.50, H 8.16, N 4.53. Found C 60.50, H 7.69, N 4.44.

**Preparation of Zr(4)($O^iPr$)$_2$:** $Zr(O^iPr)_4.{}^iPrOH$ (0.5 g, 1.5 mmol) was dissolved in toluene (20 $cm^3$) to which **4**$H_2$ (0.51 g, 1.28 mmol)) was added. This was stirred for 2 hours, after which time the solvent was removed *in-vacuo* and the product was recrystallised in hexane. After 7 days at – 20 ºC a crop of crystals were obtained which were filtered and dried. **$^1$H NMR** ($CDCl_3$) 0.88 (3H, d J = 6.0 Hz, $CH_3$ isopropoxide), 1.05 (3H, d J = 6.0 Hz, $CH_3$ isopropoxide), 1.14 (9H, s,

C(C*H*$_3$)$_3$), 1.23 (6H, d J = 6 Hz, $CH_3$ isopropoxide), 1.27 (9H, s, C(C*H*$_3$)$_3$), 2.68 – 2.79 (1H, m, $CH_2$), 2.83 – 2.89 (1H, m, $CH_2$), 2.93 (3H, s, $CH_3$), 3.32 (2H, d J = 13 Hz, $CH_2$), 3.51 – 3.62 (1H, m, $CH_2$), 4.14 (1H, sept J = 6 Hz, CH isopropoxide), 4.40 (1H, sept J = 6 Hz, CH isopropoxide), 4.52 (1H, d J = 13 Hz, $CH_2$), 6.69 – 6.75 (1H, m, Ar-H), 6.85 – 6.90 (2H, m, Ar-H), 7.13 (1H, dd J = 7.5 Hz, 2.0 Hz, Ar-H), 7.17 (1H, d J = 2.5 Hz, Ar-H), 7.33 – 7.40 (1H, m, Ar-H), 7.93 (1H, s, CH). **$^{13}$C{$^1$H} NMR** ($CDCl_3$) 27.2, 27.3 ($CH_3$ isopropoxide), 29.7, 32.2 (C(*C*H$_3$)$_3$), 34.4, 34.9 (*C*(CH$_3$)$_3$), 49.9 ($CH_3$), 57.8, 58.3, 66.1 ($CH_2$), 70.3 (CH isopropoxide), 117.3, 120.6 (Ar-CH), 122.7, 123.1 (Ar-C), 124.1, 124.2, 134.0, 134.9 (Ar-CH), 136.9, 137.9 (Ar-C), 159.9, 163.4 (Ar-O), 164.5 (CH). **Anal:** Calc for $C_{31}H_{48}N_2O_4Zr$ C, 61.65, H 8.01, N 4.64. Found C 59.0, H 8.35, N 3.46.

**Preparation of Hf(1)(O$^i$Pr)$_2$:** Hf(O$^i$Pr)$_4$$^i$PrOH (0.41 g, 1.28 mmol) was dissolved in toluene (20 cm$^3$) to which **1**$H_2$ (0.5 g, 1.28 mmol)) was added. This was stirred for 2 hours, after which time the solvent was removed *in-vacuo* and the product was recrystallised in hexane. After 4 days at – 20 ºC a crop of crystals were obtained which were filtered and dried. **$^1$H NMR** ($CDCl_3$) 0.89 (3H, d J = 6 Hz, $CH_3$ isopropoxide), 1.04 (3H, d J = 6 Hz, $CH_3$ isopropoxide), 1.11 (9H, s, C(C*H*$_3$)$_3$), 1.21 – 1.25 (6H, m, $CH_3$ isopropoxide), 1.26 – 1.29 (18H, m, C(C*H*$_3$)$_3$), 1.52 (9H, s, C(C*H*$_3$)$_3$), 2.74 – 2.82 (1H, m, $CH_2$), 2.88 – 2.94 (1H, m, $CH_2$), 3.36 (2H, d J = 13.0 Hz, $CH_2$), 3.64 (1H, sept J = 6.0 Hz, CH isopropoxide), 4.20 (1H, sept J = 6.0 Hz, CH isopropoxide), 4.48 – 4.58 (2H, m, $CH_2$), 6.88 (1H, d J = 2.5 Hz, Ar-H), 6.94 (1H, d J = 2.5 Hz, Ar-H), 7.20 (1H, d J = 2.5 Hz, Ar-H), 7.50 (1H, d J = 2.5 Hz, Ar-H), 7.93 (1H, s, CH). **$^{13}$C{$^1$H} NMR** ($CDCl_3$) 27.6, 27.7, 27.9, 28.0 ($CH_3$ isopropoxide), 29.7, 30.0, 31.8, 32.2 (C(*C*H$_3$)$_3$), 34.2, 34.3, 35.0, 35.6 (*C*(CH$_3$)$_3$), 50.1 ($CH_3$), 57.9, 58.2, 66.0 ($CH_2$), 69.9, 70.6 (CH isopropoxide), 122.4, 123.0 (Ar-C), 124.0, 124.3, 128.4, 129.8 (Ar-CH), 137.4, 137.6, 139.0, 139.2 (Ar-C), 160.2, 160.4 (Ar-O), 166.1 (CH). **Anal:** Calc for $C_{39}H_{64}N_2O_4Hf$ C, 58.30, H 8.03, N 3.49. Found C 57.9, H 8.03, N 3.41.

**Preparation of Hf(2)(O$^i$Pr)$_2$:** Hf(O$^i$Pr)$_4$$^i$PrOH (0.20 g, 0.491 mmol) was dissolved in toluene (10 cm$^3$) to which **2**$H_2$ (0.28 g, 0.49 mmol)) was added. This was stirred for 2 hours, after which time the solvent was removed *in-vacuo* and the product was recrystallised in hexane. After 7 days at -20 °C, a crop of crystals

were obtained which were filtered and dried. **$^{1}$H NMR** ($CDCl_3$) 0.40 (3H, d J = 6 Hz, $CH_3$ isopropoxide), 0.51 (3H, d J = 6 Hz, $CH_3$ isopropoxide), 1.17 (9H, s, C(C*H*$_3$)$_3$), 1.27 (18H, d J = 5.5 Hz, C(C*H*$_3$)$_3$), 1.32 (6H, dd J = 5.5 Hz, 2.5 Hz, $CH_3$ isopropoxide), 1.52 (9H, s, C(C*H*$_3$)$_3$), 3.33 (1H, sept J = 6.0 Hz, CH isopropoxide), 3.38 – 3.46 (1H, m, $CH_2$), 3.48 – 3.60 (2H, m, $CH_2$), 3.64 (1H, d J = 13 Hz, $CH_2$), 3.78 – 3.88 (1H, m, $CH_2$), 4.68 (1H, sept J = 6.0 Hz, CH isopropoxide), 5.13 (1H, d J = 12.5 Hz, $CH_2$), 6.82 (1H, d J = 2.5 Hz, Ar-H), 6.94 (1H, d J = 2.5 Hz, Ar-H), 7.23 (2H, t J = 8.0 Hz, Ar-H), 7.44 (2H, t J = 8.0 Hz, Ar-H),7.49 (1H, d J = 2.5 Hz, Ar-H), 7.76 (2H, d J = 8 Hz, Ar-H), 7.95 (1H, s, CH). **$^{13}$C{$^{1}$H} NMR** ($CDCl_3$) 26.9, 27.8 ($CH_3$ isopropoxide), 29.7, 30.0, 31.8, 32.2 (C(*C*H$_3$)$_3$), 34.3, 34.4, 35.1, 35.6 (*C*(CH$_3$)$_3$), 49.9, 58.4, 69.2 ($CH_2$), 69.7, 70.9 (CH isopropoxide), 122.1 (Ar-C), 122.4 (Ar-CH), 123.3 (Ar-C), 124.1, 124.4, 125.7, 128.2, 129.2, 129.8 (Ar-CH), 137.5, 137.9, 139.0, 139.3, 152.6 (Ar-C), 159.9, 160.5 (Ar-O), 166.0 (CH). **Anal:** Calc for $C_{44}H_{66}N_2O_4Hf$ C, 61.06, H 7.69, N 3.24. Found C 60.90, H 7.67, N 3.15.

**Preparation of Hf(3)(O$^{i}$Pr)$_2$: 3**$H_2$ (0.51 g, 1.28 mmol) was dissolved in toluene (20 cm$^3$) to which Hf(O$^{i}$Pr)$_4$$^{i}$PrOH (0.4 ML, 1.28 mmol) was added. This was stirred for 2 hours, after which time the solvent was removed *in-vacuo* and the product was recrystallised in hexane. After 20 days at – 20 ºC a crop of crystals were obtained which were filtered and dried. **$^{1}$H NMR** ($CDCl_3$) 0.91 (3H, d J = 6 Hz, $CH_3$ isopropoxide), 0.97 (9H, s, $CH_3$ isopropoxide), 1.04 (3H, d J = 6 Hz, $CH_3$ isopropoxide), 1.10 (9H, s, $CH_3$ isopropoxide), 1.24 (18H, s, C(C*H*$_3$)$_3$), 1.27 (18H, s, C(C*H*$_3$)$_3$), 2.19 (3H, s, $CH_3$), 2.29 (3H, s, $CH_3$), 2.76 (2H, sept J = 4.5 Hz, CH isopropoxide), 2.89 – 2.94 (1H, m, $CH_2$), 2.96 (3H, s, $CH_3$), 3.00 – 3.14 (1H, m, $CH_2$), 3.23 (1H, sept J = 4.5 Hz, CH isopropoxide), 3.29 (1H, s, $CH_2$), 3.34 (3H, s, $CH_3$), 3.35 (2H, s, $CH_2$), 3.36 – 3.41 (2H, m, $CH_2$), 3.65 – 3.73 (1H, m, $CH_2$), 4.20 (1H, sept J = 6.0 Hz, CH isopropoxide), 4.42 – 4.57 (4H, m, $CH_2$), 6.38 – 6.47 (2H, m, Ar-H), 6.64 (1H, t J = 7.5 Hz, Ar-H), 6.85 (2H, dd J = 8.0, 2.5 Hz, Ar-H), 6.87 (1H, s, CH), 6.99 (1H, dd J = 7.5, 1.5 Hz, Ar-H), 7.09 (1H, d J = 2.5 Hz, Ar-H), 7.13 – 7.16 (1H, m, Ar-H), 7.18 (1H, d J = 2.5 Hz, Ar-H), 7.30 – 7.34 (1H, m, Ar-H), 7.92 (1H, s, CH). **$^{13}$C{$^{1}$H} NMR** ($CDCl_3$) 16.6, 16.7 ($CH_3$), 27.4, 27.5, 27.7, 27.9 ($CH_3$ isopropoxide), 29.5, 29.6, 32.2 (C(*C*H$_3$)$_3$), 34.2, 34.3, 34.7, 34.8 (*C*(CH$_3$)$_3$), 49.9, 50.6 ($CH_3$), 57.6, 57.8, 58.0, 58.1, 66.0, 66.1 ($CH_2$),

69.9, 70.1, 70.4, 70.6 (CH isopropoxide), 116.5, 117.0 (Ar-CH), 122.0, 122.2, 122.8, 123.5 (Ar-C), 123.8, 124.0, 124.3 (Ar-CH), 128.1, 129.6 (Ar-C), 131.7, 132.2, 132.3, 134.6, 135.5 (Ar-CH), 136.9, 137.1, 137.3, 137.7 (Ar-C), 159.9, 160.3, 160.9, 161.9 (Ar-O), 164.8, 165.1 (CH). **Anal:** Calc for $C_{32}H_{50}N_2O_4Hf$ C, 54.50, H 7.15, N 3.97. Found C 54.0, H 7.01, N 3.81.

**Preparation of Hf(4)($O^iPr$)$_2$:** $Hf(O^iPr)_4.{}^iPrOH$ (0.50 g, 1.21 mmol) was dissolved in toluene (20 $cm^3$) to which **4**$H_2$ (0.48 g, 1.21 mmol)) was added. This was stirred for 2 hours, after which time the solvent was removed *in-vacuo* and the product was recrystallised in hexane. After 7 days at – 20 ºC a crop of crystals were obtained which were filtered and dried. **$^1$H NMR** ($CDCl_3$) 0.89 (3H, d J = 6 Hz, $CH_3$ isopropoxide), 1.03 (3H, d J = 6 Hz, $CH_3$ isopropoxide), 1.13 (6H, s $CH_3$ isopropoxide), 1.24 (9H, s, C(C$H_3$)$_3$), 1.26 (9H, s, C(C$H_3$)$_3$), 2.77 – 2.84 (1H, m $CH_2$), 2.89 – 2.92 (1H, m $CH_2$), 2.95 (3H, s, $CH_3$), 3.35 (2H, d J = 13.0 Hz, $CH_2$), 3.55 – 3.63 (1H, m, $CH_2$), 4.18 (1H, sept J = 6.0 Hz, CH isopropoxide), 4.47 (1H, sept J = 6.0 Hz, CH isopropoxide), 4.55 (1H, d J = 13.0 Hz, $CH_2$), 6.71 (1H, dd J = 7.0, 1.0 Hz, Ar-H), 6.87 (1H, d J = 2.5 Hz, Ar-H), 6.90 (1H, d J = 8.5 Hz, Ar-H), 7.12 (1H, dd J = 7.5, 2.0 Hz, Ar-H), 7.18 (1H, d J = 2.5 Hz, Ar-H), 7.36 – 7.42 (1H, m, Ar-H), 7.91 (1H, s, CH). **$^{13}$C{$^1$H} NMR** ($CDCl_3$) 27.4, 27.5 ($CH_3$ isopropoxide), 29.7, 32.2 (C(*C*$H_3$)$_3$), 34.3, 34.9 (*C*($CH_3$)$_3$), 50.2 ($CH_3$), 57.9, 58.3, 66.0 ($CH_2$), 70.0 (CH isopropoxide), 117.4, 121.2 (Ar-CH), 123.0 (Ar-C), 124.0, 124.3, 134.0, 135.1 (Ar-CH), 137.4, 137.8 (Ar-C), 160.1, 163.8 (Ar-O), 164.9 (CH). **Anal:** Calc for $C_{31}H_{48}N_2O_4Hf$ C, 53.87, H 7.00, N 4.05. Found C 52.7, H 6.66, N 3.82.

### 5.2.4 Experimental for Chapter 4

**Preparation of 1**$H_2$**:** A solution of 3,5-di-*tert*-butyl-2-hydroxybenzaldehyde (3.2 g, 0.01 mol) and methylethylene diamine (1.02 g, 1.2 ML, 0.014 mol) in methanol (20 ML) was prepared. The solution was stirred until a clear solution was observed, and left to stand for 24 hours to yield a yellow oil which was collected and dried (2.68 g, 65.9 %). **$^1$H NMR** ($CDCl_3$) 1.31 (9H, s, C($CH_3$)$_3$), 1.45 (9H, s, C($CH_3$)$_3$), 2.47 (3H, s, $CH_3$), 2.92 (2H, t J = 6 Hz, $CH_2$), 3.73 (2H, t J = 6 Hz, $CH_2$), 7.09 (1H, d J = 2.5 Hz, Ar-H), 7.39 (1H, d J = 2.5 Hz, Ar-H), 8.40 (1H, s, CH). **$^{13}$C{$^1$H} NMR** ($CDCl_3$) 29.8, 31.8 (C(*C*$H_3$)$_3$), 34.4, 35.3 (*C*($CH_3$)$_3$), 36.6

($CH_3$), 52.2, 59.8 ($CH_2$), 118.1, (Ar-C), 126.3, 127.3 (Ar-CH), 137.0, 140.5 (Ar-C), 158.3 (Ar-O), 167.5 (CH). **m/z** calc. $C_{18}H_{31}N_2O$ = 291.2437, found 291.2267. The yellow oil (1 g, 3.44 mmol) was dissolved in THF (20 $cm^3$), to which a solution of 3,5-di-tert-2-hydroxybenzyl bromide (1.029 g, 3.44 mmol) in THF (20 $cm^3$) was added. Triethylamine (0.35 g, 0.48 ML, 3.44 mmol) was added and the mixture stirred at 80 $^oC$ for three hours. The white precipitate was filtered and the solvent removed under reduced pressure. The product was isolated *via* flash chromatography to obtain the product (1.33 g, 76.2 %). **$^1$H NMR** ($CDCl_3$) 1.29 (9H, s, $C(CH_3)_3$), 1.32 (9H, s, $C(CH_3)_3$), 1.39 (9H, s, $C(CH_3)_3$), 1.46 (9H, s, $C(CH_3)_3$), 2.40 (3H, s, $CH_3$), 2.85 (2H, t J = 6.5 Hz, $CH_2$), 3.76 (2H, s, $CH_2$), 3.78 (2H, t J = 6.5 Hz, $CH_2$), 6.84 (1H, d J = 2.5 Hz, Ar-H), 7.09 (1H, d J = 2.5 Hz, Ar-H), 7.22 (1H, d J = 2.5 Hz, Ar-H), 7.40 (1H, d J = 2.5 Hz, Ar-H), 8.39 (1H, s, CH). **$^{13}$C{$^1$H} NMR** ($CDCl_3$) 29.4, 29.4, 31.5, 31.7 ($C(CH_3)_3$), 34.1, 35.0 ($C(CH_3)_3$), 41.9 ($CH_3$), 57.1, 57.3, 62.2 ($CH_2$), 117.8, 120.9, (Ar-C), 122.9, 123.2, 125.9, 127.0 (Ar-CH), 135.6, 136.6, 140.1, 140.4 (Ar-C), 154.3, 158.0 (Ar-O), 167.3 (CH). **m/z** calc. $C_{33}H_{53}N_2O_2$ = 509.4107, found 509.4145.

**Preparation of 2**$H_2$**:** A solution of 3,5-di-*tert*-butyl-2-hydroxybenzaldehyde (3.2 g, 0.014 mol) and phenylethylene diamine (1.91 g, 1.83 ML, 0.014 mol) in methanol (20 ML) was prepared. The solution was stirred until a clear solution was observed, and left to stand for 24 hours to yield a yellow powder which was collected and dried. **$^1$H NMR** ($CDCl_3$) 1.31 (9H, s, $C(CH_3)_3$), 1.46 (9H, s, $C(CH_3)_3$), 3.52 (2H, t J = 6 Hz, $CH_2$), 3.81 (2H, t J = 5.5 Hz, $CH_2$), 6.66 (2H, d J = 8 Hz, Ar-H), 6.73 (1H, t J = 7.5 Hz, Ar-H), 7.08 (1H, d J = 2.5 Hz, Ar-H), 7.19 (2H, t, J = 8 Hz, Ar-H), 7.40 (1H, d J = 2.5 Hz, Ar-H), 8.35 (1H, s, CH). **$^{13}$C{$^1$H} NMR** ($CDCl_3$) 29.7, 31.8 ($C(CH_3)_3$), 34.4, 35.3 ($C(CH_3)_3$), 44.5, 58.7 ($CH_2$), 113.5, 118.0, 126.3, 127.5, 129.6 (Ar-CH), 137.0, 140.5, 147.9 (Ar-C), 158.3 (Ar-O), 168.0 (CH). **m/z** calc. $C_{23}H_{33}N_2O$ = 353.2593, found 353.2569. The yellow powder (1 g, 2.84 mmol) was dissolved in THF (20 $cm^3$), to which a solution of 3,5-di-tert-2-hydroxybenzyl bromide (0.85 g, 2.84 mmol) in THF (20 $cm^3$) was added. Triethylamine (0.29 g, 0.4 ML, 2.84 mmol) was added and the mixture stirred at 80 $^oC$ for three hours. The white precipitate was filtered and the solvent removed under reduced pressure. The product was isolated *via* flash chromatography to obtain the product (0.958 g, 59.2 %). **$^1$H NMR** ($CDCl_3$) 1.19

(9H, s, $C(CH_3)_3$), 1.21 (9H, s, $C(CH_3)_3$), 1.32 (9H, s, $C(CH_3)_3$), 1.36 (9H, s, $C(CH_3)_3$), 3.42 (2H, t J = 6.5 Hz, $CH_2$), 3.58 (2H, t J = 6.5 Hz, $CH_2$), 4.32 (2H, s, CH2), 6.87 (1H, d J = 2.5 Hz, Ar-H), 6.90 (1H, d J = 2.5 Hz, Ar-H), 6.93 – 6.99 (1H, m, Ar-H), 7.09 – 7.16 (3H, m, Ar-H), 7.21 – 7.27 (2H, m, Ar-H), 7.29 (1H, d J =2.5 Hz, Ar-H), 8.07 (1H, s, CH). **$^{13}$C{$^{1}$H} NMR** ($CDCl_3$) 29.8, 30.0, 31.8, 32.0 ($C(CH_3)_3$), 34.4, 34.5, 35.2, 35.4 ($C(CH_3)_3$), 52.8, 56.9, 57.9 ($CH_2$), 118.1 (Ar-C), 121.0, (Ar-CH), 121.5 (Ar-C), 123.4, 123.7, 124.3, 126.2, 127.4, 129.7 (Ar-CH), 136.2, 137.0, 140.5, 141.7, 149.2 (Ar-C), 154.0, 158.3 (Ar-O), 167.9 (CH). **m/z** calc. $C_{38}H_{54}N_2O_2^+$ = 571.4264, found 571.4270.

**Preparation of 3**$H_2$**:** A solution of 2-hyrdroxy-3-methylbenzaldehyde (0.75 g, 0.66 ML, 5.51 mmol) and methylethylene diamine (0.41 g, 0.48 ML, 5.51 mol) in methanol (10 ML) was prepared. The solution was stirred until a clear solution was observed, and left to stand for 24 hours to yield a yellow oil which was collected and dried (0.83 g, 78.0 %). **$^{1}$H NMR** ($CDCl_3$) 2.21 (3H, s, $CH_3$), 2.39 (3H, s, $CH_3$), 2.83 (2H, t J = 5.5 Hz, $CH_2$), 3.64 (2H, t J = 5.5 Hz, $CH_2$), 6.72 (1H, t J = 7.5 Hz, Ar-H), 7.03 (1H, d J = 7.5 Hz, Ar-H), 7.11 (1H, d J = 7.0 Hz, Ar-H), 8.28 (1H, s, CH). **$^{13}$C{$^{1}$H} NMR** ($CDCl_3$) 15.6, 36.4 ($CH_3$), 51.9, 59.4 ($CH_2$), 117.9 (Ar-C), 118.2 (Ar-CH), 125.9 (Ar-C), 129.1, 133.3 (Ar-CH), 159.4 (Ar-O), 166.2 (CH). **m/z** calc. $C_{11}H_{17}N_2O$ = 193.1341, found 193.1352. The yellow oil (0.79 g, 4.08 mmol) was dissolved in THF (30 $cm^3$), to which a solution of 3,5-di-*tert*-2-hydroxybenzyl bromide (1.22 g, 4.08 mmol) in THF (30 $cm^3$) was added. Triethylamine (0.41 g, 0.57 ML, 4.08 mmol) was added and the mixture stirred at 80 $^{o}$C for three hours. The white precipitate was filtered and the solvent removed under reduced pressure. The product was isolated *via* flash chromatography to obtain the product (0.21 g, 13.0 %). **$^{1}$H NMR** ($CDCl_3$) 1.31 (9H, s, $C(CH_3)_3$), 1.40 (9H, s, $C(CH_3)_3$), 2.30 (3H, s, $CH_3$), 2.41 (3H, s, $CH_3$), 2.86 (2H, t J = 6.5 Hz, $CH_2$), 3.76 (2H, s, $CH_2$), 3.79 (2H, t J = 6.5 Hz, $CH_2$), 6.80 (1H, t J = 7.5 Hz, Ar-H), 6.85 (1H, d J = 2.5 Hz, Ar-H), 7.11 (1H, d J = 7.5 Hz, Ar-H), 7.20 (1H, d J = 7.5 Hz, Ar-H), 7.24 (1H, d J = 2.5 Hz, Ar-H), 8.37 (1H, s, CH). **$^{13}$C{$^{1}$H} NMR** ($CDCl_3$) 15.8 ($CH_3$), 29.9, 30.7 ($C(CH_3)_3$), 31.9, 32.0 ($C(CH_3)_3$), 34.5, 35.2 ($C(CH_3)_3$), 42.3 ($CH_3$), 57.3, 57.8, 62.6 ($CH_2$), 118.3 (Ar-C), 118.5 (Ar-CH), 121.3 (Ar-C), 123.3, 123.6 (Ar-CH), 126.2 (Ar-C), 129.4, 133.7 (Ar-CH), 136.0,

140.8 (Ar-C), 154.6, 159.6 (Ar-O), 166.8 (CH). **m/z** calc. $C_{26}H_{39}N_2O_2$ = 411.3012, found 411.2993.

**Preparation of 4**$H_2$**:** A solution of salicylaldehyde (2.74 g, 2.39 ML, 0.02 mol) and methylethylene diamine (1.66 g, 1.96 ML, 0.02 mol) in methanol (20 ML) was prepared. The solution was stirred until a clear solution was observed, and left to stand for 24 hours to yield a yellow oil which was collected and dried (3.34 g, 84.1 %). **$^1$H NMR** ($CDCl_3$) 2.36 (3H, s, $CH_3$), 2.81 (2H, s(br), $CH_2$), 3.62 (2H, s(br), $CH_2$), 6.76 – 6.87 (2H, m, Ar-H), 7.14 – 7.20 (2H, m, Ar-H), 8.28 (1H, s, CH). **$^{13}$C{$^1$H} NMR** ($CDCl_3$) 36.4 ($CH_3$), 51.9, 59.5 ($CH_2$), 117.0, 118.7, 131.4, 132.3 (Ar-CH), 138.7 (Ar-C), 161.4 (Ar-O), 166.0 (CH). **m/z** calc. $C_{10}H_{14}N_2O$ = 179.1184, found 179.1177. The yellow oil (2.58 g, 0.014 mol) was dissolved in THF (60 $cm^3$), to which a solution of 3,5-di-*tert*-2-hydroxybenzyl bromide (4.33 g, 0.014 mol) in THF (60 $cm^3$) was added. Triethylamine (1.46 g, 2.01 ML, 0.014 mol) was added and the mixture stirred at 80 $^oC$ for three hours. The white precipitate was filtered and the solvent removed under reduced pressure. The product was isolated *via* flash chromatography to obtain the product (3.20 g, 56.5 %). **$^1$H NMR** ($CDCl_3$) 1.31 (9H, s, $C(CH_3)_3$), 1.40 (9H, s, $C(CH_3)_3$), 2.40 (3H, s, $CH_3$), 3.74 – 3.82 (6H, m, $CH_2$), 6.85 (1H, d J = 2.5 Hz, Ar-H), 6.89 (1H, td J = 7 Hz, 1 Hz, Ar-H), 6.98 (1H, d J = 8 Hz, Ar-H), 7.23 – 7.25 (2H, m, Ar-H), 7.29 – 7.35 (1H, m, Ar-H), 8.38 (1H, s, CH). **$^{13}$C{$^1$H} NMR** ($CDCl_3$) 29.9, 32.0 ($C(CH_3)_3$), 34.4, 35.1 ($C(CH_3)_3$), 42.3 ($CH_3$), 57.3, 57.9, 62.5 ($CH_2$), 117.2, 118.9 (Ar-CH), 119.0, 121.2 (Ar-C), 122.3, 123.6, 131.7, 132.6 (Ar-CH), 135.9, 140.8 (Ar-C), 154.6, 161.3 (Ar-O), 166.6 (CH). **m/z** calc. $C_{25}H_{36}N_2O_2Na$ = 419.2674, found 419.2637.

**Preparation of 5**$H_2$**:** A solution of 2-hydroxy-3-methylbenzaldehyde (1.12 g, 1.0 ML, 8.25 mmol) and phenylethylene diamine (1.12 g, 1.08 ML, 8.25 mmol) in methanol (10 ML) was prepared. The solution was stirred until a clear solution was observed, and left to stand for 24 hours to yield a yellow oil which was collected and dried (1.92 g, 92.0 %). **$^1$H NMR** ($CDCl_3$) 2.29 (3H, s, $CH_3$), 3.51 (2H, t J = 5.5 Hz, $CH_2$), 3.83 (2H, t J = 5.5 Hz, $CH_2$), 6.64 (2H, dd J = 7.5 Hz, 1.0 Hz, Ar-H), 6.73 (1H, t J = 7.5 Hz, Ar-H), 6.81 (1H, t J = 7.5 Hz, Ar-H), 7.10 (1H, dd J = 7.5 Hz, 1.0 Hz, Ar-H), 7.19 (3H, td J = 7.5 Hz, 1.0 Hz, Ar-H), 8.32

(1H, s, CH). **$^{13}C\{^{1}H\}$ NMR** ($CDCl_3$) 15.1 ($CH_3$), 52.8, 54.9 ($CH_2$), 113.8, 120.6, 123.4 (Ar-H), 124.5, 126.4 (Ar-C), 128.9, 129.5, 133.9 (Ar-CH), 146.1 (Ar-C), 157.5 (CH), 161.2 (Ar-O). **m/z** calc. $C_{16}H_{19}N_2O$ = 255.1498, found 255.1563. The yellow oil (1.92 g, 7.55 mmol) was dissolved in THF (60 $cm^3$), to which a solution of 3,5-di-*tert*-2-hydroxybenzyl bromide (4.20 g, 14.04 mmol) in THF (60 $cm^3$) was added. Triethylamine (1.42 g, 1.96 ML, 14.04 mmol) was added and the mixture stirred at 80 $^oC$ for 72 hours. The white precipitate was filtered and the solvent removed under reduced pressure. The product was isolated *via* flash chromatography to obtain the product (1.31 g, 37.0 %). **$^{1}H$ NMR** ($CDCl_3$) 1.34 (9H, s, $C(CH_3)_3$), 1.47 (9H, s, $C(CH_3)_3$), 2.33 (3H, s, $CH_3$), 3.56 (2H, t J = 6.0 Hz, $CH_2$), 3.72 (2H, t J = 6.0 Hz, $CH_2$), 4.45 (2H, s, $CH_2$), 6.83 (1H, d J = 7.5 Hz, Ar-H), 6.93 (1H, br s, Ar-H), 7.04 (1H, d J = 6.5 Hz, Ar-H), 7.07 – 7.12 (2H, m, Ar-H), 7.21 – 7.23 (2H, m, Ar-H), 7.31 (1H, br s, Ar-H), 7.37 (1H, d J = 7.5 Hz, Ar-H), 7.43 (1H, d J = 8.0 Hz, Ar-H), 8.19 (1H, s, CH). **$^{13}C\{^{1}H\}$ NMR** ($CDCl_3$) 15.5 ($CH_3$), 29.7, 31.7 ($C(CH_3)_3$), 34.3, 34.9 ($C(CH_3)_3$), 45.5, 52.1, 57.5 ($CH_2$), 117.9 (Ar-C), 118.2, 120.7 (Ar-CH), 121.1 (Ar-C), 123.2, 123.4, 124.0 (Ar-CH), 126.0 (Ar-C), 129.1, 129.5, 133.4 (Ar-CH), 135.9, 141.4, 148.8 (Ar-C), 153.7, 159.4 (Ar-O), 166.7 (CH). **m/z** calc. $C_{31}H_{41}N_2O_2$ = 473.3168, found 473.3235.

**Preparation of 6$H_2$:** A solution of salicylaldehyde (2.54 g, 2.22 ML, 0.02 mol) and phenylethylene diamine (2.83 g, 2.71 ML, 0.02 mol) in methanol (20 ML) was prepared. The solution was stirred until a clear solution was observed, and left to stand for 24 hours to yield a yellow oil which was collected and dried (4.04 g, 84.0 %). **$^{1}H$ NMR** ($CDCl_3$) 3.57 (2H, t J = 6.0 Hz, $CH_2$), 3.88 (2H, t J = 5.5 Hz, $CH_2$), 6.72 (2H, dd J = 8.5 Hz, 1.0 Hz, Ar-H), 6.83 (1H, t J = 7.5 Hz, Ar-H), 6.98 (1H, td J = 7.5 Hz, 1.0 Hz, Ar-H), 7.08 (1H, d J = 8.0 Hz, Ar-H), 7.28 – 7.33 (3H, m, Ar-H), 7.41 (1H, td J = 7.5 Hz, 1.0 Hz, Ar-H), 8.38 (1H, s, CH). **$^{13}C\{^{1}H\}$ NMR** ($CDCl_3$) 44.4, 58.6 ($CH_2$), 113.4, 117.3, 118.0, 129.6, 131.7, 132.7 (Ar-CH), 147.7 (Ar-C), 161.3 (Ar-O), 166.8 (CH). **m/z** calc. $C_{15}H_{16}N_2O$ = 241.1335, found 241.1341. The yellow oil (3.00 g, 0.012 mol) was dissolved in THF (60 $cm^3$), to which a solution of 3,5-di-*tert*-2-hydroxybenzyl bromide (3.74 g, 0.012 mol) in THF (60 $cm^3$) was added. Triethylamine (1.26 g, 1.76 ML, 0.012 mol) was added and the mixture stirred at 80 $^oC$ for three hours. The white precipitate

was filtered and the solvent removed under reduced pressure. The product was isolated *via* flash chromatography to obtain the product (4.64 g, 79.6 %). **$^{1}$H NMR** ($CDCl_3$) 1.34 (9H, s, $C(CH_3)_3$), 1.46 (9H, s, $C(CH_3)_3$), 3.55 (2H, t J = 6.5 Hz, $CH_2$), 3.72 (2H, t J = 6.5 Hz, $CH_2$), 4.44 (2H, s, $CH_2$), 6.68 (1H, d J = 8.0 Hz, Ar-H), 6.91 (1H, d J = 7.5 Hz, Ar-H), 7.00 (2H, dd J = 5.0 Hz, J = 2.5 Hz, Ar-H), 7.10 (1H, t J = 7.5 Hz, Ar-H), 7.20 (2H, d J = 8.0 Hz, Ar-H), 7.23 (1H, br s, Ar-H), 7.31 (1H, br s, Ar-H), 7.34 – 7.41 (2H, d J = 7.5 Hz, Ar-H), 8.20 (1H, s, CH). **$^{13}$C{$^{1}$H} NMR** ($CDCl_3$) 29.7, 31.7 ($C(CH_3)_3$), 34.3, 34.9 ($C(CH_3)_3$), 45.6, 52.5, 57.8 ($CH_2$), 117.1, 118.6 (Ar-CH), 118.7 (Ar-C), 120.8 (Ar-CH), 121.1 (Ar-C), 123.3, 123.4, 124.0, 129.5, 131.4, 132.4 (Ar-CH), 135.9, 141.4, 148.9 (Ar-C), 153.7, 161.1 (Ar-O), 166.5 (CH). **m/z** calc. $C_{30}H_{39}N_2O_2$ = 459.3012, found 459.3095.

**Preparation of 7$H_2$:** A solution of 3,5-dichlorosalicylaldehyde (1.5 g, 7.85 mmol) and methylethylene diamine (0.58g, 0.68 ML, 7.85 mmol) in methanol (10 ML) was prepared. The solution was stirred until a clear solution was observed, and left to stand for 2 hours to yield a yellow powder which was collected and dried (1.88 g, 97.0 %). **$^{1}$H NMR** ($CDCl_3$) 2.41 (3H, s, $CH_3$), 2.93 (2H, br s, $CH_2$), 3.44 (2H, br s, $CH_2$), 7.06 (1H, d J = 2.5 Hz, Ar-H), 7.32 (1H, d J = 2.5 Hz, Ar-H) NO IMINE RESONANCE PRESENT. **$^{13}$C{$^{1}$H} NMR** ($CDCl_3$) 37.3 ($CH_3$), 52.6 ($CH_2$), 121.0, 122.4, 122.7 (Ar-C), 128.6, 131.0 (Ar-CH), 155.5 (Ar-O) NO IMINE RESONANCE PRESENT. **m/z** calc. $C_{10}H_{12}N_2OCl_2$ = 247.0405, found 247.0401. The yellow powder (1.50 g, 6.07 mmol) was dissolved in THF (120 $cm^3$), to which a solution of 3,5-di-*tert*-2-hydroxybenzyl bromide (1.82 g, 6.07 mmol) in THF (120 $cm^3$) was added. Triethylamine (0.61 g, 0.85 ML, 6.07 mmol) was added and the mixture stirred at 80 $^{o}$C for 72 hours. The white precipitate was filtered and the solvent removed under reduced pressure. The product was isolated *via* flash chromatography to obtain the product (2.07 g, 73.1 %). **$^{1}$H NMR** ($CDCl_3$) 1.28 (9H, s, $C(CH_3)_3$), 1.34 (9H, s, $C(CH_3)_3$), 2.38 (3H, s, $CH_3$), 2.86 (2H, t J = 6.5 Hz, $CH_2$), 3.73 (2H, s, $CH_2$), 3.82 (2H, t J = 5.5 Hz, $CH_2$), 6.82 (1H, d J = 2.5 Hz, Ar-H), 7.16 (1H, d J = 2.5 Hz, Ar-H), 7.20 (1H, d J = 2.5 Hz, Ar-H), 7.41 (1H, d J = 2.5 Hz, Ar-H), 8.28 (1H, s, CH). **$^{13}$C{$^{1}$H} NMR** ($CDCl_3$) 29.6, 31.8 ($C(CH_3)_3$), 34.3, 34.9 ($C(CH_3)_3$), 42.2 ($CH_3$), 50.9, 51.9, 56.9 ($CH_2$), 120.8, 122.8 (Ar-C), 123.3, 123.4, 129.3, 130.5, 132.4 (Ar-CH), 135.8,

140.8 (Ar-C), 154.2, 156.7 (Ar-O), 165.0 (CH). **m/z** calc. $C_{25}H_{34}N_2O_2Cl_2Na$ = 487.1895, found 487.1877.

**Preparation of 8**$H_2$**:** A solution of 3,5-dichlorosalicylaldehyde (2.5 g, 0.013 mol) and phenylethylene diamine (1.78 g, 1.71 ML, 0.013 mol) in methanol (10 ML) was prepared. The solution was stirred until a clear solution was observed, and left to stand for 24 hours to yield a yellow powder which was collected and dried (2.28 g, 57.2 %). **$^1$H NMR** ($CDCl_3$) 3.52 (2H, t J = 5.5 Hz, $CH_2$), 3.84 (2H, t J = 5.5 Hz, $CH_2$), 6.62 (2H, dt J = 7.5 Hz, 1.0 Hz, Ar-H), 6.74 (1H, tt J = 7.5 Hz, 1.0 Hz, Ar-H), 7.10 (1H, d J = 2.5 Hz, Ar-H), 7.17 – 7.22 (2H, m, Ar-H), 7.40 (1H, d J = 2.5 Hz, Ar-H), 8.17 (1H, s, CH). **$^{13}$C{$^1$H} NMR** ($CDCl_3$) 44.2, 57.6 ($CH_2$), 113.4, 118.3 (Ar-CH), 119.5, 122.8 (Ar-C), 129.4, 129.8, 132.7 (Ar-CH), 147.4 (Ar-C), 157.4 (Ar-O), 165.3 (CH). **m/z** calc. $C_{15}H_{14}N_2OCl_2$ = 309.05614, found 309.0566. The yellow powder (2.00 g, 0.006 mol) was dissolved in THF (30 $cm^3$), to which a solution of 3,5-di-*tert*-2-hydroxybenzyl bromide (1.94 g, 0.006 mol) in THF (30 $cm^3$) was added. Triethylamine (0.65 g, 0.90 ML, 0.006 mol) was added and the mixture stirred at 80 $^o$C for 24 hours. The white precipitate was filtered and the solvent removed under reduced pressure. The product was isolated *via* flash chromatography to obtain the product (2.73 g, 80.0 %). **$^1$H NMR** ($CDCl_3$) 1.28 (9H, s, $C(CH_3)_3$), 1.38 (9H, s, $C(CH_3)_3$), 3.50 (2H, t J = 6.5 Hz, $CH_2$), 3.71 (2H, t J = 6.5 Hz, $CH_2$), 4.36 (2H, s, $CH_2$), 6.92 (1H, d J = 2.5 Hz, Ar-H), 7.06 (1H, d J = 2.5 Hz, Ar-H), 7.17 – 7.18 (1H, m, Ar-H), 7.19 – 7.23 (3H, m, Ar-H), 7.25 (1H, d J = 2.5 Hz, Ar-H), 7.34 – 7.36 (1H, m, Ar-H), 7.40 (1H, m, Ar-H), 8.06 (1H, s, CH). **$^{13}$C{$^1$H} NMR** ($CDCl_3$) 29.7, 31.8 ($C(CH_3)_3$), 34.3, 34.9 ($C(CH_3)_3$), 52.2, 56.1, 58.4 ($CH_2$), 113.1, 118.1 (Ar-CH), 119.5, 120.9 (Ar-C), 121.1 (Ar-CH), 122.7, 122.9 (Ar-C), 123.6, 129.1, 129.5, 129.6, 132.3 (Ar-CH), 136.0, 141.5, 148.7 (Ar-C), 153.7, 156.6 (Ar-O), 165.0 (CH). **m/z** calc. $C_{30}H_{37}N_2O_2Cl_2$ = 527.2232, found 527.2232.

**Preparation of Al(1)Me: 1**$H_2$ (0.75 g, 1.48 mmol) was dissolved in toluene (30 ML) to which $AlMe_3$ (0.75 ML of a 2.0 M solution in hexane, 1.48 mmol) was added. This was stirred for 2 hours, after which time the solvent was removed *in-vacuo* and the product was recrystallised in hexane. After 1 day at – 20 $^o$C a crop of crystals were obtained which were filtered and dried. **$^1$H NMR** ($C_6D_6$) -0.46

(3H, s, $CH_3$), 1.36 (9H, s, $C(CH_3)_3$), 1.46 (9H, s, $C(CH_3)_3$), 1.77 (3H, s, $CH_3$), 1.82 (18H, d J = 5.0 Hz, $C(CH_3)_3$), 1.86 (1H, br s, $CH_2$), 1.99 – 2.14 (1H, m, $CH_2$), 2.42 (1H, dt J = 14.5 Hz, 4.5 Hz, $CH_2$), 2.68 (1H, d J = 12.0 Hz, $CH_2$), 2.80 – 2.94 (1H, m, $CH_2$), 3.69 (1H, d J = 12.0 Hz, $CH_2$), 6.78 (1H, d J = 2.5 Hz, Ar-H), 6.95 (1H, d J = 2.5 Hz, Ar-H), 7.31 (1H, s CH), 7.63 (1H, d J = 2.5 Hz, Ar-H), 7.75 (1H, d J = 2.5 Hz, Ar-H). **$^{13}C\{^1H\}$ NMR** ($C_6D_6$) -9.1, (Al-$CH_3$), 30.8, 30.9 ($C(CH_3)_3$), 32.2, 32.8 ($C(CH_3)_3$), 44.8 ($CH_3$), 52.6, 55.3, 59.9 ($CH_2$), 118.4, 123.1 (Ar-C), 124.6, 128.9, 132.5 (Ar-CH), 137.6, 138.9, 139.4, 142.1 (Ar-C), 157.4, 166.6 (Ar-O), 173.8 (CH). **Anal:** Calc for $C_{34}H_{53}N_2O_2Al$ C, 74.41, H 9.73, N 5.11. Found C 74.32, H 9.59, N 4.68.

**Preparation of Al(2)Me:** **2**$H_2$ (0.37 g, 0.64 mmol) was dissolved in toluene (5 $cm^3$) to which $AlMe_3$ (0.32 ML of a 2.0 M solution in hexane, 0.64 mmol) was added. This was stirred for 2 hours, after which time the solvent was removed *in-vacuo* and the product was recrystallised in hexane. After 7 days at – 20 ºC a crop of crystals were obtained which were filtered and dried. **$^1H$ NMR** ($C_6D_6$) -0.45 (3H, s, $CH_3$), 1.30 (9H, s, $C(CH_3)_3$), 1.35 (9H, s, $C(CH_3)_3$), 1.77 (9H, s, $C(CH_3)_3$), 1.88 (9H, s, $C(CH_3)_3$), 2.68 – 2.75 (2H, m, $CH_2$), 3.00 (1H, td J = 12.0 Hz, 4.0 Hz, $CH_2$), 3.20 (1H, td J = 12.0 Hz, 4.0 Hz, $CH_2$), 3.37 (1H, d J = 11.5 Hz, $CH_2$), 4.21 (1H, d J = 11.5 Hz, $CH_2$), 6.67 (1H, d J = 2.5 Hz, Ar-H), 6.78 (1H, d J = 2.5 Hz, Ar-H), 6.82 (1H, d J = 7.5 Hz, Ar-H), 6.89 (2H, d J = 7.5 Hz, Ar-H), 6.97 (2H, t J = 7.5 Hz, Ar-H), 7.25 (1H, s, CH), 7.57 (1H, d J = 2.5 Hz, Ar-H), 7.76 (1H, d J = 2.5 Hz, Ar-H). **$^{13}C\{^1H\}$ NMR** ($C_6D_6$) -8.2 (Al-$CH_3$), 30.1, 30.5, 31.6, 32.0 ($C(CH_3)_3$), 34.2, 35.8 ($C(CH_3)_3$), 50.8, 53.9, 59.0 ($CH_2$), 118.4 (Ar-C), 121.2, 123.2, 123.7 (Ar-CH), 124.2 (Ar-C), 128.3, 129.8, 132.1 (Ar-CH), 136.7, 138.0, 138.6, 139.1, 141.4 (Ar-CH), 149.1, 156.7 (Ar-O), 173.3 (CH).

**Preparation of Al(3)Me:** **3**$H_2$ (0.50 g, 1.22 mmol) was dissolved in toluene (20 $cm^3$) to which $AlMe_3$ (0.6 ML of a 2.0 M solution in hexane, 1.22 mmol) was added. This was stirred for 2 hours, after which time the solvent was removed *in-vacuo* and the product was recrystallised in hexane. After 5 days at – 20 ºC a crop of crystals were obtained which were filtered and dried. **$^1H$ NMR** ($C_6D_6$) -0.42 (3H, s, $CH_3$), 1.46 (9H, s, $C(CH_3)_3$), 1.65 – 1.76 (1H, m, $CH_2$), 1.79 (9H, s, $C(CH_3)_3$), 1.80 (3H, s, $CH_3$), 2.10 – 2.23 (1H, m, $CH_2$), 2.43 – 2.52 (1H, m, $CH_2$),

2.53 (3H, s, $CH_3$), 2.59 (1H, d J = 12.0 Hz, $CH_2$), 2.66 – 2.79 (1H, m, $CH_2$), 3.56 (1H, d J = 12.0 Hz, $CH_2$), 6.56 (1H, t J = 7.5 Hz, Ar-H), 6.76 (1H, dd J = 7.5 Hz, J = 1.0 Hz, Ar-H), 6.92 (1H, d J = 2.5 Hz, Ar-H), 7.23 (1H, d J = 7.0 Hz, Ar-H), 7.35 (1H, s, CH), 7.60 (1H, d J = 2.5 Hz, Ar-H). **$^{13}$C{$^{1}$H} NMR** ($C_6D_6$) -9.2, (Al-$CH_3$), 16.5 (CH3), 30.1, 32.3 (C(*C*$H_3$)$_3$), 34.4, 35.5 (*C*($CH_3$)$_3$), 44.1 ($CH_3$), 51.2, 54.4, 59.2 ($CH_2$), 115.3 (Ar-CH), 117.2, 122.1 (Ar-C), 123.8, 124.0 (Ar-CH), 131.2 (Ar-C), 131.4, 137.1 (Ar-CH) 138.2, 138.7 (Ar-C), 156.9, 167.2 (Ar-O), 172.7 (CH). **Anal:** Calc for $C_{27}H_{39}N_2O_2Al$ C, 71.97, H 8.72, N 6.22. Found C 71.6, H 8.65, N 6.08.

**Preparation of Al(4)Me: 5**$H_2$ (0.48 g, 1.22 mmol) was dissolved in toluene (20 $cm^3$) to which $AlMe_3$ (0.6 ML of a 2.0 M solution in hexane, 1.22 mmol) was added. This was stirred for 2 hours, after which time the solvent was removed *in-vacuo* and the product was recrystallised in hexane. After 30 days at – 20 ºC a crop of crystals were obtained which were filtered and dried. **$^{1}$H NMR** ($C_6D_6$) -0.39 (3H, s, $CH_3$), 1.44 (9H, s, C($CH_3$)$_3$), 1.78 (9H, s, C($CH_3$)$_3$), 1.79 (3H, s, $CH_3$), 1.84 (1H, t J = 5.0 Hz, $CH_2$), 2.07 – 2.16 (1H, m, $CH_2$), 2.53 (1H, dt J = 14.5 Hz, J = 5.0 Hz, $CH_2$), 2.62 – 2.67 (1H, m, $CH_2$), 2.69 (1H, d J = 12.0 Hz, $CH_2$), 3.46 (1H, d J = 12.0 Hz, $CH_2$), 6.48 – 6.53 (1H, m, Ar-H), 6.79 (1H, d J = 7.5 Hz, Ar-H), 6.89 (1H, d J = 2.5 Hz, Ar-H), 7.15 (1H, s, Ar-H), 7.16 – 7.18 (1H, m, Ar-H), 7.30 (1H, s, CH), 7.58 (1H, d J = 2.5 Hz, Ar-H). **$^{13}$C{$^{1}$H} NMR** ($C_6D_6$) -11.0 (Al-$CH_3$), 30.1, 32.3 (C(*C*$H_3$)$_3$), 34.4, 35.6 (*C*($CH_3$)$_3$), 44.0 ($CH_3$), 51.3, 53.9, 59.4 ($CH_2$), 115.4 (Ar-CH), 118.3, 121.9 (Ar-C), 122.9, 123.7, 123.9, 133.8, 137.2 (Ar-CH), 138.3, 138.7 (Ar-C), 156.8, 168.7 (Ar-O), 172.6 (CH). **Anal:** Calc for $C_{26}H_{37}N_2O_2Al$ C, 71.5, H 8.54, N 6.42. Found C 71.52, H 8.54, N 6.39.

**Preparation of Al(5)Me: 4**$H_2$ (0.45 g, 0.96 mmol) was dissolved in toluene (10 $cm^3$) to which $AlMe_3$ (0.5 ML of a 2.0 M solution in hexane, 0.96 mmol) was added. This was stirred for 2 hours, after which time the solvent was removed *in-vacuo* and the product was recrystallised in hexane. After 5 days at – 20 ºC a crop of crystals were obtained which were filtered and dried. **$^{1}$H NMR** ($C_6D_6$) -0.38 (3H, s, $CH_3$), 1.29 (9H, s, C($CH_3$)$_3$), 1.85 (9H, s, C($CH_3$)$_3$), 2.53 (3H, s, $CH_3$), 2.63 (1H, dq J = 12.5 Hz, J = 2.5 Hz, $CH_2$), 2.74 (1H, dd J = 14.5 Hz, J = 4.5 Hz, $CH_2$), 2.85 (1H, td J = 11.5 Hz, J = 4.0 Hz, $CH_2$), 3.10 (1H, sextet J = 6.0 Hz,

$CH_2$), 3.60 (1H, d J = 12.0 Hz, $CH_2$), 3.93 (1H, d J = 12.0 Hz, $CH_2$), 6.56 (1H, t J = 7.5 Hz, Ar-H), 6.66 (1H, d J = 2.5 Hz, Ar-H), 6.71 – 6.79 (2H, m, Ar-H), 6.89 – 6.98 (4H, m, Ar-H), 7.20 (1H, s, Ar-H), 7.23 (1H, s, CH), 7.52 (1H, d J = 2.5 Hz, Ar-H). **$^{13}C\{^1H\}$ NMR** ($C_6D_6$) -8.2 (Al-$CH_3$), 16.6 ($CH_3$), 30.4, 32.0 (C($CH_3$)$_3$), 34.2, 35.5 ($C$($CH_3$)$_3$), 50.8, 52.4, 60.2 ($CH_2$), 116.2 (Ar-CH), 117.7 (Ar-C), 123.1 (Ar-CH), 123.3 (Ar-C), 123.6, 125.0, 125.1, 128.6 (Ar-CH), 131.2 (Ar-C), 131.7, 137.3 (Ar-CH), 138.5, 138.6, 148.1 (Ar-C), 157.0, 165.8 (Ar-O), 172.2 (CH). **Anal:** Calc for $C_{32}H_{41}N_2O_2Al$ C, 75.0, H 8.06, N 5.47. Found C 69.9, H 7.84, N 5.54.

**Preparation of Al(6)Me: 6H$_2$** (0.50 g, 1.09 mmol) was dissolved in toluene (10 $cm^3$) to which $AlMe_3$ (0.545 ML of a 2.0 M solution in hexane, 1.09 mmol) was added. This was stirred for 2 hours, after which time the solvent was removed *in-vacuo* and the product was recrystallised in hexane. After 48 hours at – 20 ºC a crop of crystals were obtained which were filtered and dried. **$^1H$ NMR** ($C_6D_6$) -0.35 (3H, s, $CH_3$), 1.29 (9H, s, C($CH_3$)$_3$), 1.85 (9H, s, C($CH_3$)$_3$), 2.69 (1H, dq J = 12.5 Hz, J = 2.5 Hz, $CH_2$), 2.83 (1H, dd J = 14.5 Hz, J = 4.5 Hz, $CH_2$), 3.06 – 3.16 (2H, m, $CH_2$), 3.58 (1H, d J = 12.0 Hz, $CH_2$), 3.90 (1H, d J = 12.0 Hz, $CH_2$), 6.54 (1H, m, Ar-H), 6.68 (1H, d J = 2.5 Hz, Ar-H), 6.73 (1H, dd J = 8.5 Hz, J = 1.0 Hz, Ar-H), 6.77 (2H, tt J = 7.0 Hz, J = 1.5 Hz, Ar-H), 6.88 – 6.94 (4H, m, Ar-H), 7.12 (1H, s, CH), 7.18 (1H, d J = 2.0 Hz, Ar-H), 7.52 (1H, d J = 2.0 Hz, Ar-H). **$^{13}C\{^1H\}$ NMR** ($C_6D_6$) -8.3 (Al-$CH_3$), 30.3, 32.0 (C($CH_3$)$_3$), 34.2, 35.5 ($C$($CH_3$)$_3$), 49.7, 53.0, 59.2 ($CH_2$), 116.5 (Ar-CH), 118.7 (Ar-C), 122.2, 122.8 (Ar-CH), 123.6 (Ar-C), 123.8, 124.3, 125.3, 128.8, 134.0 (Ar-CH), 136.3 (Ar-C), 137.3 (Ar-CH), 138.6, 138.9 (Ar-C), 148.3, 156.6 (Ar-O), 172.3 (CH).

**Preparation of Al(7)Me: 7**$H_2$ (0.72 g, 1.53 mmol) was dissolved in toluene (10 $cm^3$) to which $AlMe_3$ (0.7700 ML of a 2.0 M solution in hexane, 1.53 mmol) was added. This was stirred for 2 hours, after which time the solvent was removed *in-vacuo* and the product was recrystallised in hexane. After 7 days at – 20 ºC a crop of crystals were obtained which were filtered and dried. **$^1H$ NMR** ($C_6D_6$) -0.48 (3H, s, $CH_3$), 1.44 (9H, s, C($CH_3$)$_3$), 1.73 (3H, s, $CH_3$), 1.79 (9H, s, C($CH_3$)$_3$), 1.94 – 2.14 (2H, m, $CH_2$), 2.46 (1H, dt J = 14.5 Hz, J = 5.0 Hz, $CH_2$), 2.61 (1H, d J = 12.0 Hz, $CH_2$), 2.65 – 2.78 (1H, m, $CH_2$), 3.49 (1H, d J = 12.0 Hz, $CH_2$), 6.58

(1H, d J = 2.5 Hz, Ar-H), 6.90 (1H, d J = 2.5 Hz, Ar-H), 6.98 (1H, s, CH), 7.38 (1H, d J = 2.5 Hz, Ar-H), 7.59 (1H, d J = 2.5 Hz, Ar-H). **$^{13}C\{^1H\}$ NMR** ($C_6D_6$) - 9.4 (Al-$CH_3$), 30.1, 32.2 (C($CH_3$)$_3$), 34.4, 35.5 ($C$($CH_3$)$_3$), 44.0 ($CH_3$), 51.5, 54.0, 59.3 ($CH_2$), 118.5, 118.8, 121.7 (Ar-C), 123.7, 124.2, 130.7, 135.8 (Ar-CH), 138.6, 139.0 (Ar-C), 156.5, 161.8 (Ar-O), 171.3 (CH).

**Preparation of Al(8)Me: 8**$H_2$ (0.68 g, 1.28 mmol) was dissolved in toluene (20 $cm^3$) to which $AlMe_3$ (0.64 ML of a 2.0 M solution in hexane, 1.28 mmol) was added. This was stirred for 2 hours, after which time the solvent was removed *in-vacuo* and the product was recrystallised in hexane. After 48 hours at – 20 ºC a crop of crystals were obtained which were filtered and dried. **$^1H$ NMR** ($C_6D_6$) - 0.47 (3H, s, $CH_3$), 1.26 (9H, s, C($CH_3$)$_3$), 1.90 (9H, s, C($CH_3$)$_3$), 2.58 (2H, td J = 12.5 Hz, J = 5.5 Hz, $CH_2$), 2.78 (1H, td J = 12.0 Hz, J = 4.5 Hz, $CH_2$), 3.00 (1H, td J = 12.0 Hz, J = 6.0 Hz, $CH_2$), 3.51 (1H, d J = 12.0 Hz, $CH_2$), 3.82 (1H, d J = 12.0 Hz, $CH_2$), 6.55 (2H, t J = 2.5 Hz, Ar-H), 6.73 (1H, t J = 7.0 Hz, Ar-H), 6.83 (1H, s, CH), 6.87 (2H, d J = 7.5 Hz, Ar-H), 6.96 (2H, d J = 8.0 Hz, Ar-H), 7.36 (1H, d J = 2.5 Hz, Ar-H), 7.49 (1H, d J = 2.5 Hz, Ar-H). **$^{13}C\{^1H\}$ NMR** ($C_6D_6$) - 7.8 (Al-$CH_3$), 30.2, 32.0 (C($C$$H_3$)$_3$), 34.2, 35.6 ($C$($CH_3$)$_3$), 51.1, 51.6, 61.1 ($CH_2$), 119.1, 119.7, 122.3 (Ar-C), 123.8, 124.0, 124.5, 126.5, 128.7, 130.8, 135.9 (Ar-CH), 138.7, 138.8, 147.1 (Ar-C) 156.9, 161.0 (Ar-O), 170.3 (CH). **Anal:** Calc for $C_{31}H_{37}N_2O_2AlCl_2$ C, 65.61, H 6.57, N 4.94. Found C 62.20, H 6.38, N 4.68.

## 5.3 Polymerisation Procedures

### 5.3.1 Solvent-free polymerisation of *rac*-LA

For solvent-free polymerisations the monomer: initiator ratio employed was 300: 1 at a temperature of 130 °C. For Chapters 2 and 3, 2 g of *rac*-LA was used. After the reaction time, methanol was added to quench the reaction and the resulting solid dissolved in dichloromethane. The solvents were removed *in vacuo* and the resulting solid was washed with copious amounts of methanol to remove any unreacted monomer. $^1$H NMR spectroscopy ($CDCl_3$) and GPC (THF) were used to determine tacticity and molecular weights ($M_n$ and $M_w$) of the polymers

produced; $P_r$ (the probability of heterotactic linkages) were determined by analysis of the methine region of the homonuclear decoupled $^1$H NMR spectra.

### 5.3.2 Solution polymerisation of *rac*-LA

For solution polymerisations a monomer: initiator ratio of 100:1 was used. In all cases 0.7 g of lactide and the appropriate amount of initiator were dissolved in toluene (10 ML) these were placed in a pre-heated oil bath at the desired temperature and heated for the desired amount of time. One equivalent of benzyl alcohol was added to the solution polymerisations in Chapter 4. The reaction was quenched by the addition of methanol (20 ML). $^1$H NMR spectroscopy ($CDCl_3$) and GPC (THF) were used to determine tacticity and molecular weights ($M_n$ and $M_w$) of the polymers produced; $P_r$ (the probability of heterotactic linkages) were determined by analysis of the methine region of the homonuclear decoupled $^1$H NMR spectra.

### 5.3.3 Solvent-free polymerisation of *rac*-LA and isosorbide

For solvent-free polymerisations the monomer: initiator ratio employed was 300:1 at a temperature of 130 °C, in all cases 2 g of *rac*-LA was used. The amount of isosorbide was varied to give a 300:10:1, 300:20:1 and 300:30:1 ratio of *rac*-LA: isosorbide: initiator. After the reaction time (120 minutes) methanol (20 ML) was added to quench the reaction and the resulting solid was dissolved in dichloromethane. The solvents were removed *in vacuo* and the resulting solid was washed with copious amounts of methanol to remove any unreacted lactide monomer and copious amounts of water to remove any unreacted isosorbide. $^1$H NMR spectroscopy ($CDCl_3$) and GPC (THF) were used to determine tacticity and molecular weights ($M_n$ and $M_w$) of the polymers produced; $P_r$ (the probability of heterotactic linkages) were determined by analysis of the methine region of the homonuclear decoupled $^1$H NMR spectra.

### 5.3.4 Solution polymerisation of 1,3-dioxan-2-one (TMC)

For solution polymerisations the monomer: initiator ratio employed was 100:1 at a temperature of 80 °C, in all cases 0.493 g of 1,3-dioxan-2-one was used. After the reaction time (24 hours) and any resulting solid was dissolved in

dichloromethane. The solvents were removed *in vacuo* and the resulting solid was washed with copious amounts of methanol to remove any unreacted monomer. GPC (THF) was used to determine molecular weights ($M_n$ and $M_w$) of the polymers produced.

### 5.3.5 Solvent-free polymerisation of *rac*-LA and 1,3-dioxan-2-one (TMC)

For solvent-free polymerisations the monomer: initiator ratio employed was 300:1 at a temperature of 130 °C, in all cases 2 g of *rac*-LA were used. The amount of 1,3-dioxan-2-one was varied to give a 300:10:1, 300:20:1 and 300:30:1 ratio of *rac*-LA: 1,3-dioxan-2-one: initiator. After the reaction time (120 minutes) methanol (20 ML) was added to quench the reaction and the resulting solid was dissolved in dichloromethane. The solvents were removed *in vacuo* and the resulting solid was washed with copious amounts of methanol to remove any unreacted monomer. $^1$H NMR spectroscopy ($CDCl_3$) and GPC (THF) were used to determine tacticity and molecular weights ($M_n$ and $M_w$) of the polymers produced; $P_r$ (the probability of heterotactic linkages) was determined by analysis of the methine region of the homonuclear decoupled $^1$H NMR spectra.

## 5.4 Kinetic Studies

### 5.4.1 Kinetic Procedure for Chapter 2

*rac*-LA (0.05 g) in $d_8$-toluene (0.6 ML) was prepared with an initial concentration of 0.578 mol dm$^{-3}$, in a monomer to initiator ratio of 100: 1 using initiators Ti(**1/3**)O$^i$Pr, {Zr(**1/3**)O$^i$Pr}$_2$ and {Hf(**1/3**)O$^i$Pr}$_2$. The $^1$H NMR spectra of the samples were obtained at 80 °C over a period of 13 hours at 15 minute intervals. The relative concentrations of the monomer and polymer were determined from analysis of the $^1$H NMR spectra and a plot of $\ln[LA]_o/[LA]_t$ *vs* time was plotted.

### 5.4.2 Kinetic Procedure for Chapter 3

*rac*-LA (0.05 g) in $d_8$-toluene or $CDCl_3$ (0.6 ML) was prepared with an initial concentration of 0.578 mol $dm^{-3}$ and a monomer to initiator ratio of 100: 1. For initiators Ti(**1-4**)($O^iPr$)$_2$, Zr(**1/2**)($O^iPr$)$_2$ and Hf(**1/2**)($O^iPr$)$_2$, the solvent used was $d_8$-toluene and the $^1$H NMR spectra of the sample was obtained at 80 °C over a period of 13 hours at 15 minute intervals for Ti(**1-3**)($O^iPr$)$_2$. The $^1$H NMR spectra of the sample for Ti(**4**)($O^iPr$)$_2$ were also collected at 80 °C but over a period 2 hours at 15 minute intervals. For the initiators Zr(**3**)($O^iPr$)$_2$ and Hf(**3**)($O^iPr$)$_2$, the solvent used was $CDCl_3$ and the $^1$H NMR spectra of the sample was obtained at 25 °C over a period 13 hours at one hour intervals. The $^1$H NMR spectra of the samples for Zr(**4**)($O^iPr$)$_2$ and Hf(**4**)($O^iPr$)$_2$ were collected at 25 °C but over a period of 2 hours at 15 minute intervals.

For the determination of the rate of degradation of the polymer, a solution of *rac*-LA (0.05 g) in $CDCl_3$ (0.6 ML) was prepared with an initial concentration of 0.578 mol $dm^{-3}$ with a monomer to initiator ratio of 100:1 using Hf(**3/4**)($O^iPr$)$_2$ as the initiator. After a period of 110 minutes, the sample was removed and 0.1 ML of $CD_3OD$ was added. The sample was returned and the spectra recorded for a further 55 minutes. The mole fractions of the polymer/methyl lactate/monomer were recorded and a plot of mole fraction *vs* time was plotted.

### 5.4.3 Kinetic Procedure for Chapter 4

A solution of either *rac*-LA, *L*-LA or *D*-LA (0.05 g) in $d_8$-toluene (0.6 ML) was prepared with an initial concentration of 0.578 mol $dm^{-3}$ with a monomer to initiator ratio of 100: 1 using initiators Al(**1/3/5**)Me. One equivalent of benzyl alcohol (5 μl) was added to generate the initiator *in situ*. The $^1$H NMR spectra of the samples were obtained at 80 °C over a period of 24 hours at 15 minute intervals. The relative concentrations of the monomer and polymer were determined from analysis of the $^1$H NMR spectra and a plot of $\ln[LA]_o/[LA]_t$ *vs* time was plotted.

1. B. M. Chamberlain, M. Cheng, D. R. Moore, T. M. Ovitt, E. B. Lobkovsky and G. W. Coates, *J. Am. Chem. Soc.*, 2001, **123**, 3229-3238.
2. G. M. Sheldrick, *University of Gottingen, Germany*, 1997.
3. A. Sokolowski, J. Muller, T. Weyhermuller, R. Schnepf, P. Hildebrandt, K. Hildenbrand, E. Bothe and K. Wieghardt, *J. Am. Chem. Soc.*, 1997, **119**, 8889-8900.
4. T. Ariga, T. Takata and T. Endo, *J. Polym. Sci., Part A: Polym. Chem.*, 1993, **31**, 581-584.

# Appendix

## X-ray Crystal Structure Data

# X-ray Crystal Structure Data for Chapter 2

Ti(**1**)O$^{i}$Pr: There was a 13 % twinning about the reciprocal 0,0,1 direction

| | |
|---|---|
| Identification code | k08mdj10 |
| Empirical formula | C39 H55 N O4 Ti |
| Formula weight | 649.74 |
| Temperature | 150(2) K |
| Wavelength | 0.71073 Å |
| Crystal system, space group | Triclinic, *P*-1 |
| Unit cell dimensions | a = 10.8850(4)Å α = 82.401(3) °<br>b = 11.8990(5)Å β = 80.713(2) °<br>c = 14.7140(5)Å γ = 76.743(1) ° |
| Volume | 1821.65(12) Å$^3$ |
| Z, Calculated density | 2, 1.185 Mg/m$^3$ |
| Absorption coefficient | 0.274 mm$^{-1}$ |
| F(000) | 700 |
| Crystal size | 0.50 x 0.40 x 0.20 mm |
| Theta range for data collection | 3.54 to 25.24$^{o}$ |
| Limiting indices | -12≤h≤12; -14≤k≤14; -17≤l≤17 |
| Reflections collected | 17487 |
| Independent reflections | 17487 [R(int) = 0.0000] |
| Reflections observed (>2□) | 14118 |
| Data Completeness | 0.968 |
| Absorption correction | Semi-empirical from equivalents |
| Max. and min. transmission | 0.92 and 0.88 |
| Refinement method | Full-matrix least-squares on F$^2$ |
| Data / restraints / parameters | 17487 / 0 / 421 |
| Goodness-of-fit on F$^2$ | 1.116 |
| Final R indices [I>2σ(I)] | $R_1$ = 0.0762 $wR_2$ = 0.1717 |
| R indices (all data) | $R_1$ = 0.0982 $wR_2$ = 0.1888 |
| Largest diff. peak and hole | 0.825 and -0.423 eÅ$^{-3}$ |

Ti(**2**)O$^{i}$Pr

| | |
|---|---|
| Identification code | k08mdj12 |
| Empirical formula | C40 H57 N O4 Ti |
| Formula weight | 663.77 |
| Temperature | 150(2) K |
| Wavelength | 0.71073 A |
| Crystal system, space group | Triclinic, *P*-1 |
| Unit cell dimensions | a = 10.9500(5) A α = 66.472(2) °<br>b = 14.0800(6) A β = 74.247(2) °<br>c = 14.2790(8) A γ = 86.724(2) ° |
| Volume | 1939.37(16) Å$^3$ |
| Z, Calculated density | 2, 1.137 Mg/m$^3$ |
| Absorption coefficient | 0.258 mm^-1 |
| F(000) | 716 |
| Crystal size | 0.15 x 0.10 x 0.10 mm |
| Theta range for data collection | 3.64 to 25.01 ° |
| Limiting indices | -12≤h≤13, -16≤k≤16, -16≤l≤16 |
| Reflections collected / unique | 17062 / 6752 [R(int) = 0.0529] |
| Completeness to theta = 25.01 | 98.9 % |
| Absorption correction | None |
| Max. and min. transmission | 0.9746 and 0.9623 |
| Refinement method | Full-matrix least-squares on F$^2$ |
| Data / restraints / parameters | 6752 / 0 / 430 |
| Goodness-of-fit on F^2 | 1.029 |
| Final R indices [I>2σ(I)] | $R_1$ = 0.0554, $wR_2$ = 0.1342 |
| R indices (all data) | $R_1$ = 0.0829, $wR_2$ = 0.1524 |
| Largest diff. peak and hole | 0.901 and -0.587 e.Å$^{-3}$ |

Ti(**3**)O$^{i}$Pr

| | |
|---|---|
| Identification code | h09mdj05 |
| Empirical formula | C43 H63 N O4 Ti |
| Formula weight | 705.84 |
| Temperature | 150(2) K |
| Wavelength | 0.71073 A |
| Crystal system, space group | Monoclinic, $P2_1/a$ |
| Unit cell dimensions | a = 11.3930(3) Å α = 90 °<br>b = 27.2830(5) Å β = 97.5310(10) °<br>c = 13.1530(4) Å γ = 90 ° |
| Volume | 4053.15(18) Å$^3$ |
| Z, Calculated density | 4, 1.157 Mg/m$^3$ |
| Absorption coefficient | 0.251 mm$^{-1}$ |
| F(000) | 1528 |
| Crystal size | 0.20 x 0.13 x 0.10 mm |
| Theta range for data collection | 3.74 to 25.08 ° |
| Limiting indices | -13≤h≤13, -32≤k≤32, -15≤l≤15 |
| Reflections collected / unique | 56867 / 7168 [R(int) = 0.1222] |
| Completeness to theta = 25.08 | 99.4 % |
| Absorption correction | None |
| Max. and min. transmission | 0.9753 and 0.9515 |
| Refinement method | Full-matrix least-squares on F$^2$ |
| Data / restraints / parameters | 7168 / 0 / 459 |
| Goodness-of-fit on F^2 | 1.037 |
| Final R indices [I>2σ(I)] | $R_1$ = 0.0523, w$R_2$ = 0.1246 |
| R indices (all data) | $R_1$ = 0.0955, w$R_2$ = 0.1510 |
| Largest diff. peak and hole | 0.351 and -0.495 e.A$^{-3}$ |

Ti(**4**)O$^{i}$Pr

| | |
|---|---|
| Identification code | h08mdj06 |
| Empirical formula | C39 H54 Cl N O4 Ti |
| Formula weight | 684.18 |
| Temperature | 150(2) K |
| Wavelength | 0.71073 Å |
| Crystal system, space group | Triclinic, *P*-1 |
| Unit cell dimensions | a = 11.0570(4) A α = 75.615(2) °<br>b = 12.0150(5) A β = 89.264(2) °<br>c = 16.4190(5) A γ = 62.851(2) ° |
| Volume | 1867.26(12) $A^3$ |
| Z, Calculated density | 2, 1.217 $Mg/m^3$ |
| Absorption coefficient | 0.340 $mm^{-1}$ |
| F(000) | 732 |
| Crystal size | 0.20 x 0.12 x 0.10 mm |
| Theta range for data collection | 3.55 to 25.00 ° |
| Limiting indices | -13≤h≤13, -14≤k≤14, -19≤l≤19 |
| Reflections collected / unique | 27486 / 6556 [R(int) = 0.1261] |
| Completeness to theta = 25.00 | 99.4 % |
| Absorption correction | None |
| Max. and min. transmission | 0.9668 and 0.9352 |
| Refinement method | Full-matrix least-squares on $F^2$ |
| Data / restraints / parameters | 6556 / 0 / 430 |
| Goodness-of-fit on $F^2$ | 1.035 |
| Final R indices [I>2σ(I)] | $R_1$ = 0.0597, $wR_2$ = 0.1469 |
| R indices (all data) | $R_1$ = 0.0913, $wR_2$ = 0.1693 |
| Largest diff. peak and hole | 1.118 and -0.621 $e.A^{-3}$ |

{Zr(**1**)O$^{i}$Pr}$_2$

| | |
|---|---|
| Identification code | k08mdj11 |
| Empirical formula | C49.50 H67 N O4 Zr |
| Formula weight | 831.26 |
| Temperature | 150(2) K |
| Wavelength | 0.71073 A |
| Crystal system, space group | Monoclinic, $P2_1/n$ |
| Unit cell dimensions | a = 12.7140(2) A α = 90 °<br>b = 15.7070(3) A β = 91.6470(10) °<br>c = 22.6870(4) A γ = 90 ° |
| Volume | 4528.69(14) A$^3$ |
| Z, Calculated density | 4, 1.219 Mg/m$^3$ |
| Absorption coefficient | 0.285 mm$^{-1}$ |
| F(000) | 1772 |
| Crystal size | 0.20 x 0.15 x 0.10 mm |
| Theta range for data collection | 3.52 to 24.98 ° |
| Limiting indices | -15≤h≤14, -18≤k≤18, -26≤l≤26 |
| Reflections collected / unique | 37439 / 7897 [R(int) = 0.1143] |
| Completeness to theta = 24.98 | 99.4 % |
| Absorption correction | None |
| Max. and min. transmission | 0.9720 and 0.9451 |
| Refinement method | Full-matrix least-squares on F$^2$ |
| Data / restraints / parameters | 7897 / 0 / 530 |
| Goodness-of-fit on F$^2$ | 1.019 |
| Final R indices [I>2σ(I)] | $R_1$ = 0.0429, $wR_2$ = 0.0833 |
| R indices (all data) | $R_1$ = 0.0754, $wR_2$ = 0.0951 |
| Largest diff. peak and hole | 0.407 and -0.459 e.A$^{-3}$ |

{Zr(**2**)O$^{i}$Pr}$_2$

| | |
|---|---|
| Identification code | k08mdj13 |
| Empirical formula | C46 H71 N O4 Zr |
| Formula weight | 793.26 |
| Temperature | 150(2) K |
| Wavelength | 0.71073 A |
| Crystal system, space group | Triclinic, *P*-1 |
| Unit cell dimensions | a = 11.3350(3) A α = 103.5680(10) °<br>b = 13.6260(3) A β = 101.1950(10) °<br>c = 15.5330(4) A γ = 96.8930(10) ° |
| Volume | 2253.01(10) A$^3$ |
| Z, Calculated density | 2, 1.169 Mg/m$^3$ |
| Absorption coefficient | 0.283 mm$^{-1}$ |
| F(000) | 852 |
| Crystal size | 0.20 x 0.15 x 0.10 mm |
| Theta range for data collection | 3.52 to 24.03 ° |
| Limiting indices | -12≤h≤12, -15≤k≤15, -17≤l≤17 |
| Reflections collected / unique | 16007 / 6966 [R(int) = 0.0442] |
| Completeness to theta = 24.03 | 98.2 % |
| Absorption correction | None |
| Max. and min. transmission | 0.9722 and 0.9455 |
| Refinement method | Full-matrix least-squares on F$^2$ |
| Data / restraints / parameters | 6966 / 0 / 487 |
| Goodness-of-fit on F$^2$ | 1.004 |
| Final R indices [I>2σ(I)] | $R_1$ = 0.0446, $wR_2$ = 0.1084 |
| R indices (all data) | $R_1$ = 0.0600, $wR_2$ = 0.1193 |
| Largest diff. peak and hole | 0.912 and -0.461 e.A^$^{-3}$ |

{Zr(**3**)O$^{i}$Pr}$_2$

| | |
|---|---|
| Identification code | k09mdj01 |
| Empirical formula | C46 H70 N O4 Zr |
| Formula weight | 792.25 |
| Temperature | 150(2) K |
| Wavelength | 0.71073 Å |
| Crystal system, space group | Triclinic, *P*-1 |
| Unit cell dimensions | a = 11.6110(2) A α = 67.638(2) °<br>b = 14.8520(3) A β = 76.3320(10) °<br>c = 16.3050(4) A γ = 67.9660(10) ° |
| Volume | 2395.97(9) A$^3$ |
| Z, Calculated density | 2, 1.098 Mg/m$^3$ |
| Absorption coefficient | 0.266 mm$^{-1}$ |
| F(000) | 850 |
| Crystal size | 0.20 x 0.10 x 0.10 mm |
| Theta range for data collection | 3.63 to 25.05 ° |
| Limiting indices | -13≤h≤13, -17≤k≤17, -19≤l≤19 |
| Reflections collected / unique | 37634 / 8400 [R(int) = 0.0658] |
| Completeness to theta = 25.05 | 99.1 % |
| Absorption correction | None |
| Max. and min. transmission | 0.9738 and 0.9486 |
| Refinement method | Full-matrix least-squares on F$^2$ |
| Data / restraints / parameters | 8400 / 0 / 487 |
| Goodness-of-fit on F$^2$ | 1.078 |
| Final R indices [I>2σ(I)] | $R_1$ = 0.0576, $wR_2$ = 0.1586 |
| R indices (all data) | $R_1$ = 0.0742, $wR_2$ = 0.1712 |
| Largest diff. peak and hole | 1.900 and -0.523 e.A$^{-3}$ |

{Hf(**1**)O$^{i}$Pr}$_2$

| | |
|---|---|
| Identification code | k10mdj19 |
| Empirical formula | C49.50 H67 Hf N O4 |
| Formula weight | 918.53 |
| Temperature | 150(2) K |
| Wavelength | 0.71073 Å |
| Crystal system, space group | Monoclinic, $P2_1/n$ |
| Unit cell dimensions | a = 12.7000(3) Å α = 90 °<br>b = 15.7100(3) Å β = 91.878(1) °<br>c = 22.5950(6) Å γ = 90 ° |
| Volume | 4505.67(18) A$^3$ |
| Z, Calculated density | 4, 1.354 Mg/m$^3$ |
| Absorption coefficient | 2.358 mm$^{-1}$ |
| F(000) | 1900 |
| Crystal size | 0.20 x 0.10 x 0.10 mm |
| Theta range for data collection | 3.52 to 27.50 ° |
| Limiting indices | -16≤h≤16, -20≤k≤20, -29≤l≤29 |
| Reflections collected / unique | 75384 / 10293 [R(int) = 0.0823] |
| Completeness to theta = 27.50 | 99.4 % |
| Absorption correction | Semi-empirical from equivalents |
| Max. and min. transmission | 0.7984 and 0.6499 |
| Refinement method | Full-matrix least-squares on F$^2$ |
| Data / restraints / parameters | 10293 / 0 / 450 |
| Goodness-of-fit on F$^2$ | 1.059 |
| Final R indices [I>2σ(I)] | $R_1$ = 0.0416, $wR_2$ = 0.0962 |
| R indices (all data) | $R_1$ = 0.0636, $wR_2$ = 0.1072 |
| Largest diff. peak and hole | 1.999 and -1.408 e.A$^{-3}$ |

# X-ray Crystal Structure Data for Chapter 3

Ligand **2**$H_2$

| | |
|---|---|
| Identification code | k10mdj23 |
| Empirical formula | C38 H54 N2 O2 |
| Formula weight | 570.83 |
| Temperature | 150(2) K |
| Wavelength | 0.71073 Å |
| Crystal system, space group | triclinic, *P*-1 |
| Unit cell dimensions | a = 10.5980(2) Å α = 104.833(1)°<br>b = 12.5280(2) Å β = 102.041(1) °<br>c = 14.7130(3) Å γ = 103.977(1)° |
| Volume | 1754.65(6) $A^3$ |
| Z, Calculated density | 2, 1.080 $Mg/m^3$ |
| Absorption coefficient | 0.066 $mm^{-1}$ |
| F(000) | 624 |
| Crystal size | 0.40 x 0.30 x 0.20 mm |
| Theta range for data collection | 3.54 to 27.52 ° |
| Limiting indices | -13≤h≤13, -16≤k≤16, -19≤l≤19 |
| Reflections collected / unique | 33522 / 7998 [R(int) = 0.0594] |
| Completeness to theta = 27.52 | 99.1 % |
| Absorption correction | None |
| Max. and min. transmission | 0.9870 and 0.9743 |
| Refinement method | Full-matrix least-squares on $F^2$ |
| Data / restraints / parameters | 7998 / 0 / 403 |
| Goodness-of-fit on $F^2$ | 1.012 |
| Final R indices [I>2σ(I)] | $R_1$ = 0.0478, $wR_2$ = 0.1171 |
| R indices (all data) | $R_1$ = 0.0776, $wR_2$ = 0.1352 |
| Largest diff. peak and hole | 0.185 and -0.225 $e.A^{-3}$ |

Ti(**1**)($O^iPr$)$_2$

| | |
|---|---|
| Identification code | h09mdj07 |
| Empirical formula | C39 H64 N2 O4 Ti |
| Formula weight | 672.82 |
| Temperature | 150(2) K |
| Wavelength | 0.71073 A |
| Crystal system, space group | Monoclinic, $P2_1/c$ |
| Unit cell dimensions | a = 14.5370(3) Å α = 90 °<br>b = 20.9780(4) Å β = 114.4370(10) °<br>c = 14.0970(2) Å γ = 90 ° |
| Volume | 3913.86(12) $A^3$ |
| Z, Calculated density | 4, 1.142 $Mg/m^3$ |
| Absorption coefficient | 0.257 $mm^{-1}$ |
| F(000) | 1464 |
| Crystal size | 0.20 x 0.20 x 0.15 mm |
| Theta range for data collection | 3.72 to 26.01 ° |
| Limiting indices | -17≤h≤17, -25≤k≤25, -17≤l≤17 |
| Reflections collected / unique | 51088 / 7670 [R(int) = 0.0767] |
| Completeness to theta = 26.01 | 99.5 % |
| Absorption correction | None |
| Refinement method | Full-matrix least-squares on $F^2$ |
| Data / restraints / parameters | 7670 / 0 / 466 |
| Goodness-of-fit on $F^2$ | 1.000 |
| Final R indices [I>2sigma(I)] | $R_1$ = 0.0408, $wR_2$ = 0.0960 |
| R indices (all data) | $R_1$ = 0.0651, $wR_2$ = 0.1105 |
| Largest diff. peak and hole | 0.237 and -0.379 $e.A^{-3}$ |

Ti(**2**)($O^iPr$)$_2$

| | |
|---|---|
| Identification code | k09mdj15 |
| Empirical formula | C44 H66 N2 O4 Ti |
| Formula weight | 734.89 |
| Temperature | 150(2) K |
| Wavelength | 0.71073 A |
| Crystal system, space group | Monoclinic, *C2/c* |
| Unit cell dimensions | a = 24.0590(3) Å α = 90 °<br>b = 18.0360(3) Å β = 102.7400(10) °<br>c = 20.0870(3) Å γ = 90 ° |
| Volume | 8501.7(2) $A^3$ |
| Z, Calculated density | 8, 1.148 $Mg/m^3$ |
| Absorption coefficient | 0.242 $mm^{-1}$ |
| F(000) | 3184 |
| Crystal size | 0.25 x 0.25 x 0.20 mm |
| Theta range for data collection | 3.85 to 27.47 ° |
| Limiting indices | -29≤h≤31, -23≤k≤23, -26≤l≤26 |
| Reflections collected / unique | 18758 / 9698 [R(int) = 0.0265] |
| Completeness to theta = 27.47 | 99.4 % |
| Absorption correction | None |
| Refinement method | Full-matrix least-squares on $F^2$ |
| Data / restraints / parameters | 9698 / 0 / 511 |
| Goodness-of-fit on $F^2$ | 1.016 |
| Final R indices [I>2σ(I)] | $R_1$ = 0.0413, $wR_2$ = 0.0980 |
| R indices (all data) | $R_1$ = 0.0603, $wR_2$ = 0.1088 |
| Largest diff. peak and hole | 0.307 and -0.395 $e.A^{-3}$ |

Zr(**1**)($O^iPr$)$_2$

| | |
|---|---|
| Identification code | k10mdj08 |
| Empirical formula | C39 H64 N2 O4 Zr |
| Formula weight | 716.14 |
| Temperature | 150(2) K |
| Wavelength | 0.71073 A |
| Crystal system, space group | Monoclinic, $P2_1/c$ |
| Unit cell dimensions | a = 14.6670(2) Å α = 90 °<br>b = 21.1850(4) Å β = 114.0370(10) °<br>c = 14.0480(3) Å γ = 90 ° |
| Volume | 3986.48(13) $A^3$ |
| Z, Calculated density | 4, 1.193 $Mg/m^3$ |
| Absorption coefficient | 0.314 $mm^{-1}$ |
| F(000) | 1536 |
| Crystal size | 0.20 x 0.20 x 0.20 mm |
| Theta range for data collection | 3.52 to 27.50 ° |
| Limiting indices | -18≤h≤19, -24≤k≤27, -18≤l≤17 |
| Reflections collected / unique | 84036 / 9117 [R(int) = 0.0638] |
| Completeness to theta = 27.50 | 99.6 % |
| Absorption correction | None |
| Max. and min. transmission | 0.9399 and 0.9399 |
| Refinement method | Full-matrix least-squares on $F^2$ |
| Data / restraints / parameters | 9117 / 0 / 463 |
| Goodness-of-fit on $F^2$ | 1.051 |
| Final R indices [I>2σ(I)] | $R_1$ = 0.0333, $wR_2$ = 0.0767 |
| R indices (all data) | $R_1$ = 0.0474, $wR_2$ = 0.0829 |
| Largest diff. peak and hole | 0.593 and -0.599 $e.A^{-3}$ |

$Zr(\mathbf{2})(O^iPr)_2$

| | |
|---|---|
| Identification code | k09mdj13 |
| Empirical formula | C44 H66 N2 O4 Zr |
| Formula weight | 778.21 |
| Temperature | 150(2) K |
| Wavelength | 0.71073 Å |
| Crystal system, space group | Monoclinic, *C2/c* |
| Unit cell dimensions | a = 24.3950(3) Å α = 90 °<br>b = 17.9500(3) Å β = 102.6020(10) °<br>c = 20.0070(3) Å γ = 90 ° |
| Volume | 8549.8(2) $A^3$ |
| Z, Calculated density | 8, 1.209 $Mg/m^3$ |
| Absorption coefficient | 0.298 $mm^{-1}$ |
| F(000) | 3328 |
| Crystal size | 0.25 x 0.10 x 0.10 mm |
| Theta range for data collection | 3.61 to 27.48 ° |
| Limiting indices | -31≤h≤31, -23≤k≤23, -25≤l≤25 |
| Reflections collected / unique | 82109 / 9779 [R(int) = 0.1021] |
| Completeness to theta = 27.48 | 99.7 % |
| Absorption correction | None |
| Refinement method | Full-matrix least-squares on $F^2$ |
| Data / restraints / parameters | 9779 / 0 / 511 |
| Goodness-of-fit on $F^2$ | 1.131 |
| Final R indices [I>2σ(I)] | R1 = 0.0599, wR2 = 0.1115 |
| R indices (all data) | R1 = 0.0953, wR2 = 0.1229 |
| Largest diff. peak and hole | 0.832 and -0.835 $e.A^{-3}$ |

Hf(**1**)($O^iPr$)$_2$

| | |
|---|---|
| Identification code | k10mdj14 |
| Empirical formula | C39 H64 Hf N2 O4 |
| Formula weight | 803.41 |
| Temperature | 150(2) K |
| Wavelength | 0.71073 Å |
| Crystal system, space group | monoclinic, $P2_1/c$ |
| Unit cell dimensions | a = 14.6520(3) Å α = 90 °<br>b = 21.1300(5) Å β = 114.074(2) °<br>c = 14.0640(4) Å γ = 90 ° |
| Volume | 3975.44(17) $A^3$ |
| Z, Calculated density | 4, 1.342 $Mg/m^3$ |
| Absorption coefficient | 2.662 $mm^{-1}$ |
| F(000) | 1664 |
| Crystal size | 0.20 x 0.10 x 0.10 mm |
| Theta range for data collection | 3.52 to 27.48 ° |
| Limiting indices | -19≤h≤18, -27≤k≤27, -18≤l≤18 |
| Reflections collected / unique | 73379 / 9085 [R(int) = 0.0512] |
| Completeness to theta = 27.48 | 99.7 % |
| Absorption correction | None |
| Max. and min. transmission | 0.7767 and 0.6181 |
| Refinement method | Full-matrix least-squares on $F^2$ |
| Data / restraints / parameters | 9085 / 0 / 458 |
| Goodness-of-fit on $F^2$ | 1.074 |
| Final R indices [I>2σ(I)] | R1 = 0.0249, wR2 = 0.0556 |
| R indices (all data) | R1 = 0.0316, wR2 = 0.0586 |
| Largest diff. peak and hole | 1.554 and -0.956 $e.A^{-3}$ |

Hf(**2**)($O^iPr$)$_2$

| | |
|---|---|
| Identification code | h10mdj08 |
| Empirical formula | C44 H66 Hf N2 O4 |
| Formula weight | 865.48 |
| Temperature | 150(2) K |
| Wavelength | 0.71073 Å |
| Crystal system, space group | Monoclinic, *C*2/*c* |
| Unit cell dimensions | a = 24.3640(2) Å α = 90 °<br>b = 17.9370(2) Å β = 102.8010(10) °<br>c = 20.0680(2) Å γ = 90 ° |
| Volume | 8552.08(15) $A^3$ |
| Z, Calculated density | 8, 1.344 $Mg/m^3$ |
| Absorption coefficient | 2.480 $mm^{-1}$ |
| F(000) | 3584 |
| Crystal size | 0.20 x 0.20 x 0.10 mm |
| Theta range for data collection | 3.86 to 27.49 ° |
| Limiting indices | -31≤h≤31, -23≤k≤23, -23≤l≤26 |
| Reflections collected / unique | 65155 / 9780 [R(int) = 0.0631] |
| Completeness to theta = 27.49 | 99.6 % |
| Absorption correction | multi-scan |
| Max. and min. transmission | 0.7895 and 0.6368 |
| Refinement method | Full-matrix least-squares on $F^2$ |
| Data / restraints / parameters | 9780 / 0 / 541 |
| Goodness-of-fit on $F^2$ | 1.093 |
| Final R indices [I>2σ(I)] | $R_1$ = 0.0314, $wR_2$ = 0.0656 |
| R indices (all data) | $R_1$ = 0.0431, $wR_2$ = 0.0727 |
| Largest diff. peak and hole | 0.986 and -1.312 $e.A^{-3}$ |

Hf(**3**)($O^iPr$)$_2$

| | |
|---|---|
| Identification code | k10mdj17 |
| Empirical formula | C38 H64 Hf N2 O4 |
| Formula weight | 791.40 |
| Temperature | 150(2) K |
| Wavelength | 0.71073 A |
| Crystal system, space group | Monoclinic, $P2_1/c$ |
| Unit cell dimensions | a = 11.05200(10) Å α = 90 °<br>b = 24.7750(3) Å β = 97.6680(10) °<br>c = 14.5020(2) Å γ = 90 ° |
| Volume | 3935.33(8) $A^3$ |
| Z, Calculated density | 4, 1.336 $Mg/m^3$ |
| Absorption coefficient | 2.688 $mm^{-1}$ |
| F(000) | 1640 |
| Crystal size | 0.20 x 0.10 x 0.10 mm |
| Theta range for data collection | 2.95 to 27.46 ° |
| Limiting indices | -14≤h≤14, -32≤k≤31, -18≤l≤18 |
| Reflections collected / unique | 56183 / 8956 [R(int) = 0.0972] |
| Completeness to theta = 27.46 | 99.6 % |
| Absorption correction | Semi-empirical from equivalents |
| Max. and min. transmission | 0.7748 and 0.6154 |
| Refinement method | Full-matrix least-squares on $F^2$ |
| Data / restraints / parameters | 8956 / 0 / 420 |
| Goodness-of-fit on $F^2$ | 1.063 |
| Final R indices [I>2σ(I)] | $R_1$ = 0.0347, $wR_2$ = 0.0679 |
| R indices (all data) | $R_1$ = 0.0544, $wR_2$ = 0.0743 |
| Largest diff. peak and hole | 0.955 and -1.466 $e.A^{-3}$ |

# X-ray Crystal Structure Data for Chapter 4

Al(**2**)Me

| | |
|---|---|
| Identification code | k11mdj22 |
| Empirical formula | C39 H55 Al N2 O2 |
| Formula weight | 610.83 |
| Temperature | 150(2) K |
| Wavelength | 0.71073 Å |
| Crystal system, space group | Orthorhombic, *Pcab* |
| Unit cell dimensions | a = 10.0400(5) Å α = 90 °<br>b = 22.8750(14) Å β = 90 °<br>c = 31.7450(18) Å γ = 90 ° |
| Volume | 7290.7(7) $A^3$ |
| Z, Calculated density | 8, 1.113 $Mg/m^3$ |
| Absorption coefficient | 0.090 $mm^{-1}$ |
| F(000) | 2656 |
| Crystal size | 0.50 x 0.20 x 0.10 mm |
| Theta range for data collection | 3.56 to 25.02 ° |
| Limiting indices | -11≤h≤11, -25≤k≤27, -36≤l≤37 |
| Reflections collected / unique | 58588 / 6295 [R(int) = 0.1130] |
| Completeness to theta = 25.02 | 98.0 % |
| Absorption correction | None |
| Refinement method | Full-matrix least-squares on $F^2$ |
| Data / restraints / parameters | 6295 / 0 / 410 |
| Goodness-of-fit on $F^2$ | 1.041 |
| Final R indices [I>2σ(I)] | $R_1$ = 0.0583, $wR_2$ = 0.1168 |
| R indices (all data) | $R_1$ = 0.1157, $wR_2$ = 0.1393 |
| Largest diff. peak and hole | 0.576 and -0.324 $e.A^{-3}$ |

Al(**3**)Me

| | |
|---|---|
| Identification code | h10mdj22 |
| Empirical formula | C27 H39 Al N2 O2 |
| Formula weight | 450.58 |
| Temperature | 150(2) K |
| Wavelength | 0.71073 Å |
| Crystal system, space group | Triclinic, *P*-1 |
| Unit cell dimensions | a = 9.7286(7) Å α = 110.181(4) °<br>b = 12.5296(10) Å β = 109.510(4) °<br>c = 13.0282(10) Å γ = 103.090(5) ° |
| Volume | 1295.98(17) $A^3$ |
| Z, Calculated density | 2, 1.155 $Mg/m^3$ |
| Absorption coefficient | 0.103 $mm^{-1}$ |
| F(000) | 488 |
| Crystal size | 0.10 x 0.10 x 0.10 mm |
| Theta range for data collection | 3.01 to 24.84 ° |
| Limiting indices | -11≤h≤10, -14≤k≤14, -15≤l≤15 |
| Reflections collected / unique | 10691 / 4417 [R(int) = 0.0835] |
| Completeness to theta = 24.84 | 98.2 % |
| Absorption correction | None |
| Refinement method | Full-matrix least-squares on $F^2$ |
| Data / restraints / parameters | 4417 / 0 / 302 |
| Goodness-of-fit on $F^2$ | 1.021 |
| Final R indices [I>2σ(I)] | $R_1$ = 0.0615, $wR_2$ = 0.1466 |
| R indices (all data) | $R_1$ = 0.1144, $wR_2$ = 0.1797 |
| Largest diff. peak and hole | 0.197 and -0.265 $e.A^{-3}$ |

Al(7)Me

| | |
|---|---|
| Identification code | h11mdj09 |
| Empirical formula | C26 H35 Al Cl2 N2 O2 |
| Formula weight | 505.44 |
| Temperature | 150(2) K |
| Wavelength | 0.71073 Å |
| Crystal system, space group | Triclinic, *P*-1 |
| Unit cell dimensions | a = 9.708(4) Å α = 82.591(15) °<br>b = 9.824(4) Å β = 75.027(16) °<br>c = 15.270(4) Å γ = 72.308(17) ° |
| Volume | 1338.3(9) $A^3$ |
| Z, Calculated density | 2, 1.254 $Mg/m^3$ |
| Absorption coefficient | 0.300 $mm^{-1}$ |
| F(000) | 536 |
| Crystal size | 0.10 x 0.10 x 0.10 mm |
| Theta range for data collection | 3.96 to 25.15 ° |
| Limiting indices | -11≤h≤11, -11≤k≤11, -18≤l≤17 |
| Reflections collected / unique | 15193 / 4732 [R(int) = 0.0781] |
| Completeness to theta = 25.15 | 98.7 % |
| Absorption correction | None |
| Refinement method | Full-matrix least-squares on $F^2$ |
| Data / restraints / parameters | 4732 / 0 / 306 |
| Goodness-of-fit on $F^2$ | 1.008 |
| Final R indices [I>2σ(I)] | $R_1$ = 0.0502, $wR_2$ = 0.1101 |
| R indices (all data) | $R_1$ = 0.0973, $wR_2$ = 0.1316 |
| Largest diff. peak and hole | 0.237 and -0.300 $e.A^{-3}$ |

Al(**8**)Me

| | |
|---|---|
| Identification code | k11mdj20 |
| Empirical formula | C31 H37 Al Cl2 N2 O2 |
| Formula weight | 567.51 |
| Temperature | 150(2) K |
| Wavelength | 0.71073 Å |
| Crystal system, space group | Monoclinic, $P2_1/n$ |
| Unit cell dimensions | a = 15.0450(3) Å α = 90 °<br>b = 11.7530(3) Å β = 100.5930(10) °<br>c = 17.2050(5) Å γ = 90 ° |
| Volume | 2990.41(13) $A^3$ |
| Z, Calculated density | 4, 1.261 $Mg/m^3$ |
| Absorption coefficient | 0.277 $mm^{-1}$ |
| F(000) | 1200 |
| Crystal size | 0.20 x 0.10 x 0.05 mm |
| Theta range for data collection | 3.62 to 25.70 ° |
| Limiting indices | -18≤h≤18, -13≤k≤14, -20≤l≤18 |
| Reflections collected / unique | 35301 / 5671 [R(int) = 0.1508] |
| Completeness to theta = 25.70 | 99.5 % |
| Absorption correction | None |
| Max. and min. transmission | 0.9863 and 0.9467 |
| Refinement method | Full-matrix least-squares on $F^2$ |
| Data / restraints / parameters | 5671 / 0 / 364 |
| Goodness-of-fit on $F^2$ | 1.018 |
| Final R indices [I>2σ(I)] | $R_1$ = 0.0610, $wR_2$ = 0.1255 |
| R indices (all data) | $R_1$ = 0.1187, $wR_2$ = 0.1536 |
| Largest diff. peak and hole | 0.822 and -0.922 $e.A^{-3}$ |

# Publications